

Reactivity Studies of Catalytically Relevant Palladium Model Complexes

by

Ansis Maleckis

A dissertation submitted in partial fulfillment
of the requirements for the degree of
Doctor of Philosophy
(Chemistry)
in The University of Michigan
2014

Doctoral Committee:

Professor Melanie S. Sanford, Chair
Professor Mark Banaszak Holl
Professor Erdogan Gulari
Professor John P. Wolfe

© Ansis Maleckis

2014

Acknowledgements

I would like to thank my advisor, Professor Melanie Sanford for having me as a member of her research group. I thank you for your ideas, suggestions and unceasing enthusiasm for research and science. You taught me how to explore, write and present chemistry. I am extremely grateful to you also for your infinite understanding and tolerance towards my unruly and idiosyncratic personality.

I thank my dissertation committee members, Professors John P. Wolfe, Mark Banaszak Holl and Erdogan Gulari for their invaluable time and advice. I must thank the department staff for all the help they have provided. DRs. Eugenio Alvarado and Chris Kojiro for assistance with NMR experiments, DRs Jim Windak and Paul Lennon for Mass spectrometry analyses and Dr Jeff W. Kampf for X-ray structures.

Table of Contents

Acknowledgments.....	ii
List of Tables	vi
List of Schemes.....	vii
List of Figures.....	xii
Abstract.....	xv

Chapter 1

Introduction.....	1
1.1 Reactivity Studies of Well Defined Palladium(IV) Centers	1
1.2 Studies towards Nickel and Palladium Catalyzed Trifluoromethylation	6
1.3 References	9

Chapter 2

Design and Synthesis of Palladium(IV) Model Complexes Supported by Facial Tridentate Ligands	11
---	----

2.1 Introduction.....	11
2.2 Synthesis of Supporting <i>fac</i> -L ₂ X Ligands	11
2.3 Preparation of (<i>fac</i> -L ₂ X)Pd ^{II} (Aryl)(CF ₃) Complexes	13
2.4 Preparation and Reactivity of (<i>fac</i> -L ₂ X)Pd ^{IV} (Aryl)(CF ₃)(Hal) Complexes.....	17
2.5 Conclusions.....	29
2.6 Experimental Section	29
2.7 References.....	59

Chapter 3

Investigation of C–H Activation at Palladium(IV).....	61
3.1 Introduction.....	61
3.2 Synthesis of the [(Py ₃ CH)Pd ^{IV} (biphenyl)Cl ₂]X Model System.....	64
3.3 Reactivity of the Model Complexes	68
3.4 Proposed Mechanism of C–H Activation at Palladium(IV)	71
3.5 Ligand Substitution at Palladium(IV).....	73
3.6 Rotation about the Pd ^{IV} –C _{Aryl} Bond.....	78
3.7 Configurational Isomerization at Pd ^{IV} via Berry Pseudorotation	80
3.8 Acetate Assisted C–H Cleavage at Palladium(IV)	82
3.9 Regioselectivity of C–H Activation at Palladium(IV).....	85
3.10 Conclusions.....	87
3.11 Experimental Section	88
3.12 References.....	140

Chapter 4

Synthesis of Trifluoromethyl Complexes Using TFAA as CF ₃ Source	142
4.1 Introduction.....	142
4.2 Decarbonylative Synthesis of Nickel Trifluoromethyl Complexes	146
4.3 Decarbonylative Synthesis of Pd ^{II} Trifluoromethyl Complexes.....	150
4.4 Reactivity of the Perfluoroalkyl Nickel and Palladium Complexes	156
4.5 Conclusions.....	157
4.6 Experimental Section	158
4.7 References.....	179

Chapter 5

Catalytic Cycle of Trifluoromethylation with TFAA as a CF ₃ Source.....	181
5.1 Introduction.....	181
5.2 Oxidative Addition of TFA Esters to (RuPhos) _n Pd ⁰	184
5.3 Decarbonylative Decomposition of (RuPhos)Pd(COR _f)(OCOR _f).....	186
5.4 Transmetalation and Reductive Elimination.....	189
5.5 Conclusions.....	191
5.6 Experimental Section	191
5.7 References.....	205

List of Tables

Chapter 2

Design and Synthesis of Palladium(IV) Model Complexes Supported by Facial Tridentate Ligands

Table 2.1 Preparation of (<i>fac</i> -L ₂ X)Pd ^{IV} (Aryl)(CF ₃)(Cl) complexes.....	19
Table 2.2 Reactions of (dpaa)Pd ^{II} (Aryl)(CF ₃) with NFTPT	20

Chapter 3

Investigation of C–H Activation at Palladium(IV)

Table 3.1 Spin-lattice relaxation times (<i>T</i> ₁) for complexes 7 , 8 and 9	66
Table 3.2 MS data of [(Py ₃ CH)Pd ^{IV} ([1,1'-biphenyl]-2,2'-diyl)(Cl)] ⁺ (12).....	137
Table 3.3 MS data for intramolecular KIE determination	137

List of Schemes

Chapter 1

Introduction

Scheme 1.1 Diastereoselective Csp ³ -H iodination.....	2
Scheme 1.2 Acetoxylation and arylation of unactivated Csp ³ -H bonds	2
Scheme 1.3 Synthesis of TP and BiPy supported Pd ^{IV} complexes	3
Scheme 1.4 Formation of Pd ^{IV} via oxidative addition of aryl iodide to Pd ^{II}	4
Scheme 1.5 Oxidative Pd ^{IV} mediated fluorination of arylboronic acids	4
Scheme 1.6 Directed Pd ^{IV} mediated C–H chlorination	5
Scheme 1.7 Directed Pd ^{IV} mediated C–H sulfonylation.....	5
Scheme 1.8 Catalytic cycle for proposed trifluoromethylation reaction	8

Chapter 2

Design and Synthesis of Palladium(IV) Model Complexes Supported by Facial Tridentate Ligands

Scheme 2.1 Synthesis of <i>fac</i> -L ₂ X ligands 2 and 3	13
Scheme 2.2 Synthesis of <i>fac</i> -L ₂ X ligand 4	13
Scheme 2.3 Preparation of <i>cis</i> -(4-Mepy) ₂ Pd(4-MeC ₆ H ₄)(CF ₃)	14

Scheme 2.4 Preparation of $(\text{Tp})\text{Pd}^{\text{II}}(4\text{-MeC}_6\text{H}_4)(\text{CF}_3)$	15
Scheme 2.5 Preparation of $(\text{L}_2\text{X})\text{Pd}^{\text{II}}(4\text{-MeC}_6\text{H}_4)(\text{CF}_3)$ complexes	15
Scheme 2.6 Preparation of $(\text{Tp})\text{Pd}^{\text{IV}}(\text{Aryl})(\text{CF}_3)(\text{Cl})$	18
Scheme 2.7 Reactivity of $(\text{Tp})\text{Pd}^{\text{IV}}(\text{Aryl})(\text{CF}_3)(\text{Cl})$	18
Scheme 2.8 Reaction of $(\text{dpsa})\text{Pd}^{\text{IV}}(\text{Aryl})(\text{CF}_3)(\text{F})$ with TMSOTf	23
Scheme 2.9 Synthesis of $(\text{dpph})\text{Pd}^{\text{IV}}(\text{Aryl})(\text{CF}_3)(\text{Cl})$	24
Scheme 2.10 Reactivity of $(\text{dpph})\text{Pd}^{\text{IV}}(\text{Aryl})(\text{CF}_3)(\text{Cl})$ with L-type ligands	26
Scheme 2.11 Reactivity of $(\text{dpph})\text{Pd}^{\text{IV}}(\text{Aryl})(\text{CF}_3)(\text{Cl})$ with X-type ligands.....	27
Scheme 2.12 Preparation of $(\text{dpph})\text{Pd}^{\text{IV}}(\text{biphe})(\text{Cl})$	28

Chapter 3

Investigation of C–H Activation at Palladium(IV)

Scheme 3.1 para-Selective arylation of monosubstituted arenes.....	61
Scheme 3.2 Oxidative dimerization of 2-arylpyridines	62
Scheme 3.3 Carboamination of alkenes.....	62
Scheme 3.4 Intramolecular C–H activation at a Pd^{IV}	63
Scheme 3.5 Preparation of $[(\text{Py}_3\text{CH})\text{Pd}^{\text{IV}}([\text{1,1'-biphenyl}]\text{-2-yl})(\text{Cl})_2][\text{X}]$ Complexes	64
Scheme 3.6 Binding of chloride counterion to $[(\text{Py}_3\text{CH})\text{Pd}^{\text{IV}}([\text{1,1'-biphenyl}]\text{-2-yl})(\text{Cl})_2]$	67
Scheme 3.7 Thermal decomposition of $[(\text{Py}_3\text{CH})\text{Pd}^{\text{IV}}([\text{1,1'-biphenyl}]\text{-2-yl})(\text{Cl})_2][\text{Cl}]$	68
Scheme 3.8 Reactions of $[(\text{Py}_3\text{CH})\text{Pd}^{\text{IV}}([\text{1,1'-biphenyl}]\text{-2-yl})(\text{Cl})_2][\text{Cl}]$ with bases	69
Scheme 3.9 Concerted metallation-deprotonation (CMD) mechanism.....	69
Scheme 3.10 Acetate promoted C–H activation at Pd^{IV}	70

Scheme 3.11 Proposed mechanism for acetate-assisted C–H activation at Pd ^{IV}	72
Scheme 3.12 Chloride-to-acetate ligand substitution at Pd ^{IV}	73
Scheme 3.13 Detection of [(Py ₃ CH)Pd ^{IV} ([1,1'-biphenyl]-2-yl)(Cl)(OAc)] ⁺ by NMR	74
Scheme 3.14 Preparation of Pd ^{IV} bromide and azide complexes	74
Scheme 3.15 Preparation of [(Py ₃ CH)Pd ^{IV} ([1,1'-biphenyl]-2,2'-diyl)(Br)][TfO]	76
Scheme 3.16 Reaction of [(Py ₃ CCH ₃)Pd ^{IV} (biphenyl-2,2'-diyl)(Br)][TfO] with AgOAc	77
Scheme 3.17 Chloride-to-bromide ligand exchange rate at Pd ^{IV}	78
Scheme 3.18 Rotation about the Pd ^{IV} –C _{Aryl} bond.....	79
Scheme 3.19 Isomerization of [(Py ₃ CH)Pd ^{IV} ([1,1'-biphenyl]-2-yl)(Br) ₂][IBr ₂].....	81
Scheme 3.20 Determination of intramolecular KIE	83
Scheme 3.21 Determination of intermolecular KIE	84
Scheme 3.22 Regioselective acetate-assisted C–H activation at Pd ^{IV}	85
Scheme 3.23 C–O bond forming reductive elimination process at Pd ^{IV} center.....	86
Scheme 3.24 General procedure for the synthesis of iodobiphenyls	90
Scheme 3.25 Synthesis of 2,6-dideutero-4-(<i>t</i> -butyl)-5'-fluoro-2'-iodobiphenyl (S14)	94
Scheme 3.26 Synthesis of 2-deutero-2'-iodo-1,1'-biphenyl (S15)	97
Scheme 3.27 Equilibrium between conformers of (Py ₃ CH)Pd ^{II} (biphen-2-yl)(I).....	99

Chapter 4

Synthesis of Trifluoromethyl Complexes Using TFAA as CF₃ Source

Scheme 4.1. Swarts reaction	142
Scheme 4.2. McLoughlin-Throrer reaction.....	143

Scheme 4.3. Cross coupling of aryl iodides with Ruppert's reagent	143
Scheme 4.4. Copper mediated decarboxylative trifluoromethylation	144
Scheme 4.5 General mechanism of decarbonylative coupling reactions.....	145
Scheme 4.6. Palladium catalyzed decarbonylative coupling	145
Scheme 4.7 Preparation of transition metal CF ₃ complexes.....	146
Scheme 4.8 Preparation of (PPh ₃) ₂ Ni(CF ₃)(OCCF ₃).....	147
Scheme 4.9 Preparation of (dppe)Ni(CF ₃)(OCCF ₃)	148
Scheme 4.10 Preparation of (dppe)Ni(R _f)(X) complexes.....	150
Scheme 4.11 Synthesis of (PPh ₃) ₂ Pd(COCF ₃)(OCOCF ₃)	151
Scheme 4.12 Reactivity of (PPh ₃) ₂ Pd(COCF ₃)(OCOCF ₃)	151
Scheme 4.13 Viable mechanism for decarbonylation at Ni ^{II}	153
Scheme 4.14 Viable mechanism for decarbonylation at Pd ^{II}	153
Scheme 4.15 Synthesis of (P(<i>o</i> -Tol) ₃) ₂ Pd(COCF ₃)(OCOCF ₃).....	153
Scheme 4.16 Decarbonylative decomposition of (P(<i>o</i> -Tol) ₃) ₂ Pd(COCF ₃)(OCOCF ₃) ...	154
Scheme 4.17 Preparation of (dppe)Pd(R _f)(OCOR _f) complexes	155
Scheme 4.18 Preparation of (dppe)Pd(CHF ₂)(Cl)	156
Scheme 4.19 Preparation of (dppe)Pd(R _f)(C ₆ H ₅) complexes	157
Scheme 4.20 Preparation of (dppe)Pd(CF ₃)(CH ₃).....	157

Chapter 5

Catalytic Cycle of Trifluoromethylation with TFAA as a CF₃ Source

Scheme 5.1 Palladium catalyzed trifluoroacetylation.....	182
Scheme 5.2 Mechanism of palladium catalyzed trifluoroacetylation.....	182
Scheme 5.3 Trifluoromethylation developed by Buchwald and coworkers.....	183
Scheme 5.4 Reaction of (RuPhos) _n Pd ⁰ with TFAA.....	184
Scheme 5.5 Reaction of (RuPhos) _n Pd ⁰ with C ₆ F ₅ OCOCF ₃	185
Scheme 5.6 Synthesis of (RuPhos)Pd(COR _f)(OCOR _f) via ligand exchange.....	186
Scheme 5.7 Preparation of (RuPhos)Pd(R _f)(OCOR _f) complexes.....	187
Scheme 5.8 Formation of [(RuPhos) ₂ Pd ₂](CF ₃ COO) ₂	188
Scheme 5.9 Transmetallation and reductive elimination reactions.....	189

List of Figures

Chapter 1

Introduction

Figure 1.1. Examples of trifluoromethylated pharmaceuticals and agrochemicals 7

Chapter 2

Design and Synthesis of Palladium(IV) Model Complexes Supported by Facial Tridentate Ligands

Figure 2.1 Selected (*fac*-L₂X) supporting ligands 12

Figure 2.2 Determination of stereochemistry for (*fac*-L₂X)Pd^{II}(Aryl)(CF₃) complexes .. 16

Figure 2.3 Thermal ellipsoid plot of (dpph)Pd^{II}(Aryl)(CF₃) (**14**)..... 17

Figure 2.4 Stereochemical assignment for (*fac*-L₂X)Pd^{IV}(Aryl)(CF₃)(X) complexes..... 21

Figure 2.5 Thermal ellipsoid plots of (dpsa)Pd^{IV}(Aryl)(CF₃)(X) complexes 22

Figure 2.6 ¹H NMR spectra of (dpph)Pd^{IV}(Aryl)(CF₃)(Cl) (**27**) at 20 °C and 0 °C..... 25

Figure 2.7 Thermal ellipsoid plot of (dpph)Pd^{IV}(Aryl)(CF₃)(NPhth)..... 27

Chapter 3

Investigation of C–H Activation at Palladium(IV)

Figure 3.1 Possible intermediates	63
Figure 3.2 $^1\text{H}/^1\text{H}$ ROESY spectrum of $[(\text{Py}_3\text{CH})\text{Pd}^{\text{IV}}([\text{1,1}'\text{-biphenyl}]\text{-2-yl})(\text{Cl})_2][\text{ICl}_2]$..	65
Figure 3.3 ORTEP drawing of $[(\text{Py}_3\text{CH})\text{Pd}^{\text{IV}}([\text{1,1}'\text{-biphenyl}]\text{-2-yl})(\text{Cl})_2][\text{ICl}_2]$	67
Figure 3.4 ORTEP drawing of $[(\text{Py}_3\text{CH})\text{Pd}^{\text{IV}}([\text{1,1}'\text{-biphenyl}]\text{-2,2'-diy})\text{(Cl)}][\text{Cl}]$	71
Figure 3.5 ORTEP drawing of $[(\text{Py}_3\text{CH})\text{Pd}^{\text{IV}}([\text{1,1}'\text{-biphenyl}]\text{-2-yl})(\text{Br})_2][\text{IBr}_2]$	75
Figure 3.6 $^1\text{H}/^1\text{H}$ ROESY spectrum of $[(\text{Py}_3\text{CH})\text{Pd}^{\text{IV}}([\text{1,1}'\text{-biphenyl}]\text{-2-yl})(\text{Br})_2][\text{IBr}_2]$.	80
Figure 3.7 Ortep drawing of $(\text{Py}_3\text{CH})\text{Pd}^{\text{II}}([\text{1,1}'\text{-biphenyl}]\text{-2-yl})(\text{I})$ (6)	100
Figure 3.8 Absorbance of complex 24 as a function of added bromide	134
Figure 3.9 UV-Vis traces (480 nm) of reaction between complex 9 and bromide	135
Figure 3.10 UV-Vis traces (480 nm) of reaction between complex 24 and bromide	136
Figure 3.11 Array of ^{19}F NMR spectra showing conversion of 34 to the product 35	138
Figure 3.12 Plot of 35 formed and 34 consumed as a function of time	139
Figure 3.13 Array of ^{19}F NMR spectra showing conversion of 38 to the product 39	139
Figure 3.14 Plot of 39 formed and 38 consumed as a function of time	139

Chapter 4

Synthesis of Trifluoromethyl Complexes Using TFAA as CF_3 Source

Figure 4.1 ^{19}F NMR spectrum of $(\text{dppe})\text{Ni}(\text{CF}_3)(\text{OOC}\text{CF}_3)$	148
Figure 4.2 $^{31}\text{P}\{^1\text{H}\}$ NMR spectrum of $(\text{dppe})\text{Ni}(\text{CF}_3)(\text{OOC}\text{CF}_3)$	149

Figure 4.3 Screened Pd⁰(L)_n complexes 152

Chapter 5

Catalytic Cycle of Trifluoromethylation with TFAA as a CF₃ Source

Figure 5.1 ¹⁹F- and ³¹P{¹H}-NMR spectra of RuPhosPd(CF₃)(OCOCF₃) 187

Abstract

Recently high oxidation state palladium chemistry has emerged as efficient tool for direct C–H bond functionalization that does not require prefunctionalized starting materials. Investigation of transition metal model complexes is an efficient approach for optimization of known reactions and development of new methodologies. This dissertation describes reactivity studies of Pd^{IV} model systems with an aim to gain better understanding of Pd^{IV} mediated C–H bond functionalization reactions. In addition, investigation of Pd^{II} model complexes to assess the feasibility of hypothetical Pd^{0/II} catalyzed trifluoromethylation reaction with trifluoroacetic anhydride as a CF₃ source is also described.

In order to obtain detailed information about processes occurring at Pd^{IV} during catalysis, relatively stable yet reactive model systems had to be identified. First, we designed and synthesized a number of Pd^{IV} complexes supported by facial tridentate NNN and NCN ligands and investigated their reactivity. Next, we identified appropriate model system for detailed investigation of C–H bond cleavage at Pd^{IV} centers. Mechanistic information about this transformation was obtained through the following: (i) extensive one- and two-dimensional NMR analysis, (ii) reactivity studies of a series of substituted analogues, and (iii) isotope effect studies. These experiments suggest that C–H activation at [(Py₃CH)Pd^{IV}(biphenyl)Cl₂]⁺ model system occurs via a multistep process involving chloride-to-acetate ligand exchange followed by conformational and

configurational isomerization and then C–H cleavage. The data also suggest that C–H cleavage proceeds via an acetate-assisted mechanism with the carboxylate likely serving as an intramolecular base.

In a unrelated project we propose a catalytic cycle for nickel(0/II) or palladium(0/II) catalyzed decarbonylative trifluoromethylation using trifluoroacetic esters as CF₃ sources. The catalytic cycle consists of four elementary steps: (1) oxidative addition of a trifluoroacetic ester to M⁰ center, (2) CO deinsertion from the resulting trifluoroacyl M^{II} complex, (3) transmetalation of a zinc-aryl to M^{II}, and (4) aryl–CF₃ bond-forming reductive elimination. We demonstrated that the use of RuPhos as the supporting ligand for palladium enables each of these steps to proceed under mild conditions. These studies set the stage for the development of catalytic arene trifluoromethylation and perfluoroalkylation reactions using inexpensive trifluoroacetic acid-derived CF₃ sources.

Chapter 1: Introduction

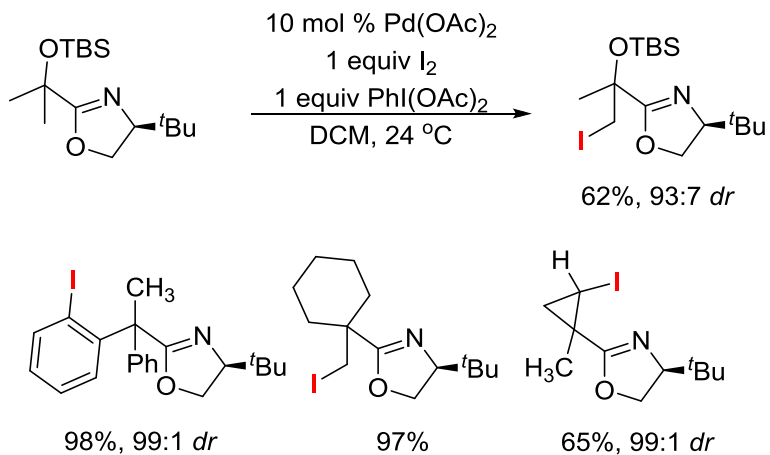
Reactivity studies of well defined complexes have been an invaluable tool for the elucidation of transition metal catalyzed reaction mechanisms^{1,2} as well as for development and refinement of important industrial scale processes.^{3,4} This dissertation describes design, synthesis and reactivity studies of Pd model complexes with a goal to understand and optimize already known Pd catalyzed reactions as well as to develop new synthetic methodology. Specifically, Pd^{IV} mediated C–H functionalization and Pd^{II} mediated trifluoromethylation reactions are the main research subjects in this dissertation.

1.1 Reactivity Studies of Well Defined Palladium(IV) Centers

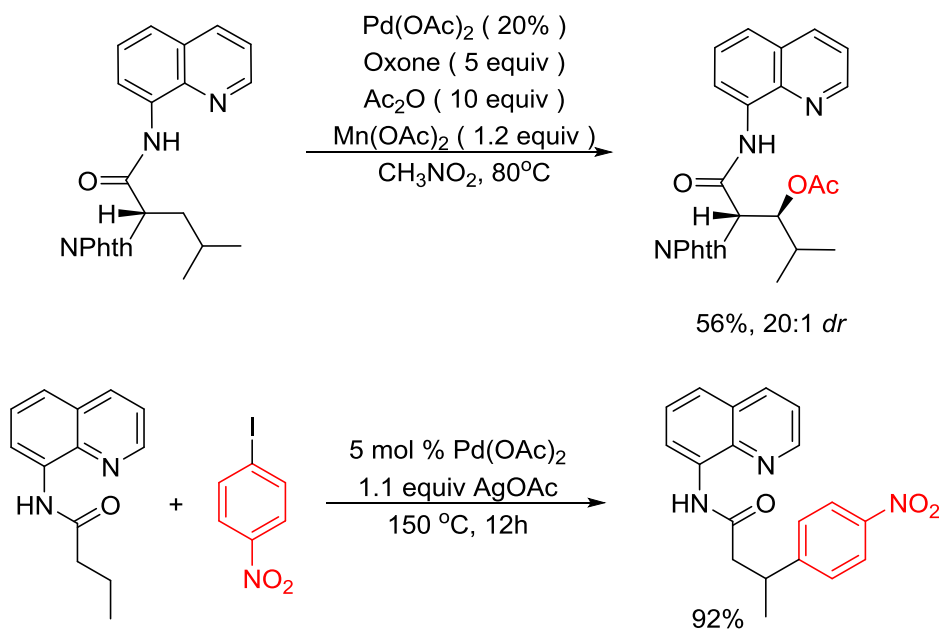
Pd^{IV} mediated C–H bond functionalization reactions have emerged as practically useful methodology complementary to the conventional Pd^{0/II} catalyzed processes.⁵ In particular, Pd catalyzed oxidative amination, arylation, acetoxylation and alkylation of arenes and directed functionalization of unactivated aliphatic C–H bonds are extremely efficient transformations that do not require prefunctionalized starting materials.⁶ Directing groups and temporary directing auxiliaries ensure high regioselectivities in these C–H functionalization reactions. Scheme 1.1 and Scheme 1.2 show particularly noteworthy examples. For instance, highly diastereoselective C^{sp}³-H and C^{sp}²-H iodinations of substrates bearing chiral oxazoline auxiliary were achieved with Pd(OAc)₂

catalyst (Scheme 1.1).⁷ 8-Aminoquinoline, in turn, is a versatile temporary auxiliary for acetoxylation and arylation of carboxylic acids (Scheme 1.2).^{8,9}

Scheme 1.1 Diastereoselective Csp³-H iodination

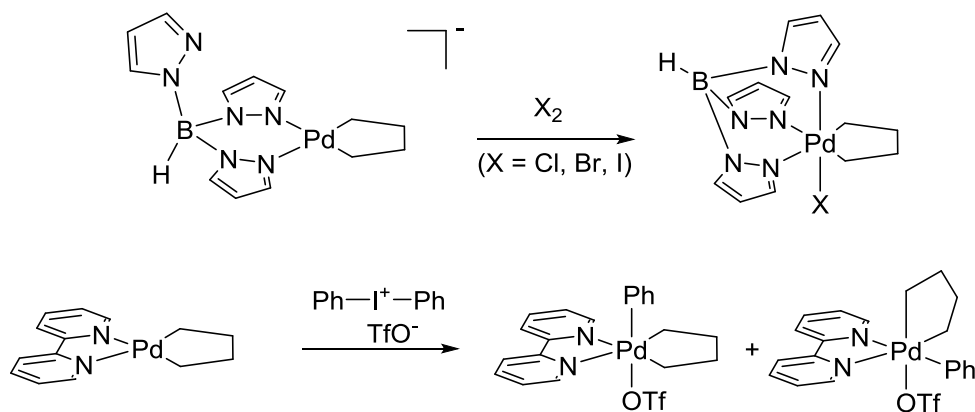


Scheme 1.2 Acetoxylation and arylation of unactivated Csp³-H bonds



The exact mechanism of Pd^{IV} mediated reactions is often unclear. Better understanding of processes occurring at Pd^{IV} would allow improvement of C–H functionalization regioselectivities and expansion of the substrate scope. A large number of model complexes have been investigated with an aim to gain insight in Pd^{IV} mediated C–H functionalization processes.^{5a} Pd^{IV} complexes are typically obtained via oxidation of appropriate Pd^{II} precursor. Chlorine, bromine, iodine(III) compounds, peroxides, reactive alkylating agents and wide array of other reagents have been used as oxidants. Pd^{IV} species undergo facile reductive elimination therefore, chelating supporting ligands such as bipyridine (BiPy) and hydrotris(pyrazolyl)borate (TP) are commonly used for stabilization of Pd^{IV} complexes. Scheme 1.3 shows examples of BiPy and TP supported complexes reported by Canty and coworkers.¹⁰

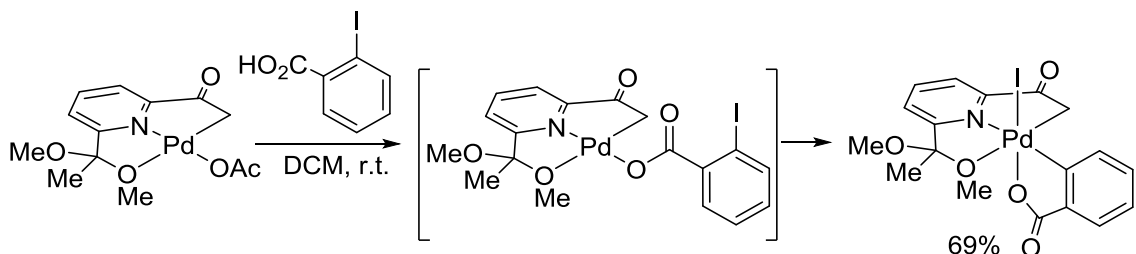
Scheme 1.3 Synthesis of TP and BiPy supported Pd^{IV} complexes



It has been demonstrated that even aryl iodides can undergo oxidative addition to Pd^{II} to form Pd^{IV} species (Scheme 1.4).¹¹ This suggests that Pd^{IV} species might be involved not only in oxidative C–H functionalization reactions but also in conventional catalytic

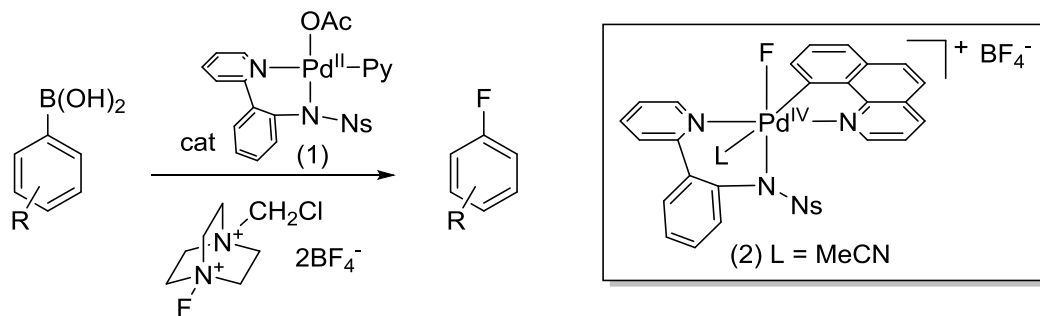
processes such as Heck and Suzuki reactions that have been generally considered to proceed strictly via Pd^{0/II} catalytic cycle.^{5a,12}

Scheme 1.4 Formation of Pd^{IV} via oxidative addition of aryl iodide to Pd^{II}

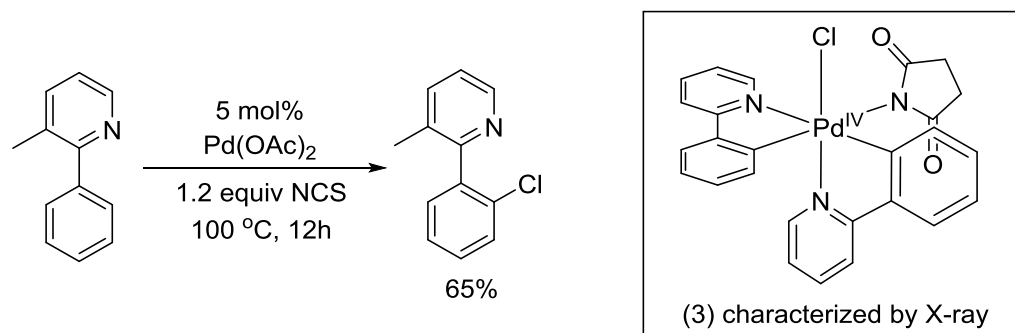


In several cases the intermediacy of Pd^{IV} in the catalytic turnover has been verified via synthesis of Pd^{IV} model complexes.¹³ For example, investigation of complex **2** confirmed that Pd^{IV} species are involved in oxidative fluorination of arylboronic acids catalyzed by complex **1** (Scheme 1.5).¹⁴ In another study, Pd^{IV} species such as **3** were demonstrated to be likely intermediates in directed C–H chlorination of phenylpyridines with *N*-chlorosuccinimide as an oxidant (Scheme 1.6).^{15,16}

Scheme 1.5 Oxidative Pd^{IV} mediated fluorination of arylboronic acids

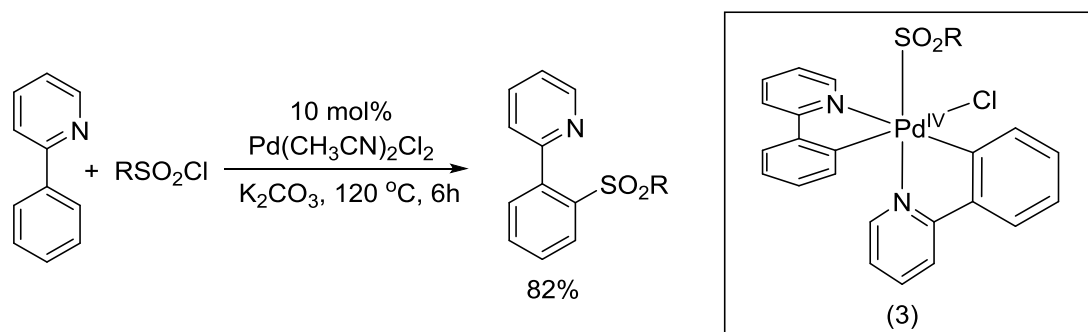


Scheme 1.6 Directed Pd^{IV} mediated C–H chlorination



Synthesis and investigation of Pd^{IV} model complexes can also aid to disprove certain mechanistic hypothesis. For example, it was proposed that Pd catalyzed C–H sulfonation of phenylpyridine proceeds with intermediacy of Pd^{IV} species such as **3** (Scheme 1.7). Pure model complex **3** was obtained through independent synthesis. Further studies showed that even though complex **3** does reductively eliminate sulfonated phenylpyridine, **3** is not kinetically competent catalyst in sulfonation of phenyl pyridines, which means that this transformation proceeds through a different pathway.^{17,18}

Scheme 1.7 Directed Pd^{IV} mediated C–H sulfonation



Most catalytically relevant Pd^{IV} complexes are very reactive and unstable species, which greatly hampers investigation of fundamental Pd^{IV} chemistry. This issue is

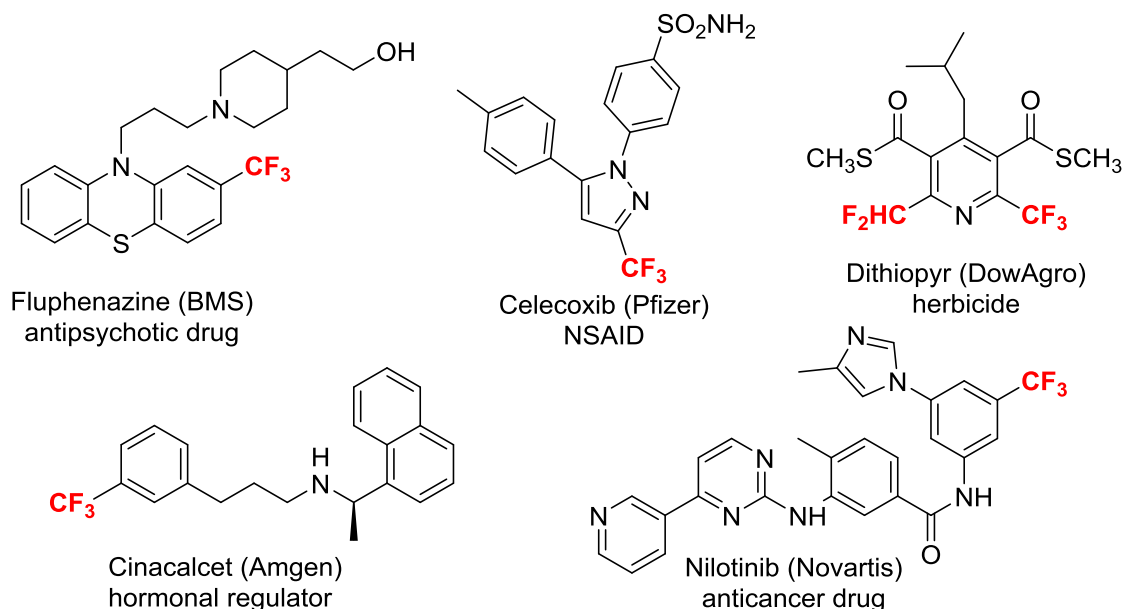
addressed in Chapter 2 which describes design and synthesis of new Pd^{IV} complexes stabilized by several diverse tridentate, facially coordinating ligands. The goal of Chapter 2 is to elucidate the relationship between electronic and steric properties of supporting ligands and reactivity at Pd^{IV} as well as development of model systems for investigation of ligand exchange, migratory insertion and C–H activation at Pd^{IV}.

C–H activation at Pd^{IV} has been proposed to be a key process in several recently reported C–H functionalization reactions¹⁹ however, comprehensive understanding of this process is lacking. Previous results from our group²⁰ led to identification of appropriate model system for studies of C–H activation at Pd^{IV}. Chapter 3 describes detailed mechanistic investigation of acetate assisted C–H cleavage at Pd^{IV}. It is demonstrated that concerted metallation-deprotonation (CMD) with acetate acting as an intramolecular base is a viable pathway for C–H activation at Pd^{IV}.

1.2 Studies towards Nickel and Palladium Catalyzed Trifluoromethylation

Trifluoromethyl moiety is used to modulate metabolic stability, lipophilicity and binding affinity of biologically active ingredients in many pharmaceuticals and agrochemicals (Figure 1.1).²¹ Medium and large scale syntheses of trifluoromethylated arenes are often inefficient and expensive processes. The lack of cheap, environmentally friendly and broadly applicable methods for the late stage trifluoromethylation of complex molecules has greatly impeded development and wider application of trifluoromethylated compounds in medicine and agriculture.

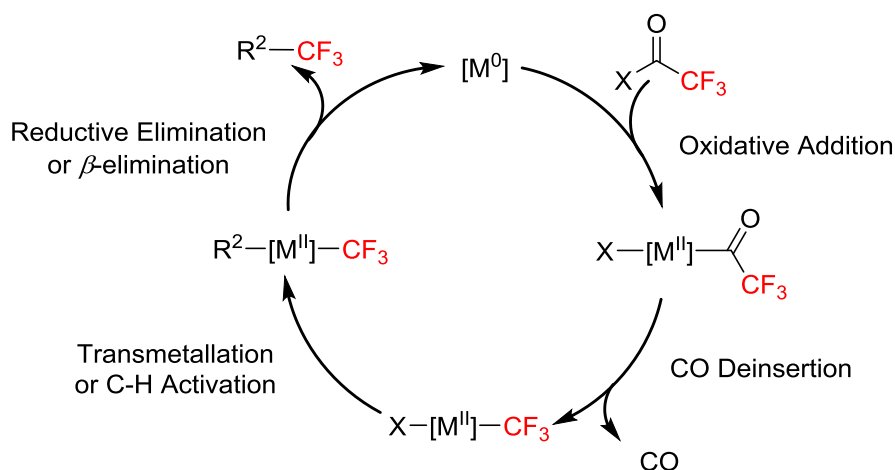
Figure 1.1. Examples of trifluoromethylated pharmaceuticals and agrochemicals



In Chapter 4 a novel approach towards the synthesis of trifluoromethylated compounds is presented. We propose a theoretical Ni and/or Pd catalyzed trifluoromethylation reaction that would employ trifluoroacetic anhydride (TFAA) and TFA esters as cheap and available CF_3 sources. The catalytic cycle for this reaction is shown in Scheme 1.8. Such a trifluoromethylation reaction would be efficient and broadly applicable addition to the currently available methodologies.

The proposed trifluoromethylation reaction seems reasonable. Step 1 (oxidative addition of trifluoroacetic esters to Pd^0)²² as well as step 3 (transmetallation at Pd^{II})^{23,24,25} both have significant precedent in the literature. In addition, the feasibility of aryl- CF_3 bond-forming reductive elimination from Pd^{II} (step iv) has also been confirmed by several reported examples. Grushin has achieved this transformation at $(\text{Xantphos})\text{Pd}^{\text{II}}(\text{aryl})(\text{CF}_3)$ complexes,⁴ while Buchwald has demonstrated the use of BrettPhos and RuPhos as ligands for this coupling.⁴

Scheme 1.8 Catalytic cycle for proposed trifluoromethylation reaction



However, decarbonylation (step iii) has not been reported previously at trifluoroacetyl palladium and trifluoroacetyl nickel complexes.²⁶ Other second and third row transition metal trifluoroacetyl complexes are known to undergo decarbonylation; however, these transformations typically require high temperatures and long reaction times.^{27,28,29,30} Thus, we anticipated that CO deinsertion could present a major bottleneck for the envisioned trifluoromethylation reaction. For this reason, before attempting catalytic reaction, we decided to prepare Ni and Pd model complexes and investigate CO deinsertion step in detail with an aim that obtained information could then be used for development and optimization of catalytic trifluoromethylation reaction. Chapter 4 describes study of decarbonylation of trifluoroacetyl ligand at Ni and Pd centers. The relationship between steric properties of the supporting ligand and facility of the decarbonylation process at Pd^{II} center is elucidated. In addition, new method for the synthesis of fluoroalkyl- Ni and Pd complexes via oxidative addition and CO deinsertion sequence is developed.

After the key processes of decarbonylation had been worked out, an attempt was made to find a single supporting ligand that would promote all the elementary steps of

catalytic cycle shown in Scheme 1.8. In Chapter 5 investigation of 2-dicyclohexylphosphino-2',6'-diisopropoxybiphenyl (RuPhos) supported Pd complexes in the context of decarbonylative trifluoromethylation is described.

1.3 References

-
- (1) For example, studies of several distinct hydrogenation mechanisms (a) Chan, A. S. C.; Pluth, J. J.; Halpern, J. *Inorg. Chim. Acta* **1979**, *37*, L477-L479. (b) Halpern, J.; Riley, D. P.; Chan, A. S. C.; Pluth, J. J. *J. Am. Chem. Soc.* **1977**, *99*, 8055-8057. (c) Chen, A. S. C.; Halpern, J. *J. Am. Chem. Soc.* **1980**, *102*, 838-840. (a) Crabtree, R. H.; Felkin, H.; Fillebeen-Khan, T.; Morris, G. E. *J. Organomet. Chem.* **1979**, *168*, 183-195. (b) Crabtree, R. H.; Lavin, M. *J. Chem. Soc. Commun.* **1985**, 1661-1662. Daley, C. J. A.; Bergens, S. H. *J. Am. Chem. Soc.* **2002**, *124*, 3680-3691.
 - (2) Studies of platinum(IV) mediated C-H functionalization (a) Stahl, S. S.; Labinger, J. A.; Bercaw, J. E. *Angew. Chem. Int. Ed.* **1998**, *37*, 2180-2192. (b) Stahl, S. S.; Labinger, J. A.; Bercaw, J. E. *J. Am. Chem. Soc.* **1996**, *118*, 5961-5976. (c) Johansson, L.; Ryan, O. B.; Tilset, M.; *J. Am. Chem. Soc.* **1999**, *121*, 1974-1975.
 - (3) Investigation of carbonylation of methanol (a) Adamson, G. W.; Daly, J. J. *J. Organomet. Chem.* **1974**, *71*, C17-C19. (b) Adams, H.; Bailey, N. A.; Mann, B. E.; Manuel, C. P.; Spencer, C. M.; Kent, A. G. *J. Chem. Soc. Dalton. Trans.* **1988**, 489-496. (c) Haynes, A.; Mann, B. E.; Morris, G. E.; Maitlis, P. M. *J. Am. Chem. Soc.* **1993**, *115*, 4093-4100.
 - (4) Investigation of hydroformylation of alkenes Heck, R. F.; Breslow, D. S. *J. Am. Chem. Soc.* **1961**, *83*, 4023-4027.
 - (5) (a) Xu, L. M.; Li, B. J.; Yang, Z.; Shi, Z. J. *Chem. Soc. Rev.* **2010**, *39*, 712-733. (b) Sehnal, P.; Taylor, R. J. K.; Fairlamb, I. J. S. *Chem. Rev.* **2010**, *110*, 824-889.
 - (6) Lyons, T. W.; Sanford, M. S. *Chem. Rev.* **2010**, *110*, 1147-1169.
 - (7) Giri, R.; Chen, X.; Yu, J.-Q. *Angew. Chem. Int. Ed.* **2005**, *44*, 2112-2115.
 - (8) Reddy, B. V. S.; Reddy, L. R.; Corey, E. J. *Org. Lett.* **2006**, *15*, 3391-3394.
 - (9) Zaitsev, V. G.; Shabashov, D.; Daugulis, O. *J. Am. Chem. Soc.* **2005**, *127*, 13154-13155.
 - (10) (a) Canty, A. J.; Jin, H.; Roberts, A. S.; Skelton, B. W.; White, A. H. *Organometallics*, **1996**, *15*, 5713-5722. (b) Canty, A. J.; Patel, J.; Rodemann, T.; Ryan, J. H.; Skelton, B. W.; White, A. H. *Organometallics*, **2004**, *23*, 3466-3473.
 - (11) Vincente, J.; Arcas, A.; Juliá-Hernández, F.; Bautista, D. *Angew. Chem. Int. Ed.* **2011**, *50*, 6896-6899.
 - (12) (a) Gerber, R.; Blacque, O.; Frech, C. M. *ChemCatChem* **2009**, *1*, 393-400. (b) Sjövall, S.; Wendt, O. F.; Andersson, C. *J. Chem. Soc. Dalton Trans.* **2002**, 1396-1400. (c) Ohff, M.; Ohff, A.; Milstein, D. *Chem. Commun.* **1999**, 357-358.

-
- (13) (a) McCall, A. S.; Wang, H.; Desper, J. M.; Kraft, S. *J. Am. Chem. Soc.* **2011**, *133*, 1832-1848. (b) Oloo, W.; Zavalij, P. Y.; Zhang, J.; Khasin, E.; Vedernikov, A. N. *J. Am. Chem. Soc.* **2010**, *132*, 14400-14402. (c) Shabashov, D.; Daugulis, O. *J. Am. Chem. Soc.* **2010**, *132*, 3965-3972.
- (14) (a) Furuya, T.; Ritter, T. *J. Am. Chem. Soc.* **2008**, *130*, 10060-10061. (b) Furuya, T.; Benitez, D.; Tkatchouk, E.; Storm, A. E.; Tang, P.; Goddard, W. A.; Ritter, T. *J. Am. Chem. Soc.* **2010**, *132*, 3793-3807.
- (15) Kalyani, D.; Dick, A. R.; Anani, W. Q.; Sanford, M. S. *Org. Lett.* **2006**, *8*, 2523-2526.
- (16) Whitfield, S. R.; Sanford, M. S. *J. Am. Chem. Soc.* **2007**, *129*, 15142-15143.
- (17) Zhao, X. D.; Dimitrijević, E.; Dong, V. M. *J. Am. Chem. Soc.* **2009**, *131*, 3466-3467.
- (18) Zhao, X. D.; Dong, V. M. *Angew. Chem. Int. Ed.* **2011**, *50*, 932-934.
- (19) (a) Hickman, A. J.; Sanford, M. S. *ACS Catal.* **2011**, *1*, 170-174. (b) Pilarski, L. T.; Selander, N.; Bose, D.; Szabo, K. J. *Org. Lett.* **2009**, *11*, 5518-5521. (c) Kawai, H.; Kobayashi, Y.; Oi, S.; Inoue, Y. *Chem. Commun.* **2008**, 1464-1466. (d) Sibbald, P. A.; Rosewall, C. F.; Swartz, R. D.; Michael, F. E. *J. Am. Chem. Soc.* **2009**, *131*, 15945-15951. (e) Rosewall, C. F.; Sibbald, P. A.; Liskin, D. V. Michael, F. E. *J. Am. Chem. Soc.* **2009**, *131*, 9488-9489. (f) Wang, X.; Leow, D.; Yu, J.-Q. *J. Am. Chem. Soc.* **2011**, *133*, 13864-13867.
- (20) Racowski, J. M.; Ball, N. D.; Sanford, M. S. *J. Am. Chem. Soc.* **2011**, *133*, 18022-18025.
- (21) Purser, S.; Moore, P. R.; Swallow, S.; Gouverneur, V. *Chem. Soc. Rev.* **2008**, *37*, 320-330.
- (22) (a) Nagayama, K.; Shimizu, I.; Yamamoto, A. *Bull. Chem. Soc. Jpn.* **1999**, *72*, 799-803. (b) Kakino, R.; Shimizu, I.; Yamamoto, A. *Bull. Chem. Soc. Jpn.* **2001**, *74*, 371-376.
- (23) For examples for transmetallation from zinc and lithium to Pd(II), see Negishi, E.; Takahashi, T.; Akiyoshi, K. *J. Organomet. Chem.* **1987**, *334*, 181-194.
- (24) For examples for transmetallation from magnesium to Pd(II), see Stockland Jr., R. A.; Anderson, G. K.; Rath, N. P. *Organometallics* **1997**, *16*, 5096-5101.
- (25) For examples for transmetallation from boron to Pd(II), see (a) Furuya, T.; Ritter, T. *J. Am. Chem. Soc.* **2008**, *130*, 10060-10061. (b) Furuya, T.; Kaiser, H. M.; Ritter, T. *Angew. Chem. Int. Ed.* **2008**, *47*, 5993-5996.
- (26) For an example of decarbonylation of non-fluorinated acyl ligands at Pd(II), see: Otsuka, S.; Nakamura, A.; Yoshida, T.; Naruto, M.; Ataka, K. *J. Am. Chem. Soc.* **1973**, *93*, 3180-3188.
- (27) For reviews, see: (a) Brothers, P. J.; Roper, W. R. *Chem. Rev.* **1988**, *88*, 1293-1326. (b) Morrison, J. A. *Adv. Inorg. Chem. Radiochem.* **1983**, *27*, 293-316.
- (28) For the synthesis of first row metal trifluoromethyl complexes via decarbonylation, see: (a) King, R. B. *Acc. Chem. Res.* **1970**, *3*, 417-427. (b) McClellan, W. R. *J. Am. Chem. Soc.* **1961**, *83*, 1598-1600.
- (29) Synthesis of second row metal trifluoromethyl complexes via decarbonylation: Panthi, B. D.; Gipson, S. L.; Franken, A. *Organometallics*, **2010**, *29*, 5890-5896.
- (30) Ir trifluoromethyl complexes via decarbonylation: (a) Brothers, P. J.; Burrell, A. K.; Clark, G. R. Rickard, C. E. F.; Roper, W. R. *J. Organomet. Chem.* **1990**, *394*, 615-642. (b) Blake, D. M.; Shields, S.; Wyman, L. *Inorg. Chem.* **1974**, *13*, 1595-1600.

Chapter 2: Design and Synthesis of Palladium(IV) Model Complexes Supported by Facial Tridentate Ligands¹

2.1 Introduction

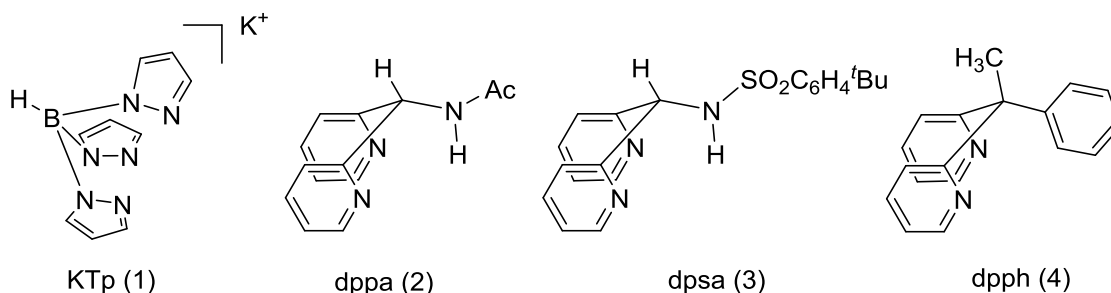
At the outset of this project our goal was to design and synthesize isolable yet reactive Pd^{IV} complexes, investigate electronic and steric effects of supporting ligands on reactivity of Pd^{IV} and elucidate mechanistic nuances of C–H activation at Pd^{IV}. With these goals in mind, we sought to identify ligands that would stabilize Pd^{IV} complexes, thereby slowing the relative rate of reductive elimination versus that of other transformations. Our studies targeted complexes of general structure (*fac*-L₂X)Pd^{IV}(CF₃)(aryl)(halide). The trifluoromethyl (CF₃) ligand was selected in order to stabilize the Pd^{IV} center and render competing reductive elimination reactions relatively slow.² The halide was anticipated to be a labile ligand that could serve as a site of reactivity at the high-oxidation-state Pd center.

2.2 Synthesis of Supporting *fac*-L₂X Ligands

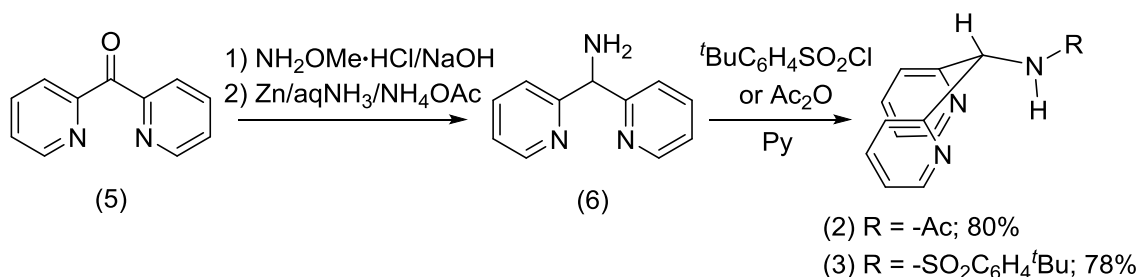
For this study facially coordinated monoanionic tridentate supporting ligands (*fac*-L₂X) were selected, because these are known to stabilize a number of isolable organometallic Pd^{IV} complexes.^{3,4,5} Scheme 2.1 shows the structures of the ligands **1-4** that were targeted for the preparation of (*fac*-L₂X)Pd^{IV}(CF₃)(aryl)(halide) complexes. Ligands **1-4** differ with steric and electronic properties. Specifically, ligands **1-4** bear a

progressively stronger σ donor which might enhance the reactivity of Pd^{IV} complexes toward X-type ligand substitution and reductive elimination. The σ -aryl in NNC donor ligand **4** is expected to have especially large trans influence.⁶ Notably, while *mer*-NNC and *mer*-NCN pincer ligands have been widely used in high-valent Pd chemistry analogous *fac*-NNC ligands have not been well studied at Pd^{IV}. It was anticipated that by screening number of diverse ligands we would be able to find a good balance between stability and reactivity at Pd^{IV} center.

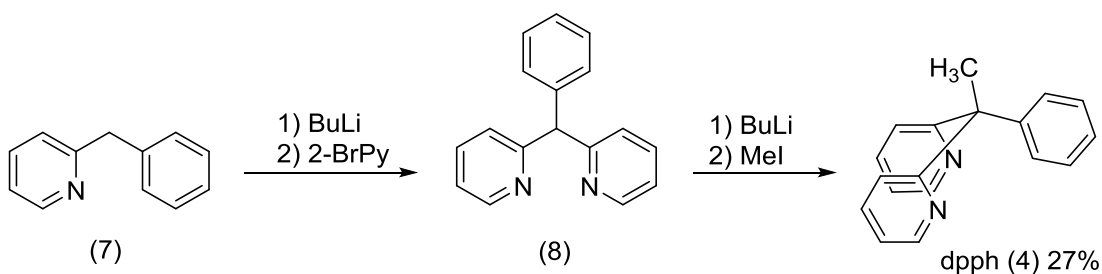
Figure 2.1 Selected (*fac*-L₂X) supporting ligands



Scheme 2.1 Synthesis of *fac*-L₂X ligands **2** and **3**



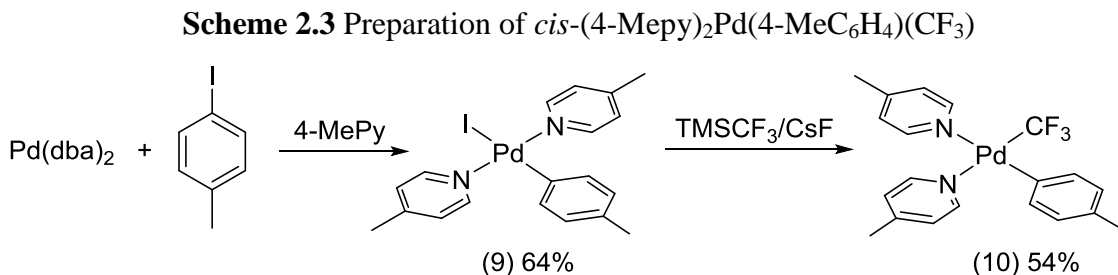
Scheme 2.2 Synthesis of *fac*-L₂X ligand **4**



2.3 Preparation of (*fac*-L₂X)Pd^{II}(Aryl)(CF₃) Complexes

We anticipated that targeted Pd^{IV} complexes could be synthesized via a two step procedure: first ligation of ligands **1-4** to appropriate Pd^{II} precursor would afford (*fac*-L₂X)Pd^{II}(Aryl)(CF₃) intermediates which would then be oxidized to (*fac*-L₂X)Pd^{IV}(Aryl)(CF₃)(X). Our initial synthetic efforts focused on identifying a (L)(L')Pd^{II}(Aryl)(CF₃) precursor that could be used for the synthesis of diverse (*fac*-L₂X)Pd^{II}(Aryl)(CF₃) intermediates. It was of particular importance that L and L' be easily displaced by ligands **1-4**. Previous reports have shown that (tmeda)Pd^{II}(CH₃)₂ and (tmeda)Pd^{II}(CH₃)(C₆H₅) undergo facile ligand exchange with monophosphines, diphosphines, and bipyridine;⁸ as such, we initially hypothesized that (tmeda)Pd^{II}(Aryl)(CF₃) would be a convenient palladium starting material. While the

synthesis of $(\text{tmeda})\text{Pd}^{\text{II}}(\text{Aryl})(\text{CF}_3)$ was straightforward and high yielding, clean ligand exchange was not observed with the *fac*- L_2X ligands **1-4** investigated in this study. As such, we next targeted the Pd^{II} complex *cis*-(4-Mepy) $_2\text{Pd}(4\text{-MeC}_6\text{H}_4)(\text{CF}_3)$ (**10**; 4-Mepy = 4-methylpyridine), which contains more labile monodentate 4-Mepy ligands.

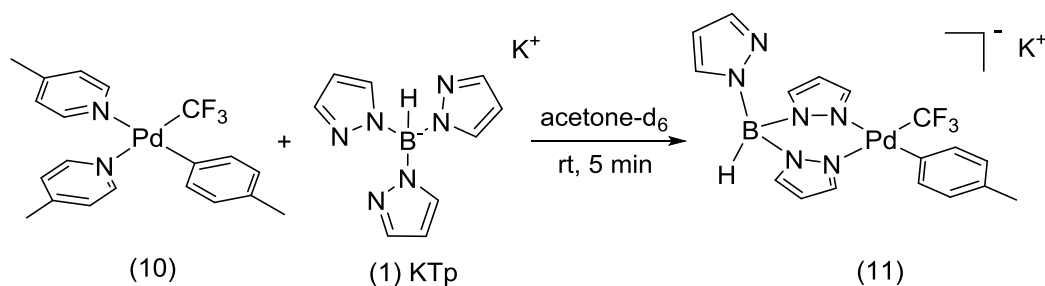


As shown in Scheme 2.3, complex **10** was prepared in two straightforward steps. First, oxidative addition of 4-iodotoluene to $\text{Pd}(\text{dba})_2$ in the presence of 10 equiv of 4-methylpyridine afforded *trans*-(4-Me-py) $_2\text{Pd}(4\text{-MeC}_6\text{H}_4)(\text{I})$ (**9**) in 64% yield. Since it was not stable in solution, complex **9** was carried forward crude. In the second step, the treatment of **9** with excess $\text{CsF}/\text{TMSCF}_3$ provided **10** in 54% yield as a white solid. Notably, the use of dry CsF and anhydrous solvent was essential in order to obtain reproducible yields of **10**. The product was characterized by ^{19}F , ^{13}C , and ^1H NMR spectroscopy. Complex **10** decomposes slowly over 24 h in CDCl_3 solution with concomitant release of Pd black; however, it is stable in the solid state for several weeks at room temperature.

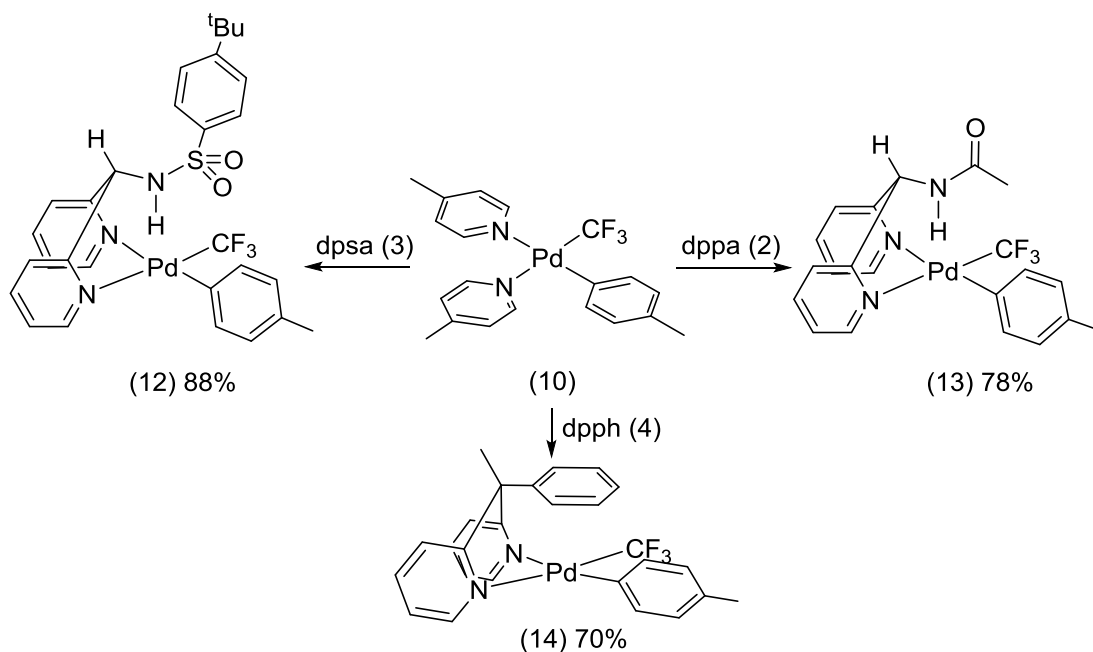
Complex **10** turned out to be a practical precursor for targeted (*fac*- L_2X) $\text{Pd}^{\text{II}}(\text{Aryl})(\text{CF}_3)$ intermediates. For instance, when **10** was treated with slight excess of **KTp** (**1**) in acetone- d_6 solution and reaction progress was monitored by ^1H and ^{19}F NMR spectroscopy, it was observed that complete conversion of **10** to **11** occurred within

5 minutes (Scheme 2.4). The ionic nature of **11** prevented its isolation in a pure form therefore; crude **11** was carried forward for the preparation of Pd^{IV} complex without further purification. In contrast, treatment of **10** with 1.15 equiv of ligands **2-4** at room temperature afforded isolable Pd^{II} products **12-14** (Scheme 2.5). Complexes **12-14** were characterized by ¹H, ¹³C, and ¹⁹F NMR spectroscopy, and all resonances were assigned by 2D ¹H/¹H COSY, ¹H/¹³C HSQC, and ¹H/¹³C HMBC NMR spectra.

Scheme 2.4 Preparation of (Tp)Pd^{II}(4-MeC₆H₄)(CF₃)

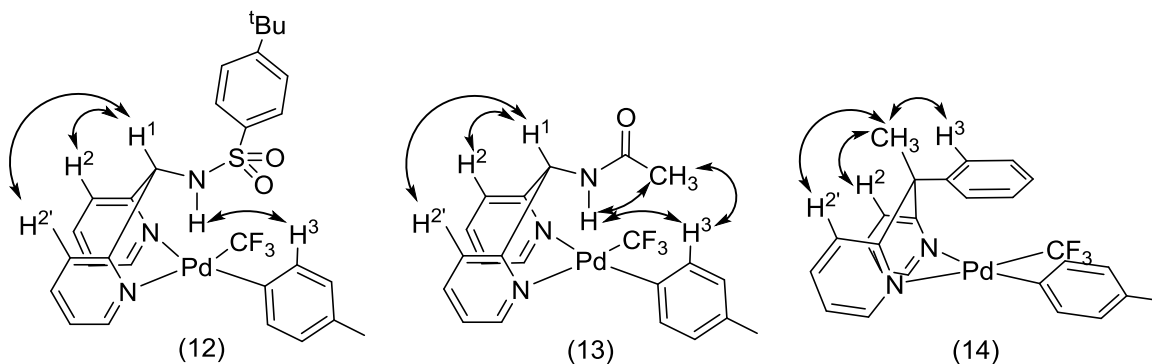


Scheme 2.5 Preparation of (L₂X)Pd^{II}(4-MeC₆H₄)(CF₃) complexes



The configurations of complexes **12-14** were established using 2D $^1\text{H}/^1\text{H}$ ROESY NMR experiments. Important correlations are shown in Figure 2.2. For $(\text{dpsa})\text{Pd}^{\text{II}}(4\text{-MeC}_6\text{H}_4)(\text{CF}_3)$ (**12**) and $(\text{dpaa})\text{Pd}^{\text{II}}(4\text{-MeC}_6\text{H}_4)(\text{CF}_3)$ (**13**), the amide functionality is in the endo position over the square plane of palladium, as evidenced by (1) an NOE correlation between the NH proton of the amide and H^3 and (2) strong correlation between H^1 and $\text{H}^2/\text{H}^{2'}$ as well as by (3) the lack of NOE correlations between the NH proton and H^2 and $\text{H}^{2'}$. The preference for the endo isomer may be a consequence of a noncovalent interaction between the palladium and the NH proton.

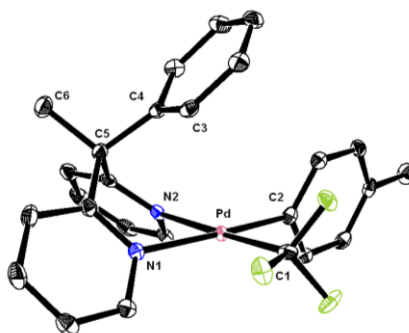
Figure 2.2 Determination of stereochemistry for $(\text{fac-L}_2\text{X})\text{Pd}^{\text{II}}(\text{Aryl})(\text{CF}_3)$ complexes



The stereochemistry of **14** was also elucidated via a $^1\text{H}/^1\text{H}$ ROESY experiment: $\text{H}^2/\text{H}^{2'}$ protons of the pyridine rings show NOE correlations with the endo methyl group but not with ortho protons of the endo phenyl ring (Figure 2.2). The structure and endo configuration of **14** was confirmed by single-crystal X-ray diffraction analysis. Crystals of **14** were obtained by slow evaporation of a saturated ethyl acetate solution at room temperature. A thermal ellipsoid plot of **14** as well as key bond distances and bond angles are shown in Figure 2.3. The phenyl ring above the square plane of palladium is inclined toward the trifluoromethyl group, with a $\text{C}_6\text{-C}_5\text{-C}_4\text{-C}_3$ torsion angle 103.80° . The

Pd–C4 (2.992 Å) and Pd–C3 (3.153 Å) distances are considerably longer than is typical (2.1–2.2 Å) in stable late-transition-metal η^2 -arene complexes;⁹ however, they are shorter than the sum of the van der Waals radii of the corresponding atoms. This apparent weak noncovalent interaction between palladium and the phenyl ring is likely the reason why **14** is formed as a single endo isomer.

Figure 2.3 Thermal ellipsoid plot of (dpph)Pd^{II}(Aryl)(CF₃) (**14**)

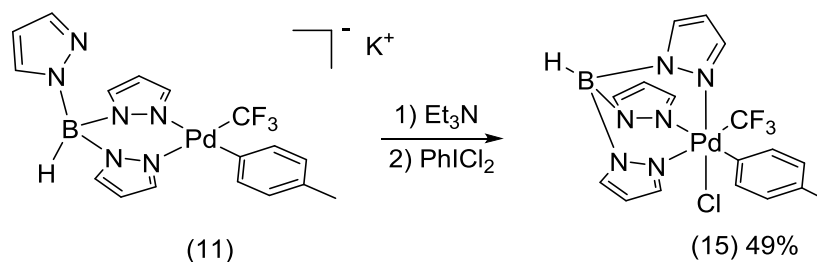


Thermal ellipsoids are shown at 50% probability. H atoms have been omitted for clarity. Selected bond lengths (Å) and angles (deg): Pd–C1, 2.013; Pd–C2, 1.99; Pd–N1, 2.155; Pd–N2, 2.121; Pd–C4, 2.992; Pd–C3, 3.153; C6–C5–C4–C3, 103.80.

2.4 Preparation and Reactivity of (*fac*-L₂X)Pd^{IV}(Aryl)(CF₃)(Hal) Complexes

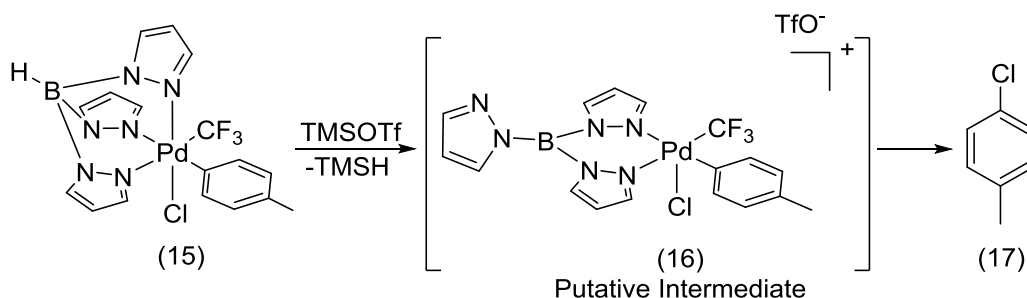
With (*fac*-L₂X)Pd^{II}(Aryl)(CF₃) precursors **12-14** in hand, we examined the synthesis and reactivity of (*fac*-L₂X)Pd^{IV}(Aryl)(CF₃)(Cl) model complexes. Oxidation of K[(Tp)Pd^{II}(Aryl)(CF₃)] (**11**) with PhICl₂ afforded **15** which was isolated in 49% yield after purification by flash chromatography (Scheme 2.6). Complex **15** was characterized by ¹H, ¹³C, ¹⁹F, and ¹¹B NMR spectroscopy.

Scheme 2.6 Preparation of (Tp)Pd^{IV}(Aryl)(CF₃)(Cl)



Complex **15** was stable in CHCl₃ solution for several days at room temperature as well as for up to 2 h at 80 °C. Under these conditions the starting material could be recovered quantitatively from the reaction mixtures. In order to test the reactivity of **15** towards C–H activation, we attempted to open a free coordination site via an abstraction of the chloride ligand. We found that **15** is highly inert towards chloride abstraction. For example, the treatment of **15** with 10 equiv of AgOTf or AgBF₄ in CDCl₃ for 2 h at 50 °C did not afford any substitution of the chloride ligand and unchanged **15** was recovered.

Scheme 2.7 Reactivity of (Tp)Pd^{IV}(Aryl)(CF₃)(Cl)

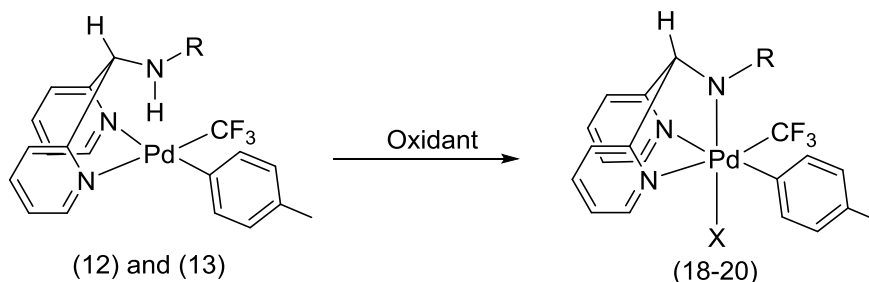


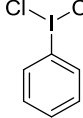
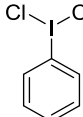
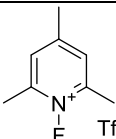
Quantitative reductive elimination of chlorotoluene (**17**) was observed when ligand exchange was attempted by treatment of **15** with 1 equivalent of trimethylsilyl triflate (TMSOTf) in CDCl₃ solution at room temperature (Scheme 2.7). Apparently,

instead of chloride, Tp hydride was abstracted and *in situ* formed cationic Pd^{IV} intermediate such as **16** underwent facile C–Cl bond forming reductive elimination. The high thermal stability of **15** is likely tied to the low lability of the Cl ligand, since ligand dissociation is the first step of many reductive elimination reactions from Pd^{IV} centers.

We reasoned that unsymmetrical *fac*-tridentate ligands **2** and **3** containing a stronger σ -donor than pyrazole might enhance the reactivity of Pd^{IV} complexes towards X-type ligand abstraction. Thus we next investigated oxidation of previously obtained Pd^{II} complexes **12** and **13** (Table 2.1).

Table 2.1 Preparation of (*fac*-L₂X)Pd^{IV}(Aryl)(CF₃)(Cl) complexes



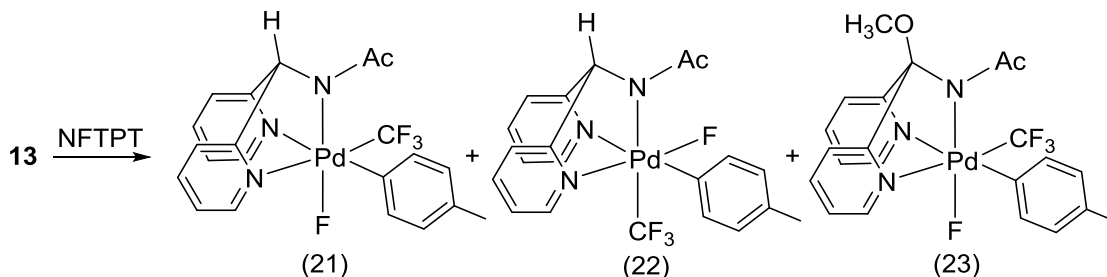
Entry	R (Complex)	Oxidant	X	Yield (Product)
1	<i>p</i> - ^t BuC ₆ H ₄ SO ₂ (12)	 (PhICl ₂)	Cl	42% (18)
2	Ac (13)	 (PhICl ₂)	Cl	47% (19)
3	<i>p</i> - ^t BuC ₆ H ₄ SO ₂ (12)	 (NFTPT) TfO ⁻	F	68% (20)

As shown in Table 2.1, the treatment of **12** and **13** with PhICl₂ at room temperature in CH₂Cl₂ afforded **18** (42% yield) and **19** (47% yield), respectively.

Complex **12** also reacted with *N*-fluoro-2,4,6-trimethylpyridinium triflate (NFTPT) to afford the corresponding Pd^{IV} fluoride **20** in 68% yield. In all three of these reactions, a single stereoisomer was detected in both the crude and isolated products. Complexes **18-20** were all purified via column chromatography on silica gel.

In contrast to the reactions in Table 2.1, the oxidation of **13** with NFTPT in CH₂Cl₂ at room temperature afforded two different isomeric products **21** and **22** (Table 2.2). These compounds were purified by an aqueous work-up followed by chromatography on silica gel and were isolated in 40% and 33% yield, respectively. Interestingly, when **13** was treated with NFTPT in CH₂Cl₂ and crude reaction mixture was subjected directly to column chromatography with 10% MeOH in THF as mobile phase, complexes **21** and **23** were isolated in 39% and 24% yield. Moreover, when the reaction solvent was changed from CH₂Cl₂ to MeCN, **21** was obtained as sole reaction product in 53% isolated yield.

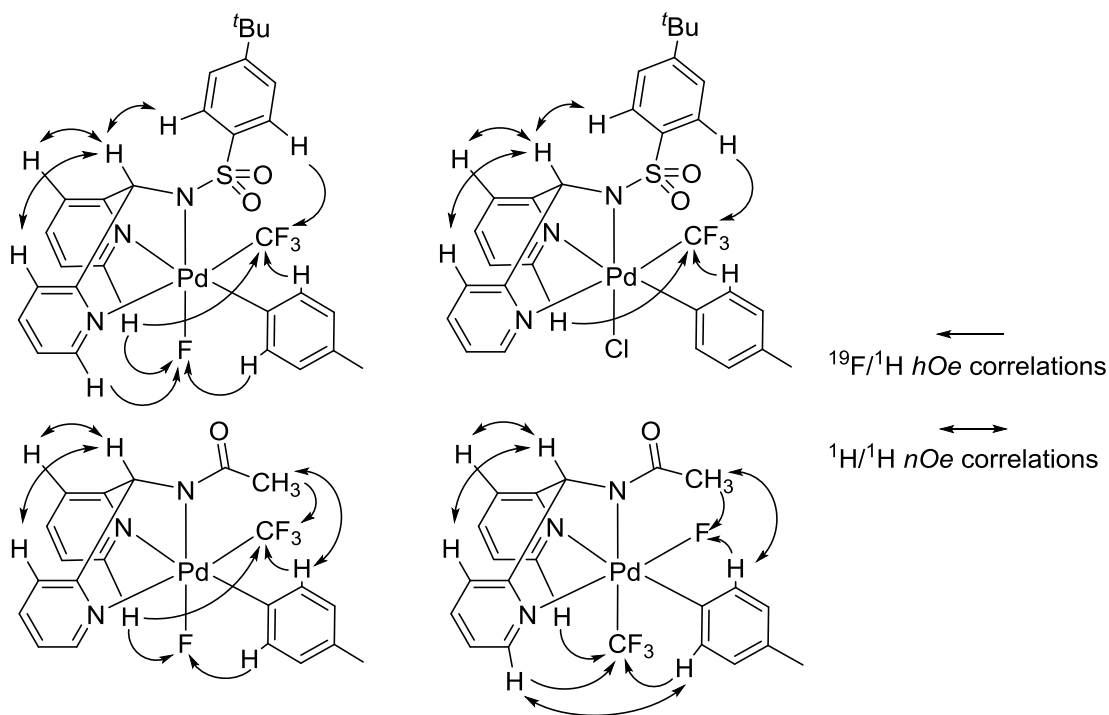
Table 2.2 Reactions of (dpaa)Pd^{II}(Aryl)(CF₃) with NFTPT



Entry	Solvent	Isolated yield of 21 (%)	Isolated yield of 22 (%)	Isolated yield of 23 (%)
1	CH ₂ Cl ₂	40	33	0
2	CH ₂ Cl ₂ /MeOH	39	0	24
3	MeCN	53	0	0

Complexes **18-23** were characterized by ^1H , ^{13}C , and ^{19}F NMR spectroscopy, and all resonances were assigned by 2D ^1H - ^1H COSY, ^1H - ^{13}C HSQC, and ^1H - ^{13}C HMBC NMR experiments. For amide complexes **18**, **20**, **21**, and **22**, the stereochemistry about the Pd^{IV} centers was established via ^{19}F - ^1H HOESY and ^1H - ^1H ROESY NMR experiments. Significant *hOe* and *nOe* correlations are shown in Figure 2.4. The stereochemistry of complex **19** was assigned based on a very similar pattern of ^1H NMR resonances to that of complex **21**.

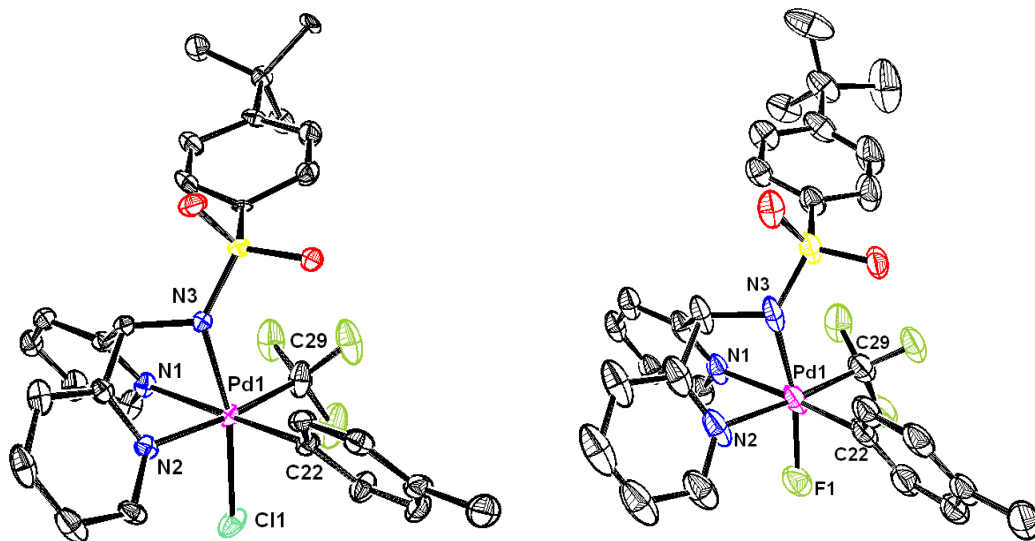
Figure 2.4 Stereochemical assignment for (*fac*- L_2X) Pd^{IV} (Aryl)(CF_3)(X) complexes



The structure and stereochemistry of the Pd^{IV} sulfonamide complexes **18** and **20** were further confirmed by single crystal X-ray diffraction analysis. Crystals of **18** and **20** were obtained by slow diffusion of MTBE into a MeCN solution at $-20\text{ }^\circ\text{C}$. In each case, the solid-state structure was fully consistent with the solution NMR data presented above.

Thermal ellipsoid plots of **18** and **20** are shown in Figure 2.5. Thermal ellipsoids are shown at 50% probability.

Figure 2.5 Thermal ellipsoid plots of (dpsa)Pd^{IV}(Aryl)(CF₃)(X) complexes



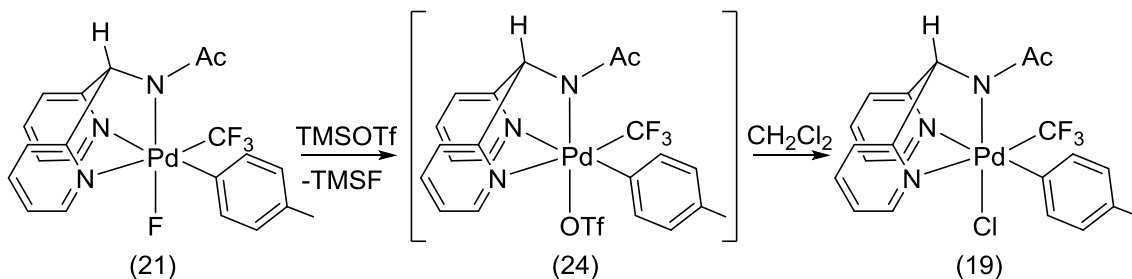
Compounds **18-23** were inert toward carbon–halogen and/or carbon–CF₃ bond forming reductive elimination. For example, they were stable in CDCl₃ solution for at least 2 weeks at room temperature. Complexes **18-23** did decompose after heating at 80 °C for several hours in DMSO solution. However, this transformation yielded an intractable mixture of organic and inorganic products that precluded definitive characterization.

We next examined the reactivity of **18-23** toward ligand substitution. Remarkably, despite the relatively large trans influence of amide X-type ligands,¹⁰ complexes **18-23** showed no reaction upon treatment with 10 equiv of AgOTf or AgBF₄ in CDCl₃ or DMSO-*d*₆ for 2 h at room temperature. In the reactions with Ag salts in CDCl₃, ¹H NMR

spectroscopic analysis of the crude mixtures showed some shifting of the amide ligand resonances; however, quenching with NBu_4I returned only starting material.

In contrast, these complexes did show reactivity with the highly electrophilic reagent TMSOTf. For example, the treatment of **21** with 1 equiv of TMSOTf in CD_2Cl_2 solution at room temperature produced chloride complex **19** in quantitative yield (Scheme 2.8). This transformation presumably occurs via *in situ* generation of complex **24**, which abstracts chloride from a molecule of solvent. Intermediate **24** was not detected by ^1H or ^{19}F NMR spectroscopy in CD_2Cl_2 ; however, when the reaction was conducted in CDCl_3 , this putative intermediate was observed but underwent fast decomposition (over 2 h at room temperature) to a complex mixture of unidentified products.

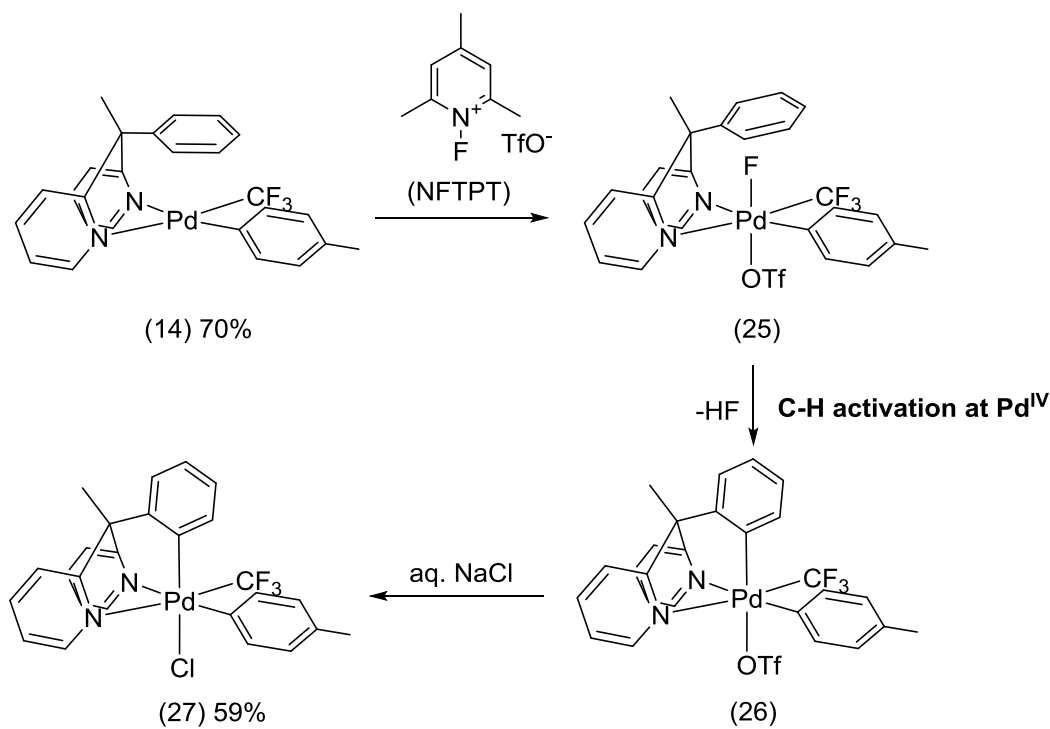
Scheme 2.8 Reaction of $(\text{dpsa})\text{Pd}^{\text{IV}}(\text{Aryl})(\text{CF}_3)(\text{F})$ with TMSOTf



We next pursued complexes containing facial tridentate NNC donor ligands where N = pyridine and C = σ -aryl. The σ -aryl is expected to have a large trans influence,¹⁰ thereby facilitating dissociation of a trans X-type ligand. On the basis of the results discussed above (and prior work from our group),² we reasoned that NFTPT could oxidize **14** to form Pd^{IV} complex **25** (Scheme 2.9). We have also recently shown that

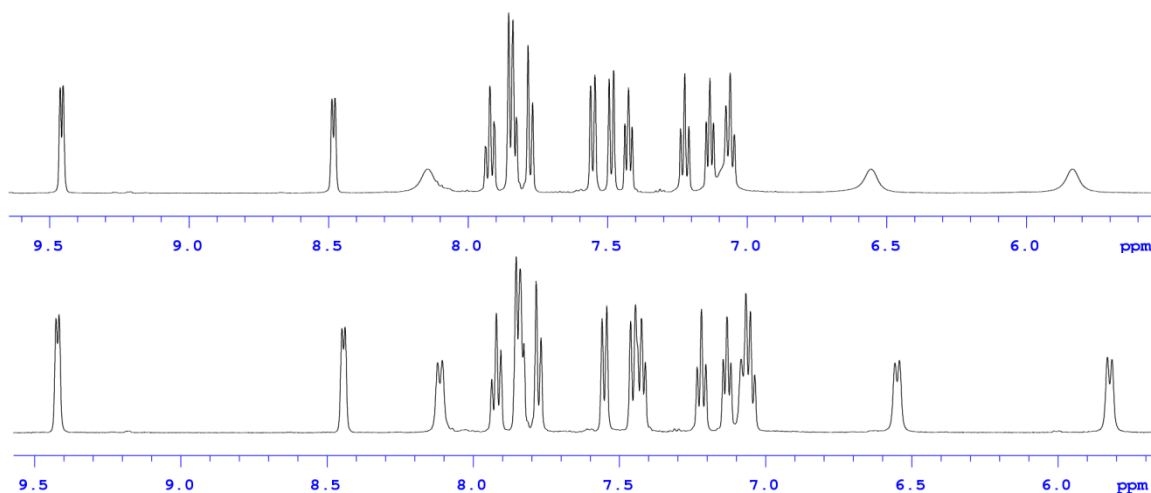
analogues of **25** can undergo intramolecular C–H activation to generate cyclometalated Pd^{IV} species.¹¹ Thus, we hypothesized that **25** might be capable of C–H activation to generate the NNC ligated product **26**. Gratifyingly, the treatment of **14** with NFTPT for 5 min in CH₂Cl₂ at room temperature afforded **26**. Notably, neither **25**, nor any other intermediates were detected in this transformation. An analogue of **14** without a methyl group in the benzylic position of the ligand gave only a complex mixture of products upon oxidation with NFTPT. This observation suggests that very close proximity between Pd and the C–H bond is necessary to achieve C–H activation at Pd^{IV} in this system. The triflate ligand of **26** was highly labile, and washing a CH₂Cl₂ solution of **26** with aqueous NaCl afforded the readily isolable chloride product **27** in 59% yield.

Scheme 2.9 Synthesis of (dpph)Pd^{IV}(Aryl)(CF₃)(Cl)



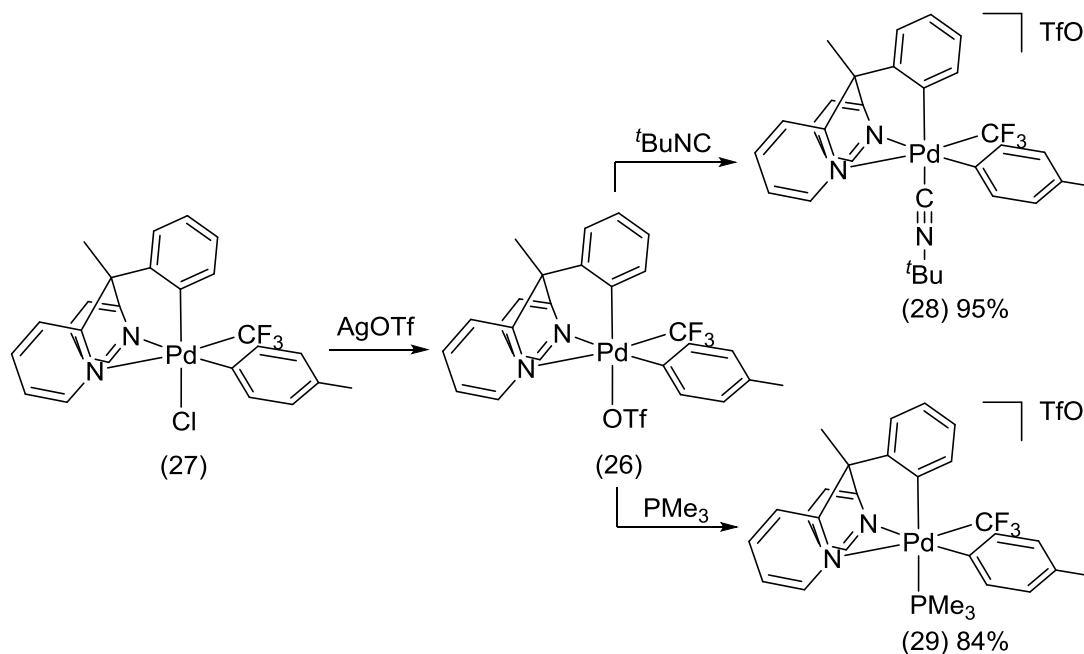
Complex **27** was characterized by ^1H , ^{13}C , and ^{19}F NMR spectroscopy. Interestingly, rotation about the Pd-tolyl bond in **27** is slow on the NMR timescale. At room temperature, four broad but distinct ^1H NMR signals are observed for the aromatic protons of this ligand. When the temperature is lowered to $0\text{ }^\circ\text{C}$, these resonances resolve into four sharp doublets (Figure 2.6).

Figure 2.6 ^1H NMR spectra of $(\text{dpph})\text{Pd}^{\text{IV}}(\text{Aryl})(\text{CF}_3)(\text{Cl})$ (**27**) at $20\text{ }^\circ\text{C}$ and $0\text{ }^\circ\text{C}$



The strongly σ -donating aryl arm of the tridentate ligand rendered this complex highly reactive towards X-type ligand substitution. For example, sonication of **27** with 1.2 equiv of AgOTf for 10 min at room temperature in dichloromethane afforded complex **26** *in situ*. As shown in Scheme 2.10, this compound reacted with *tert*-butylisocyanide to afford **28** in 95% yield and with PMe_3 to generate **29** in 84% yield. Notably, examples of stable phosphine Pd^{IV} complexes like **29** remain rare,¹² while **28** is, to our knowledge, the first example of a Pd^{IV} complex containing an isocyanide ligand.

Scheme 2.10 Reactivity of of (dpph)Pd^{IV}(Aryl)(CF₃)(Cl) with L-type ligands



Chloride complex **27** also underwent facile substitution with X-type ligands. Relatively basic X-type ligands like *p*-nitrophenolate and phthalimide were introduced in high yield by reaction of **27** with the corresponding sodium or potassium salts (Scheme 2.11). Examples of isolable Pd^{IV} phenolate and imide Pd^{IV} complexes remain rare in the literature,¹³ likely because these basic ligands tend to destabilize Pd^{IV} and participate in fast reductive elimination processes. X-ray quality crystals of phthalimide complex **30** were obtained by vapor diffusion of hexanes into a CHCl₃ solution at -20 °C. X-ray structure of **30** is shown in Figure 2.7.

Scheme 2.11 Reactivity of $(\text{dppe})\text{Pd}^{\text{IV}}(\text{Aryl})(\text{CF}_3)(\text{Cl})$ with X-type ligands

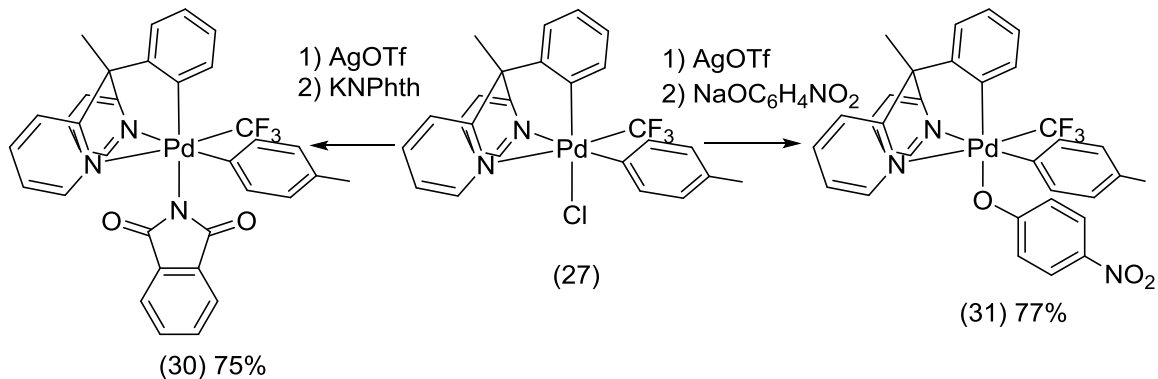
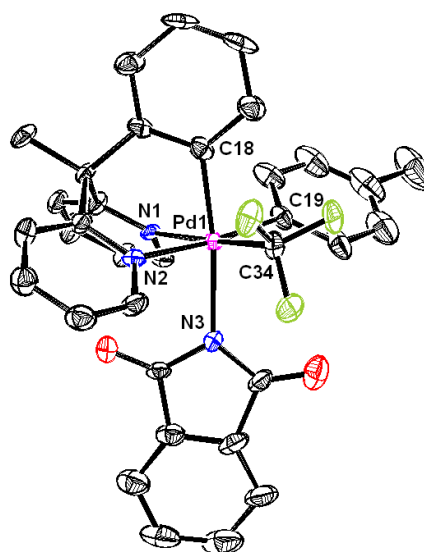


Figure 2.7 Thermal ellipsoid plot of $(\text{dppe})\text{Pd}^{\text{IV}}(\text{Aryl})(\text{CF}_3)(\text{NPhth})$



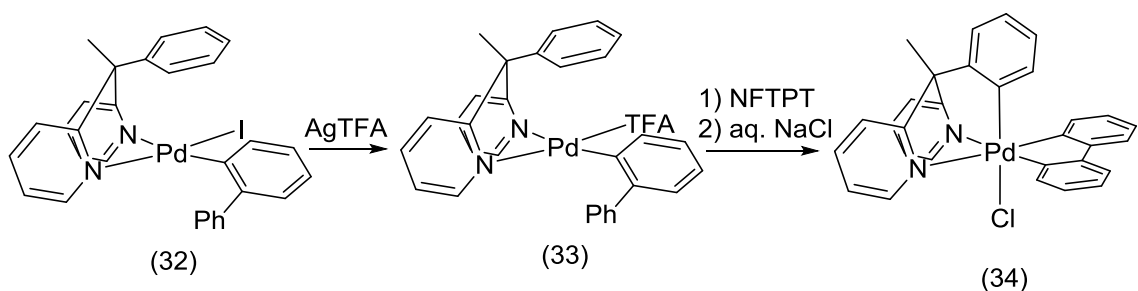
Thermal ellipsoids are shown at 50% probability. H atoms omitted for clarity.

Despite the fast rates of ligand substitution at **27**, this complex is still highly inert towards reductive elimination. For example, **27** was stable for several weeks in CHCl_3 at room temperature. Furthermore, only ~20% decomposition was observed after heating to $110\text{ }^\circ\text{C}$ for 2 h in $\text{DMSO}-d_6$. One possible explanation is that the restricted rotation about the Pd–tolyl bond precludes the complex from assuming the conformation required for

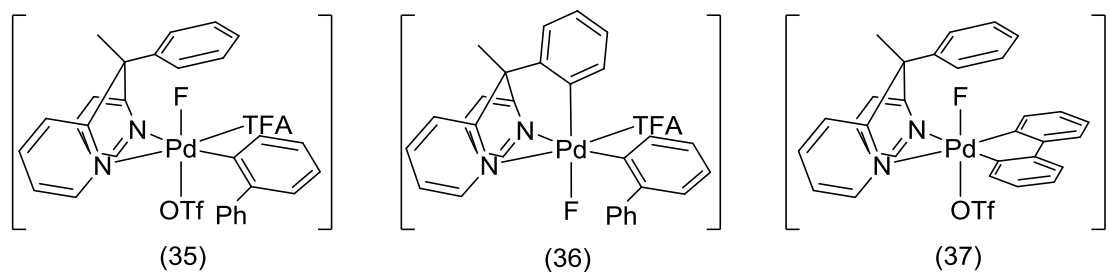
aryl-CF₃ bond-forming reductive elimination. Complexes **28-31** were also stable for several days in CDCl₃ solution at room temperature. When heated above 50 °C, dissociation/decomposition of the labile ligand occurred, and complex mixtures of products were obtained.

A final set of studies focused on the reactivity of these NNC-ligated complexes towards oxidatively induced C-H activation processes. As shown in Scheme 2.12, treatment of *in situ*-generated (dpph)Pd(2-PhC₆H₄)(TFA) (**32**) with NFTPT followed by aqueous NaCl at room temperature resulted in double C-H activation to generate the cyclometalated chloride complex **34**. We propose that this transformation proceeds via intermediates like **35-37**.¹¹ This suggests the possibility that a single Pd^{IV} center can mediate more than one C-H activation event, a type of transformation that could potentially be exploited in catalytic C-C bond-forming reactions.

Scheme 2.12 Preparation of (dpph)Pd^{IV}(biphe)(Cl)



Possible Intermediates



2.5 Conclusions

In summary, this chapter describes the oxidation of a series of Pd^{II} precursors to form Pd^{IV}-aryl products containing *fac*-NNN and *fac*-NNC donor ligands. In all cases, the Pd^{IV} complexes were stable to reductive elimination processes for prolonged periods (at minimum several days) in solution at room temperature. The NNC-ligated Pd^{IV} center participated in facile ligand substitution reactions in which a halide and/or triflate ligand were displaced by phosphine, isocyanide, phenoxide, or phthalimide donors. Furthermore, several examples of oxidatively-induced C–H activation have been demonstrated. These systems add to a growing body of evidence that high oxidation state Pd centers are capable of participating in a diverse set of organometallic reactions beyond simply reductive elimination processes.

2.6 Experimental Section

General Procedures. All syntheses were conducted under a nitrogen atmosphere unless otherwise stated. All reagents were purchased from commercial sources and used as received. Bis(dibenzylideneacetone)palladium was obtained as described in literature.¹⁴ Tetrahydrofuran, dichloromethane and diethyl ether were purified using an Innovative Technologies (IT) solvent purification system consisting of a copper catalyst, activated alumina, and molecular sieves. NMR spectra were acquired using 400, 500 and 700 MHz Varian spectrometers. All ¹H/¹H NOESY and ¹H/¹H ROESY correlation spectra were acquired on a 500 MHz instrument. ¹H, ¹⁹F and ¹³C chemical shifts are reported in parts per million (ppm) relative to TMS, with the residual solvent peak used

as an internal reference. ^1H and ^{19}F multiplicities are reported as follows: singlet (s), doublet (d), triplet (t), quartet (q), broad resonance (br) and multiplet (m).

Preparation of *N*-Di(2-pyridyl)methylacetamide (dpa) (2). To a solution of di(pyridin-2-yl)methylamine (**6**) (0.75 g; 4.05 mmol) in pyridine (5 mL) was added acetic anhydride (1.0 mL). The reaction mixture was stirred at rt for 2 h, then water (1 mL) was added, and stirring was continued for 30 min. The reaction mixture was poured into a saturated aq. NaHCO_3 solution (50 mL), and the resulting solution was extracted with EtOAc (6×50 mL). The combined organic phases were washed with brine (100 mL) and dried over anhydrous MgSO_4 . The volatiles were evaporated under reduced pressure, and the resulting residue was suspended in diethyl ether (15 mL) and collected by filtration. The solid was washed with hexanes and dried under reduced pressure. Yield: 0.74 g (80%) of white crystals. $\text{Mp} = 77\text{-}79$ °C. ^1H NMR (CDCl_3): δ 8.51 (d, $J = 3.6$ Hz, 2H), 7.88 (bs, 1H), 7.60 (t, $J = 7.4$ Hz, 2H), 7.39 (d, $J = 7.6$ Hz, 2H), 7.12 (t, $J = 5.9$ Hz, 2H), 6.19 (d, $J = 6.8$ Hz, 1H), 2.09 (s, 3H). $^{13}\text{C}\{^1\text{H}\}$ NMR (CDCl_3): δ 169.55, 158.88, 149.20, 136.81, 122.45, 122.20, 59.06, 23.36. HRMS electrospray (m/z): $[\text{M} + \text{H}]^+$ calcd for $\text{C}_{13}\text{H}_{14}\text{N}_3\text{O}$, 228.1131; found, 228.1131.

Preparation of 4-*tert*-Butyl-*N*-[di(pyridin-2-yl)methyl]benzenesulfonamide (dpsa) (3). 4-*tert*-Butylbenzenesulfonyl chloride (1.05 g; 4.50 mmol) was added to a solution of di(pyridin-2-yl)methylamine (**6**) (0.75 g; 4.05 mmol) in pyridine (5 mL). The reaction mixture was stirred at rt for 2 h and then water (1 mL) was added. The solution was allowed to stir for 30 min. The reaction mixture was poured into water (100 mL), and the resulting suspension was extracted with EtOAc (100 mL). The organic phase was washed with water (3×50 mL) and brine (100 mL) and dried over anhydrous MgSO_4 .

The solvent was evaporated under reduced pressure and the residue was suspended in hexane (100 mL) and collected by filtration. Yield: 1.20 g (78%) of yellow crystals. Mp = 178 °C. ^1H NMR (CDCl_3): δ 8.41 (d, J = 4.4 Hz, 2H), 7.61 (d, J = 8.5 Hz, 2H), 7.49 (t, J = 6.4 Hz, 2H), 7.24 (multiple peaks, 5H), 7.05 (dd, J = 7.2, 5.0 Hz, 2H), 5.62 (d, J = 6.2 Hz, 1H), 1.23 (s, 9H). $^{13}\text{C}\{^1\text{H}\}$ NMR (CDCl_3): δ 157.84, 155.86, 148.75, 136.87, 136.71, 126.99, 125.59, 122.52, 122.17, 62.08, 34.93, 31.00. HRMS electrospray (m/z): $[\text{M} + \text{H}]^+$ calcd for $\text{C}_{21}\text{H}_{24}\text{N}_3\text{O}_2\text{S}$, 382.1584; found, 382.1584.

Preparation of di-(2-pyridyl)phenylmethane (8). Di-(2-pyridyl)phenylmethane (**8**) was obtained as described in literature.¹⁵

Preparation of 1,1-di(2-pyridyl)phenylethane (dppe) (4). Butyllithium (2.5 M in hexanes, 4.8 mL, 12.0 mmol) was slowly added to a cooled (-78 °C) solution of dipyridylphenylmethane (**8**) (2.50 g; 10.15 mmol) in dry THF (50 mL). The resulting suspension was warmed to -20 °C over the period of 1 h, and then methyl iodide (1.25 mL; 20.0 mmol) was added. The reaction mixture was stirred at rt for 3 h, then the volatiles were removed under reduced pressure. The resulting residue was suspended in diethyl ether, this suspension was filtered, and the filtrate was collected and concentrated under vacuum. The crude product was purified on a silica gel column (mobile phase: hexanes/EtOAc with gradient from 4/1 to 1/1) to yield thick oil that crystallized upon standing. Yield: 2.04 g (77%) of a colorless solid. Mp = 69-71 °C. ^1H NMR (CDCl_3): δ 8.60 (d, J = 4.7 Hz, 2H), 7.55 (td, J = 8.0 and 1.6 Hz, 2H), 7.27 (m, 2H), 7.21 (m, 1H), 7.10 (multiple peaks, 4H), 7.05 (d, J = 8.0 Hz, 2H), 2.30 (s, 3H). $^{13}\text{C}\{^1\text{H}\}$ NMR (CDCl_3): δ 166.48, 148.77, 147.61, 135.85, 128.47, 128.06, 126.21, 123.48, 121.07, 57.56, 28.33. HRMS electrospray (m/z): $[\text{M} + \text{H}]^+$ calcd for $\text{C}_{18}\text{H}_{17}\text{N}_2$, 261.1386; found, 261.1386.

Preparation of (4-MePy)₂Pd(4-MeC₆H₄)(I) (9). Pd(dba)₂ (1.25 g; 2.17 mmol) was added to a solution of 4-iodotoluene (1.20 g; 5.50 mmol) and 4-methylpyridine (2.05 g; 22.0 mmol) in THF (20 mL) at rt. The resulting homogenous solution was stirred at rt. After 15 min, product started to precipitate from solution. The thick suspension was stirred at room temperature for another 30 min, then hexane (30 mL) was added. The precipitate was filtered and washed with diethyl ether (4 × 50 mL) and hexanes (4 × 50 mL). Yield: 1.42 g (64%) of yellow crystals. The crude product contains some minor impurities, but it was used directly in the next step as decomposition was observed during purification attempts. ¹H NMR (CDCl₃): δ 8.69 (d, *J* = 5.9 Hz, 4H), 7.00 (d, *J* = 5.9 Hz, 4H), 6.87 (d, *J* = 7.6 Hz, 2H), 6.66 (d, *J* = 7.6 Hz, 2H), 2.27 (s, 6H), 2.13 (s, 3H). ¹³C{¹H} NMR (CDCl₃): δ 154.49, 153.02, 149.27, 132.82, 132.66, 127.86, 125.57, 21.06, 20.61.

Preparation of (4-MePy)₂Pd(4-MeC₆H₄)(CF₃) (10). Cesium fluoride (1.06 g; 7.0 mmol) was placed in a Schlenk flask and dried under vacuum at 100 °C for 2 h. The flask was then cooled to rt under an atmosphere of nitrogen, (4-MePy)₂Pd(4-MeC₆H₄)(I) (9) (0.75 g; 1.7 mmol) was added, and the flask was then flushed with nitrogen and sealed with a rubber septum. Dry THF (20 mL) and TMSCF₃ (1.1 mL; 7.0 mmol) were added via cannula. The resulting suspension was stirred at rt for 15 min. During this period, the color of the solution changed from yellow to dark green and some Pd black precipitate was observed. The volatiles were removed under reduced pressure at room temperature. The residue was suspended in dichloromethane (40 mL) and filtered through a pad of celite. The solution was evaporated under reduced pressure. The resulting residue was suspended in diethyl ether (10 mL) and collected by filtration. The solid was washed with

ethyl acetate (4 × 3 mL) and dried under reduced pressure. Yield: 0.36 g (54%) of white crystals. ¹H NMR (CDCl₃): δ 8.53 (d, *J* = 5.9 Hz, 2H), 8.14 (d, *J* = 5.9 Hz, 2H), 7.41 (d, *J* = 7.5 Hz, 2H), 7.12 (d, *J* = 5.5 Hz, 2H), 6.94 (d, *J* = 5.5 Hz, 2H), 6.81 (d, *J* = 7.5 Hz, 2H), 2.34 (s, 3H), 2.23 (s, 3H), 2.20 (s, 3H). ¹³C{¹H} NMR (CDCl₃): δ 150.39, 150.04, 149.48 (q, *J* = 9.3 Hz), 149.40, 149.37, 135.96, 134.89 (q, *J* = 364 Hz), 131.36, 127.21, 125.72, 125.66, 21.07, 20.96, 20.94. ¹⁹F NMR (CDCl₃): δ -21.00 (s).

Preparation of (dpsa)Pd^{II}(4-MeC₆H₄)(CF₃) (12). (4-MePy)₂Pd(4-MeC₆H₄)(CF₃) (10) (81 mg; 0.18 mmol) was added to a solution of 4-*tert*-butyl-*N*-[di(pyridin-2-yl)methyl]benzenesulfonamide (3) (80 mg; 0.21 mmol) in EtOAc (2 mL) at rt. The reaction mixture was stirred at rt for 10 min, then filtered through a pad of celite. The volume of the solution was reduced to 1 mL and then hexane (10 mL) was added. The precipitate was collected by filtration, washed with a 1/1 mixture of hexane/diethyl ether (3 × 3 mL), and dried under reduced pressure. Yield: 106 mg (78%) of a white powder. ¹H NMR (CDCl₃): δ 8.80 (multiple peaks, 2H), 8.04 (d, *J* = 4.1 Hz, 1H), 7.68 (d, *J* = 6.9 Hz, 2H), 7.65 (td, *J* = 7.7, 1.5 Hz, 1H), 7.48 (td, *J* = 7.5, 1.5 Hz, 1H), 7.45 (d, *J* = 7.7 Hz, 1H), 7.38 (d, *J* = 6.9 Hz, 2H), 7.21 (d, *J* = 8.3 Hz, 2H), 7.13 (multiple peaks, 2H), 7.04 (t, *J* = 5.6 Hz, 1H), 6.87 (d, *J* = 7.5 Hz, 2H), 5.72 (d, *J* = 9.4 Hz, 1H), 2.23 (s, 3H), 1.21 (s, 9H). ¹³C{¹H} NMR (CDCl₃): δ 156.49, 154.18, 153.48, 153.23, 152.69, 150.01 (q, *J* = 9.5 Hz), 139.41, 138.59, 136.71, 135.70, 134.58 (q, *J* = 364 Hz), 132.41, 127.99, 127.04, 126.99, 125.94, 124.96, 124.70, 124.14, 63.11, 34.97, 30.98, 20.97. ¹⁹F NMR (CDCl₃): δ -20.29 (s). HRMS electrospray (*m/z*): [M - F]⁺ calcd for C₂₉H₃₀F₂N₃O₂PdS, 628.1056; found, 628.1058.

Preparation of (dpaa)Pd^{II}(4-MeC₆H₄)(CF₃) (13). (4-MePy)₂Pd(4-MeC₆H₄)(CF₃) (10) (120 mg; 0.26 mmol) was added to a solution of *N*-di(2-pyridyl)methylacetamide (2) (68 mg; 0.30 mmol) in CH₂Cl₂ (3 mL) at rt. After the solution was stirred at rt for 5 min, it was filtered through a pad of celite. The volume of the CH₂Cl₂ solution was reduced to 1 mL under reduced pressure, and the product was then precipitated with hexanes (15 mL). The precipitate was collected by filtration, washed with diethyl ether (3 × 2 mL) and dried under reduced pressure. Yield: 115 mg (88%) of a white powder. ¹H NMR (CDCl₃): δ 9.07 (d, *J* = 8.7 Hz, 1H), 8.99 (d, *J* = 5.1 Hz, 1H), 8.10 (d, *J* = 5.1 Hz, 1H), 7.86 (td, *J* = 7.8 Hz, 1.1 Hz, 1H), 7.73 (td, *J* = 6.6, 1.1 Hz, 1H), 7.61 (multiple peaks, 2H), 7.40 (t, *J* = 6.6 Hz, 1H), 7.31 (d, *J* = 7.3 Hz, 2H), 7.10 (t, *J* = 6.4 Hz, 1H), 6.88 (d, *J* = 7.3 Hz, 2H), 6.34 (d, *J* = 8.7 Hz, 1H), 2.25 (s, 3H), 2.21 (s, 3H). ¹³C{¹H} NMR (CDCl₃): δ 169.86, 155.34, 154.47, 153.38, 152.76, 150.01 (q, *J* = 9.3 Hz), 139.35, 139.11, 135.74, 134.82 (q, *J* = 363 Hz), 132.39, 127.93, 125.40, 125.12, 124.66, 124.52, 59.62, 23.32, 20.95. ¹⁹F NMR (CDCl₃): -20.39 (s). HRMS electrospray (*m/z*): [M - F]⁺ calcd for C₂₁H₂₀F₂N₃OPd, 474.0604; found, 474.0605.

Preparation of (dpPh)Pd^{II}(4-MeC₆H₄)(CF₃) (14). (4-MePy)₂Pd(4-MeC₆H₄)(CF₃) (10) (300 mg; 0.66 mmol) was added to a solution of 1,1-di(2-pyridyl)phenylethane (dpPh) (4) (182 mg; 0.70 mmol) in EtOAc (15 mL) at rt. After the solution was stirred at rt for 5 min, it was filtered through a pad of celite. The volume of the solution was reduced to 3 mL, and the product then started to crystallize. This suspension was cooled at -20 °C for 2 h, and then the precipitate was collected by filtration, washed with ethyl acetate (3 × 1 mL), and dried under reduced pressure. Yield: 208 mg (60%) of a white powder. The mother liquor was evaporated under reduced pressure. The residue was

suspended in diethyl ether, collected by filtration and dried under reduced pressure to yield another 35 mg (10%) of the product. For complex **10** at room temperature there is a hindered rotation about palladium-tolyl and C-phenyl bonds on a NMR timescale. In order to resolve broad resonances ^1H - and ^{13}C -NMR spectra were measured at 50 °C and 46 °C. ^1H NMR (CDCl_3 at 50 °C): δ 9.09 (d, $J = 4.9$ Hz, 1H), 8.25 (d, $J = 5.3$ Hz, 1H), 7.87 (td, $J = 7.8, 1.5$ Hz, 1H), 7.77 (multiple peaks, 3H), 7.41 (t, $J = 7.6$ Hz, 2H), 7.36 (t, $J = 7.4$ Hz, 1H), 7.33 (t, $J = 6.5$ Hz, 1H), 7.03 (td, $J = 7.2$ Hz, 1.7 Hz, 1H), 6.97 (d, $J = 7.0$ Hz, 2H), 6.78 (d, $J = 7.8$ Hz, 2H), 6.73 (d, $J = 7.6$ Hz, 2H), 2.24 (s, 3H), 2.18 (s, 3H). $^{13}\text{C}\{^1\text{H}\}$ NMR (CDCl_3 at 46 °C): δ 162.24, 160.53, 153.38, 152.78, 151.70 (q, $J = 9.8$ Hz), 148.27, 138.35, 138.10, 135.96, 134.61 (q, $J = 366$ Hz), 131.19, 128.87, 127.87, 127.12, 127.06, 123.04, 122.99, 122.78, 122.54, 57.52, 29.76, 20.91. ^{19}F (CDCl_3 at 25 °C): δ -21.82 (s). HRMS electrospray (m/z): $[\text{M} - \text{F}]^+$ calcd for $\text{C}_{26}\text{H}_{23}\text{F}_2\text{N}_3\text{Pd}$, 507.0859; found, 507.0855.

Preparation of (Tp)Pd^{IV}(4-MeC₆H₄)(CF₃)(Cl) (15). (4-MePy)₂Pd(4-MeC₆H₄)(CF₃) (**10**) (100 mg; 0.22 mmol) was added to the solution of KTp (58 mg; 0.23 mmol) in acetone (10 mL) at rt. The reaction mixture was stirred for 5 min at rt and then triethylamine (25 mg; 0.25 mmol) and iodobenzene dichloride (61 mg; 0.22 mmol) were added. The solution was stirred at rt for 10 min and then the volatiles were removed under reduced pressure. The resulting residue was purified on a silica gel column (mobile phase: hexanes/EtOAc with gradient from 10/1 to 6/1). Yield: 56 mg (49%) of yellow crystals. ^1H NMR (CDCl_3): δ 8.00 (d, $J = 1.4$ Hz, 1H), 7.83 (d, $J = 2.2$ Hz, 1H), 7.71 (d, $J = 2.2$ Hz, 1H), 7.67 (d, $J = 2.2$ Hz, 1H), 7.51 (d, $J = 2.1$ Hz, 1H), 7.33 (d, $J = 1.9$ Hz, 1H), 6.84 (d, $J = 8.6$ Hz, 2H), 6.80 (d, $J = 8.6$ Hz, 2H), 6.31 (multiple peaks, 2H), 6.16 (t, $J =$

2.2 Hz, 1H), 4.1-5.0 (br, 1H), 2.30 (s, 3H). $^{13}\text{C}\{^1\text{H}\}$ NMR (CDCl_3): δ 149.35 (q, $J = 2.2$ Hz), 142.15 (q, $J = 2.1$ Hz), 141.40, 141.36, 136.62, 136.08, 134.96, 134.89, 134.75, 129.01, 114.25 (q, $J = 376$ Hz), 106.81, 106.32, 106.10, 20.40. ^{19}F NMR (CDCl_3): δ -17.30 (s). ^{11}B NMR (CDCl_3): δ -3.44 (d, $J = 74$ Hz). HRMS electrospray (m/z): $[\text{M} - \text{Cl} + \text{MeCN}]^+$ calcd for $\text{C}_{19}\text{H}_{20}\text{BF}_3\text{N}_7\text{Pd}$, 520.0855; found 520.0849.

Preparation of (dpsa)Pd^{IV}(4-MeC₆H₄)(CF₃)(Cl) (18). Iodobenzene dichloride (60 mg; 0.22 mmol) was added to a solution of (dpsa)Pd^{II}(4-MeC₆H₄)(CF₃) (12) (130 mg; 0.20 mmol) in MeCN (4 mL) at rt. The reaction mixture was stirred at rt for 15 min and then the volatiles were removed under reduced pressure. The crude product was purified on a silica gel column (mobile phase: hexane/EtOAc = 1/1). Fractions containing pure product (TLC control) were evaporated under reduced pressure. The resulting residue was dissolved in dichloromethane (~0.5 mL), and the product was precipitated with the addition of hexane (20 mL). The precipitate was collected by filtration, washed with diethyl ether and dried under reduced pressure. Yield: 57 mg (42%) of a yellow powder. ^1H NMR (CDCl_3): δ 9.01 (d, $J = 5.2$ Hz, 1H), 8.57 (d, $J = 5.2$ Hz, 1H), 7.83 (td, $J = 7.8$, 1.0 Hz, 1H), 7.79 (td, $J = 7.6$, 1.0 Hz, 1H), 7.64 (d, $J = 7.7$ Hz, 1H), 7.55 (d, $J = 8.4$ Hz, 2H), 7.50 (d, $J = 7.7$ Hz, 1H), 7.38 (t, $J = 6.5$ Hz, 1H), 7.28 (t, $J = 6.4$ Hz, 1H), 7.24 (d, $J = 8.4$ Hz, 2H), 7.22 (d, $J = 8.6$ Hz, 2H), 6.82 (d, $J = 8.6$ Hz, 2H), 6.14 (s, 1H), 2.26 (s, 3H), 1.24 (s, 9H). $^{13}\text{C}\{^1\text{H}\}$ NMR (CDCl_3): δ 158.69, 157.62, 154.63, 149.79, 149.76, 146.96, 140.67, 140.30, 139.66, 135.70, 135.52, 129.11, 126.60, 125.22, 124.48, 124.14, 120.66, 120.59, 115.03 (q, $J = 378$ Hz), 74.80, 34.83, 31.08, 20.42. ^{19}F NMR (CDCl_3): δ -11.90 (s). HRMS electrospray (m/z): $[\text{M} + \text{Na}]^+$ calcd for $\text{C}_{29}\text{H}_{29}\text{ClF}_3\text{N}_3\text{NaO}_2\text{PdS}$, 704.0548; found, 704.0548.

Preparation of (dpaa)Pd^{IV}(4-MeC₆H₄)(CF₃)(Cl) (19). Iodobenzene dichloride (77 mg; 0.28 mmol) was added to a solution of (dpaa)Pd^{II}(4-MeC₆H₄)(CF₃) (13) (110 mg; 0.22 mmol) in acetonitrile (5 mL) at rt. The reaction mixture was stirred at rt for 20 min, then solvent was removed under reduced pressure. The residue was purified on a silica gel column that was eluted first with ethyl acetate, then with THF, and finally with 10% methanol in THF. Fractions that contained pure product (TLC control) were evaporated under reduced pressure, and the resulting residue was dissolved in diethyl ether (20 mL). This solution was filtered through a cotton plug, and the volume of the solution was reduced to 10 mL. The product was then precipitated with hexanes (30 mL), collected by filtration, washed with hexanes, and dried under reduced pressure. Yield: 55 mg (47%) of an orange powder. ¹H NMR (CDCl₃): δ 9.03 (d, *J* = 5.0 Hz, 1H), 8.49 (d, *J* = 5.3 Hz, 1H), 7.87 (multiple peaks, 2H), 7.73 (multiple peaks, 2H), 7.43 (t, *J* = 6.0 Hz, 1H), 7.25 (multiple peaks, 2H), 6.95 (broad d, *J* = 8.1 Hz, 2H), 6.79 (d, *J* = 8.1 Hz, 2H), 2.25 (s, 3H), 1.69 (s, 3H). ¹³C{¹H} NMR (CDCl₃): δ 175.06, 158.16, 158.10, 149.75, 149.49, 148.94 (q, *J* = 2.9 Hz), 140.43, 140.17, 135.76, 135.55, 129.15, 124.40, 124.19, 121.66, 121.32, 116.42 (q, *J* = 376 Hz), 71.72, 24.89 (q, *J* = 2.7 Hz), 20.40. ¹⁹F NMR (CDCl₃): δ -13.08 (s). HRMS electrospray (m/z): [M + H]⁺ calcd for C₂₁H₂₀ClF₃N₃OPd, 528.0276; found, 528.0269.

Preparation of (dpsa)Pd^{IV}(4-MeC₆H₄)(CF₃)(F) (20). NFTPT (64 mg; 0.22 mmol) was added to a solution of complex 12 (130 mg; 0.20 mmol) in MeCN (3 mL) at rt. The reaction mixture was stirred at rt for 15 min. The volatiles were removed under reduced pressure. The resulting residue was dissolved in CH₂Cl₂ (15 mL), and this solution was washed with water (4 × 15 mL), dried over anhydrous Na₂SO₄, and evaporated under

reduced pressure. The crude product was purified on a silica gel column that was eluted first with ethyl acetate and then with THF. Fractions containing pure product (TLC control) were evaporated under reduced pressure. The resulting residue was dissolved dichloromethane (0.5 mL), and the product was precipitated with the addition of hexane (20 mL). This precipitate was collected by filtration, washed with diethyl ether and dried under reduced pressure. Yield: 91 mg (68%) of a yellow powder. ^1H NMR (CDCl_3): δ 8.82 (d, $J = 5.1$ Hz, 1H), 8.30 (d, $J = 5.2$ Hz, 1H), 7.70 (d, $J = 8.8$ Hz, 2H), 7.67 (td, $J = 6.7, 1.5$ Hz, 1H), 7.60 (multiple peaks, 3H), 7.50 (td, $J = 7.7, 1.3$ Hz, 1H), 7.28 (t, $J = 6.8$ Hz, 1H), 7.24 (d, $J = 8.8$ Hz, 2H), 7.12 (t, $J = 6.4$ Hz, 1H), 6.90 (d, $J = 8.6$ Hz, 2H), 6.26 (d, $J = 5.4$ Hz, 1H), 2.28 (s, 3H), 1.22 (s, 9H). $^{13}\text{C}\{^1\text{H}\}$ NMR (CDCl_3): δ 157.94, 157.10, 155.10, 150.88 (m), 149.27, 148.23, 140.07, 139.52, 136.07, 131.58, 131.53, 129.08, 127.09, 125.28, 124.18, 124.02, 121.64, 121.08, 114.69 (q, $J = 378$ Hz), 74.26, 34.86, 31.07, 20.51. ^{19}F NMR (CDCl_3): δ -20.44 (d, $J = 4.8$ Hz), -285.11 (br. m). HRMS electrospray (m/z): $[\text{M} + \text{H}]^+$ calcd for $\text{C}_{29}\text{H}_{30}\text{F}_4\text{N}_3\text{O}_2\text{PdS}$, 666.1024; found, 666.1021.

Preparation of (dpaa)Pd^{IV}(4-MeC₆H₄)(CF₃)(F) (21) and (22). (dpaa)Pd^{II}(4-MeC₆H₄)(CF₃) (13) (58 mg; 0.12 mmol) was dissolved in CH_2Cl_2 (4 mL) and NFTPT (38 mg; 0.13 mmol) was added at rt. The reaction mixture was stirred at rt for 20 min. The CH_2Cl_2 solution was then washed with water (4×5 mL), dried over anhydrous Na_2SO_4 , filtered, and evaporated under reduced pressure. ^1H -NMR and ^{19}F -NMR analysis of the crude residue showed the presence of two Pd(IV) complexes in an approximately 2:1 ratio. These compounds were separated by preparative TLC (mobile phase: 10% methanol in THF) to yield the major isomer **21** (24 mg 40%) and minor isomer **22** (20

mg; 33%) as yellow powders. When oxidation was conducted in acetonitrile only **21** isomer was formed (53% isolated yield).

Analytical data for 21: ^1H NMR (CDCl_3): δ 9.01 (d, $J = 5.4$ Hz, 1H), 8.25 (d, $J = 5.4$ Hz, 1H), 7.91 (multiple peaks, 2H), 7.74 (multiple peaks, 2H), 7.48 (t, $J = 5.4$ Hz, 1H), 7.27 (t, $J = 6.1$ Hz, 1H), 7.14 (d, $J = 5.4$ Hz, 1H; coupled with F), 7.09 (multiple peaks, 2H), 6.90 (d, $J = 7.8$ Hz, 2H), 2.32 (s, 3H), 1.82 (s, 3H). $^{13}\text{C}\{^1\text{H}\}$ NMR (CDCl_3): δ 175.19 (d, $J = 3.1$ Hz), 157.69, 157.56, 152.01 (m), 149.22, 149.00, 140.46, 140.21, 136.01, 132.34 (d, $J = 6.6$ Hz), 129.05, 124.33, 124.25, 121.80, 121.33, 116.84 (q, $J = 376$ Hz), 71.03, 24.75 (m), 20.51. ^{19}F NMR (CDCl_3): δ -290.85 (m), -23.84 (d, $J = 3.8$ Hz). HRMS electrospray (m/z): $[\text{M} + \text{H}]^+$ calcd for $\text{C}_{21}\text{H}_{20}\text{F}_4\text{N}_3\text{OPd}$, 512.0572; found, 512.0574.

Analytical data for 22: ^1H NMR (CDCl_3): δ 8.98 (d, $J = 5.1$ Hz, 1H), 8.55 (d, $J = 5.5$ Hz, 1H), 8.03 (t, $J = 7.7$ Hz, 1H), 7.89 (t, $J = 7.7$ Hz, 1H), 7.85 (d, $J = 8.0$ Hz, 1H), 7.80 (d, $J = 7.7$ Hz, 1H), 7.26 (multiple peaks, 2H), 7.07 (s, 1H), 6.90 (d, $J = 8.0$ Hz, 2H), 6.81 (multiple peaks, 2H), 2.32 (s, 3H) and 1.43 (s, 3H). $^{13}\text{C}\{^1\text{H}\}$ NMR (CDCl_3): δ 175.94, 161.56, 158.30, 151.35 (m), 151.21 (m), 150.16, 141.64, 140.00, 136.46, 130.67 (d, $J = 16.4$ Hz), 129.50, 125.24, 124.37, 122.80, 122.21, 121.90 (q, $J = 384$ Hz) 69.97, 22.98 (d, $J = 4$ Hz), 20.49. ^{19}F NMR (CDCl_3): δ -312.97 (m), -33.80 (d, $J = 3.2$ Hz). HRMS electrospray (m/z): $[\text{M} + \text{H}]^+$ calcd for $\text{C}_{21}\text{H}_{19}\text{F}_4\text{N}_3\text{OPd}$, 512.0572; found, 512.0570.

Preparation of (MeO-dpaa)Pd^{IV}(4-MeC₆H₄)(CF₃)(F) (23). When the reaction of **13** with NFTPT was carried out under slightly different conditions, compound **23** was formed as a by-product. The procedure that generated **23** is as follows: (dpaa)Pd^{II}(4-

MeC₆H₄)(CF₃) (**13**) (150 mg; 0.30 mmol) was dissolved in CH₂Cl₂ (5 mL), and NFTPT (110 mg; 0.38 mmol) was added. The reaction mixture was stirred at rt for 20 min. The solvent was then removed under reduced pressure, and the crude mixture was purified on a silica gel column that was eluted first with ethyl acetate, then with THF, and finally with 10% methanol in THF. The major isomer **21** eluted first followed by the minor side product **23**. Both products **21** (60 mg; 39%) and **23** (38 mg; 24%) were obtained as yellow powders. Analytical data for **23**: ¹H NMR (CDCl₃): δ 8.88 (d, *J* = 5.2 Hz, 1H), 8.25 (d, *J* = 5.2 Hz, 1H), 7.93 (multiple peaks, 3H), 7.74 (d, *J* = 7.9 Hz, 1H), 7.41 (m, 1H), 7.28 (multiple peaks, 3H), 6.92 (d, *J* = 8.1 Hz, 2H), 3.16 (s, 3H), 2.32 (s, 3H), 1.86 (s, 3H). ¹³C{¹H} NMR (CDCl₃): δ 182.17, 158.95, 158.58, 152.52 (m), 147.98, 147.86, 140.42, 140.11, 135.98, 132.04, 132.00, 129.12, 125.04, 124.50, 121.34, 120.94, 116.81 (q, *J* = 378 Hz), 99.87, 52.69, 26.11 (m), 20.56. ¹⁹F NMR (CDCl₃): δ -284.40 (s), -25.58 (s). HRMS electrospray (*m/z*): [M + H]⁺ calcd for C₂₂H₂₂F₄N₃O₂Pd, 542.0678; found, 542.0678.

Preparation of (dpph)Pd^{IV}(4-MeC₆H₄)(CF₃)(Cl) (27**).** NFTPT (230 mg; 0.80 mmol) was added to a solution of (dpph)Pd^{II}(4-MeC₆H₄)(CF₃) (**14**) (340 mg; 0.64 mmol) in CH₂Cl₂ (30 mL) at rt. The reaction mixture was stirred at rt for 10 min, and then it was washed with water (4 × 15 mL) and brine (2 × 15 mL). The CH₂Cl₂ layer was collected, dried over anhydrous Na₂SO₄, and evaporated under reduced pressure. The resulting residue was suspended in ethyl acetate (5 mL), and the suspended solids were collected by filtration and washed with ethyl acetate (2 × 3 mL). The resulting white powder was dissolved in chloroform (4 mL) from which a crystalline product started to precipitate. This product was collected by filtration and dried under reduced pressure. Yield: 213 mg

(59%) of a white powder. In order to resolve broad resonances, the ^1H - and ^{13}C -NMR spectra were obtained at 0 °C. Rotation around palladium-tolyl bond at room temperature and below is slow on the NMR timescale, so there is a distinct signal for each tolyl CH in both the ^1H - and ^{13}C -NMR spectra. ^1H NMR (CD_2Cl_2 at 0 °C): δ 9.42 (d, $J = 5.4$ Hz, 1H), 8.44 (d, $J = 5.1$ Hz, 1H), 8.12 (d, $J = 7.8$ Hz, 1H), 7.92 (t, $J = 7.7$ Hz, 1H), 7.84 (multiple peaks, 2H), 7.78 (d, $J = 8.1$ Hz, 1H), 7.55 (d, $J = 7.8$ Hz, 1H), 7.44 (multiple peaks, 2H), 7.22 (t, $J = 7.3$ Hz, 1H), 7.13 (t, $J = 6.6$ Hz, 1H), 7.06 (multiple peaks, 2H), 6.55 (d, $J = 7.8$ Hz, 1H), 5.83 (d, $J = 7.7$ Hz, 1H), 2.71 (br. s, 3H), 2.27 (s, 3H). $^{13}\text{C}\{^1\text{H}\}$ NMR (CD_2Cl_2 at 0 °C): δ 159.84 (q, $J = 2.4$ Hz), 157.27, 156.78, 155.57 (q, $J = 3.9$ Hz), 154.20, 152.64, 139.96, 139.88, 137.35, 136.73, 136.47, 134.97, 134.35, 128.22, 128.13, 127.66, 126.20, 126.07 (q, $J = 369$ Hz), 124.84, 123.58, 123.27, 121.58, 121.26, 56.50, 23.24, 20.44. ^{19}F NMR (CD_2Cl_2 at 0 °C): δ -23.89 (s). HRMS electrospray (m/z): $[\text{M} - \text{Cl}]^+$ calcd for $\text{C}_{26}\text{H}_{22}\text{F}_3\text{N}_2\text{Pd}$, 525.0764; found, 525.0763.

Preparation of [(dpph)Pd^{IV}(4-MeC₆H₄)(CF₃)(*t*-BuNC)]OTf (28). A suspension of (dpph)Pd^{IV}(4-MeC₆H₄)(CF₃)(Cl) (27) (110 mg; 0.20 mmol) and silver triflate (62 mg; 0.24 mmol) in CH_2Cl_2 (15 mL) was sonicated for 15 min at rt. The AgCl precipitate was removed by filtration, *tert*-butyl isocyanide (25.0 mg; 0.30 mmol) was added, and the resulting solution was stirred for 3 min. The volatiles were removed under reduced pressure, and the product was suspended in diethyl ether (10 mL), filtered, washed with diethyl ether (3×3 mL), and dried under reduced pressure. Yield: 114 mg (95%) of a white powder. In order to resolve broad resonances, the ^1H - and ^{13}C -NMR spectra were measured at 0 °C. Rotation around the palladium-tolyl bond at room temperature and below is slow on the NMR timescale so there is a distinct signal for each tolyl CH

fragment in both ^1H - and ^{13}C -NMR spectra. Several overlapping signals in the ^{13}C -NMR spectrum were resolved by ^1H - ^{13}C HSQC, ^1H - ^{13}C HMBC, ^{19}F - ^{13}C HSQC, and ^{19}F - ^{13}C HMBC NMR experiments. Because of a very low intensity, the carbon resonance of the CF_3 group could not be observed directly in the ^{13}C -NMR spectrum. This value was extracted from the ^{19}F - ^{13}C HSQC NMR spectrum. ^1H NMR (CDCl_3 at 0°C): δ 8.87 (d, J = 4.9 Hz, 1H), 8.12 (multiple peaks, 4H), 7.93 (d, J = 5.1 Hz, 1H), 7.69 (d, J = 8.1 Hz, 1H), 7.51 (multiple peaks 2H), 7.42 (d, J = 8.1 Hz, 1H), 7.29 (t, J = 6.4 Hz, 1H), 7.22 (t, J = 7.6 Hz, 1H), 7.06 (multiple peaks, 2H), 6.63 (d, J = 8.1 Hz, 1H), 5.81 (d, J = 8.1 Hz, 1H), 2.77 (br, 3H), 2.27 (s, 3H), 1.55 (s, 9H). $^{13}\text{C}\{^1\text{H}\}$ NMR (CDCl_3 at 0°C): δ 159.77, 157.55, 157.17, 152.77, 151.80, 150.83, 142.32, 141.88, 137.18, 136.07 (two overlapping resonances), 135.60 (two overlapping resonances), 133.80, 130.38, 128.89, 128.84, 127.23, 125.84 (shift for the CF_3 group extracted from the ^{19}F - ^{13}C HSQC spectrum), 125.49, 124.71, 124.69, 124.50 (two overlapping resonances), 120.75 (q, J = 321 Hz $\text{CF}_3\text{SO}_2\text{O}^-$), 59.71, 57.41, 29.52, 23.36, 20.72. ^{19}F (CDCl_3 at 0°C): -20.12 (s), -78.28 (s). HRMS electrospray (m/z): $[\text{M} - \text{OTf}]^+$ calcd for $\text{C}_{31}\text{H}_{31}\text{F}_3\text{N}_3\text{Pd}$, 608.1499; found, 608.1500. IR (KBr): ν 3490 (s, br), 2987 (s, br), 2225 (s), 1602 (s), 1561 (w), 1470 (s), 1275 cm^{-1} (s, br).

Preparation of $[(\text{dpph})\text{Pd}^{\text{IV}}(\text{4-MeC}_6\text{H}_4)(\text{CF}_3)(\text{PMe}_3)]\text{OTf}$ (29**).** A suspension of $(\text{dpph})\text{Pd}^{\text{IV}}(\text{4-MeC}_6\text{H}_4)(\text{CF}_3)(\text{Cl})$ (**27**) (110 mg; 0.20 mmol) and silver triflate (62 mg; 0.24 mmol) in CH_2Cl_2 (15 mL) was sonicated for 15 min at rt. The AgCl precipitate was removed by filtration, PMe_3 (50.0 mg; 0.66 mmol) was added, and the resulting solution was stirred for 3 min. The volatiles were removed under reduced pressure, and the product was suspended in diethyl ether (10 mL). The suspended solids were collected by

filtration, washed with diethyl ether (3×3 mL), and dried under reduced pressure. Yield: 124 mg (84%) of a white powder. ^1H NMR (CD_2Cl_2): δ 8.86 (d, $J = 5.4$ Hz, 1H), 8.18 (multiple peaks, 4H), 8.08 (d, $J = 5.6$ Hz, 1H), 7.32 (t, $J = 6.1$ Hz, 1H), 7.58 (multiple peaks, 2H), 7.48 (dd, $J = 9.6, 8.4$ Hz, 1H), 7.40 (t, $J = 6.2$ Hz, 1H), 7.25 (t, $J = 7.5$ Hz, 1H), 7.17 (dd, $J = 8.2, 1.9$ Hz, 1H), 7.09 (m, 1H), 6.78 (d, $J = 7.9$ Hz, 1H), 6.09 (d, $J = 7.9$ Hz, 1H), 2.82 (br. s, 3H), 2.34 (s, 3H), 1.11 (d, $J = 8.8$ Hz, 9H). $^{13}\text{C}\{^1\text{H}\}$ NMR (CD_2Cl_2): δ 163.27 (d, $J = 133.5$ Hz), 158.78, 158.10, 153.77, 151.42 (d, $J = 3.4$ Hz), 150.87 (d, $J = 4.1$ Hz), 142.12, 141.88, 137.19, 136.48 (d, $J = 13.6$ Hz), 136.24, 135.86, 134.32, 130.22, 128.87, 128.58 (d, $J = 10.9$ Hz), 127.47 (shift for the CF_3 group extracted from the $^{19}\text{F}/^{13}\text{C}$ ASAPHMQC spectrum), 126.87, 125.48 (d, $J = 9.5$ Hz), 124.70, 124.51, 124.34, 124.17, 120.97 (q, $J = 321.5$ Hz), 57.31, 23.78, 20.31, 13.45 (d, $J = 19.1$ Hz). ^{19}F NMR (CDCl_3): δ -18.11 (d, $J = 20.7$ Hz), -76.88 (s). $^{31}\text{P}\{^1\text{H}\}$ NMR (CD_2Cl_2): -16.38 (q, $J = 20.8$ Hz). HRMS electrospray (m/z): $[\text{M} - \text{OTf}]^+$ calcd for $\text{C}_{29}\text{H}_{31}\text{F}_3\text{N}_2\text{PPd}$, 601.1206; found, 601.1196.

Preparation of $[(\text{dpph})\text{Pd}^{\text{IV}}(4\text{-MeC}_6\text{H}_4)(\text{CF}_3)(\text{NPhth})]$ (30). A suspension of $(\text{dpph})\text{Pd}^{\text{IV}}(4\text{-MeC}_6\text{H}_4)(\text{CF}_3)(\text{Cl})$ (**27**) (50.0 mg; 0.089 mmol) and silver triflate (29 mg; 0.11 mmol) in CH_2Cl_2 (15 mL) was sonicated for 15 min at rt. The AgCl precipitate was removed by filtration, and the resulting CH_2Cl_2 solution was washed with solution of potassium phthalimide (74 mg; 0.40 mmol) in water (2 mL). The CH_2Cl_2 solution was then washed with water (3×5 mL) and dried over anhydrous Na_2SO_4 . The solvent was removed under reduced pressure, and the product was suspended in diethyl ether (10 mL). The suspended solids were collected by filtration, washed with diethyl ether (3×3 mL), and dried under reduced pressure. Yield: 45 mg (75%) of a white powder. In order

to resolve broad resonances, the ^1H - and ^{13}C -NMR spectra were measured at $-51\text{ }^\circ\text{C}$. Rotation around palladium-tolyl and palladium-NPhth bond at $-51\text{ }^\circ\text{C}$ is slow on the NMR timescale, so there is a distinct signal for each tolyl and NPhth atom in both ^1H - and ^{13}C -NMR spectra. ^1H NMR (CDCl_3 at $-51\text{ }^\circ\text{C}$): δ 9.37 (d, $J = 8.3$ Hz, 1H), 8.89 (d, $J = 5.1$ Hz, 1H), 8.08 (d, $J = 5.1$ Hz, 1H), 7.92 (multiple peaks, 2H), 7.84 (multiple peaks, 2H), 7.78 (d, $J = 7.3$ Hz, 1H), 7.56 (d, $J = 8.1$ Hz, 1H), 7.52 (t, $J = 7.2$ Hz, 1H), 7.43 (d, $J = 8.1$ Hz, 1H), 7.28 (t, $J = 7.2$ Hz, 1H), 7.10-7.22 (multiple peaks, 4H), 7.02 (t, $J = 7.5$ Hz, 1H), 6.96 (t, $J = 6.4$ Hz, 1H), 6.40 (d, $J = 8.3$ Hz, 1H), 5.55 (d, $J = 8.3$ Hz, 1H), 2.96 (t, $J = 12.5$ Hz, 1H), 2.78 (t, $J = 12.8$ Hz, 1H), 2.71 (t, $J = 12.6$ Hz, 1H), 2.22 (s, 3H). $^{13}\text{C}\{^1\text{H}\}$ NMR (CDCl_3 at $-51\text{ }^\circ\text{C}$): δ 180.67, 180.52, 159.04, 156.40, 156.21, 155.66, 153.40, 150.28, 140.02 (two overlapping signals as evident in the $^1\text{H}/^{13}\text{C}$ ASAPHMQC spectrum), 139.72, 139.50, 138.27, 137.06, 135.63, 134.32, 134.21, 132.06, 131.68, 128.04, 128.01, 127.82, 125.98, 125.59 (shift for the CF_3 group extracted from the $^{19}\text{F}/^{13}\text{C}$ ASAPHMQC spectrum), 124.68, 123.81 (two overlapping signals as evident in the $^1\text{H}/^{13}\text{C}$ ASAPHMQC spectrum), 123.36, 121.89, 121.52, 120.76, 56.78, 24.00, 20.98. ^{19}F NMR (CDCl_3 at $-51\text{ }^\circ\text{C}$): δ -23.03 (s). HRMS electrospray (m/z): $[\text{M} - \text{NPhth}]^+$ calcd for $\text{C}_{26}\text{H}_{22}\text{F}_3\text{N}_2\text{Pd}$, 525.0764; found, 525.0769.

Preparation of $[(\text{dpph})\text{Pd}^{\text{IV}}(4\text{-MeC}_6\text{H}_4)(\text{CF}_3)(4\text{-NO}_2\text{-C}_6\text{H}_4\text{O})]$ (31). A suspension of $(\text{dpph})\text{Pd}^{\text{IV}}(4\text{-MeC}_6\text{H}_4)(\text{CF}_3)(\text{Cl})$ (**27**) (55 mg; 0.10 mmol) and silver triflate (33 mg; 0.13 mmol) in CH_2Cl_2 (15 mL) was sonicated for 15 min at rt. The AgCl precipitate was removed by filtration, and the resulting CH_2Cl_2 solution was washed with solution of sodium 4-nitrophenolate (21 mg; 0.13 mmol) in water (2 mL). The CH_2Cl_2 solution was then washed with water (5×5 mL) and dried over anhydrous Na_2SO_4 . The

solvent was removed under reduced pressure, and the product was suspended in diethyl ether (10 mL). The suspended solids were collected by filtration, washed with diethyl ether (3 × 3 mL), and dried under reduced pressure. Yield: 50 mg (77%) of a yellow powder. In order to resolve broad resonances, the ¹H- and ¹³C-NMR spectra were measured at -27 °C and -21 °C, respectively. Rotation around palladium-tolyl bond at room temperature and below is slow on the NMR timescale so there is a distinct signal for each tolyl CH fragment in both ¹H- and ¹³C-NMR spectra. ¹H NMR (CD₂Cl₂ at -27 °C): δ 8.94 (d, *J* = 5.3 Hz, 1H), 8.32 (d, *J* = 8.1 Hz, 1H), 7.97 (multiple peaks, 2H), 7.89 (d, *J* = 8.1 Hz, 1H), 7.83 (t, *J* = 7.5 Hz, 1H), 7.64 (d, *J* = 5.2 Hz, 1H), 7.55 (d, *J* = 7.9 Hz, 1H), 7.52 (d, *J* = 7.9 Hz, 1H), 7.46 (d, *J* = 9.1 Hz, 2H), 7.29 (t, *J* = 6.6 Hz, 1H), 7.24 (t, *J* = 7.2 Hz, 1H), 7.20 (d, *J* = 7.9 Hz, 1H), 7.10 (t, *J* = 7.4 Hz, 1H), 6.87 (t, *J* = 6.4 Hz, 1H), 6.62 (d, *J* = 7.6 Hz, 1H), 5.99 (d, *J* = 7.9 Hz, 1H), 5.33 (d, *J* = 8.9 Hz, 2H), 2.73 (br. s, 3H), 2.29 (s, 3H). ¹³C{¹H} NMR (CD₂Cl₂ at -21 °C): δ 178.23, 159.18, 158.99, 158.75, 156.74, 154.37, 153.29, 142.45, 142.38, 138.68, 137.99, 137.71, 136.99, 136.14, 135.54, 130.68, 130.57, 130.16, 128.24, 127.99, 126.86, 126.77 (shift for the CF₃ group extracted from the ¹⁹F/¹³C ASAPHMQC spectrum), 125.96, 125.67, 124.22, 123.93, 121.50, 58.62, 24.97, 22.50. ¹⁹F NMR (CD₂Cl₂ at -21 °C): δ -29.67 (s). HRMS electrospray (*m/z*): [M - NO₂C₆H₄O]⁺ calcd for C₂₆H₂₂F₃N₂Pd, 525.0764; found, 525.0771.

Preparation of (dpph)Pd^{II}(2-PhC₆H₄)(I) (32). Pd(dba)₂ (316 mg; 0.66 mmol) was added to a solution of 2-iodobiphenyl (390 mg; 1.40 mmol) and 4-*tert*-butylpyridine (300 mg; 2.2 mmol) in THF (12 mL) at rt. The resulting homogenous solution was stirred at rt for 1 h, and then 1,1-di-(2-pyridyl)phenylethane (dpph) (**6**) (364 mg; 1.40 mmol) was added. The reaction mixture was stirred for 5 min and then filtered through a pad of

celite. The volatiles were removed under reduced pressure. The resulting residue was suspended in hexanes (30 mL), and the suspended solids were collected by filtration and washed with diethyl ether (5×15 mL). The crude product was obtained as a yellowish powder (387 mg; 46%) and it was typically used without further purification. A sample for characterization was obtained by crystallization from ethyl acetate. Rotation around C-phenyl bond is slow on the NMR timescale at room temperature. In order to resolve broad resonances, the ^1H - and ^{13}C -NMR spectra were measured at 46 °C. ^1H NMR (CDCl_3 at 46 °C): δ 9.52 (d, $J = 4.5$ Hz, 1H), 8.47 (d, $J = 6.2$ Hz, 2H), 8.04 (d, $J = 5.2$ Hz, 1H), 7.83 (t, $J = 7.6$ Hz, 1H), 7.73 (multiple peaks, 2H), 7.68 (d, $J = 7.2$ Hz, 1H), 7.40 (multiple peaks, 5H), 7.28 (t, $J = 6.6$ Hz, 1H), 7.21 (multiple peaks, 2H), 6.96 (dd, $J = 5.3, 9.1$ Hz, 1H), 6.84 (t, $J = 7.2$ Hz, 1H), 6.74 (bs, 2H), 6.62 (t, $J = 6.9$ Hz, 1H), 6.52 (br. s, 1H), 2.19 (s, 3H). $^{13}\text{C}\{^1\text{H}\}$ NMR (CDCl_3 at 46 °C): δ 161.80, 159.86, 155.36, 153.03, 148.03, 145.31, 144.77, 142.47, 138.66, 137.97, 137.76, 130.59, 129.46, 129.28, 128.95, 127.43, 127.32, 126.07, 123.59, 123.40, 123.25, 123.17, 123.11, 122.45, 57.89, 30.30. HRMS electrospray (m/z): $[\text{M} - \text{I}]^+$ calcd for $\text{C}_{30}\text{H}_{25}\text{N}_2\text{Pd}$, 519.1047; found, 519.1052.

Preparation of (dpph)Pd^{IV}(biphe)(Cl) (34). Silver trifluoroacetate (77 mg; 0.35 mmol) was added to a solution of (dpph)Pd^{II}(2-PhC₆H₄)(I) (**32**) (200 mg; 0.31 mmol) in CH_2Cl_2 (10 mL) at rt. The reaction mixture was stirred at rt for 15 min, and then this mixture was filtered through a pad of celite. The volume of the solution was reduced to 15 mL. NFTPT (116 mg; 0.4 mmol) was added, and the reaction was stirred at room temperature for 15 min. The reaction mixture was then washed with water (3×10 mL) and brine (2×10 mL), dried over anhydrous Na_2SO_4 , and concentrated under reduced pressure. The resulting residue was dissolved in minimal amount of CH_2Cl_2 and

filtered through a plug of silica gel that had been pre-equilibrated with a 1/1 mixture of MeOH and CH₂Cl₂. The filtrate was collected and evaporated under reduced pressure, and the resulting residue was suspended in ethyl acetate (5 mL), and the suspended solids were collected by filtration, washed with ethyl acetate (3 × 3 mL), and dried under vacuum. Yield: 89 mg (52%) of a white powder. ¹H NMR (CD₂Cl₂): δ 9.26 (dd, *J* = 5.5, 1.7 Hz, 2H), 7.95 (td, *J* = 7.7, 1.7 Hz, 2H), 7.88 (d, *J* = 8.3 Hz, 2H), 7.74 (dd, *J* = 7.6 Hz, 1.6 Hz, 2H), 7.54 (dd, *J* = 7.9, 1.2 Hz, 1H), 7.48 (t, *J* = 4.5 Hz, 2H), 7.20 (t, *J* = 7.4 Hz, 2H), 7.00 (t, *J* = 5.3 Hz, 1H), 6.83 (td, *J* = 7.4, 1.4 Hz, 2H), 6.73 (d, *J* = 7.9 Hz, 2H), 6.64 (t, *J* = 5.4 Hz, 1H), 6.46 (dd, *J* = 7.9, 1.2 Hz, 1H), 2.77 (s, 3H). ¹³C{¹H} NMR (CD₂Cl₂): δ 169.60, 157.85, 152.98, 151.22, 149.69, 139.49, 137.28, 136.60, 130.57, 126.84, 125.97, 125.25, 125.12, 124.75, 123.67, 123.11, 121.15, 56.24, 23.40. HRMS electrospray (m/z): [M + Na]⁺ calcd for C₃₀H₂₃ClN₂NaPd, 575.0477; found 575.0479.

X-ray structure determination for (dpph)Pd^{II}(4-MeC₆H₄)(CF₃) (14). Colorless needles of **14** were grown from an ethyl acetate solution of the compound at 23 deg. C. A crystal of dimensions 0.14 x 0.10 x 0.09 mm was mounted on a Rigaku AFC10K Saturn 944+ CCD-based X-ray diffractometer equipped with a low temperature device and Micromax-007HF Cu-target micro-focus rotating anode ($\lambda = 1.54187$ Å) operated at 0.2 kW power (20 kV, 10 mA). The X-ray intensities were measured at 85(1) K with the detector placed at a distance 42.00 mm from the crystal. A total of 1561 images were collected with an oscillation width of 2.0° in ω . The exposure time was 20 sec. for the low angle images, 45 sec. for high angle. The integration of the data yielded a total of 23642 reflections to a maximum 2θ value of 136.46° of which 3880 were independent

and 3814 were greater than $2\sigma(I)$. The final cell constants were based on the xyz centroids of 22979 reflections above $10\sigma(I)$. Analysis of the data showed negligible decay during data collection; the data were processed with CrystalClear 2.0 and corrected for absorption. The structure was solved and refined with the Bruker SHELXTL (version 2008/4) software package, using the space group $P1\bar{1}$ with $Z = 2$ for the formula $C_{26}H_{23}N_2F_3Pd, 2(C_{24}H_{20}B)$. Full matrix least-squares refinement based on F^2 converged at $R1 = 0.0173$ and $wR2 = 0.0425$ [based on $I > 2\sigma(I)$], $R1 = 0.0176$ and $wR2 = 0.0427$ for all data. There is a minor substitutional site disorder of the $-CF_3$ group bonded to palladium, which was refined as the contribution of 6.0% iodide. Additional details are presented below.

Crystal data and structure refinement for **14**.

Identification code	am352
Empirical formula	$C_{25.94} H_{23} F_{2.82} I_{0.06} N_2 Pd$
Formula weight	529.95
Temperature	85(2) K
Wavelength	1.54178 Å
Crystal system, space group	Triclinic, $P-1$
Unit cell dimensions	$a = 9.6736(2)$ Å $\alpha = 73.482(5)$ deg. $b = 11.0702(2)$ Å $\beta = 75.138(5)$ deg. $c = 11.2344(8)$ Å $\gamma = 73.681(5)$ deg.
Volume	$1086.38(8)$ Å ³
Z, Calculated density	2, 1.620 Mg/m ³
Absorption coefficient	7.850 mm ⁻¹
F(000)	533.1
Crystal size	0.14 x 0.10 x 0.09 mm
Theta range for data collection	4.18 to 68.23 deg.
Limiting indices	$-11 \leq h \leq 11, -13 \leq k \leq 13, -13 \leq l \leq 13$
Reflections collected / unique	23642 / 3880 [$R(int) = 0.0297$]
Completeness to $\theta = 68.23$	97.5%
Absorption correction	Semi-empirical from equivalents
Max. and min. transmission	0.521 and 0.411
Refinement method	Full-matrix least-squares on F^2

Data / restraints / parameters	3880 / 0 / 301
Goodness-of-fit on F^2	1.034
Final R indices [$I > 2\sigma(I)$]	R1 = 0.0173, wR2 = 0.0425
R indices (all data)	R1 = 0.0176, wR2 = 0.0427
Largest diff. peak and hole	0.299 and -0.381 e. \AA^{-3}

Atomic coordinates ($\times 10^4$) and equivalent isotropic displacement parameters ($\text{\AA}^2 \times 10^3$) for **14**. U(eq) is defined as one third of the trace of the orthogonalized U_{ij} tensor.

	x	y	z	U(eq)
Pd(1)	3046(1)	3185(1)	7036(1)	9(1)
F(1)	5380(1)	1940(1)	8416(1)	17(1)
F(2)	5321(1)	881(1)	7105(1)	20(1)
F(3)	6249(1)	2565(1)	6435(1)	23(1)
N(1)	2260(1)	1721(1)	6654(1)	11(1)
N(2)	896(2)	4288(1)	6870(1)	12(1)
C(1)	3019(2)	1070(2)	5759(2)	14(1)
C(2)	2533(2)	143(2)	5477(2)	18(1)
C(3)	1236(2)	-162(2)	6186(2)	22(1)
C(4)	433(2)	510(2)	7109(2)	20(1)
C(5)	952(2)	1476(2)	7306(2)	13(1)
C(6)	42(2)	2351(2)	8214(2)	13(1)
C(7)	-268(2)	3745(2)	7403(2)	13(1)
C(8)	-1670(2)	4427(2)	7211(2)	18(1)
C(9)	-1873(2)	5678(2)	6468(2)	20(1)
C(10)	-678(2)	6222(2)	5928(2)	18(1)
C(11)	693(2)	5499(2)	6148(2)	14(1)
C(12)	821(2)	2288(2)	9276(2)	13(1)
C(13)	2013(2)	1302(2)	9605(2)	14(1)
C(14)	2554(2)	1208(2)	10672(2)	17(1)
C(15)	1902(2)	2094(2)	11423(2)	18(1)
C(16)	722(2)	3086(2)	11097(2)	20(1)
C(17)	191(2)	3184(2)	10032(2)	16(1)
C(18)	-1394(2)	1923(2)	8894(2)	20(1)
C(19)	3626(2)	4623(2)	7395(2)	12(1)
C(20)	3963(2)	5673(2)	6427(2)	14(1)
C(21)	4180(2)	6754(2)	6695(2)	16(1)
C(22)	4111(2)	6816(2)	7928(2)	15(1)
C(23)	3827(2)	5749(2)	8890(2)	15(1)
C(24)	3585(2)	4674(2)	8631(2)	14(1)
C(25)	4309(2)	8007(2)	8211(2)	22(1)
C(26)	5072(3)	2136(2)	7254(2)	14(1)
I(1)	5682(3)	1962(2)	6990(2)	15(1)

X-ray structure determination for (dpsa)Pd^{IV}(4-MeC₆H₄)(CF₃)(Cl) (18).

Yellow, block-like crystals of **18** were grown from an acetonitrile/methyl *t*-butyl ether solution at 23 deg. C. A crystal of dimensions 0.15 x 0.13 x 0.12 mm was mounted on a Rigaku AFC10K Saturn 944+ CCD-based X-ray diffractometer equipped with a low temperature device and Micromax-007HF Cu-target micro-focus rotating anode ($\lambda = 1.54187$ Å) operated at 0.2 kW power (20 kV, 10 mA). The X-ray intensities were measured at 85(1) K with the detector placed at a distance 42.00 mm from the crystal. A total of 1506 images were collected with an oscillation width of 2.0° in ω . The exposure time was 10 sec. per image for low angle and 30 seconds for high angle images. The integration of the data yielded a total of 34052 reflections to a maximum 2θ value of 136.44° of which 5929 were independent and 5842 were greater than $2\sigma(I)$. The final cell constants were based on the xyz centroids of 18798 reflections above $10\sigma(I)$. Analysis of the data showed negligible decay during data collection; the data were processed with CrystalClear 2.0 and corrected for absorption. The structure was solved and refined with the Bruker SHELXTL (version 2008/4) software package, using the space group P1bar with $Z = 2$ for the formula C₂₉H₃₅ClF₃N₅O₂PdS, 2(C₂H₃N). Full matrix least-squares refinement based on F^2 converged at $R1 = 0.0297$ and $wR2 = 0.0729$ [based on $I > 2\sigma(I)$], $R1 = 0.0304$ and $wR2 = 0.0734$ for all data. The acetonitrile solvates and the *t*-butylphenylsulfonamido ligand are disordered. Additional details are presented in below.

Crystal data and structure refinement for **18**.

Identification code	am341
Empirical formula	C33 H35 Cl F3 N5 O2 Pd S
Formula weight	764.57
Temperature	85(2) K
Wavelength	1.54178 Å
Crystal system, space group	Triclinic, P -1
Unit cell dimensions	a = 9.9337(2) Å alpha = 67.070(5) deg. b = 13.4448(3) Å beta = 78.111(5) deg. c = 14.1447(10) Å gamma = 73.844(5) deg.
Volume	1660.93(13) Å ³
Z, Calculated density	2, 1.529 Mg/m ³
Absorption coefficient	6.306 mm ⁻¹
F(000)	780
Crystal size	0.15 x 0.13 x 0.12 mm
Theta range for data collection	3.41 to 68.22 deg.
Limiting indices	-11<=h<=11, -16<=k<=16, -17<=l<=17
Reflections collected / unique	34052 / 5929 [R(int) = 0.0485]
Completeness to theta = 68.22	97.6%
Absorption correction	Semi-empirical from equivalents
Max. and min. transmission	0.474 and 0.416
Refinement method	Full-matrix least-squares on F ²
Data / restraints / parameters	5929 / 183 / 560
Goodness-of-fit on F ²	1.056
Final R indices [I>2sigma(I)]	R1 = 0.0270, wR2 = 0.0694
R indices (all data)	R1 = 0.0273, wR2 = 0.0696
Largest diff. peak and hole	0.472 and -0.599 e.Å ⁻³

Atomic coordinates (x 10⁴) and equivalent isotropic displacement parameters (Å² x 10³) for **18**. U(eq) is defined as one third of the trace of the orthogonalized Uij tensor.

	x	y	z	U(eq)
S(1)	2806(1)	1439(1)	3965(1)	23(1)
Pd(1)	4004(1)	2579(1)	1436(1)	14(1)
Cl(1)	4659(1)	3494(1)	-277(1)	28(1)
F(1)	1478(1)	3814(1)	2163(1)	43(1)
F(2)	2453(2)	4834(1)	774(1)	49(1)
F(3)	3350(1)	4303(1)	2192(1)	42(1)
O(1)	1414(1)	1705(1)	3672(1)	33(1)
O(2)	3273(1)	362(1)	4725(1)	27(1)
N(1)	5352(2)	1056(1)	1368(1)	15(1)
N(2)	5860(2)	2751(1)	1917(1)	18(1)
N(3)	3908(2)	1560(1)	2954(1)	16(1)
C(1)	5718(2)	689(2)	580(1)	22(1)
C(2)	6599(2)	-335(2)	680(2)	32(1)
C(3)	7126(2)	-982(2)	1615(2)	31(1)
C(4)	6761(2)	-598(2)	2429(2)	24(1)
C(5)	5856(2)	425(1)	2283(1)	16(1)
C(6)	5402(2)	998(1)	3066(1)	16(1)
C(7)	6300(2)	1857(1)	2733(1)	17(1)
C(8)	7515(2)	1716(2)	3148(1)	21(1)
C(9)	8305(2)	2524(2)	2693(2)	24(1)
C(10)	7839(2)	3447(2)	1855(2)	28(1)
C(11)	6600(2)	3541(2)	1491(2)	24(1)
C(12)	2914(5)	2488(4)	4440(3)	20(1)
C(13)	1882(4)	3498(3)	4323(3)	21(1)
C(14)	1888(4)	4209(3)	4815(3)	22(1)
C(15)	2910(4)	3984(3)	5458(3)	19(1)
C(16)	3910(5)	3037(4)	5561(4)	19(1)
C(17)	3986(5)	2293(4)	5066(3)	16(1)
C(18)	2748(4)	4730(3)	6082(3)	17(1)
C(19)	4049(5)	4509(4)	6600(4)	29(1)
C(20)	1543(5)	4447(4)	6948(4)	27(1)
C(21)	2352(6)	5973(4)	5409(4)	26(1)
C(12A)	2773(6)	2318(4)	4612(3)	24(1)
C(13A)	1494(4)	2957(3)	4779(3)	23(1)
C(14A)	1455(4)	3644(3)	5310(3)	26(1)
C(15A)	2650(5)	3681(3)	5654(3)	18(1)
C(16A)	3980(7)	3000(5)	5419(4)	25(1)
C(17A)	3989(6)	2318(5)	4891(4)	24(1)
C(18A)	2526(5)	4457(4)	6246(4)	20(1)
C(19A)	3811(5)	4083(4)	6869(4)	31(1)
C(20A)	1182(6)	4495(5)	6987(4)	19(1)

C(21A)	2565(6)	5622(4)	5453(4)	23(1)
C(22)	2337(2)	2251(2)	1059(1)	18(1)
C(23)	2057(2)	1210(2)	1580(1)	18(1)
C(24)	944(2)	953(2)	1322(1)	21(1)
C(25)	127(2)	1709(2)	552(1)	24(1)
C(26)	445(2)	2746(2)	32(2)	27(1)
C(27)	1554(2)	3021(2)	277(2)	26(1)
C(28)	-1077(2)	1420(2)	288(2)	33(1)
C(29)	2736(2)	3958(2)	1644(2)	31(1)
N(4)	3174(4)	8335(3)	3452(4)	53(1)
C(30)	2120(5)	8741(3)	3769(3)	33(1)
C(31)	725(6)	9325(4)	4106(4)	33(1)
N(6)	-232(4)	8106(4)	3241(4)	48(1)
C(34)	266(5)	8481(4)	3667(4)	36(1)
C(31A)	941(7)	8930(4)	4198(4)	35(1)
N(5)	183(4)	8098(3)	2542(3)	38(1)
C(32)	1184(4)	7462(3)	2492(3)	24(1)
C(33)	2550(3)	6687(2)	2334(2)	41(1)
N(7)	3496(4)	8367(3)	2271(3)	40(1)
C(35)	3107(5)	7639(3)	2259(3)	32(1)
C(33A)	2550(3)	6687(2)	2334(2)	41(1)

X-ray structure determination for (dpsa)Pd^{IV}(4-MeC₆H₄)(CF₃)(F) (20).

Yellow plates of **20** were grown from an acetonitrile/methyl t-butyl ether solution at 23 deg. C. A crystal of dimensions 0.20 x 0.10 x 0.06 mm was mounted on a Rigaku AFC10K Saturn 944+ CCD-based X-ray diffractometer equipped with a low temperature device and Micromax-007HF Cu-target micro-focus rotating anode ($\lambda = 1.54187 \text{ \AA}$) operated at 0.25 kW power (25 kV, 10 mA). The X-ray intensities were measured at 85(1) K with the detector placed at a distance 42.00 mm from the crystal. A total of 3147 images were collected with an oscillation width of 1.0° in ω . The exposure time was 10 sec. per image for low angle and 40 seconds for high angle images. The integration of the data yielded a total of 67691 reflections to a maximum 2θ value of 136.46° of which 5932 were independent and 5725 were greater than $2\sigma(I)$. The final cell were based on

the xyz centroids of 67691 reflections above $10\sigma(I)$. Analysis of the data showed negligible decay during data collection; the data were processed with CrystalClear 2.0 and corrected for absorption. The structure was solved and refined with the Bruker SHELXTL (version 2008/4) software package, using the space group C2/c with Z = 8 for the formula $C_{29}H_{29}F_4N_3O_2PdS$, (C_2H_3N) , $(C_5H_{12}O)_{0.5}$. Full matrix least-squares refinement based on F^2 converged at $R_1 = 0.0470$ and $wR_2 = 0.1170$ [based on $I > 2\sigma(I)$], $R_1 = 0.0482$ and $wR_2 = 0.1181$ for all data. The acetonitrile and methyl t-butyl ether solvates are disordered. Additional details are presented in below.

Crystal data and structure refinement for **20**.

Identification code	am355
Empirical formula	$C_{33.50}H_{38}F_4N_4O_{2.50}PdS$
Formula weight	751.14
Temperature	85(2) K
Wavelength	1.54178 Å
Crystal system, space group	Monoclinic, C2/c
Unit cell dimensions	a = 17.4944(3) Å $\alpha = 90$ deg. b = 22.1204(4) Å $\beta = 114.778(8)$ deg. c = 18.4391(13) Å $\gamma = 90$ deg.
Volume	6478.7(5) Å ³
Z, Calculated density	8, 1.540 Mg/m ³
Absorption coefficient	5.760 mm ⁻¹
F(000)	3080
Crystal size	0.20 x 0.10 x 0.06 mm
Theta range for data collection	3.43 to 68.23 deg.
Limiting indices	$-21 \leq h \leq 21$, $-26 \leq k \leq 26$, $-22 \leq l \leq 22$
Reflections collected / unique	67911 / 5932 [R(int) = 0.0499]
Completeness to $\theta = 68.23$	100.0%
Absorption correction	Semi-empirical from equivalents
Max. and min. transmission	0.712 and 0.544
Refinement method	Full-matrix least-squares on F^2
Data / restraints / parameters	5932 / 75 / 479
Goodness-of-fit on F^2	1.069
Final R indices [$I > 2\sigma(I)$]	$R_1 = 0.0470$, $wR_2 = 0.1170$
R indices (all data)	$R_1 = 0.0482$, $wR_2 = 0.1181$
Largest diff. peak and hole	1.075 and -1.361 e.Å ⁻³

Atomic coordinates (x 10⁴) and equivalent isotropic displacement parameters (Å² x 10³) for **20**. U(eq) is defined as one third of the trace of the orthogonalized Uij tensor.

	x	y	z	U(eq)
S(1)	4127(1)	2737(1)	5379(1)	31(1)
Pd(1)	4866(1)	1952(1)	4238(1)	34(1)
F(1)	5390(1)	1590(1)	3595(1)	47(1)
F(2)	5830(2)	2740(1)	3773(2)	63(1)
F(3)	4736(1)	3162(1)	3793(2)	53(1)
F(4)	5833(1)	3024(1)	4877(1)	47(1)
O(1)	4985(1)	2844(1)	5926(1)	37(1)
O(2)	3537(1)	2567(1)	5705(1)	35(1)
N(1)	3678(2)	2088(1)	3193(2)	31(1)
N(2)	4261(2)	1128(1)	4285(2)	43(1)
N(3)	4124(2)	2215(1)	4776(2)	35(1)
C(1)	3534(2)	2129(1)	2425(2)	34(1)
C(2)	2717(2)	2160(1)	1840(2)	34(1)
C(3)	2054(2)	2159(1)	2052(2)	34(1)
C(4)	2210(2)	2109(2)	2854(2)	35(1)
C(5)	3035(2)	2066(1)	3410(2)	31(1)
C(6)	3322(2)	1903(1)	4291(2)	36(1)
C(7)	3523(2)	1234(2)	4321(2)	41(1)
C(8)	2992(3)	766(2)	4302(2)	49(1)
C(9)	3245(3)	178(2)	4226(2)	59(1)
C(10)	3982(3)	78(2)	4183(2)	60(1)
C(11)	4509(3)	568(2)	4220(2)	53(1)
C(12)	3728(2)	3426(1)	4866(2)	32(1)
C(13)	2875(2)	3496(1)	4389(2)	33(1)
C(14)	2574(2)	4052(2)	4047(2)	37(1)
C(15)	3120(3)	4551(2)	4176(2)	42(1)
C(16)	3958(3)	4461(2)	4640(3)	55(1)
C(17)	4273(3)	3907(2)	4993(3)	50(1)
C(18)	2759(3)	5173(2)	3818(2)	47(1)
C(19)	2199(4)	5398(2)	4185(3)	74(2)
C(20)	2309(3)	5137(2)	2918(2)	49(1)
C(21)	3482(4)	5646(2)	4025(4)	93(2)
C(22)	5916(2)	1734(2)	5224(2)	40(1)
C(23)	5864(2)	1579(2)	5924(2)	40(1)
C(24)	6601(2)	1401(2)	6588(2)	43(1)
C(25)	7374(2)	1374(2)	6545(2)	42(1)
C(26)	7397(2)	1515(2)	5818(2)	44(1)
C(27)	6672(2)	1698(2)	5156(2)	44(1)
C(28)	8168(2)	1214(2)	7262(2)	48(1)
C(29)	5364(2)	2767(2)	4179(2)	39(1)
N(4)	5405(5)	9481(4)	3613(5)	65(2)
C(30)	5247(6)	9883(4)	3180(5)	57(2)

C(31)	5079(10)	10418(4)	2646(8)	69(3)
N(5)	5372(5)	9061(4)	3373(6)	76(2)
C(32)	5176(5)	8636(4)	2984(5)	58(2)
C(33)	4888(5)	8078(4)	2522(7)	53(3)
O(3)	4718(4)	4896(3)	8126(3)	50(1)
C(34)	5197(6)	5432(4)	8427(5)	54(2)
C(35)	5020(20)	4554(3)	7500(30)	72(3)
C(36)	4321(6)	4006(4)	7395(6)	56(2)
C(37)	4621(6)	4914(4)	6777(5)	59(2)
C(38)	5798(5)	4350(5)	7897(6)	56(2)

X-ray structure determination for [(dpph)Pd^{IV}(4-MeC₆H₄)(CF₃)(NPhth)]

(30). Colorless needles of **30** were grown from a chloroform solution at 23 deg. C. A crystal of dimensions 0.14 x 0.12 x 0.08 mm was mounted on a Rigaku AFC10K Saturn 944+ CCD-based X-ray diffractometer equipped with a low temperature device and Micromax-007HF Cu-target micro-focus rotating anode ($\lambda = 1.54187$ Å) operated at 0.3 kW power (30 kV, 10 mA). The X-ray intensities were measured at 85(1) K with the detector placed at a distance 42.00 mm from the crystal. A total of 1239 images were collected with an oscillation width of 1.5° in ω . The exposure time was 15 sec. per image for low angle and 35 seconds for high angle images. The integration of the data yielded a total of 53247 reflections to a maximum 2θ value of 136.48° of which 7380 were independent and 6784 were greater than $2\sigma(I)$. The final cell constants were based on the xyz centroids of 41264 reflections above $10\sigma(I)$. Analysis of the data showed negligible decay during data collection; the data were processed with CrystalClear 2.0 and corrected for absorption. The structure was solved and refined with the Bruker SHELXTL (version 2008/4) software package, using the space group P2(1)/n with $Z = 4$ for the formula C₃₄H₂₆F₃N₃O₂Pd, 3(CHCl₃). All non-hydrogen atoms were refined anisotropically with

the hydrogen atoms placed in idealized positions. The dichloromethane solvate molecules are disordered and were modeled as diffuse scattering by use of the SQUEEZE subroutine of the PLATON program suite. Full matrix least-squares refinement based on F^2 converged at $R1 = 0.0504$ and $wR2 = 0.1316$ [based on $I > 2\sigma(I)$], $R1 = 0.0556$ and $wR2 = 0.1331$ for all data. Additional details are presented in below.

Crystal data and structure refinement for **30**.

Identification code	am3201
Empirical formula	C ₃₇ H ₂₉ Cl ₉ F ₃ N ₃ O ₂ Pd
Formula weight	1030.08
Temperature	85(2) K
Wavelength	1.54178 Å
Crystal system, space group	Monoclinic, P 1 2 ₁ /n 1
Unit cell dimensions	a = 9.8196(2) Å alpha = 90 deg. b = 19.3578(4) Å beta = 98.596(7) deg. c = 21.4850(15) Å gamma = 90 deg.
Volume	4038.1(3) Å ³
Z, Calculated density	4, 1.694 Mg/m ³
Absorption coefficient	9.641 mm ⁻¹
F(000)	2056
Crystal size	0.14 x 0.12 x 0.08 mm
Theta range for data collection	3.09 to 68.24 deg.
Limiting indices	-11 ≤ h ≤ 11, -23 ≤ k ≤ 22, -25 ≤ l ≤ 25
Reflections collected / unique	53247 / 7380 [R(int) = 0.0644]
Completeness to theta = 68.24	99.8%
Absorption correction	Semi-empirical from equivalents
Max. and min. transmission	0.726 and 0.423
Refinement method	Full-matrix least-squares on F ²
Data / restraints / parameters	7380 / 0 / 391
Goodness-of-fit on F ²	1.097
Final R indices [I > 2σ(I)]	R1 = 0.0524, wR2 = 0.1316
R indices (all data)	R1 = 0.0556, wR2 = 0.1331
Largest diff. peak and hole	0.850 and -1.138 e.Å ⁻³

Atomic coordinates ($\times 10^4$) and equivalent isotropic displacement parameters ($\text{\AA}^2 \times 10^3$) for **30**.U(eq) is defined as one third of the trace of the orthogonalized U_{ij} tensor.

	x	y	z	U(eq)
Pd(1)	5488(1)	1266(1)	1998(1)	16(1)
F(1)	3657(2)	2041(2)	1109(1)	34(1)
F(2)	2718(3)	1101(2)	1404(1)	33(1)
F(3)	2874(3)	2003(2)	1996(1)	33(1)
O(1)	6875(3)	-184(2)	1484(2)	34(1)
O(2)	2914(4)	18(2)	2364(2)	43(1)
N(1)	7505(3)	959(2)	2347(2)	17(1)
N(2)	6042(3)	1181(2)	1072(2)	17(1)
N(3)	4951(3)	154(2)	1931(2)	22(1)
C(1)	7724(4)	491(2)	2812(2)	22(1)
C(2)	9024(4)	248(2)	3044(2)	25(1)
C(3)	10112(5)	482(3)	2748(2)	35(1)
C(4)	9893(4)	955(2)	2280(2)	28(1)
C(5)	8571(4)	1201(2)	2066(2)	20(1)
C(6)	8224(4)	1730(2)	1544(2)	17(1)
C(7)	7305(4)	1407(2)	976(2)	21(1)
C(8)	7706(5)	1349(2)	389(2)	30(1)
C(9)	6781(5)	1072(2)	-119(2)	28(1)
C(10)	5505(5)	848(2)	-12(2)	30(1)
C(11)	5179(5)	907(2)	588(2)	26(1)
C(12)	9585(4)	1989(2)	1336(2)	26(1)
C(13)	7452(4)	2345(2)	1797(2)	19(1)
C(14)	8009(5)	3005(2)	1820(2)	31(1)
C(15)	7340(5)	3557(2)	2072(3)	36(1)
C(16)	6131(6)	3457(2)	2283(3)	37(1)
C(17)	5544(5)	2797(2)	2259(2)	31(1)
C(18)	6220(4)	2250(2)	2027(2)	22(1)
C(19)	5115(5)	1427(2)	2915(2)	24(1)
C(20)	6158(6)	1682(3)	3353(2)	40(1)
C(21)	5928(7)	1784(3)	3982(3)	50(2)
C(22)	4667(8)	1655(3)	4156(3)	59(2)
C(23)	3577(8)	1389(3)	3704(3)	54(2)
C(24)	3844(6)	1277(3)	3093(2)	38(1)
C(25)	4351(11)	1798(4)	4817(4)	86(3)
C(26)	5797(4)	-308(2)	1684(2)	22(1)
C(27)	5238(5)	-1019(2)	1704(2)	31(1)
C(28)	5672(6)	-1660(3)	1513(2)	43(1)
C(29)	4883(7)	-2236(3)	1612(3)	51(2)
C(30)	3705(8)	-2169(4)	1890(3)	60(2)
C(31)	3244(7)	-1539(3)	2084(3)	50(2)
C(32)	4031(5)	-975(3)	1974(2)	34(1)
C(33)	3883(5)	-203(3)	2128(2)	28(1)
C(34)	3601(4)	1627(2)	1614(2)	25(1)

2.7 References

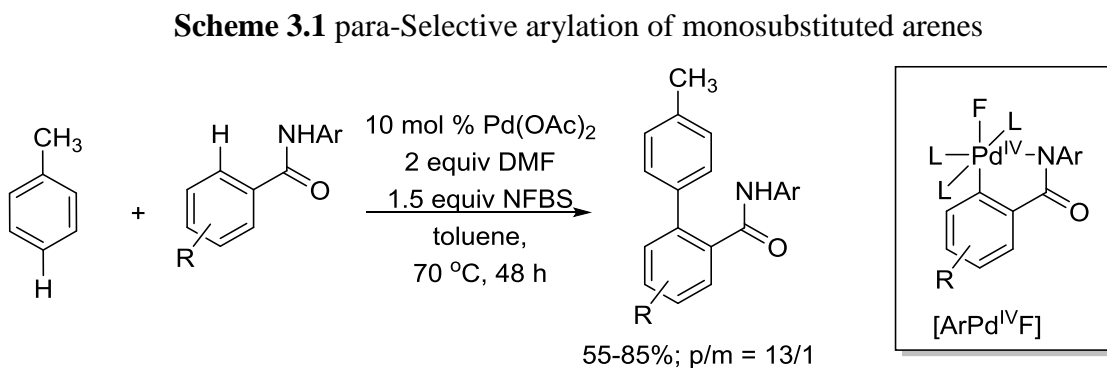
- (1) Excerpts of Chapter 2 reprinted with permission from Maleckis, A.; Sanford, M. S. Facial Tridentate Ligands for Stabilizing Palladium(IV) Complexes. *Organometallics* **2011**, *30*, 6617-6627. Copyright 2011. American Chemical Society.
- (2) (a) Ball, N. D.; Gary, J. B.; Ye, Y.; Sanford, M. S. *J. Am. Chem. Soc.* **2011**, *133*, 7577-7584. (b) Ball, N. D.; Kampf, J.; Sanford, M. S. *J. Am. Chem. Soc.* **2010**, *132*, 2878-2879.
- (3) Pd^{IV} complexes of neutral tridentate (L₃-type) ligands: (a) Klaui, W.; Glaum, M.; Wagner, T.; Bennett, M. A. *J. Organomet. Chem.* **1994**, *472*, 355-358. (b) Bennett, M. A.; Canty, A. J.; Felixberger, J. K.; Rendina, L. M.; Sutherland, C.; Willis, A. C. *Inorg. Chem.* **1993**, *32*, 1951-1958. (c) Brown, D. G.; Byers, P. K.; Canty, A. J. *Organometallics* **1990**, *9*, 1231-1235. (d) Byers, P. K.; Canty, A. J.; Skelton, B. W.; White, A. H. *Organometallics* **1990**, *9*, 826-832.
- (4) Pd^{IV} tris(pyrazoyl)borate complexes: (a) Campora, J.; Palma, P.; del Rio, D.; Lopez, J. A.; Alvarez, E. *Organometallics* **2005**, *24*, 3624-3628. (b) Campora, J.; Palma, P.; del Rio, D.; Lopez, J. A.; Valerga, P. *Chem. Commun.* **2004**, 1490-1491. (c) Campora, J.; Palma, P.; del Rio, D.; Carmona, E. *Organometallics* **2003**, *22*, 3345-3347. (d) Canty, A. J.; Jin, H.; Penny, J. D. *J. Organomet. Chem.* **1999**, *573*, 30-35. (e) Canty, A. J.; Jin, H.; Roberts, A. S.; Skelton, B. W.; White, A. H. *Organometallics* **1996**, *15*, 5713-5722.
- (5) Pd^{IV} pincer complexes: (a) Canty, A. J.; Rodemann, T.; Skelton, B. W.; White, A. H. *Organometallics* **2006**, *25*, 3996-4001. (b) Lagunas, M.-C.; Gossage, R. A.; Spek, A. L.; van Koten, G. *Organometallics* **1998**, *17*, 731-741. (c) Alsters, P. L.; Engel, P. F.; Hogerheide, M. P.; Copijn, M.; Spek, A. L.; van Koten, G. *Organometallics* **1993**, *12*, 1831-1844.
- (6) Coe, B. J.; Glenwright, S. J. *Coord. Chem. Rev.* **2000**, *203*, 5-80.
- (7) Chang, J.; Plummer, S.; Berman, E. S. F.; Striplin, D.; Blauch, D. *Inorg. Chem.* **2004**, *43*, 1735-1742.
- (8) (a) Markies, B. A.; Canty, A. J.; de Graaf, W.; Boersma, J.; Janssen, M. D.; Hogerheide, M. P.; Smeets, W. J. J.; Spek, A. L.; van Koten, G. *J. Organomet. Chem.* **1994**, *482*, 191-199. (b) de Graaf, W.; Boersma, J.; van Koten, G. *Organometallics* **1990**, *9*, 1479-1484. (c) de Graaf, W.; Boersma, J.; Smeets, W. J. J.; Spek, A. L.; van Koten, G. *Organometallics* **1989**, *8*, 2907-2917.
- (9) (a) Iverson, C. N.; Lachicotte, R. J.; Müller.; Jones, W. D. *Organometallics* **2002**, *21*, 5320-5333. (b) Reinartz, S.; White, P. S.; Brookhart, M.; Tempelton, J. L. *J. Am. Chem. Soc.* **2001**, *123*, 12724-12725. (c) Chin, R. M.; Dong, L.; Duckett, S. B.; Partridge, M. G.; Jones, W. D.; Perutz, R. N. *J. Am. Chem. Soc.* **1993**, *115*, 7685-7695.
- (10) Coe, B. J.; Glenwright, S. J. *Coord. Chem. Rev.* **2000**, *203*, 5-80.
- (11) Racowski, J. M.; Ball, N. D.; Sanford, M. S. *J. Am. Chem. Soc.* **2011**, *133*, 18022-18025.
- (12) Rare examples of Pd^{IV} phosphine complexes: (a) Bayer, A.; Canty, A. J.; Edwards, P. G.; Skelton, B. W.; White, A. H. *J. Chem. Soc., Dalton Trans.* **2000**, 3325-330. (b) Bayer, A.; Canty, A. J.; Skelton, B. W.; White, A. H. *J. Organomet. Chem.* **2000**, *595*, 296-299.

-
- (13) (a) Whitfield, S. R.; Sanford, M. S. *J. Am. Chem. Soc.* **2007**, *129*, 15142-15143. (b) Yamamoto, Y.; Ohno, T.; Itoh, K. *Angew. Chem. Int. Ed.* **2002**, *41*, 3662-3665.
- (14) Takahashi, Y.; Ito, Ts.; Sakai, S.; Ishii, Y. *J. Chem. Soc. D*, **1970**, *17*, 1065-1066.
- (15) Ihara, E.; Koyama, K.; Yasuda, H.; Kanehisa, N.; Kai, Y. *J. Organomet. Chem.* **1999**, *574*, 40-49.

Chapter 3: Investigation of C–H Activation at Palladium(IV)¹

3.1 Introduction

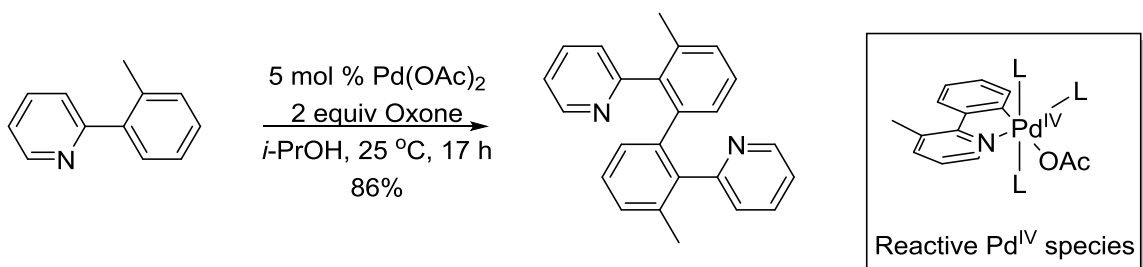
Synthesis of biaryls via traditional Pd^{0/II} catalyzed cross-coupling reactions (*e.g.*, Suzuki, Kumada, Stille, Hiyama) require prefunctionalized starting materials. Oxidative C–H/C–H cross-coupling present a much more efficient process. Until now poor regio- and substrate chemo- selectivities have been considered a major limitation of the oxidative coupling approach. However, in 2011 Yu and coworkers reported regioselective oxidative C–H/C–H coupling of benzamides with monosubstituted arenes (Scheme 3.1).² Extremely high C–H activation regioselectivities and unusual substrate selectivities were rationalized by the unique reactivity of [ArPd^{IV}F] species.



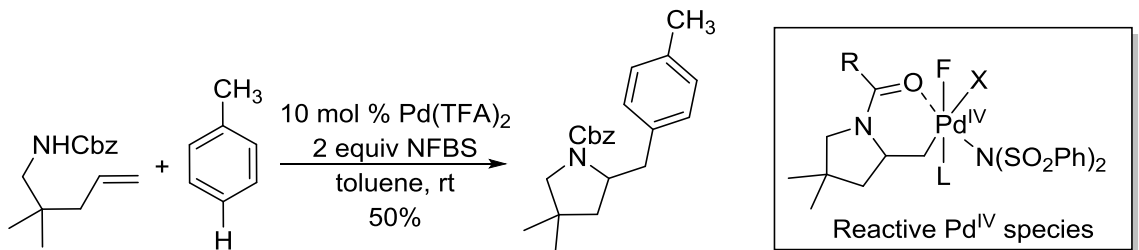
C–H activation at Pd^{IV} has been proposed to be a key process in several other catalytic reactions.³ For example, mechanistic studies have provided evidence that palladium catalyzed oxidative dimerization of 2-arylpyridines⁴ (Scheme 3.2) and *N*-

fluorobenzenesulfonimide (NFBS) promoted carboamination of olefins⁵ (Scheme 3.3) involve C–H cleavage at Pd^{IV} as important step in the catalytic turnover. This example demonstrates remarkable selectivity of Pd^{IV} towards C–H cleavage that potentially can be exploited to develop wide variety of very efficient C–H functionalization reactions.

Scheme 3.2 Oxidative dimerization of 2-arylpyridines



Scheme 3.3 Carboamination of alkenes

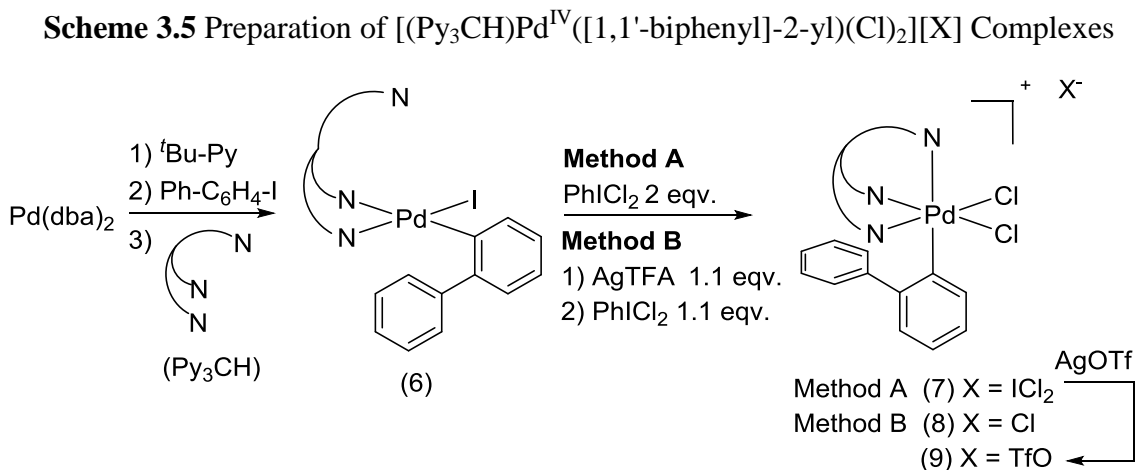


In order to improve currently known C–H functionalization and oxidative cross-coupling reactions and to develop new methodologies, a better understanding of processes occurring at Pd^{IV} is necessary. As such, stoichiometric studies of the mechanism, selectivity, and relative rates of such fundamental reactions at Pd^{IV} centers could provide key insights for designing, and improving catalytic processes. While numerous studies have been published on reductive elimination from Pd^{IV},⁶ C–H activation at isolated, high oxidation state Pd centers is not a thoroughly investigated and

a thorough mechanistic investigation of the C–H activation reaction. Canty and co-workers have previously reported several organometallic Pd^{IV} tris(2-pyridil)methane (Py₃CH) complexes that are stable to reductive elimination at room temperature.⁸ This led us to propose that the third pyridine arm of Py₃CH might impart an appropriate balance of stability and reactivity to enable C–H activation at Pd^{IV}.

3.2 Synthesis of the [(Py₃CH)Pd^{IV}(biphenyl)Cl₂]X Model System

Initial synthetic efforts targeted Pd^{IV} complexes of the general structure [(Py₃CH)Pd^{IV}(biphenyl)Cl₂]X (Scheme 3.5). The tris(2-pyridil)methane (Py₃CH) ligand was prepared in 1 step from α -picoline and 2-fluoropyridine (see Experimental Section for complete details). Pd^{II} precursor **6** was obtained via oxidative addition of iodobiphenyl to Pd(dba)₂ and subsequent ligation of (4-^tBuPy)₂Pd^{II}(biphenyl)(I) intermediate to Py₃CH ligand.

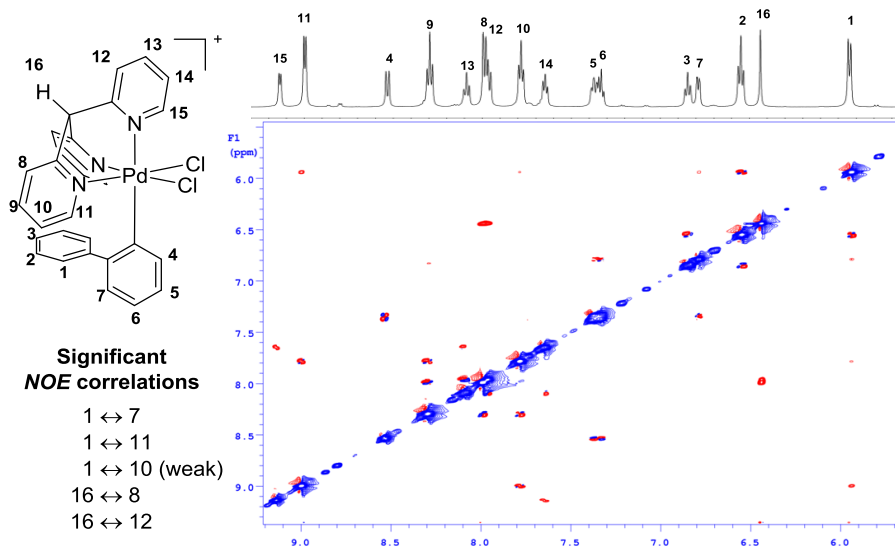


The treatment of (Py₃CH)Pd^{II}(biphenyl)(I) (**6**) with 2 equivalents of PhICl₂ in CH₂Cl₂ at room temperature (Scheme 3.5, method A) afforded the desired cationic Pd^{IV}

product **7** in 85% yield as the ICl_2^- salt. The corresponding chloride salt (**8**) was obtained under slightly modified reaction conditions (Scheme 3.5, method B). Finally, the treatment of **7** with 2 equiv of AgOTf resulted in smooth conversion to the triflate salt **9**. As predicted, complexes **7-9** are significantly more stable than **2**, and they can be stored in the solid state at room temperature for at least 4 weeks without detectable decomposition.

The solution stereochemistry and conformations of **7-9** were elucidated via 1D ^1H NMR and 2D $^1\text{H}/^1\text{H}$ NOESY and ROESY NMR spectra. The ROESY NMR spectrum and peak assignments for **7** are shown in Figure 3.2.

Figure 3.2 $^1\text{H}/^1\text{H}$ ROESY spectrum of $[(\text{Py}_3\text{CH})\text{Pd}^{\text{IV}}([\text{1,1'-biphenyl}]\text{-2-yl})(\text{Cl})_2][\text{ICl}_2]$



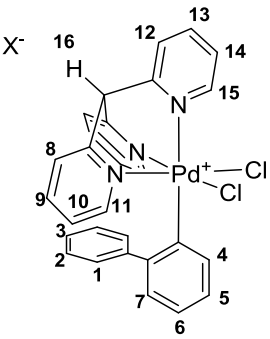
(spectrum acquired at 500 MHz)

The most notable feature of the structure **7** is the orientation of the phenyl ring of the biaryl ligand underneath two of the pyridine rings. This conformation was assigned on the basis of the shielding of the aromatic protons H-1 and H-2 (to 5.9 and 6.6 ppm,

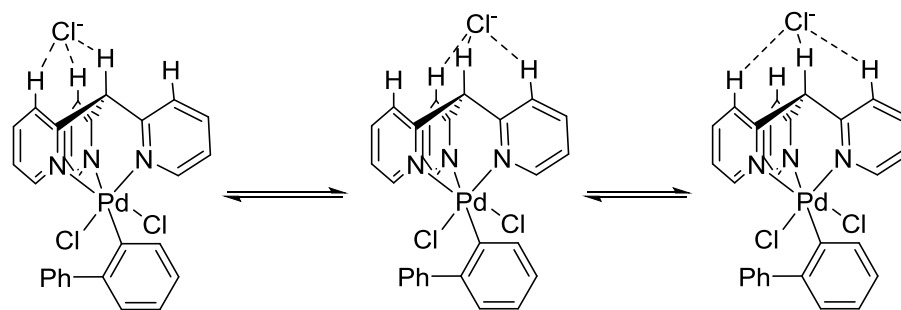
respectively) as well as by NOE correlations between H-1 and H-10/H-11. This conformation is likely due to favorable π - π interactions between the biphenyl and tripyridylmethane ligands.

The ^1H NMR spectra of **7-9** are highly dependent on the counterion X. The spin-lattice relaxation times (T_1) for **7** and **8** in CDCl_3 at 25 °C show that the ICl_2^- and Cl^- counterions have close interactions with H(8), H(12), and H(16) of the Py_3CH ligand (Table 3.1). This is likely due to equilibration of the counterion between three similar sites (Scheme 3.6). Remarkably, these interactions persist even in the highly polar CD_3NO_2 . In contrast, the triflate counterion in complex **9** does not have strong interactions with the Py_3CH ligand in either CDCl_3 or CD_3NO_2 . Related binding of halide counterions to the ligand periphery of cationic Pd^{IV} complexes has been documented by Kraft and Canty.⁹

Table 3.1 Spin-lattice relaxation times (T_1) for complexes **7**, **8** and **9**

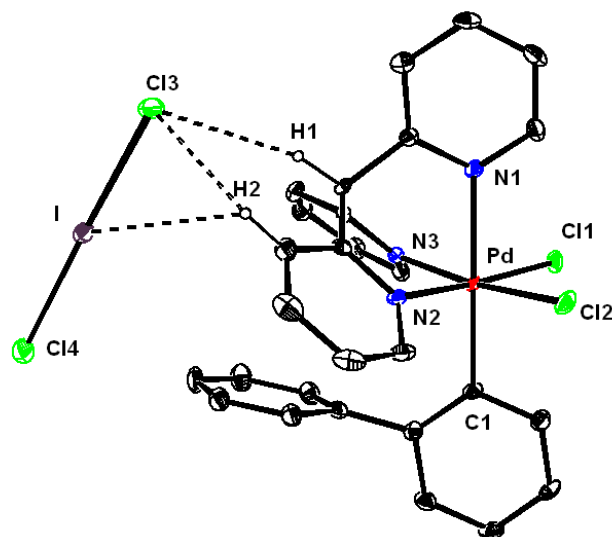
 (7) X = ICl_2^- or (8) X = Cl^- or (9) X = TfO^-	Position	T_1 (X = ICl_2^-)	T_1 (X = Cl^-)	T_1 (X = TfO^-)
	1	1,336	1,206	1,948
2	0,769	0,673	1,802	
3	0,592	0,542	1,888	
4	2,216	2,108	2,367	
5	1,783	1,627	1,575	
6	1,641	1,656	2,173	
7	1,926	1,765	2,027	
8	0,099	0,088	1,363	
9	0,589	0,493	1,782	
10	1,123	0,929	1,661	
11	1,679	1,546	2,146	
12	0,14	0,121	1,551	
13	0,836	0,7	1,848	
14	1,404	1,255	1,751	
15	2,091	1,917	2,576	
16	0,086	0,071	1,003	

Scheme 3.6 Binding of chloride counterion to $[(\text{Py}_3\text{CH})\text{Pd}^{\text{IV}}([1,1'\text{-biphenyl}]\text{-2-yl})(\text{Cl})_2]$



The structure of complex **7** was further confirmed by mass spectrometry and single crystal X-ray diffraction analysis. High resolution ESI mass spectrometric analysis of **7-9** showed an intense peak with $m/z = 576.022$ corresponding to the cationic Pd^{IV} core. An ORTEP drawing of **7** is shown in Figure 3.3. This structure shows that, in the solid state, the ICl_2^- counterion has short contacts with the methine hydrogen [$\text{Cl}(3)\text{-H}(1) = 2.872 \text{ \AA}$] as well as with pyridine proton H2 [$\text{Cl}(3)\text{-H}(2) = 2.752 \text{ \AA}$; $\text{I-H}(2) = 3.354 \text{ \AA}$].

Figure 3.3 ORTEP drawing of $[(\text{Py}_3\text{CH})\text{Pd}^{\text{IV}}([1,1'\text{-biphenyl}]\text{-2-yl})(\text{Cl})_2][\text{ICl}_2]$

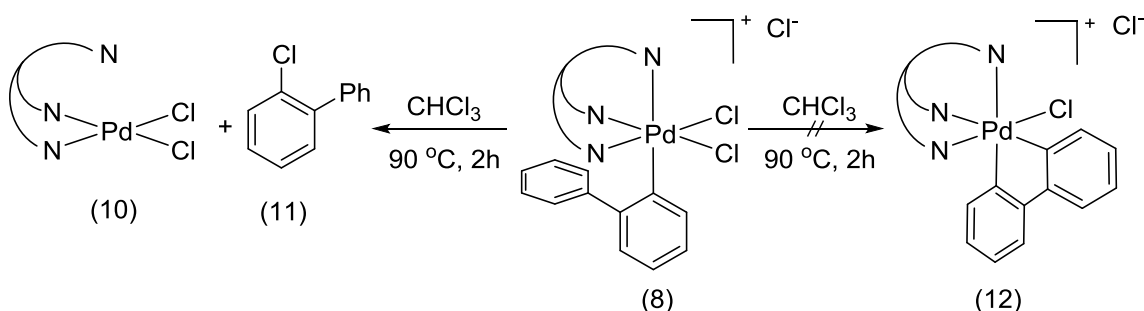


Thermal ellipsoids are drawn at 50% probability. Only hydrogen atoms involved in bonding of ICl_2^- are shown for clarity.

3.3 Reactivity of the Model Complexes

On the basis of our previous work (Scheme 3.7), we expected that heating complexes **7-9** would result in C–H activation to form products like **12** (Scheme 3.7). However, instead, heating **8** at 90 °C for 2 h in CDCl₃ resulted in C–Cl bond-forming reductive elimination to afford Pd^{II} complex **10** along with chlorobiphenyl **11**.

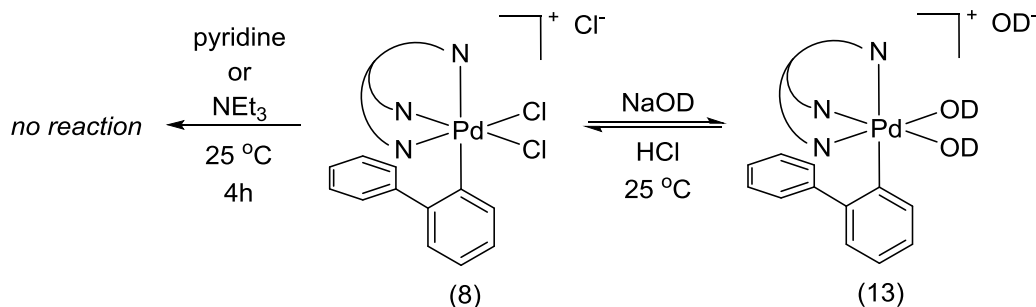
Scheme 3.7 Thermal decomposition of [(Py₃CH)Pd^{IV}([1,1'-biphenyl]-2-yl)(Cl)₂][Cl]



We next hypothesized that base might be necessary to promote C–H activation in this system. However, the treatment of **8** with an excess of triethylamine or pyridine in CH₂Cl₂ at room temperature for 4 h returned only unreacted starting material (Scheme 3.8). When this reaction was conducted at 60 °C, complex **10** underwent decomposition to generate a complex mixture of unidentified products. The desired product **12** was not detected. Complex **8** did react with NaOD at 25 °C to form a colorless D₂O-soluble Pd^{IV} product that we propose to be the deuterioxide complex **13**. Attempts to isolate **13** resulted in decomposition; however, this complex was characterized *in situ* with ¹³C{¹H}, ¹H/¹H gCOSY and NOESY NMR experiments as well as ¹H/¹³C HSQC and HMBC correlation experiments. Notably, the chloride-to-deuterioxide ligand exchange was completely

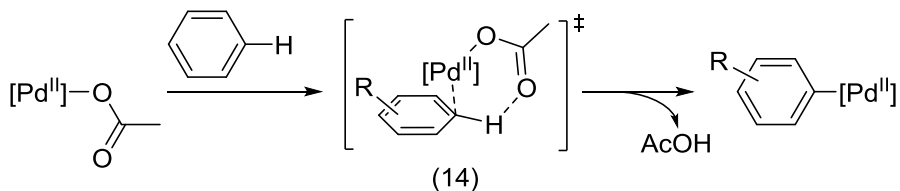
reversible. The acidification of D₂O solutions of **14** with aqueous HCl resulted in rapid and near quantitative regeneration of **8**.

Scheme 3.8 Reactions of [(Py₃CH)Pd^{IV}([1,1'-biphenyl]-2-yl)(Cl)₂][Cl] with bases

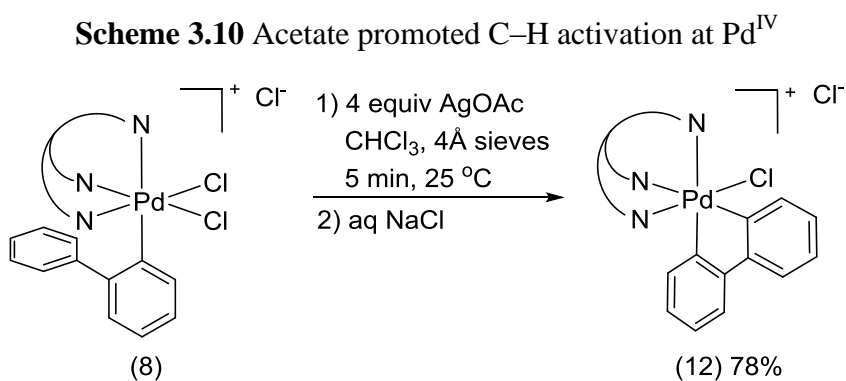


The observation of facile, reversible chloride/deuteroxide ligand exchange prompted us to test the related ligand substitution reaction of chloride for acetate. We reasoned that incorporation of an acetate ligand might trigger C–H activation at Pd^{IV} via a concerted metallation deprotonation (CMD) mechanism. It is known that carboxylate plays an intimate role in the C–H activation process at Pd^{II}. Numerous studies have implicated cyclic transition states for C–H activation at Pd^{II}, where the carbonyl group of the carboxylate ligand acts as an internal base (Scheme 3.9, **14**).^{10,11} This pathway, often referred to as concerted metallation deprotonation (CMD), is supported by extensive experimental data as well as quantum-mechanical calculations.¹²

Scheme 3.9 Concerted metallation-deprotonation (CMD) mechanism



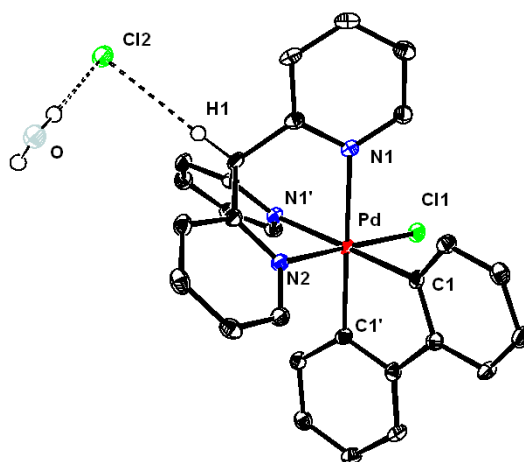
Recent work has also shown that C–H cleavage via a CMD pathway can occur at Rh^{III}, Ir^{III} and Ru^{II} centers as well.^{13,14,15} While CMD C–H activation at Pd^{II} centers has been well studied, the possibility of analogous pathways at high oxidation-state Pd centers remains unexplored. This gap in understanding is particularly noteworthy because palladium carboxylates are used as catalysts in oxidative C–H functionalization reactions¹⁶ (see Schemes 3.1-3.3 above), suggesting the possibility of CMD mechanism at Pd^{IV}.



According to the reasoning above a CDCl₃ solution of **8** was treated with 5% aqueous KOAc. This resulted in a rapid color change from orange to yellow within 5 min (Scheme 3.10). Gratifyingly, ¹H NMR analysis of the separated CDCl₃ layer showed clean conversion to the cyclometalated complex **12**. When this reaction was performed on a preparative scale, complex **12** was isolated in only 39% yield. However, optimization of the reaction conditions (through the use of anhydrous CHCl₃ as the solvent and substituting aqueous KOAc with AgOAc) led to the formation of **12** in high yield after 5 min at 25 °C (78% isolated yield, Scheme 3.10).

Complex **12** is stable at room temperature in the solid state and in CDCl_3 solution for at least two weeks. This cyclometalated compound was characterized by 1D and 2D NMR analysis as well as by single crystal X-ray diffraction. The X-ray structure of **12** is shown in Figure 3.4. In the solid-state, the chloride counterion is hydrogen-bonded to the methine hydrogen ($\text{Cl}(2)\text{-H}(1) = 2.568\text{\AA}$) as well as to a co-crystallized water molecule.

Figure 3.4 ORTEP drawing of $[(\text{Py}_3\text{CH})\text{Pd}^{\text{IV}}([\text{1,1'-biphenyl-2,2'-diyl})(\text{Cl})][\text{Cl}]$.



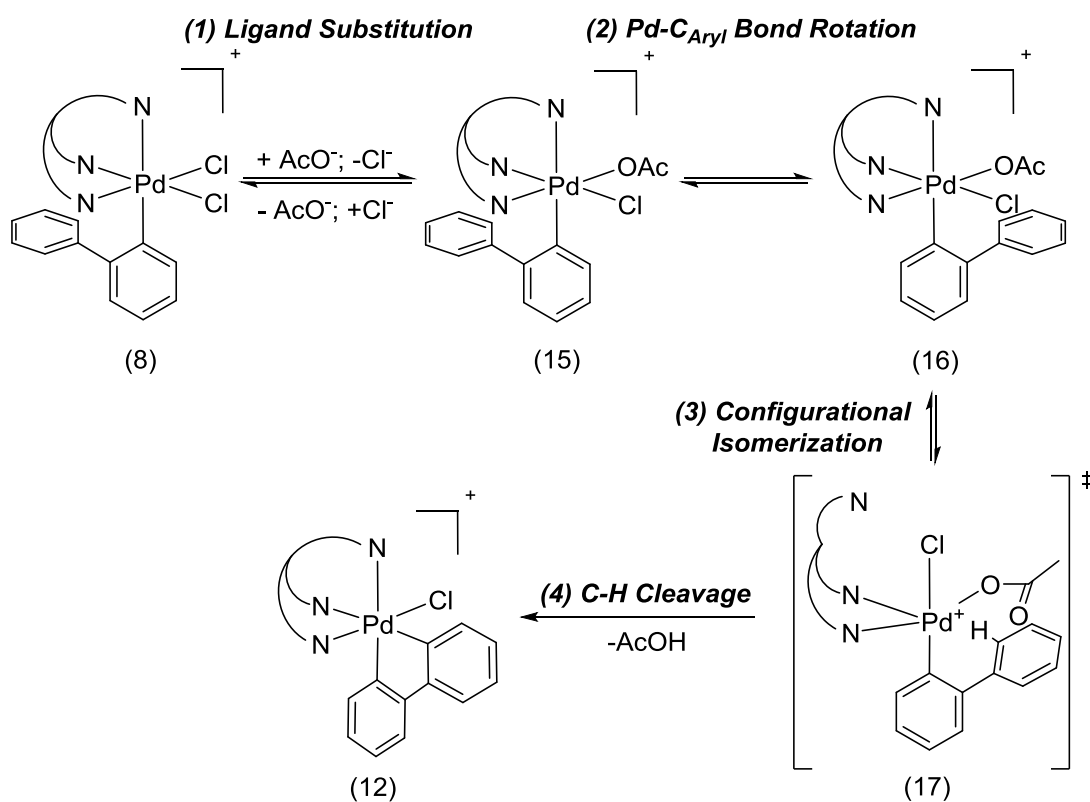
Thermal ellipsoids are drawn at 50% probability. Only hydrogen atom involved in hydrogen bonding is shown for clarity. Selected bond lengths (\AA): Pd-C(1) 2.176, Pd-Cl(1) 2.296, Pd-N(1) 2.176, Pd-N(2) 2.049. Selected bond angles (deg): N(1)-Pd-Cl(1) 91.95, Cl(1)-Pd-C(1) 88.51, C(1)-Pd-N(2) 90.58, N(2)-Pd-N(1) 88.95, C(1)-Pd-C(1') 81.46, N(1)-Pd-C(1) 179.14.

3.4 Proposed Mechanism of C–H Activation at Palladium(IV)

We next sought to gain insights into the mechanism of this C–H activation reaction. As noted in Scheme 3.8 and Scheme 3.9, acetate was the only base examined that promoted this transformation. This strongly suggests that the carboxylate is not

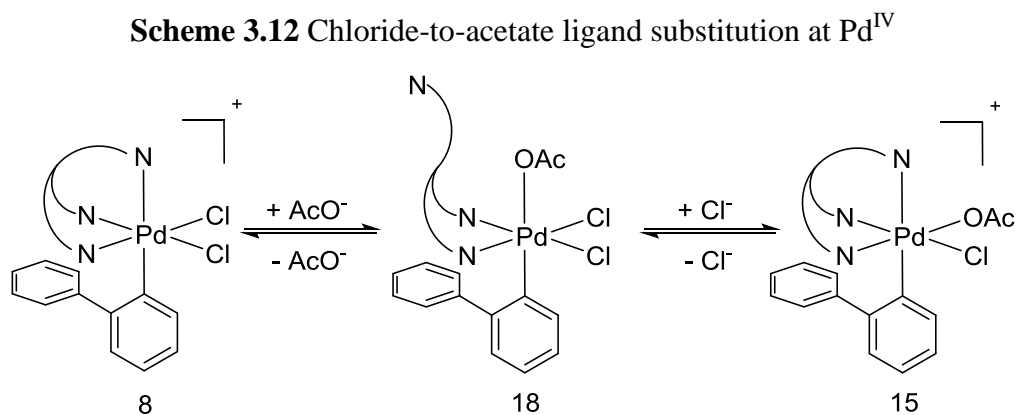
simply serving as an external base in the reaction. Furthermore, the observation of facile replacement of chloride for hydroxide (Scheme 3.8) indicates the feasibility of ligand substitution to form a Pd^{IV} acetate complex prior to C–H activation. On the basis of these preliminary observations, we hypothesized that the observed C–H activation reaction could proceed via the pathway depicted in Scheme 3.11. This involves four distinct steps: (1) chloride to acetate ligand substitution, (2) rotation about the Pd–C_{Aryl} bond, (3) configurational isomerization via Berry pseudorotation, and (4) C–H cleavage with acetate acting as an internal base. With this working mechanism in mind, we have conducted a variety of experiments to gain insights into the feasibility of each of the proposed steps. These studies are described in detail in the sections below.

Scheme 3.11 Proposed mechanism for acetate-assisted C–H activation at Pd^{IV}



3.5 Ligand Substitution at Palladium(IV)

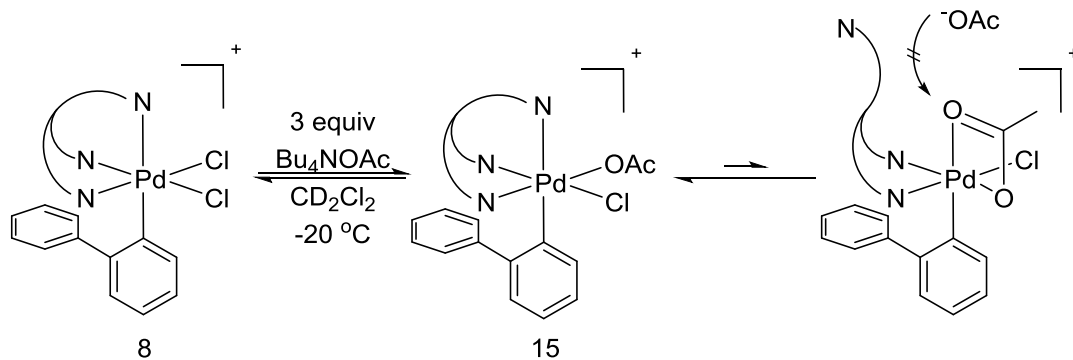
The first step of the proposed mechanism involves chloride-to-acetate ligand exchange at cationic Pd^{IV} center **8**. This most likely proceeds via reversible dissociation of one pyridine arm of the Py₃CH ligand followed by binding of acetate to generate intermediate **18** (Scheme 3.12). Subsequent chloride dissociation and re-association of the pyridine arm would then yield **15**.



We first sought to detect **15** at low temperature using ¹H NMR spectroscopy. Treatment of a CD₂Cl₂ solution of **8** with 3 equiv of Bu₄NOAc at -20 °C resulted in the formation of a new species with spectroscopic features consistent with **15** (Scheme 3.13). This compound was unstable to isolation, and underwent rapid C-H activation to form **12** upon warming to 0 °C. As such, **15** could only be characterized *in situ* by 1D ¹H NMR spectroscopy as well as 2D ¹H/¹H gCOSY and NOESY. Several diagnostic spectral features support the assignment of this species as a mono-acetate complex. Most importantly, the ¹H NMR spectrum clearly shows that this intermediate lacks a plane of symmetry, suggesting that only one chloride ligand has undergone ligand exchange with

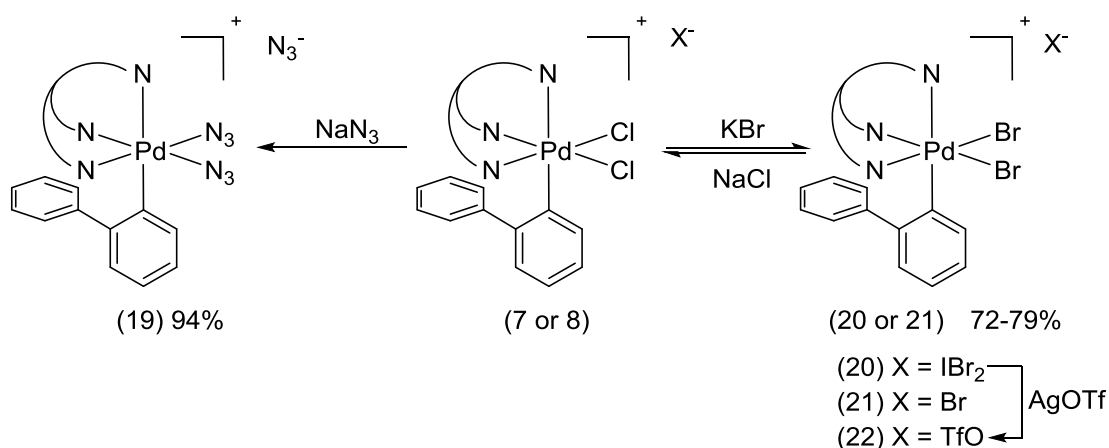
acetate. The observed exchange of only one of the chloride ligands is likely due to the possibility of κ^2 binding of the acetate to the cationic Pd^{IV} center (Scheme 3.13).¹⁷ This binding mode would inhibit association of a second acetate.

Scheme 3.13 Detection of $[(\text{Py}_3\text{CH})\text{Pd}^{\text{IV}}([\text{1,1'-biphenyl-2-yl})(\text{Cl})(\text{OAc})]^+$ by NMR



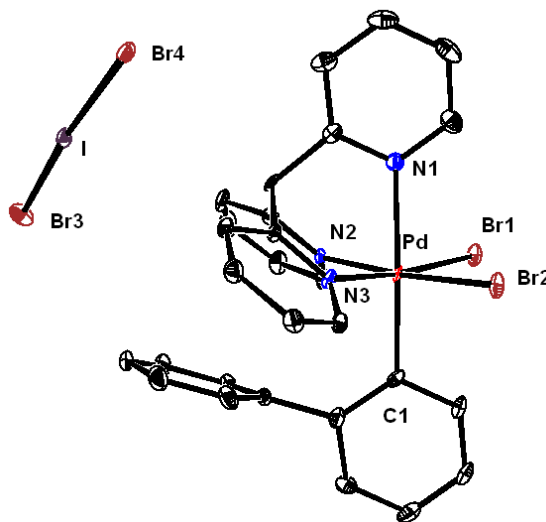
In order to gain further insights into ligand exchange processes at **8**, we examined ligand substitution reactions with other nucleophilic anions. As shown in Scheme 3.14, complexes **7** and **8** also undergoes facile ligand exchange with both bromide and azide to generate stable products **19-21**.

Scheme 3.14 Preparation of Pd^{IV} bromide and azide complexes



Complexes **19-22** were characterized by conventional 1D and 2D NMR techniques and by HRMS. All of these compounds show C_s symmetry, which indicates that both chloride ligands have been exchanged. Notably, the ^1H NMR spectrum of **19** shows several equilibrating species, suggesting that it exists as a mixture of conformational and configurational isomers (*vide infra* for further discussion). In contrast, the ^1H NMR spectra of **20-22** are each consistent with the presence of a single major isomer in solution. These latter spectra are extremely similar to that of **8**. The identity of dibromide complex **20** was further corroborated by a single crystal X-ray diffraction analysis, and the structure is shown in Figure 3.5.

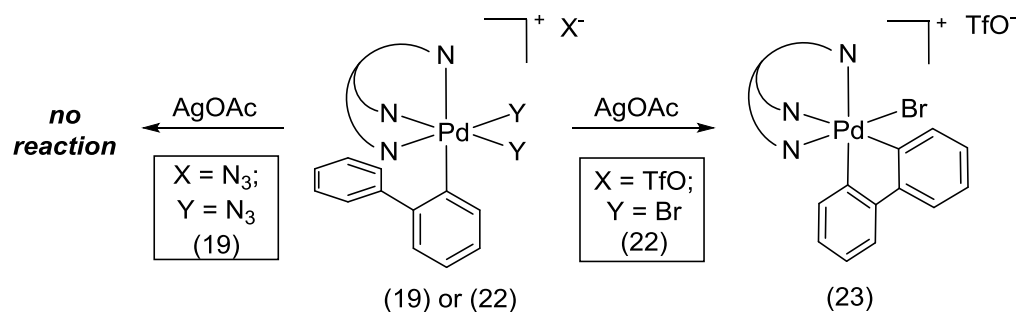
Figure 3.5 ORTEP drawing of $[(\text{Py}_3\text{CH})\text{Pd}^{\text{IV}}([\text{1,1}'\text{-biphenyl}]\text{-2-yl})(\text{Br})_2][\text{IBr}_2]$



Thermal ellipsoids are drawn at 50% probability. Hydrogen atoms are omitted for clarity. Selected bond lengths (\AA): Pd-C(1) 2.092(3), Pd-Br(1) 2.427, Pd-N(1) 2.198, Pd-N(2) 2.070. Selected bond angles (deg): N(2)-Pd-Br(1) 88.75, Br(1)-Pd-Br(2) 89.71, Br(2)-Pd-N(3) 89.16, N(3)-Pd-N(2) 91.87, N(1)-Pd-C(1) 177.51.

The chloride-to-bromide ligand exchange is readily reversible, and **20-21** reacted rapidly (within 5 min at 25 °C) with aqueous NaCl to regenerate **7** or **8** (Scheme 3.14). The presence of bromide ligands did not alter the reactivity of Pd^{IV} center towards acetate-promoted C–H activation. For example, the reaction of **22** with 4 equiv of AgOAc resulted in clean C–H cleavage to afford cyclometalated product **23** in 53% isolated yield (Scheme 3.15). In contrast, the equilibrium for chloride-to-azide exchange appears to lie far to the right, as no reaction was observed upon treatment of **19** with a large excess of aqueous NaCl. In addition, the treatment of azide complex **19** with AgOAc returned only unchanged starting material (Scheme 3.15).

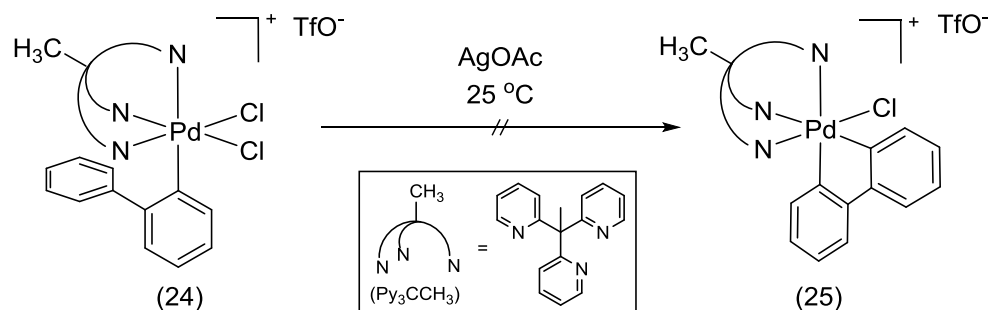
Scheme 3.15 Preparation of [(Py₃CH)Pd^{IV}([1,1'-biphenyl]-2,2'-diyl)(Br)][TfO]



We noted that both the proposed ligand substitution (step 1 in Scheme 3.11) as well as the configurational isomerization (step 3 in Scheme 3.11) involve reversible dissociation of one arm of the Py₃CH ligand. We thus hypothesized that these two steps (and thus the overall C–H activation process) would be slowed significantly by replacing the Py₃CH ligand with Py₃CCH₃ (complex **24** in Scheme 3.16). The additional methyl group in Py₃CCH₃ is expected to render **24** more rigid than Py₃CH, thus potentially slowing both ligand substitution and configurational isomerization.

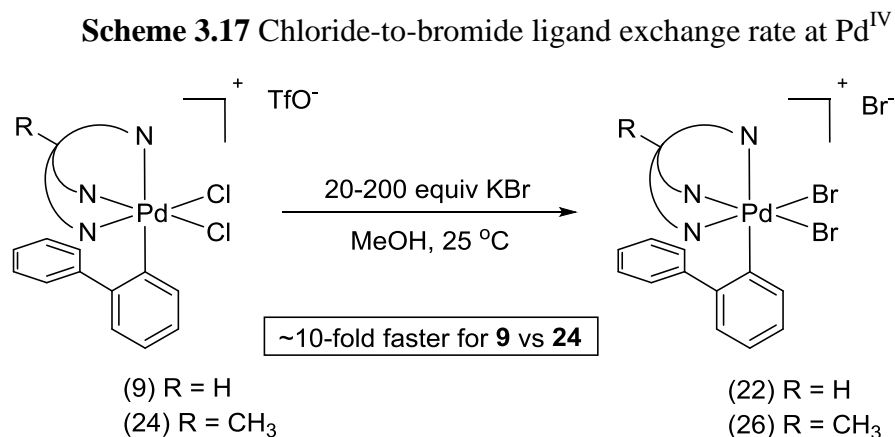
Complex **24** was synthesized using a similar procedure to that for **9** (see Experimental Section for details). As predicted, this complex showed dramatically reduced reactivity towards acetate-assisted C–H activation. Indeed, as shown in Scheme 3.16, the treatment of **24** with AgOAc or aqueous KOAc at room temperature did not lead to cyclometalation to form **25**. Instead, these conditions resulted in slow (over 1 h) decomposition of **24** to generate a complex mixture of products. These results suggest that ligand substitution and/or configurational isomerization are likely greatly impeded in this system; as such, competing decomposition pathways predominate.

Scheme 3.16 Reaction of $[(\text{Py}_3\text{CCH}_3)\text{Pd}^{\text{IV}}(\text{biphenyl-2,2}'\text{-diyl})(\text{Br})][\text{TfO}]$ with AgOAc



To directly compare ligand substitution at **24** and **9**, we studied the reaction of both complexes with KBr (Scheme 3.17). At room temperature, these reactions were too fast to be monitored by NMR spectroscopy, but they could be followed via UV-Vis spectroscopy based on the appearance of an absorbance band at 480 nm. Likely due to the presence of multiple steps with similar rate constants the kinetic behavior of these systems is complex. Despite this complexity, the experiments show that, under otherwise identical reaction conditions, ligand substitution of Cl for Br at **9** proceeds to completion

approximately 10-fold faster than the analogous transformation at **24**. This is consistent with our predications about the increased rigidity of Py₃CCH₃ versus Py₃CH.

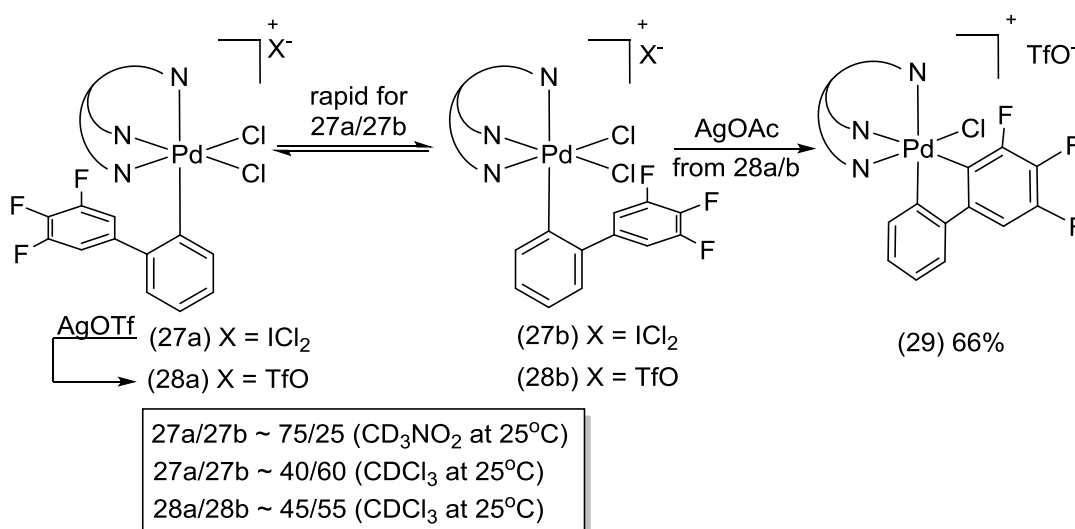


3.6 Rotation about the Pd^{IV}-C_{Aryl} Bond

As discussed above, complexes **7-9** were obtained as a single conformer with respect to rotation about the Pd-biphenyl bond. The favored conformation has the biphenyl ligand positioned under the Py₃CH. We hypothesize that this conformation is stabilized by π -stacking between the electron rich phenyl group of the biphenyl and the electron deficient pyridines. Thus, in an effort to disrupt this π - π interaction, we synthesized a complex with three electron withdrawing fluorine substituents on the biphenyl ligand (**27**). This perturbation has the predicted effect, and the 1D ¹H NMR and 2D ¹H/¹H ROESY NMR spectra of **27** show that this compound exists as a mixture of two C_s symmetric conformational isomers **27a** and **27b** (**27a:27b** = 40:60 in CDCl₃, Scheme 3.18) which interconvert on the EXSY time scale.¹⁸ Interestingly, the ratio of **27a:27b** is solvent dependent. While **27a** is the major isomer in CD₃NO₂ (**27a:27b** = 75:25), **27b** predominates in less polar CDCl₃ (**27a:27b** = 40:60). These results show that

rotation around the Pd–aryl bond is fast in **27** and that both conformations are readily accessible at room temperature. The treatment of **27a/27b** with AgOTf resulted in clean formation of the corresponding triflate complex **28** as a mixture of two isomers **28a** and **28b** (**28a:28b** = 45:55 in CDCl₃). Surprisingly, **28a** and **28b** do not interconvert on the NMR time scale (as determined by a 2D ¹H/¹H ROESY experiment in CDCl₃ at 25 °C). This observation indicates that the counterion can influence flexibility of the cationic Pd^{IV} core.

Scheme 3.18 Rotation about the Pd^{IV}–C_{Aryl} bond

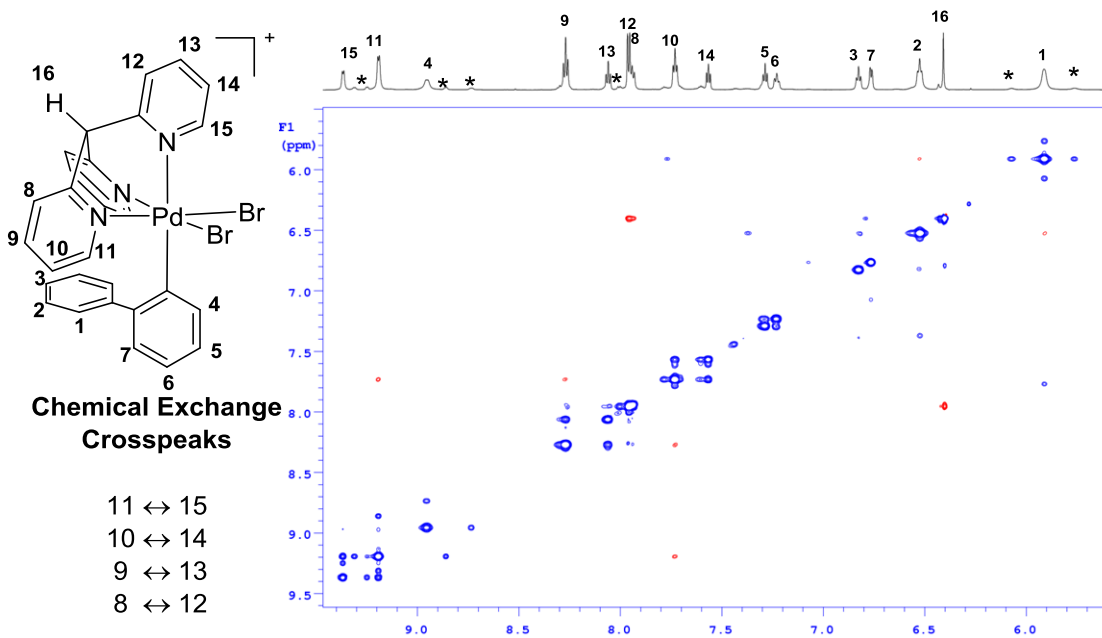


As shown in Scheme 3.18, both complex **27** and its triflate counterpart **28** participate in acetate-assisted C–H activation in a similar fashion to **7-9**. For example, the treatment of **28a/b** with 4 equiv of AgOAc in dry CHCl₃ afforded complex **29** in 66% isolated yield. Overall this series of experiments demonstrates the feasibility of rotation about the Pd^{IV}–aryl bond in complexes that undergo acetate-assisted C–H activation (and that are closely related to the parent compounds **7-9**).

3.7 Configurational Isomerization at Pd^{IV} via Berry Pseudorotation

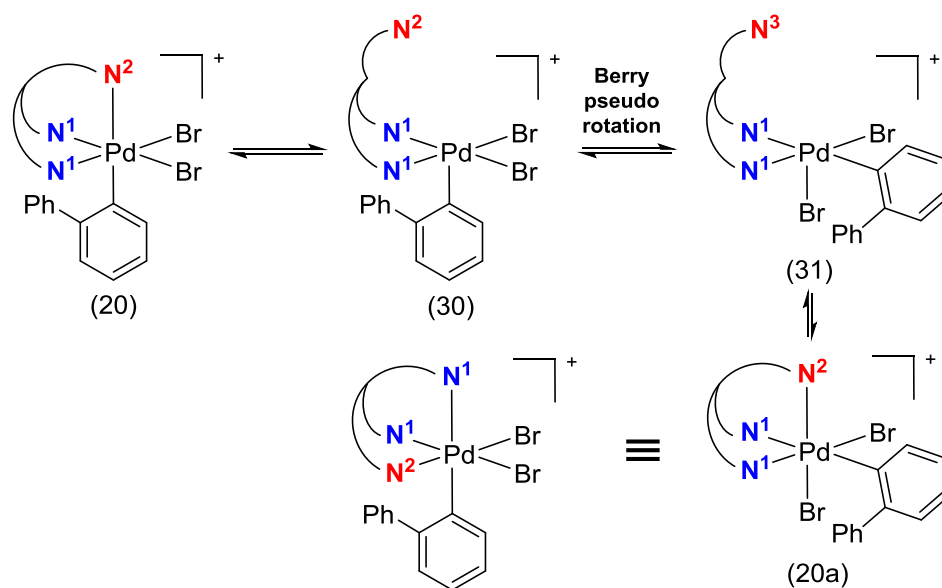
The viability of the proposed configurational isomerization process was first probed by EXSY NMR experiments in complexes of general structure [(Py₃CH)Pd(biphenyl)Y₂]⁺.¹⁸ Only one isomer was observed in the ¹H and ¹³C NMR spectra of dichloride complexes **7-9**; furthermore, ¹H/¹H ROESY and NOESY experiments show that **7-9** are configurationally stable on the NMR timescale. In contrast, as shown in Figure 3.6, the ¹H/¹H ROESY spectrum of dibromide complex **20** shows chemical exchange crosspeaks between the two equivalent pyridine rings trans to the bromides and the one distinct pyridine ring trans to the carbon.

Figure 3.6 ¹H/¹H ROESY spectrum of [(Py₃CH)Pd^{IV}([1,1'-biphenyl]-2-yl)(Br)₂][IBr₂]



(spectrum acquired at 500 MHz)

Scheme 3.19 Isomerization of $[(\text{Py}_3\text{CH})\text{Pd}^{\text{IV}}([\text{1,1'-biphenyl-2-yl})(\text{Br})_2][\text{IBr}_2]$



It is well documented that six-coordinate complexes can undergo inversion of configuration at the metal by bond-rupture mechanism via formation of a configurationally labile five-coordinate intermediate.¹⁹ As such we propose that the observed exchange in complex **20** is the result of the pathway depicted in Scheme 3.19. Here, initial dissociation of one arm of the facial tridentate pyridine ligand (labeled N² in Scheme 3.19) affords the 5-coordinate complex **30**, which can undergo configurational isomerization to form **31** via Berry pseudorotation.²⁰ N² reassociation would then afford product **20a**. Importantly, complexes **20** and **20a** are chemically equivalent, with the sole difference that N² has swapped places with one of the N¹ groups. The configurational isomerization pathway proposed in Scheme 3.19 is further corroborated by the observation of broad, low intensity resonances in the ¹H NMR and ¹H/¹H ROESY spectra of **20** (labeled with asterisks in Figure 3.6). This species is in exchange with **20** on the NMR timescale (based on ¹H/¹H ROESY analysis). Although the broad signals make it difficult to characterize definitively, we propose that this may be an intermediate like **30**

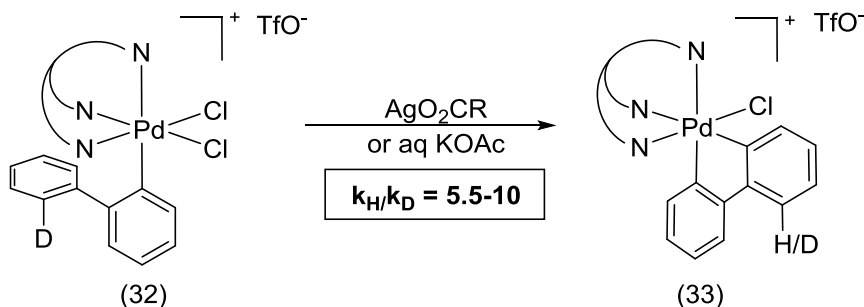
or **31**. We disfavor formulation of this species as an octahedral tribromide complex based on the fact that the addition of 2-4 equiv of NBu_4Br did not increase the equilibrium population of this compound in solution. Interestingly, no chemical exchange crosspeaks were detected in $^1\text{H}/^1\text{H}$ ROESY spectrum for $[(\text{Py}_3\text{CH})\text{Pd}(\text{biphenyl})\text{Br}_2][\text{TfO}]$ (**22**). This observation demonstrates the influence of the outer-sphere counterion on the binding properties of the Py_3CH ligand. A possible explanation to this observation is that hydrogen bonding of IBr_2^- to the Py_3CH ligand in complex **20** promotes dissociation of one pyridine ring and stabilizes a pentacoordinate intermediate like **32** or **33**.

3.8 Acetate Assisted C–H Cleavage at Palladium(IV)

A series of isotope effect studies were conducted to (a) gain insights into the nature of the transition state for C–H cleavage and (b) establish whether C–H bond activation is involved in the rate-determining step of the overall transformation.²¹ Mono-deuterated complex **32** was synthesized by analogy to the procedure shown in Scheme 3.5.²² Complex **32** was then treated with various carboxylate sources to yield the cyclopalladated product **33** (Scheme 3.20). ^1H NMR analysis of **33** showed that cleavage of the C–H bond occurred in preference to cleavage of the C–D bond with all of the carboxylates examined. Accurate values for the intramolecular KIE were obtained from ESI-MS mass spectrometric analysis. All of the carboxylate sources tested [KOAc (aqueous), AgOAc , AgOPiv , AgO_2CCF_3 , and $\text{AgO}_2\text{CC}_6\text{H}_5$] afforded product **33** with an intramolecular $k_{\text{H}}/k_{\text{D}}$ between 9 and 12 at 25 °C. Increasing the reaction temperature to 55 °C and lowering it to 0 °C had a relatively small influence on the observed isotope effect. For example, with AgOAc , $k_{\text{H}}/k_{\text{D}} = 10$ at 0 °C and 7 at 55 °C. These latter results indicate

that quantum tunneling does not contribute significantly to the isotope effect in this system.

Scheme 3.20 Determination of intramolecular KIE

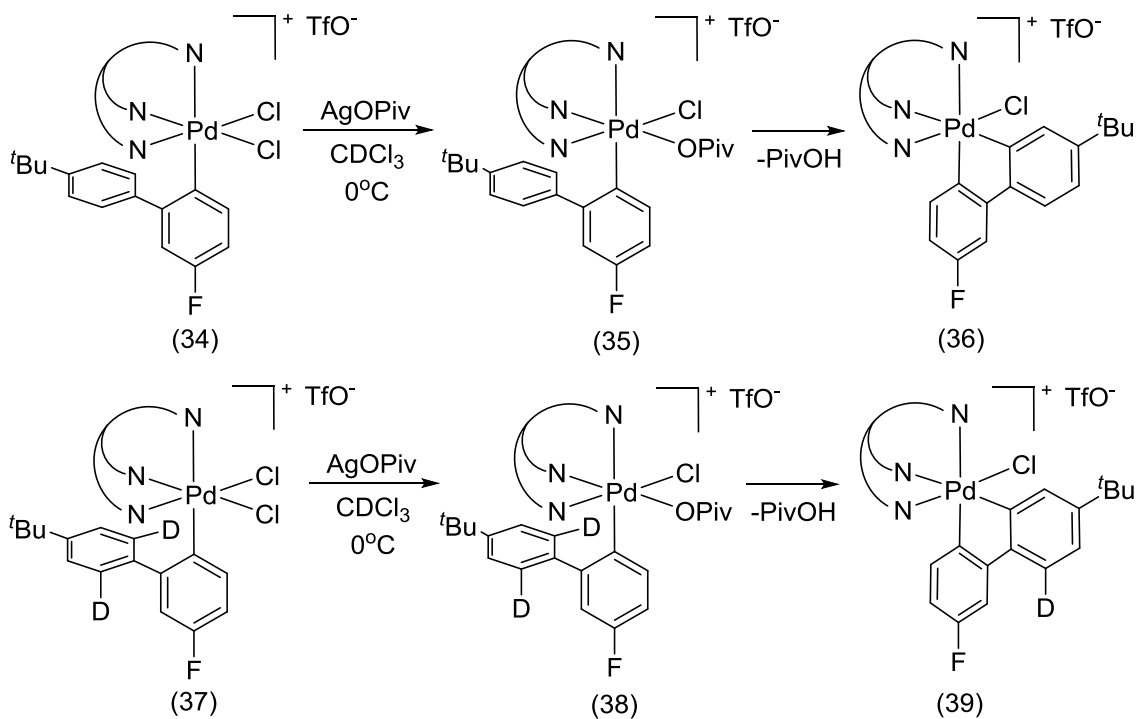


Overall, the observed large magnitude of the intramolecular isotope effect is indicative of central transition state for C–H cleavage, suggesting that the proton is transferred between two sites of similar basicity.²³ These observed values are similar to those reported for CMD C–H cleavage at Pd(II)^{12d} and Ir(III)^{14b} centers (values in the literature vary from 5-7). An intermolecular KIE of 6 was determined also for benzene mercuration, which is proposed to proceed via a cyclic transition state with acetate acting as an intramolecular base.²⁴

The intermolecular KIE for this reaction was next determined using substrates **34** and **37** (Scheme 3.21). The *t*-butyl group was introduced on the biphenyl ligand of **34** and **37** in order to enhance solubility (essential for obtaining quantitative rate data). The fluorine substituent was added to enable monitoring of reaction rate by ¹⁹F NMR spectroscopy. The use of Bu₄NOAc or AcOH/Et₃N resulted in formation of cyclopalladated products **38** or **41** in only 65% and 35% NMR yield, respectively. Competitive formation of unidentified side products did not allow us to extract reliable

rate constants for CH activation under homogenous reaction conditions with Bu_4NOAc therefore, for kinetic studies we switched to AgOPiv as carboxylate source. Thus, treatment of **34** and **37** with 3 equiv of AgOPiv resulted in smooth conversion to cyclopalladated products **36** and **39**.

Scheme 3.21 Determination of intermolecular KIE

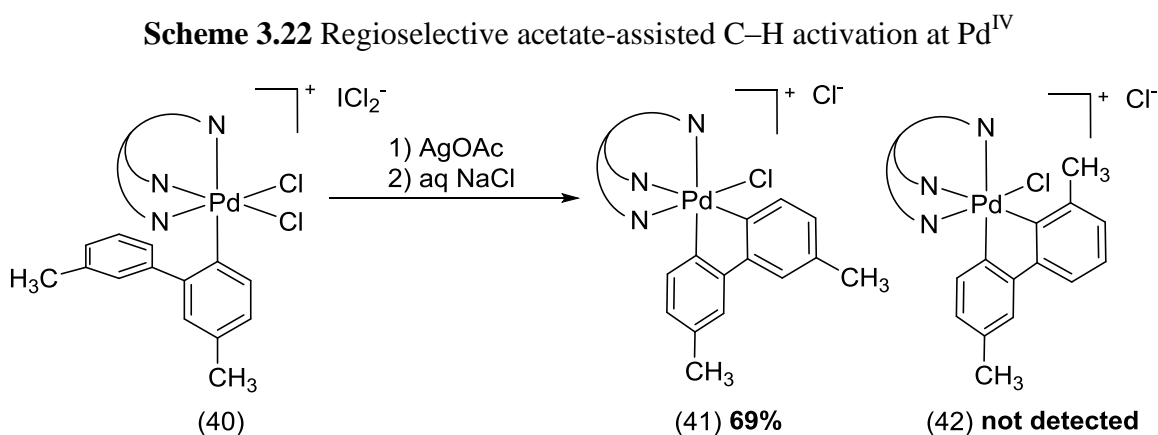


The progress of these reactions was monitored by ^{19}F NMR spectroscopy. After 5 min, both substrates **34** and **37** underwent nearly quantitatively conversion to the mono-pivalate intermediates **35** and **38**. Both intermediates **35** and **38** then underwent relatively slow conversion to **36** and **39**, respectively. The overall reaction rates for substrates **34** and **37** under these conditions were the same within the error of measurement. These observations show that that the rate of the overall transformation is not limited by the rate

of the ligand exchange or the availability of the carboxylate ligand (due to low solubility of AgOPiv) and that conformational and configurational isomerization is likely the rate-limiting step in this transformation.

3.9 Regioselectivity of C–H Activation at Palladium(IV)

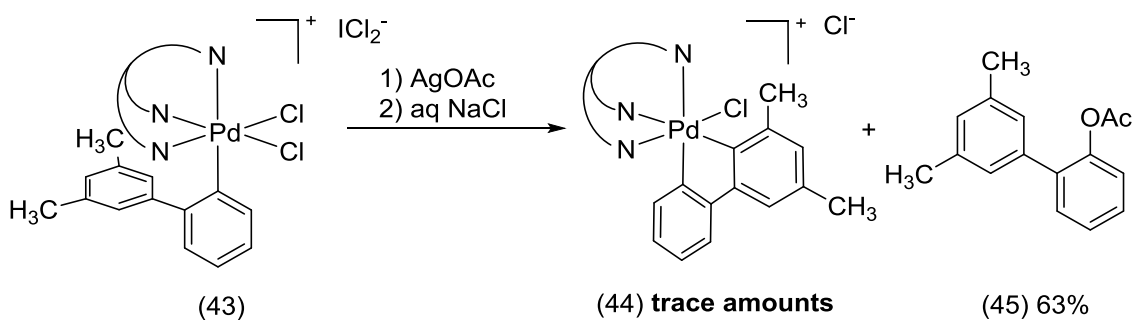
So far we we have conducted a number of experiments to elucidate details of acetate-assisted C–H activation at Pd^{IV} (Scheme 3.11). It was discussed previously that some of the Pd^{IV} mediated C–H functionalization reactions proceed with remarkably high regioselectivities even when substrate does not contain directing groups. Such high regioselectivities are likely due either to unique electronic properties of Pd^{IV} or to steric requirements of octahedral ligand environment at Pd^{IV} center. It must be noted that palladium carboxylates are typically used as catalysts in Pd^{IV} mediated C–H functionalization reactions therefore, it is plausible that the carboxylate ligand also plays role in ensuring high regioselectivities. In order to gain insight into the origin of this phenomenon, we decided to probe regioselectivity of C–H activation also in our system.



We first chose to investigate the reactivity of complex **40** which contains two electronically similar sites for C–H cleavage but one of which is sterically hindered by a methyl group (Scheme 3.22). Treatment of **40** with AgOAc followed by workup with aqueous NaCl afforded complex **41** in 69% isolated yield. No regioisomer **42** was detected in crude reaction mixture or in isolated product **41**.

We next synthesized and investigated complex **43** which has both C–H activation sites hindered by methyl groups (Scheme 3.23). Treatment of **43** with AgOAc afforded only trace amounts of C–H activation product **44** which was detected by High-resolution Mass Spectrometry (HRMS). In this reaction, acetoxybiaryl **45** was isolated as major product in 63% yield. Compound **45** is likely a result of C_{Aryl}–OAcetyl bond forming reductive elimination from Pd^{IV} center. Interestingly, while the C–H activation reaction investigated in this chapter tolerates fluorine substituent next to the reaction site (Scheme 3.18), methyl groups shut down C–H cleavage completely.

Scheme 3.23 C–O bond forming reductive elimination process at Pd^{IV} center



Experiments shown in Scheme 3.22 and Scheme 3.23 demonstrate that in Py₃CH supported complexes high regioselectivity of C–H activation is a result of steric requirements set by the octahedral ligand sphere of Pd^{IV}. While it cannot be universally

generalized to all systems, it is highly likely that steric effects play a major role also in determining regioselectivity in many catalytic C–H functionalization reactions mediated by Pd^{IV}.

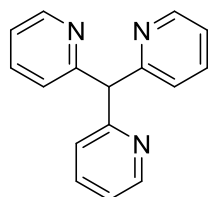
3.10 Conclusions

A model system for investigation of C–H activation at a Pd^{IV} center was developed. As discussed above, C–H activation in this system likely proceeds through a pathway involving four key steps: (1) ligand exchange, (2) Pd–C_{Aryl} bond rotation, (3) configurational isomerization via Berry pseudorotation, and (4) C–H cleavage via a concerted metallation deprotonation (CMD) transition state with an acetate ligand serving as an internal base. The feasibility of each of these steps is supported by the experiments presented above. A key feature of the investigated [(Py₃CH)Pd(biphenyl)Cl₂]X system is the semilabile tridentate tris(2-pyridil)methane ligand. This ligand stabilizes octahedral cationic Pd^{IV} centers towards reductive elimination. However, coordinatively unsaturated species can be formed via dissociation of a pyridine arm of the ligand. This ligand dissociation is believed to facilitate both the ligand exchange as well as the configurational isomerization steps. Importantly, the extremely mild conditions necessary for acetate assisted C–H cleavage at Pd^{IV} centers renders this process attractive for applications in catalytic C–H functionalization processes mediated by high oxidation state palladium.

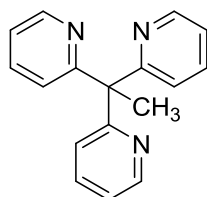
3.11 Experimental Section

General Procedures. All syntheses were conducted under ambient atmosphere unless otherwise stated. All reagents were purchased from commercial sources and used as received. Tetrahydrofuran, dichloromethane and diethyl ether were purified using an Innovative Technologies (IT) solvent purification system consisting of a copper catalyst, activated alumina, and molecular sieves. NMR spectra were acquired using 400, 500 and 700 MHz Varian spectrometers. All $^1\text{H}/^1\text{H}$ NOESY and $^1\text{H}/^1\text{H}$ ROESY correlation spectra were acquired on a 500 MHz instrument. ^1H , ^{19}F and ^{13}C chemical shifts are reported in parts per million (ppm) relative to TMS. ^1H and ^{19}F multiplicities are reported as follows: singlet (s), doublet (d), triplet (t), quartet (q) and multiplet (m).

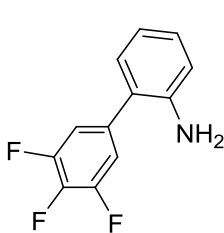
3.11.1 Synthesis and Characterization of Ligands and Organic Compounds



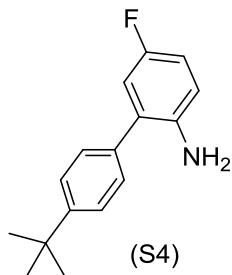
(S1) Py_3CH



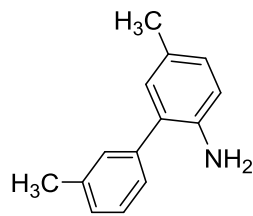
(S2) Py_3CCH_3



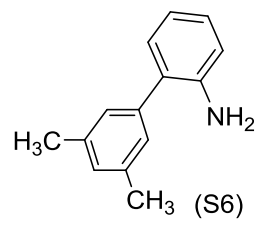
(S3)



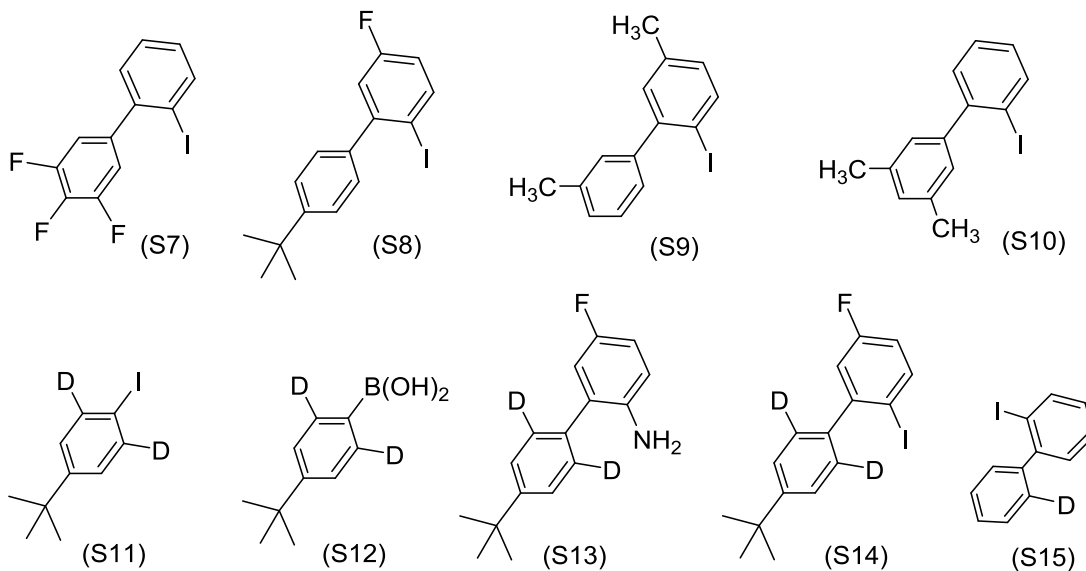
(S4)



(S5)



(S6)

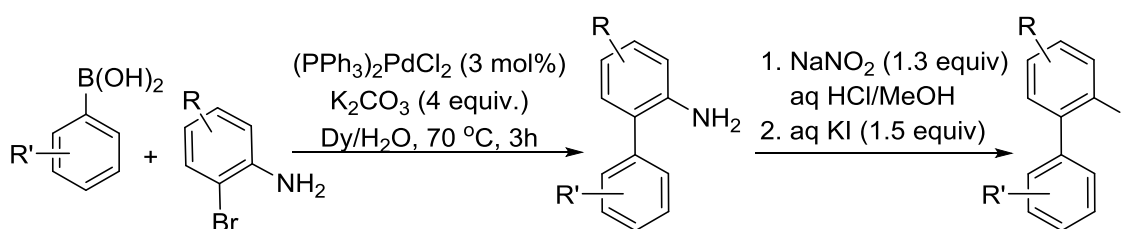


Preparation of tris(pyridin-2-yl)methane (S1). Under an atmosphere of nitrogen, butyllithium (2.5 M in hexanes, 68 mL, 170 mmol) was slowly added to a cooled ($-78\text{ }^{\circ}\text{C}$) solution of 2-picoline (14.0 g; 150 mmol) in dry THF (250 mL). The resulting suspension was warmed to $0\text{ }^{\circ}\text{C}$ over the period of 1 h, and then neat 2-fluoropyridine (23.7 mL; 275 mmol) was slowly added over the period of 20 min. Next, the reaction was heated to $65\text{ }^{\circ}\text{C}$ for 3 h and then it was poured into water (300 mL) and the resulting mixture was extracted with EtOAc ($3 \times 100\text{ mL}$). The combined organic phases were washed with brine (200 mL) and dried over anhydrous MgSO_4 . The volatiles were removed under reduced pressure. Fractional vacuum distillation of the residue ($180\text{--}230\text{ }^{\circ}\text{C}$; $\sim 0.05\text{ mmHg}$) afforded di(pyridine-2-yl)methane (7.55 g; 30%) as a yellowish oil and tris(pyridine-2-yl)methane (5.23 g; 14%) as a pale brown solid. $\text{Mp} = 92\text{--}93\text{ }^{\circ}\text{C}$. $^1\text{H NMR}$ (CDCl_3): δ 8.58 (d, $J = 4.9\text{ Hz}$, 3H), 7.62 (td, $J = 7.8$ and 1.7 Hz , 3H), 7.31 (d, $J = 7.8\text{ Hz}$, 3H), 7.13 (m, 3H), 5.98 (s, 1H). $^{13}\text{C}\{^1\text{H}\}$ NMR (CDCl_3): δ 161.07, 149.49,

136.54, 124.14, 121.73, 64.07. HRMS electrospray (m/z): [M + H]⁺ calcd for C₁₆H₁₄N₃, 248.1182; Found, 248.1185.

Preparation of 1,1,1-tris(pyridin-2-yl)ethane (S2). Under an atmosphere of nitrogen, LDA (1.5 M solution in THF, 5.5 mL, 8.2 mmol) was slowly added to a cooled (-78 °C) solution of tris(pyridine-2-yl)methane (S1) (1.70 g; 6.9 mmol) in dry THF (50 mL). The resulting solution was warmed to 20 °C over the period of 1 h, and then neat methyl iodide (0.87 mL; 14 mmol) was added. Reaction mixture was stirred at 20 °C for 2 h and then volatiles were removed under reduced pressure. The residue was purified by flash chromatography on a silica gel column (mobile phase: hexanes/EtOAc with gradient from 4/1 to 1/1) to yield 1.21g (67%) of a yellowish solid. Mp = 87-88 °C. ¹H NMR (CDCl₃): δ 8.58 (m, 3H), 7.57 (td, *J* = 8.1 and 1.4 Hz, 3H), 7.01 (m, 6H), 2.33 (s, 3H). ¹³C NMR (CDCl₃): δ 165.88, 148.82, 135.99, 123.48, 121.22, 60.11, 27.33. HRMS electrospray (m/z): [M + H]⁺ calcd for C₁₇H₁₆N₃, 262.1339; Found, 262.1339.

Scheme 3.24 General procedure for the synthesis of iodobiphenyls



General procedure 1: Synthesis of 2-arylanilines. A flask was charged with corresponding 2-bromoaniline (10.0 mmol), boronic acid (11.0 mmol), K₂CO₃ (40 mmol) and (PPh₃)₂PdCl₂ (210 mg; 0.30 mmol). Dioxane (40 mL) and water (70 mL) were then added. Reaction mixture was heated to 70 °C for 3 h and then cooled to r.t. The product

was extracted from the biphasic mixture with EtOAc (3 × 50 mL). The combined organic phases were washed with brine (100 mL) and dried over anhydrous MgSO₄. The solvent was removed under reduced pressure and the residue was purified by flash chromatography on a silica gel column (mobile phase: hexanes/EtOAc with gradient from 10/0 to 10/2) to yield product as a colorless oil or colorless crystals.

Preparation of 3',4',5'-trifluoro-(1,1'-biphenyl)-2-amine (S3). S3 was obtained according to the general procedure **1** in 84% yield as colorless crystals. Mp = 57-58 °C. ¹H NMR (CDCl₃): δ 7.18 (td, *J* = 7.8 and 1.5 Hz, 1H), 7.10 (dd, *J* = 8.3 and 6.6 Hz 2H), 7.06 (dd, *J* = 7.5 and 1.5 Hz, 1H), 6.82 (td, *J* = 7.5 and 1.0 Hz, 1H), 6.76 (dd, *J* = 8.1 and 0.9 Hz, 1H), 3.73 (bs, 2H). ¹³C NMR (CDCl₃): δ 148.44 (ddd, *J* = 250.7, 19.5 and 4.1 Hz), 140.35, 136.02 (dt, *J* = 252.0 and 15.3 Hz), 132.61 (td, *J* = 8.2 and 4.8 Hz), 127.24, 126.55, 121.51, 116.00, 113.08, 110.31 (dd, *J* = 16.4 and 4.1 Hz). ¹⁹F NMR (CDCl₃): δ -133.99 (dd, *J* = 21.6 and 8.3 Hz, 2F), -162.35 (tt, *J* = 19.9 and 6.6 Hz, 1F). HRMS electrospray (m/z): [M + H]⁺ calcd for C₁₂H₈F₃N, 224.0682; Found, 224.0679.

Preparation of 4'-(tert-butyl)-5-fluoro-(1,1'-biphenyl)-2-amine (S4). S4 was obtained according to the general procedure **1** in 87% yield as a colorless oil. ¹H NMR (CDCl₃): δ 7.48 (d, *J* = 8.5 Hz, 2H), 7.38 (d, *J* = 8.5 Hz, 2H), 6.87 (m, 2H), 6.69 (dd, *J* = 8.5 and 4.9 Hz, 1H), 3.67 (br, 2H), 1.37 (s, 9H). ¹³C NMR (CDCl₃): δ 156.32 (d, *J* = 236.4 Hz), 150.53, 139.68 (d, *J* = 2.0 Hz), 135.56, 128.69 (d, *J* = 6.9 Hz), 128.53, 125.83, 116.65 (d, *J* = 22.5 Hz), 116.36 (d, *J* = 8.2 Hz), 114.60 (d, *J* = 22.5 Hz), 34.61, 31.34. ¹⁹F NMR (CDCl₃): δ -127.06 (td, *J* = 8.2 and 4.1 Hz, 1F). HRMS electrospray (m/z): [M + H]⁺ calcd for C₁₆H₁₈FN, 244.1496; Found, 244.1501.

Preparation of 4,3'-dimethyl-(1,1'-biphenyl)-2-amine (S5). S5 was obtained according to the general procedure **1** in 88% yield as a colorless oil. ^1H NMR (CDCl_3 at $25\text{ }^\circ\text{C}$): δ 7.44 (td, $J = 7.5$ and 2.2 Hz, 1H), 7.41-7.36 (m, 2H), 7.27 (d, $J = 7.3$ Hz, 1H), 7.10-7.07 (m, 2H), 6.77 (dd, $J = 8.5$ and 2.4 Hz, 1H), 3.73 (bs, 2H), 2.52 (s, 3H), 2.41 (s, 3H). $^{13}\text{C}\{^1\text{H}\}$ NMR (CDCl_3 at $25\text{ }^\circ\text{C}$): δ 141.14, 139.80, 138.47, 131.04, 129.94, 129.05, 128.76, 127.96, 127.93, 127.80, 126.21, 115.90, 21.60, 20.57. HRMS electrospray (m/z): $[\text{M} + \text{H}]^+$ calcd for $\text{C}_{14}\text{H}_{16}\text{N}$, 198.1277; Found, 198.1279.

Preparation of 3',5'-dimethyl-(1,1'-biphenyl)-2-amine (S6). S6 was obtained according to the general procedure **1** in 94% yield as a colorless oil. ^1H NMR (CDCl_3 at $25\text{ }^\circ\text{C}$): δ 7.21-7.17 (m, 2H), 7.14 (s, 2H), 7.06 (s, 1H), 6.88 (t, $J = 7.5$ Hz, 1H), 6.80 (d, $J = 7.8$ Hz, 1H), 3.84 (bs, 2H), 2.43 (s, 6H). $^{13}\text{C}\{^1\text{H}\}$ NMR (CDCl_3 at $25\text{ }^\circ\text{C}$): δ 143.54, 139.50, 138.38, 130.41, 128.85, 128.36, 127.98, 126.88, 118.63, 115.59, 21.42. HRMS electrospray (m/z): $[\text{M} + \text{H}]^+$ calcd for $\text{C}_{14}\text{H}_{16}\text{N}$, 198.1277; Found, 198.1285.

General procedure 2: Synthesis of iodobiphenyls. Water (10 mL) and conc. aq. HCl (5 mL) were added to a solution of the corresponding 2-arylaniline (6.0 mmol) in MeOH (20 mL). The resulting solution was then cooled to $0\text{ }^\circ\text{C}$ and NaNO_2 (550 mg, 8.0 mmol) in H_2O (3 mL) was added slowly over the period of 5 minutes. The reaction mixture was stirred at $0\text{ }^\circ\text{C}$ for 15 minutes and KI (1.5 g; 9 mmol) in H_2O (10 mL) was then added over the period of 5 minutes. Reaction mixture was stirred for 20 minutes at $20\text{ }^\circ\text{C}$ and then it was heated to $60\text{ }^\circ\text{C}$ for 30 minutes. To the dark brown suspension was then added aqueous Na_2SO_3 (8 g in 40 mL H_2O) and the resulting mixture was extracted with EtOAc (3×50 mL). The combined organic phases were washed with brine (100 mL) and dried over anhydrous MgSO_4 . The volatiles were removed under reduced

pressure and the residue was purified by flash chromatography on a silica gel column (mobile phase: 100% hexanes) to yield product as a colorless oil.

Preparation of 3',4',5'-trifluoro-2-iodo-1,1'-biphenyl (S7). S7 was obtained according to the general procedure 2 in 73% yield as a colorless oil. ¹H NMR (CDCl₃): δ 7.94 (dd, *J* = 8.0 and 1.2 Hz, 1H), 7.39 (td, *J* = 7.5 and 1.2 Hz, 1H), 7.24 (dd, *J* = 7.5 and 1.5 Hz, 1H), 7.07 (td, *J* = 7.8 and 1.7 Hz, 1H), 6.95 (dd, *J* = 8.2 and 6.5 Hz, 2H). ¹³C NMR (CDCl₃): δ 150.66 (ddd, *J* = 250.0, 9.5 and 4.0 Hz), 143.64, 139.80 (multiplet overlapping with singlet at 139.75), 139.75, 139.40 (dt, *J* = 252.7 and 15.0 Hz), 129.81, 129.71, 128.35, 113.80 (dd, *J* = 17.0 and 4.1 Hz), 97.79. ¹⁹F NMR (CDCl₃): δ -134.44 (dd, *J* = 21.5 and 8.3 Hz, 2F), 161.70 (tt, *J* = 21.5 and 6.6 Hz, 1F). HRMS electron impact (m/z): [M]⁺ calcd for C₁₂H₆F₃I, 333.9466; Found, 333.9459.

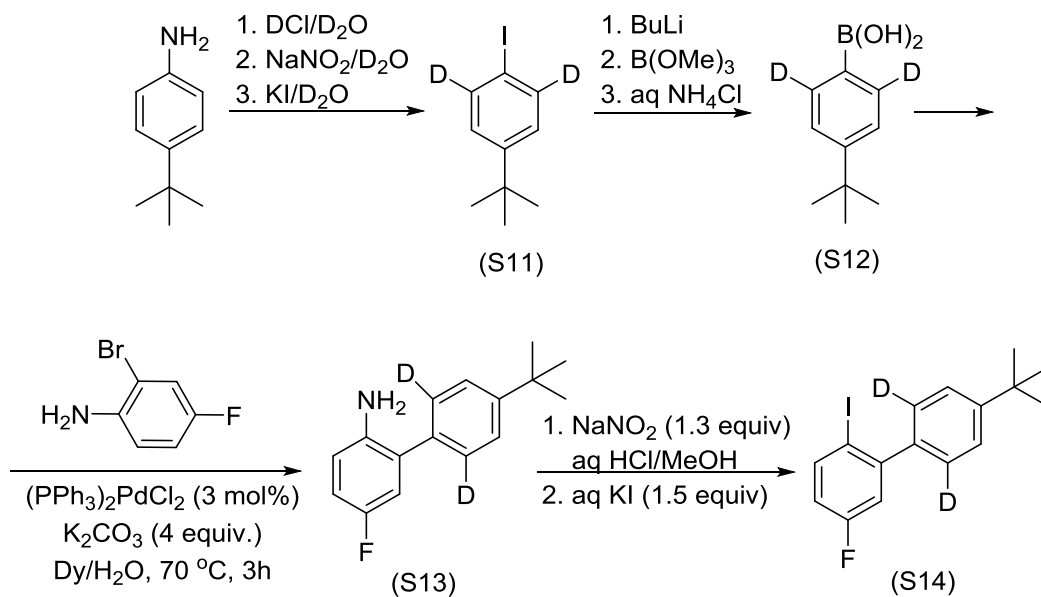
Preparation of 4-(tert-butyl)-5'-fluoro-2'-iodo-1,1'-biphenyl (S8). S8 was obtained according to the general procedure 2 in 73% yield as a colorless oil. ¹H NMR (CDCl₃): δ 7.88 (dd, *J* = 8.7 and 5.6 Hz, 1H), 7.45 (d, *J* = 8.3 Hz, 2H), 7.27 (d, *J* = 8.2 Hz, 2H), 7.05 (dd, *J* = 9.6 and 3.1 Hz, 1H), 6.79 (td, *J* = 8.2 and 2.9 Hz, 1H), 1.38 (s, 9H). ¹³C NMR (CDCl₃): δ 162.83 (d, *J* = 248.0 Hz), 151.00, 148.42 (d, *J* = 7.5 Hz), 140.63 (d, *J* = 7.5 Hz), 140.18, 128.70, 124.97, 117.47 (d, *J* = 22.5 Hz), 116.00 (d, *J* = 21.8 Hz), 51.51 (d, *J* = 2.7 Hz), 34.67, 31.36. ¹⁹F NMR (CDCl₃): δ -114.70 (m, 1F). HRMS electron impact (m/z): [M]⁺ calcd for C₁₆H₁₆FI, 354.0280; Found, 354.0275.

Preparation of 4,3'-dimethyl-2-iodo-1,1'-biphenyl (S9). S9 was obtained according to the general procedure 2 in 89% yield as a colorless oil. ¹H NMR (CDCl₃ at 25 °C): δ 7.87 (d, *J* = 8.2 Hz, 1H), 7.37 (t, *J* = 7.8 Hz, 1H), 7.26 (d, *J* = 7.5 Hz, 1H), 7.22-7.19 (m, 3H), 6.91 (d, *J* = 8.2 Hz, 1H), 2.48 (s, 3H), 2.39 (s, 3H). ¹³C{¹H} NMR (CDCl₃

at 25 °C): δ 146.57, 144.24, 139.28, 138.07, 137.54, 131.11, 130.01, 129.76, 128.32, 127.85, 126.44, 94.60, 21.59, 21.00. HRMS electron impact ionization (m/z): $[M]^+$ calcd for C₁₄H₁₃I, 308.0062; Found, 308.0057.

Preparation of 3',5'-dimethyl-2-iodo-1,1'-biphenyl (S10). S10 was obtained according to the general procedure 2 in 81% yield as a colorless oil. ¹H NMR (CDCl₃ at 25 °C): δ 7.95 (d, J = 8.0 Hz, 1H), 7.38 (t, J = 7.4 Hz, 1H), 7.30 (d, J = 7.5 Hz, 1H), 7.05 (s, 1H), 7.02 (t, J = 8.0 Hz, 1H), 6.97 (s, 2H), 2.39 (s, 6H). ¹³C{¹H} NMR (CDCl₃ at 25 °C): δ 146.86, 144.10, 139.42, 137.40, 130.04, 129.20, 128.59, 128.02, 127.08, 98.68, 21.38. HRMS electron impact ionization (m/z): $[M]^+$ calcd for C₁₄H₁₃I, 308.0062; Found, 308.0067.

Scheme 3.25 Synthesis of 2,6-dideutero-4-(*t*-butyl)-5'-fluoro-2'-iodobiphenyl (S14)



Preparation of 1,6-dideutero-4-(*tert*-butyl)-iodobenzene (S11). 4-*tert*-Butyl-aniline (6.0 g; 39.7 mmol) was heated in 10% DCl/D₂O (40 mL) to 100 °C under an inert atmosphere for 12 h. Volatiles were removed under reduced pressure and fresh portion of

DCI/D₂O (40 mL) was added and heating was continued for another 12 h. Reaction mixture was then cooled to 0 °C and NaNO₂ (3.45g; 50 mmol) in D₂O (15 mL) was slowly added over the period of 15 minutes. Reaction mixture was stirred at 0 °C for 15 minutes and KI (9.96 g; 60 mmol) in D₂O (25 mL) was then added over the period of 10 minutes. Reaction mixture was stirred for 20 minutes at 20 °C and then it was heated to 60 °C for 30 minutes. Aqueous Na₂SO₃ (20 g in 200 mL H₂O) was added to the resulting dark brown suspension and mixture was then extracted with EtOAc (3 × 100 mL). The combined organic phases were washed with brine (200 mL) and dried over anhydrous MgSO₄. The solvent was removed under reduced pressure and the residue was purified by flash chromatography on a silica gel column (mobile phase: 100% hexanes) to yield 9.80 g (94%) of a colorless oil. ¹H NMR (CDCl₃): δ 7.16 (s, 2H), 1.32 (s, 9H). ¹³C NMR (CDCl₃): δ 150.86, 136.74 (t, *J* = 25.2 Hz), 127.46, 90.40, 34.60, 31.20. HRMS electron impact (*m/z*): [M]⁺ calcd for C₁₀H₁₁D₂I, 262.0188; Found, 262.0194.

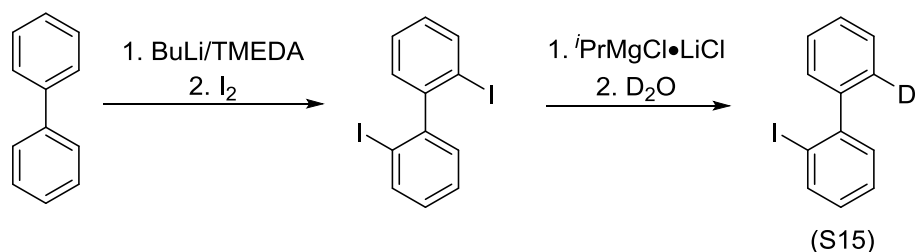
Preparation of (2,6-dideutero-4-(*tert*-butyl)phenyl)boronic acid (S12). Under the atmosphere of nitrogen butyllithium (2.5 M in hexanes, 9 mL, 22.5 mmol) was slowly added to a cooled (−78 °C) solution of 2,6-dideutero-4-(*tert*-butyl)-iodobenzene (**S11**) (5.5 g; 21 mmol) in dry THF (150 mL). Neat trimethylborate (5.6 mL; 50 mmol) was next slowly added over the period of 5 min. Reaction mixture was stirred at −78 °C for 2 h and then it was slowly warmed to 20 °C and kept at this temperature for 2 hours. Saturated aq NH₄Cl (100 mL) was then added and the resulting biphasic mixture was intensively stirred at r.t. for 2 hours. The reaction mixture was then extracted with Et₂O (3 × 100 mL). The combined organic phases were washed with brine (200 mL), dried over anhydrous MgSO₄ and the volatiles were removed under reduced pressure. The

resulting white solid (2.76 g; 73%) was used in the next step as is without characterization or further purification.

Preparation of 2',6'-dideutero-4'-(*tert*-butyl)-5-fluoro-(1,1'-biphenyl)-2-amine (S13). S13 was synthesized from (2,6-dideutero-4-(*tert*-butyl)phenyl)boronic acid (S12) according to the general procedure 1 in 96% yield (colorless oil). ¹H NMR (CDCl₃): δ 7.49 (br, 2H), 6.88 (m, 2H), 6.70 (dd, *J* = 8.5 and 4.7 Hz, 1H), 3.70 (br, 2H), 1.38 (s, 9H). ¹³C NMR (CDCl₃): δ 156.37 (d, *J* = 235.6 Hz), 150.56, 139.64 (d, *J* = 2.0 Hz), 135.38, 128.70 (d, *J* = 6.8 Hz), 128.22 (t, *J* = 24.5 Hz), 125.73, 116.67 (d, *J* = 22.5 Hz), 116.43 (d, *J* = 8.2 Hz), 114.61 (d, *J* = 21.8 Hz), 34.62, 31.35. ¹⁹F NMR (CDCl₃): δ -126.92 (m, 1F). HRMS electrospray (*m/z*): [M + H]⁺ calcd for C₁₆H₁₆D₂FN, 246.1622; Found, 246.1621.

Preparation of 2,6-dideutero-4-(*tert*-butyl)-5'-fluoro-2'-iodo-1,1'-biphenyl (S14). S14 was obtained according to the general procedure 2 in 68% yield (colorless oil). ¹H NMR (CDCl₃): δ 7.88 (dd, *J* = 8.7 and 5.6 Hz, 1H), 7.45 (d, *J* = 8.3 Hz, 2H), 7.05 (dd, *J* = 9.6 and 3.1 Hz, 1H), 6.79 (td, *J* = 8.2 and 2.9 Hz, 1H), 1.38 (s, 9H). ¹³C NMR (CDCl₃): δ 162.83 (d, *J* = 248.0 Hz), 151.00, 148.42 (d, *J* = 7.5 Hz), 140.63 (d, *J* = 7.5 Hz), 140.18, 128.70, 124.97, 117.47 (d, *J* = 22.5 Hz), 116.00 (d, *J* = 21.8 Hz), 51.51 (d, *J* = 2.7 Hz), 34.67, 31.36. ¹⁹F NMR (CDCl₃): δ - 114.70 (m, 1F). HRMS electron impact (*m/z*): [M]⁺ calcd for C₁₆H₁₆FI, 354.0280; Found, 354.0275.

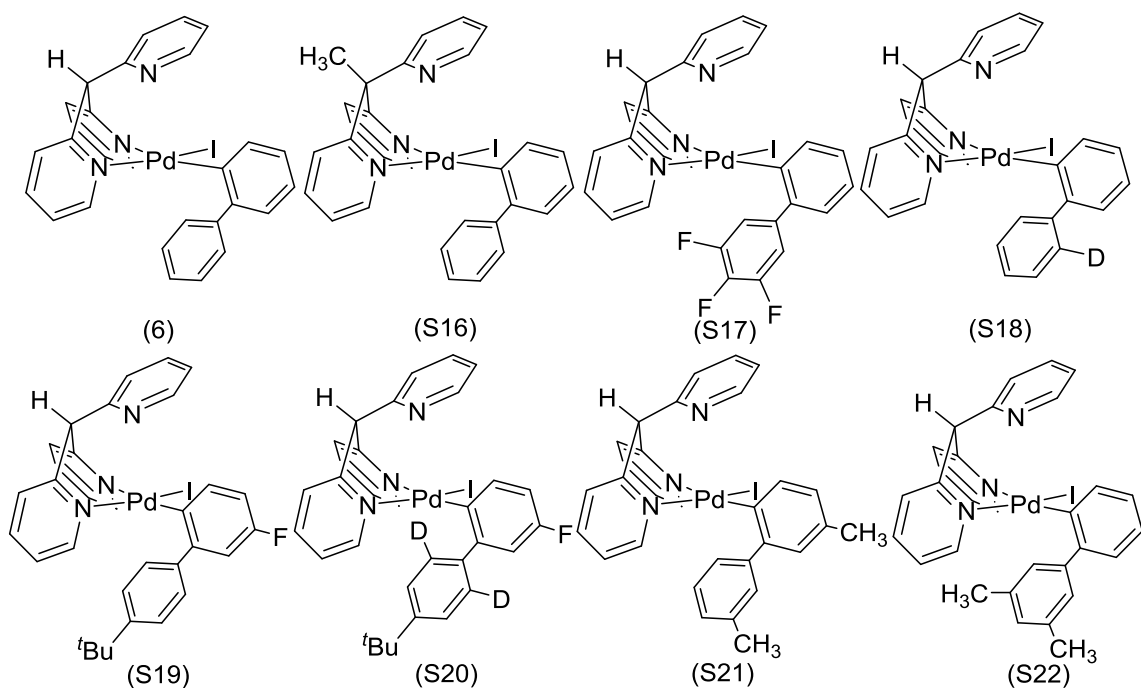
Scheme 3.26 Synthesis of 2-deutero-2'-iodo-1,1'-biphenyl (**S15**)



2,2'-Diiodo-1,1'-biphenyl was synthesized according to a published procedure.²⁵

Preparation of 2-deutero-2'-iodo-1,1'-biphenyl (S15). Under an atmosphere of nitrogen *i*PrMgCl•LiCl (1.3M in THF; 3.3 mL; 4.3 mmol) was added to a cooled (-78 °C) solution of 2,2'-diiodo-1,1'-biphenyl (1.35g, 3.33 mmol) in dry THF (30 mL). The reaction mixture was warmed to 0 °C and stirred at this temperature for 2 h. D₂O (0.2 mL; 10 mmol) was added to the solution in one portion. The reaction mixture was then partitioned between Et₂O (100 mL) and brine (100 mL). The organic phase was dried over MgSO₄ and the solvent was then removed under reduced pressure to yield colorless oil. The obtained crude product (890 mg; 95%) contained approximately 10% of unreacted starting material which was removed on a silica gel column (mobile phase: 100% hexanes) to afford 765 mg (82%) of a pure product as a colorless oil. The extent of D incorporation (99%) was calculated from the mass spectrometry data according to a published procedure.²⁶ For mass spectrometry data see pages 33-36. ¹H NMR (CDCl₃): δ 7.98 (dd, *J* = 8.0 and 0.9 Hz, 1H), 7.40 (m, 2H), 7.41 (m, 2H), 7.37 (d, *J* = 8.3 Hz, 1H), 7.33 (d, *J* = 7.5 Hz, 1H), 7.05 (t, *J* = 7.3 Hz, 1H). ¹³C NMR (CDCl₃): δ 146.63, 144.14, 139.52, 130.11, 129.28, 128.99 (t, *J* = 24.5 Hz), 128.80, 128.14, 127.98, 127.87, 127.66, 98.67. HRMS electron impact (*m/z*): [M]⁺ calcd for C₁₂H₈DI, 280.9812; Found, 280.9820.

3.11.2 Pd^{II} Precursors of (Py₃CH)Pd^{II}([1,1'-biphenyl]-2-yl)(I) General Structure

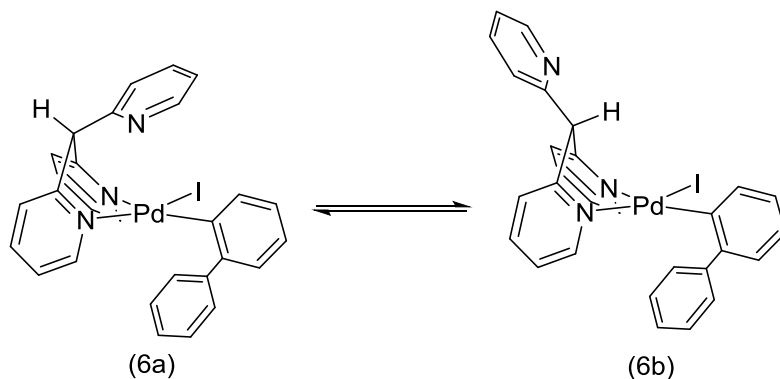


General procedure 3: Preparation of Pd^{II} complexes with (Py₃CH)Pd^{II}(biphen-2-yl)(I) general structure. A 20 mL vial was charged with 4-*tert*-butylpyridine (300 mg, 2.2 mmol), the corresponding iodobiphenyl (1.3 mmol) and THF (15 mL). Pd(dba)₂ (600mg; 1.0 mmol) was then added and the vial was sealed with a teflon lined cap. The reaction mixture was heated to 50 °C until the color of the solution changed from dark red to yellow (usually 5-10 min). Tris(pyridine-2-yl)methane (**S1**) (284 mg; 1.15 mmol) was added to the reaction mixture and the resulting solution was then filtered through a plug of diatomaceous earth. The volatiles were removed under reduced pressure and the residue was suspended in hexanes (100 mL). The solid was filtered, redissolved in CH₂Cl₂ (15 mL) and then precipitated again with hexanes (100

mL). The product was filtered and then washed with 50/50 mixture of Et₂O and hexanes (3 × 30 mL) and dried under reduced pressure.

Pd^{II} complexes with the (Py₃CH)Pd^{II}(biphen-2-yl)(I) general structure exist as a mixture of equilibrating isomers as shown in Scheme 3.27. NMR spectra for the obtained Pd^{II} complexes are very broad at 25 °C indicating that the isomerization is facile. Upon cooling to -20 °C the broad resonances resolved into sharp signals. However, as it is evident from 2D ¹H/¹H ROESY or NOESY spectra, both isomers are still in equilibrium at -20°C. Because of extensive overlap between the peaks of the two isomers, ¹H and ¹³C{¹H} NMR data for these Pd^{II} complexes is not reported in detail. The structure of Pd^{II} complex **6** was confirmed by a single crystal X-ray diffraction analysis (Figure 3.7).

Scheme 3.27 Equilibrium between conformers of (Py₃CH)Pd^{II}(biphen-2-yl)(I)

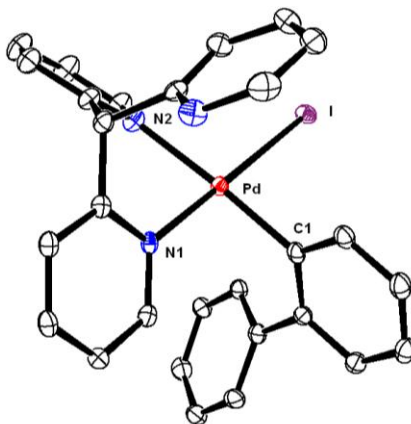


Preparation of (Py₃CH)Pd^{II}([1,1'-biphenyl]-2-yl)(I) (6**).** **6** was obtained according to the general procedure **3** in 67% yield as a yellow powder. X-ray quality crystals of **6** were obtained by slow vapor diffusion of Et₂O into CH₂Cl₂ solution of **6**. In CDCl₃ at 25 °C complex **6** exists as a mixture of two equilibrating isomers **6a** and **6b** in

approximately 1:2 ratio, however, isomer **6a** crystallized in preference to **6b** (Figure 3.7).

HRMS electrospray (m/z): $[M - I]^+$ calcd for $C_{28}H_{22}N_3Pd$, 506.0854; Found, 506.0859.

Figure 3.7 Ortep drawing of $(Py_3CH)Pd^{II}([1,1'-biphenyl]-2-yl)(I)$ (**6**)



Thermal ellipsoids are drawn at 50% probability. Hydrogen atoms are omitted for clarity. There is rotational disorder in a portion of the free pyridine ring that results in N3/C13 sites being mixed occupancy at 0.5 ratio.

Preparation of $(Py_3CCH_3)Pd^{II}([1,1'-biphenyl]-2-yl)(I)$ (S16**).** **S16** was obtained according to the general procedure **3** in 77% yield as a yellow powder. Only one stereoisomer was detected in the 1H and $^{13}C\{^1H\}$ NMR spectra of **S16**. Stereochemistry of **S16** was determined from the $^1H/^1H$ NOESY NMR experiment. 1H NMR ($CDCl_3$ at $25^\circ C$): δ 9.41 (d, $J = 4.8$ Hz, 1H), 8.64 (d, $J = 4.1$ Hz, 1H), 8.38 (d, $J = 7.5$ Hz, 2H), 7.98 (d, $J = 5.9$ Hz, 1H), 7.85 (t, $J = 6.5$ Hz, 1H), 7.76 (m, 3H), 7.70 (d, $J = 5.9$ Hz, 1H), 7.39 (t, $J = 7.6$ Hz, 2H), 7.34 (dd, $J = 6.7$ and 5.0 Hz, 1H), 7.30 (t, $J = 6.2$ Hz, 1H), 7.24 (t, $J = 7.4$ Hz, 1H), 7.20 (dd, $J = 7.4$ and 1.0 Hz, 1H), 6.98 (dd, $J = 8.9$ and 5.3 Hz, 1H), 6.88 (d, $J = 8.1$ Hz, 1H), 6.85 (t, $J = 7.6$ Hz, 1H), 6.66 (t, $J = 6.7$ Hz, 1H), 6.51 (d, $J = 7.2$ Hz, 1H), (s, 3H). ^{13}C NMR ($CDCl_3$ at $25^\circ C$): δ 165.84, 161.58, 159.12, 154.91, 152.64,

149.61, 145.76, 145.04, 143.21, 138.20, 138.02, 137.74, 137.54, 130.52, 129.32, 127.40, 126.06, 124.69, 124.01, 123.60, 123.23, 123.21, 123.18, 122.52, 122.31, 60.01, 28.05.
HRMS electrospray (m/z): [M – I]⁺ calcd for C₂₉H₂₄N₃Pd, 520.1000; Found, 520.1009.

Preparation of (Py₃CH)Pd^{II}(3',4',5'-trifluoro-[1,1'-biphenyl]-2-yl)(I) (S17).

S17 was obtained according to the general procedure **3** in 73% yield as a yellow powder. ¹⁹F NMR (CD₂Cl₂ at -25 °C) of the major isomer: δ -136.92 (dd, *J* = 20.0 and 10.0 Hz, 2F), -165.43 (tt, *J* = 21.6 and 6.6 Hz, 1F). ¹⁹F NMR (CD₂Cl₂ at -25 °C) of the minor isomer: δ -136.96 (dd, *J* = 21.6 and 8.3 Hz, 2F), -165.27 (tt, *J* = 21.6 and 6.6 Hz, 1F).
HRMS electrospray (m/z): [M – I]⁺ calcd for C₂₈H₁₉F₃N₃Pd, 560.0560; Found, 560.0571.

Preparation of (Py₃CH)Pd^{II}(2'-deutero-[1,1'-biphenyl]-2-yl)(I) (S18).

S18 was obtained according to the general procedure **3** in 79% yield as a yellow powder. HRMS electrospray (m/z): [M – I]⁺ calcd for C₂₈H₂₁DN₃Pd, 507.0906; Found, 507.0916.

Preparation of (Py₃CH)Pd^{II}(5-fluoro-4'-tert-butyl-[1,1'-biphenyl]-2-yl)(I) (S19).

S19 was obtained according to the general procedure **3** in 74% yield as a yellow powder. ¹⁹F NMR (CDCl₃ at -25°C): δ -124.24 (q, *J* = 8.3 Hz, isomer **S19a**), -123.45 (q, *J* = 9.4 Hz, isomer **S19b**). HRMS electrospray (m/z): [M – I]⁺ calcd for C₃₂H₂₉FN₃Pd, 580.1375; Found, 580.1391.

Preparation of (Py₃CH)Pd^{II}(4'-tert-butyl-2',6'-dideutero-5-fluoro-[1,1'-biphenyl]-2-yl)(I) (S20).

S20 was obtained according to the general procedure **3** in 83% yield as a yellow powder. ¹⁹F NMR (CDCl₃ at -25°C): δ -124.24 (q, *J* = 10.0 Hz, isomer **S20a**), -123.46 (q, *J* = 8.2 Hz, isomer **S20b**). HRMS electrospray (m/z): [M – I]⁺ calcd for C₃₂H₂₇D₂FN₃Pd, 582.1500; Found, 582.1515.

Preparation of (Py₃CH)Pd^{II}(4,3'-dimethyl-[1,1'-biphenyl]-2-yl)(I) (S21). S21 was obtained according to the general procedure **3** in 73% yield as a yellow powder. HRMS electrospray (m/z): [M – I]⁺ calcd for C₃₀H₂₆N₃Pd, 534.1156; Found, 534.1153.

Preparation of (Py₃CH)Pd^{II}(3',5'-dimethyl-[1,1'-biphenyl]-2-yl)(I) (S22). S22 was obtained according to the general procedure **3** in 51% yield as a yellow powder. HRMS electrospray (m/z): [M – I]⁺ calcd for C₃₀H₂₆N₃Pd, 534.1156; Found, 534.1168.

X-ray structure determination for (Py₃CH)Pd^{II}([1,1'-biphenyl]-2-yl)(I) (6). Orange blocks of **6** were grown from a dichloromethane/diethyl ether solution of the compound at 4 deg. C. A crystal of dimensions 0.06 x 0.03 x 0.03 mm was mounted on a Rigaku AFC10K Saturn 944+ CCD-based X-ray diffractometer equipped with a low temperature device and Micromax-007HF Cu-target micro-focus rotating anode ($\lambda = 1.54187$ Å) operated at 1.2 kW power (40 kV, 30 mA). The X-ray intensities were measured at 85(1) K with the detector placed at a distance 42.00 mm from the crystal. A total of 3718 images were collected with an oscillation width of 1.0° in ω . The exposure time was 1 sec. for the low angle images, 4 sec. for high angle. The integration of the data yielded a total of 60719 reflections to a maximum 2θ value of 136.46° of which 4344 were independent and 4154 were greater than $2\sigma(I)$. The final cell constants were based on the xyz centroids of 46120 reflections above $10\sigma(I)$. Analysis of the data showed negligible decay during data collection; the data were processed with CrystalClear 2.0 and corrected for absorption. The structure was solved and refined with the Bruker SHELXTL (version 2008/4) software package, using the space group P2(1)/n with Z = 4 for the formula C₂₈H₂₂N₃PdI. Full matrix least-squares refinement based on

F^2 converged at $R1 = 0.0320$ and $wR2 = 0.0825$ [based on $I > 2\sigma(I)$], $R1 = 0.0329$ and $wR2 = 0.0832$ for all data. There is rotational disorder in a portion of one ligand that results in N3/C13 sites being mixed occupancy at 0.5 ratio. Additional details are presented in below.

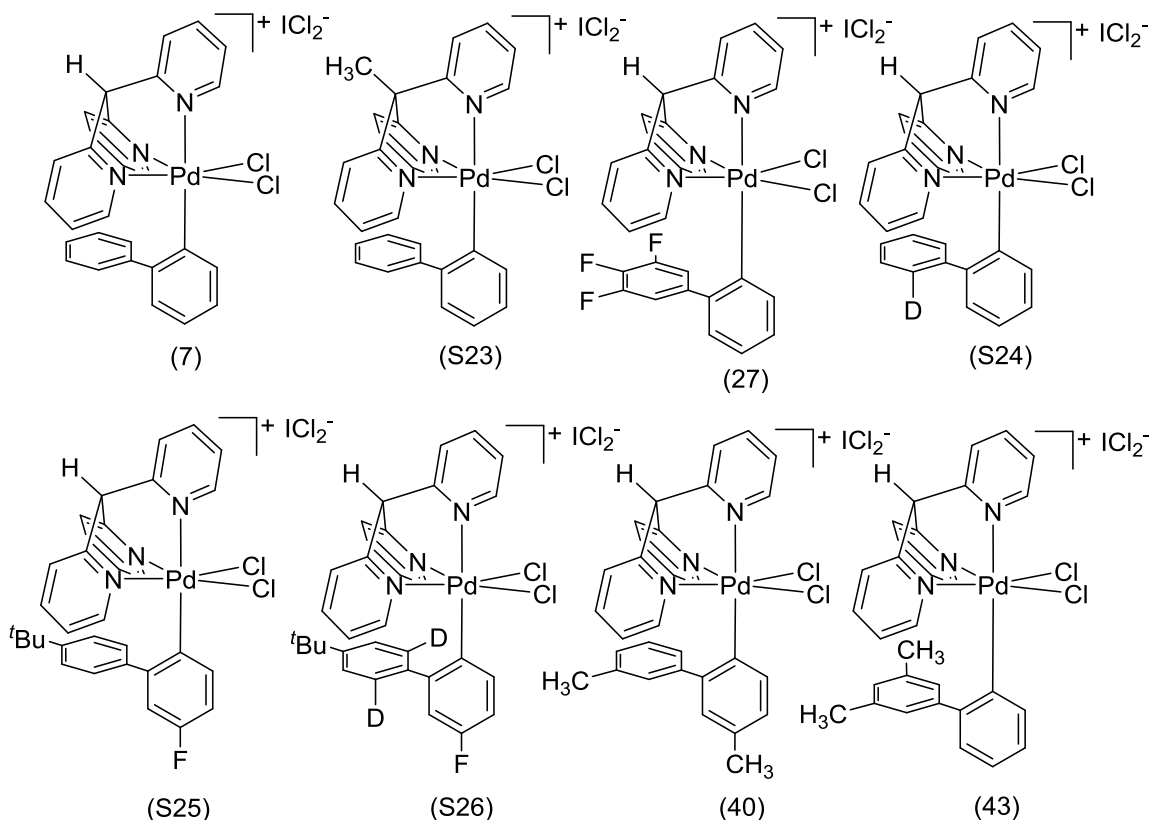
Crystal data and structure refinement for am5379 (**complex 6**).

Identification code	am5379
Empirical formula	C ₂₈ H ₂₂ I N ₃ Pd
Formula weight	633.79
Temperature	85(2) K
Wavelength	1.54178 Å
Crystal system, space group	Monoclinic, P2(1)/n
Unit cell dimensions	a = 9.3934(2) Å alpha = 90 deg. b = 14.7202(3) Å beta = 101.232(7) deg. c = 17.5207(12) Å gamma = 90 deg.
Volume	2376.23(18) Å ³
Z, Calculated density	1.772 Mg/m ³
Absorption coefficient	16.657 mm ⁻¹
F(000)	1240
Crystal size	0.06 x 0.03 x 0.03 mm
Theta range for data collection	5.15 to 68.23 deg.
Limiting indices	-11 ≤ h ≤ 11, -17 ≤ k ≤ 17, -21 ≤ l ≤ 20
Reflections collected / unique	60719 / 4344 [R(int) = 0.0687]
Completeness to theta = 68.23	99.9%
Absorption correction	Semi-empirical from equivalents
Max. and min. transmission	0.6349 and 0.4348
Refinement method	Full-matrix least-squares on F ²
Data / restraints / parameters	4344 / 0 / 298
Goodness-of-fit on F ²	1.063
Final R indices [I > 2σ(I)]	R1 = 0.0320, wR2 = 0.0825
R indices (all data)	R1 = 0.0329, wR2 = 0.0832
Largest diff. peak and hole	1.392 and -0.984 e.Å ⁻³

Atomic coordinates ($\times 10^4$) and equivalent isotropic displacement parameters ($\text{\AA}^2 \times 10^3$) for complex **6**. U(eq) is defined as one third of the trace of the orthogonalized Uij tensor.

	x	y	z	U(eq)
I(1)	4030(1)	2258(1)	1980(1)	26(1)
Pd(1)	1358(1)	2255(1)	1197(1)	21(1)
C(1)	-1923(4)	2424(3)	827(2)	25(1)
C(2)	-3297(4)	2533(3)	379(2)	27(1)
C(3)	-3443(4)	2640(3)	-417(2)	30(1)
C(4)	-2217(4)	2601(2)	-745(2)	26(1)
C(5)	-869(4)	2480(2)	-272(2)	23(1)
C(6)	493(4)	2442(3)	-617(2)	25(1)
C(7)	1249(4)	1538(3)	-442(2)	28(1)
C(8)	1355(5)	930(3)	-1038(3)	35(1)
C(9)	1987(6)	88(3)	-849(3)	43(1)
C(10)	2492(6)	-123(3)	-71(3)	45(1)
C(11)	2344(5)	508(3)	487(3)	35(1)
C(12)	1439(4)	3284(3)	-389(2)	26(1)
C(13)	2871(4)	3215(3)	-58(2)	34(1)
N(3A)	2871(4)	3215(3)	-58(2)	34(1)
C(14)	3616(5)	4007(3)	164(3)	36(1)
C(15)	2952(5)	4835(3)	34(3)	37(1)
C(16)	1529(5)	4862(3)	-344(3)	43(1)
C(17)	865(4)	3114(2)	1978(2)	24(1)
C(18)	1193(4)	4028(3)	1887(2)	29(1)
C(19)	775(4)	4699(3)	2354(3)	33(1)
C(20)	17(4)	4464(3)	2924(2)	33(1)
C(21)	-321(4)	3563(3)	3024(2)	28(1)
C(22)	97(4)	2873(3)	2561(2)	24(1)
C(23)	-331(4)	1919(3)	2693(2)	26(1)
C(24)	-1712(4)	1734(3)	2845(2)	30(1)
C(25)	-2150(4)	862(3)	2980(2)	34(1)
C(26)	-1200(5)	140(3)	2981(2)	36(1)
C(27)	187(4)	297(3)	2834(2)	30(1)
C(28)	603(4)	1179(3)	2690(2)	27(1)
N(1)	-717(3)	2400(2)	515(2)	21(1)
N(2)	1737(4)	1325(2)	310(2)	29(1)
N(3)	755(4)	4085(3)	-551(2)	34(1)
C(13A)	755(4)	4085(3)	-551(2)	34(1)

3.11.3 Complexes with $[(\text{Py}_3\text{CH})\text{Pd}^{\text{IV}}(\text{biaryl})(\text{Cl})_2][\text{ICl}_2]$ General Structure



General procedure 4: Preparation of Pd^{IV} complexes with $[(\text{Py}_3\text{CH})\text{Pd}^{\text{IV}}(\text{biphen-2-yl})(\text{Cl})_2][\text{ICl}_2]$ general structure. Iodobenzene dichloride (1.24g; 4.5 mmol) was added to a solution of the corresponding Pd^{II} complex (2.1 mmol) in CH_2Cl_2 (25 mL). The reaction mixture was stirred at ambient temperature for 5 minutes. If any precipitate had formed during this period, nitromethane (~ 5 mL) was then added to dissolve it. The resulting bright orange solution was washed with water (3×40 mL) and then with brine (2×40 mL). The organic phase was dried over anhydrous Na_2SO_4 and evaporated under reduced pressure. Et_2O (80 mL) was added to the amorphous residue and the resulting suspension was sonicated for 15 minutes at 20°C .

The crystalline product was filtered and washed with several portions of Et₂O (3 × 30 mL) and then with EtOAc (3 × 10 mL). Thus obtained orange powder was dried under high vacuum.

Preparation of [(Py₃CH)Pd^{IV}([1,1'-biphenyl]-2-yl)(Cl)₂][ICl₂] (7). **7** was obtained according to the general procedure **4** in 85% yield. X-ray quality crystals of were obtained by slow vapor diffusion of Et₂O into CD₃NO₂ solution of **7** at 4 °C. ¹H NMR (CD₃NO₂): δ 9.14 (d, *J* = 5.1 Hz, 1H), 9.00 (d, *J* = 6.1 Hz, 2H), 8.53 (d, *J* = 8.8 Hz, 1H), 8.30 (t, *J* = 7.5 Hz, 2H), 8.09 (t, *J* = 7.6 Hz, 1H), 7.97 (m, 3H), 7.78 (t, *J* = 6.9 Hz, 2H), 7.65 (t, *J* = 6.4 Hz, 1H), 7.35 (m, 2H), 6.85 (t, *J* = 7.3 Hz, 1H), 6.79 (d, *J* = 6.8 Hz, 1H), 6.55 (t, *J* = 7.6 Hz, 2H), 6.44 (s, 1H), 5.94 (d, *J* = 7.3 Hz, 2H). ¹³C NMR (CD₃NO₂): δ 155.61, 154.24, 150.29, 149.28, 148.67, 144.20, 143.56, 142.00, 141.15, 140.94, 135.60, 128.11, 127.92, 127.76, 127.68, 127.08, 125.78, 125.68, 125.57, 61.98. HRMS electrospray (*m/z*): [M – ICl₂]⁺ calcd for C₂₈H₂₂Cl₂N₃Pd, 576.0220; Found, 576.0211.

Preparation of [(Py₃CCH₃)Pd^{IV}([1,1'-biphenyl]-2-yl)(Cl)₂][ICl₂] (S23). **S23** was obtained according to the general procedure **4** in 79% yield. ¹H NMR (CD₃NO₂): δ 9.29 (d, *J* = 5.3 Hz, 1H), 9.10 (d, *J* = 5.4 Hz, 2H), 8.57 (d, *J* = 8.6 Hz, 1H), 8.32 (t, *J* = 7.4 Hz, 2H), 8.11 (m, 3H), 8.00 (d, *J* = 8.3 Hz, 1H), 7.77 (t, *J* = 6.4 Hz, 2H), 7.77 (t, *J* = 6.4 Hz, 1H), 7.37 (td, *J* = 8.9 and 1.9 Hz, 1H), 7.32 (t, *J* = 6.9 Hz, 1H), 7.23 (t, *J* = 7.4 Hz, 1H), 6.77 (dd, *J* = 6.9 and 2.1 Hz, 1H), 6.53 (t, *J* = 7.6 Hz, 2H), 5.84 (d, *J* = 7.2 Hz, 2H), 2.77 (s, 3H). ¹³C NMR (CD₃NO₂): δ 156.24, 154.94, 151.70, 151.20, 150.59, 144.01, 143.55, 141.75, 141.10, 140.96, 135.64, 127.79, 127.72 (two overlapping peaks as determined by 2D ¹H/¹³C ASAPHMQC), 127.65, 127.11, 126.16, 125.63, 125.45,

123.21, 57.87, 21.40. HRMS electrospray (m/z): $[M - ICl_2]^+$ calcd for $C_{29}H_{24}Cl_2N_3Pd$, 592.0382; Found, 592.0370.

Preparation of $[(Py_3CH)Pd^{IV}(3',4',5'\text{-trifluoro-[1,1'\text{-biphenyl]-2-yl})(Cl)_2][ICl_2]$ (27**).** **27** was obtained according to the general procedure **4** in 77% yield. Complex **27** exist as a mixture of two equilibrating isomers **27a** and **27b**. The ratio between isomers **27a** and **27b** is ~ 40/60 in $CDCl_3$ and ~ 75/25 in CD_3NO_2 at 25°C. Because of the overlap between the peaks of the two isomers 1H and $^{13}C\{^1H\}$ NMR data for **27a/b** is not reported in detail. ^{19}F NMR ($CDCl_3$ at 25°C) of the major isomer: δ - 137.88 (dd, $J = 18.4$ and 11.7 Hz, 2F), -162.93 (t, $J = 21.6$ Hz, 1F). ^{19}F NMR ($CDCl_3$ at 25°C) of the minor isomer: δ -132.61 (dd, $J = 19.9$ and 7.5 Hz, 2F), -158.61 (t, $J = 19.9$ Hz, 1F). ^{19}F NMR (CD_3NO_2 at 25°C) of the major isomer: δ -136.62 (m, 2F), -164.26 (m, 1F). ^{19}F NMR (CD_3NO_2 at 25°C) of the minor isomer: δ - 141.34 (dd, $J = 18.3$ and 8.3 Hz, 2F), -166.93 (tt, $J = 20.1$ and 6.7 Hz, 1F). HRMS electrospray (m/z): $[M - ICl_2]^+$ calcd for $C_{28}H_{19}Cl_2F_3N_3Pd$, 629.9937; Found, 629.9938.

Preparation of $[(Py_3CH)Pd^{IV}(2'\text{-deutero-[1,1'\text{-biphenyl]-2-yl})(Cl)_2][ICl_2]$ (S24**).** **S24** was obtained according to the general procedure **4** in 46% yield. 1H NMR (CD_3NO_2): δ 9.13 (d, $J = 5.3$ Hz, 1H), 8.99 (d, $J = 6.0$ Hz, 2H), 8.52 (d, $J = 9.0$ Hz, 1H), 8.29 (t, $J = 7.5$ Hz, 2H), 8.08 (t, $J = 7.7$ Hz, 1H), 7.98 (d, $J = 7.9$ Hz, 2H), 7.95 (d, $J = 7.7$ Hz, 1H), 7.77 (t, $J = 6.4$ Hz, 2H), 7.64 (t, $J = 6.4$ Hz, 1H), 7.36 (td, $J = 7.3$ and 1.5 Hz, 1H), 7.32 (t, $J = 7.0$ Hz, 1H), 6.84 (t, $J = 7.5$ Hz, 1H), 6.78 (dd, $J = 7.0$ and 1.7 Hz, 1H), 6.54 (m, 2H), 6.44 (s, 1H), 5.94 (d, $J = 7.9$ Hz, 1H). ^{13}C NMR (CD_3NO_2): δ 155.61, 154.22, 150.28, 149.27, 148.66, 144.20, 143.52, 141.99, 141.14, 140.84, 135.59, 128.11, 127.91, 127.74, 127.69, 127.62, 127.08, 126.96, 125.77, 125.68, 125.56, 61.96 (Signal of

the carbon attached to the deuterium was not observed presumably because it is a triplet of low intensity that overlaps with other more intense nearby peaks). HRMS electrospray (m/z): $[M - \text{ICl}_2]^+$ calcd for $\text{C}_{28}\text{H}_{21}\text{DCl}_2\text{N}_3\text{Pd}$, 577.0283; Found, 577.0283.

Preparation of $[(\text{Py}_3\text{CH})\text{Pd}^{\text{IV}}(\text{5-fluoro-4}'\text{-tert-butyl-[1,1}'\text{-biphenyl]-2-yl})(\text{Cl})_2][\text{ICl}_2]$ (S25). S25 was obtained according to the general procedure 4 in 60% yield. ^1H NMR (CD_3NO_2): δ 9.12 (d, $J = 4.9$ Hz, 1H), 8.98 (d, $J = 6.0$ Hz, 2H), 8.55 (dd, $J = 9.2$ and 5.8 Hz, 1H), 8.32 (t, $J = 7.5$ Hz, 2H), 8.09 (t, $J = 7.5$ Hz, 1H), 8.02 (d, $J = 7.2$ Hz, 2H), 7.95 (d, $J = 7.6$ Hz, 1H), 7.80 (t, $J = 6.4$ Hz, 2H), 7.64 (t, $J = 6.4$ Hz, 1H), 7.18 (td, $J = 8.6$ and 3.2 Hz, 1H), 6.61 (dd, $J = 9.6$ and 3.4 Hz, 1H), 6.56 (d, $J = 8.1$ Hz, 2H), 6.53 (s, 1H), 5.89 (d, $J = 8.3$ Hz, 2H), 1.19 (s, 9H). ^{13}C NMR (CD_3NO_2): δ 161.15 (d, $J = 246.6$ Hz), 154.24, 150.31, 149.11, 148.54, 148.22, 145.20 (d, $J = 7.5$ Hz), 144.34, 142.27 (d, $J = 7.5$ Hz), 142.15, 137.42, 137.14, 127.98, 127.81, 127.21, 125.87, 125.79, 123.97, 120.54 (d, $J = 21.8$ Hz), 113.79 (d, $J = 21.1$ Hz), 61.77, 33.64, 29.96. ^{19}F NMR (CD_3NO_2): δ -118.74 (q, $J = 7.3$ Hz). ^1H NMR (CDCl_3): δ 9.10 (d, $J = 5.4$ Hz, 1H), 8.92 (d, $J = 6.0$ Hz, 2H), 8.52 (dd, $J = 9.5$ and 5.7 Hz, 1H), 8.39 (d, $J = 7.5$ Hz, 2H), 8.35 (d, $J = 7.7$ Hz, 1H), 8.19 (t, $J = 7.5$ Hz, 2H), 8.01 (t, $J = 7.5$ Hz, 1H), 7.64 (t, $J = 6.4$ Hz, 1H), 7.53 (t, $J = 6.9$ Hz, 1H), 7.23 (s, 1H), 7.09 (td, $J = 7.4$ and 3.4 Hz, 1H), 6.54 (dd, $J = 9.2$ and 3.4 Hz, 1H), 6.47 (d, $J = 8.1$ Hz, 2H), 5.67 (d, $J = 8.1$ Hz, 2H), 1.20 (s, 9H). ^{13}C NMR (CDCl_3): δ 161.21 (d, $J = 249$ Hz), 153.78, 150.53, 149.35 (two overlapping resonances as revealed by 2D $^1\text{H}/^{13}\text{C}$ HSQC and HMBC), 149.14, 147.56, 144.64 (d, $J = 6.8$ Hz), 143.63, 142.58 (d, $J = 6.8$ Hz), 142.06, 136.87, 129.01, 127.18, 126.96, 126.91, 125.81, 124.21, 121.12 (d, $J = 21.5$ Hz), 114.66 (d, $J = 20.5$ Hz), 60.40, 34.27, 31.17. ^{19}F

NMR (CDCl₃): δ -115.80 (q, J = 16.6 Hz). HRMS electrospray (m/z): [M – ICl₂]⁺ calcd for C₃₂H₂₉Cl₂FN₃Pd, 650.0752; Found, 650.0757.

Preparation of [(Py₃CH)Pd^{IV}(4'-*tert*-butyl-2',6'-dideutero-5-fluoro-[1,1'-biphenyl]-2-yl)(Cl)₂][ICl₂] (S26). S26 was obtained according to the general procedure 4 in 81% yield. ¹H NMR (CD₃NO₂): δ 9.12 (d, J = 5.1 Hz, 1H), 8.98 (d, J = 6.4 Hz, 2H), 8.55 (td, J = 7.7 and 3.6 Hz, 1H), 8.32 (t, J = 7.3 Hz, 2H), 8.09 (t, J = 7.2 Hz, 1H), 8.01 (d, J = 7.5 Hz, 1H), 7.95 (d, J = 7.6 Hz, 1H), 7.80 (t, J = 6.4 Hz, 2H), 7.64 (t, J = 6.3 Hz, 1H), 7.18 (td, J = 8.9 and 3.2 Hz, 1H), 6.61 (dd, J = 9.4 and 3.1 Hz, 1H), 6.56 (br, 2H), 6.51 (s, 1H), 1.19 (s, 3H). ¹³C NMR (CD₃NO₂): δ 161.15 (d, J = 246.6 Hz), 154.24, 150.31, 149.09, 148.53, 148.24, 145.14 (d, J = 6.8 Hz), 144.36, 142.27 (d, J = 7.5 Hz), 142.15, 137.42, 136.96, 128.00, 127.81, 126.89 (t, J = 23.8 Hz), 125.88, 125.81, 123.86, 120.54 (d, J = 21.8 Hz), 113.79 (d, J = 21.1 Hz), 61.80, 33.64, 29.98. ¹⁹F NMR (CD₃NO₂): δ -118.73 (q, J = 6.7 Hz). HRMS electrospray (m/z): [M – ICl₂]⁺ calcd for C₃₂H₂₇D₂Cl₂FN₃Pd, 652.0877; Found, 652.0878.

Preparation of [(Py₃CH)Pd^{IV}(4,3'-dimethyl-[1,1'-biphenyl]-2-yl)(Cl)₂][ICl₂] (40). 40 was obtained according to the general procedure 4 in 74% yield. ¹H NMR (CDCl₃ at 25 °C): δ 9.11 (d, J = 5.1 Hz, 1H), 8.97 (d, J = 5.4 Hz, 1H), 8.91 (d, J = 4.4 Hz, 1H), 8.50 (d, J = 7.6 Hz, 1H), 8.40-8.35 (m, 3H), 8.18 (t, J = 7.3 Hz, 1H), 8.12 (t, J = 7.3 Hz, 1H), 7.96 (td, J = 7.6 and 1.2 Hz, 1H), 7.58 (t, J = 6.4 Hz, 1H), 7.53 (t, J = 6.6 Hz, 1H), 7.49 (t, J = 6.4 Hz, 1H), 7.41 (s, 1H), 7.12 (dd, J = 8.9 and 2.5 Hz, 1H), 6.77 (d, J = 7.6 Hz, 1H), 6.52 (d, J = 2.2 Hz, 1H), 6.37 (t, J = 7.8 Hz, 1H), 5.68 (s, 1H), 5.36 (d, J = 7.3 Hz, 1H), 2.35 (s, 3H), 1.89 (s, 3H). ¹³C{¹H} NMR (CDCl₃ at 25 °C): δ 153.80, 153.74, 153.14, 150.38, 149.86, 149.60, 143.38, 143.05, 142.71, 141.71, 140.85, 140.69,

137.74, 136.38 (two overlapping peaks as revealed by $^1\text{H}/^{13}\text{C}$ HMBC), 136.08, 129.33, 129.26, 128.97, 128.84, 127.68, 127.20, 126.89, 126.68, 126.13, 125.60, 124.09, 59.99, 21.35, 19.98. HRMS electrospray (m/z): $[\text{M} - \text{ICl}_2]^+$ calcd for $\text{C}_{30}\text{H}_{26}\text{Cl}_2\text{N}_3\text{Pd}$, 604.0533; Found, 604.0518.

Preparation of $[(\text{Py}_3\text{CH})\text{Pd}^{\text{IV}}(3',5'\text{-dimethyl-[1,1'-biphenyl]-2-yl)(\text{Cl})_2][\text{ICl}_2]$ (**43**). **40** was obtained according to the general procedure **4** in 53% yield. ^1H NMR (CD_3NO_2 at $25\text{ }^\circ\text{C}$): δ 9.13 (d, $J = 5.1$ Hz, 1H), 8.97 (d, $J = 5.9$ Hz, 2H), 8.52 (d, $J = 8.6$ Hz, 1H), 8.34 (t, $J = 7.6$ Hz, 2H), 8.09 (t, $J = 7.6$ Hz, 1H), 8.05 (d, $J = 7.6$ Hz, 2H), 8.00 (d, $J = 7.6$ Hz, 1H), 7.79 (t, $J = 6.6$ Hz, 2H), 7.64 (t, $J = 6.1$ Hz, 1H), 7.35 (t, $J = 6.1$ Hz, 1H), 7.30 (t, $J = 7.1$ Hz, 1H), 6.72 (d, $J = 6.6$ Hz, 1H), 6.56 (s, 1H), 6.53 (s, 1H), 5.51 (s, 2H), 1.84 (s 6H). $^{13}\text{C}\{^1\text{H}\}$ NMR (CD_3NO_2 at $25\text{ }^\circ\text{C}$): δ 155.68, 154.31, 150.30, 149.40, 148.96, 144.02, 143.73, 142.03, 141.11, 140.94, 136.33, 135.91, 128.21, 127.79, 127.68 (two overlapping signals as revealed by $^1\text{H}/^{13}\text{C}$ ASAPHMQC, see below), 127.26, 125.97, 125.78, 125.69, 61.98, 19.95. HRMS electrospray (m/z): $[\text{M} - \text{ICl}_2]^+$ calcd for $\text{C}_{30}\text{H}_{26}\text{Cl}_2\text{N}_3\text{Pd}$, 604.0533; Found, 604.0541.

X-ray structure determination for [(Py₃CH)Pd^{IV}([1,1'-biphenyl]-2-yl)(Cl)₂][ICl₂] (7).

Orange blocks of **7** were grown from a diethyl ether/nitromethane solution of the compound at 4 deg. C. A crystal of dimensions 0.08 x 0.06 x 0.06 mm was mounted on a Rigaku AFC10K Saturn 944+ CCD-based X-ray diffractometer equipped with a low temperature device and Micromax-007HF Cu-target micro-focus rotating anode ($\lambda = 1.54187$ Å) operated at 1.2 kW power (40 kV, 30 mA). The X-ray intensities were measured at 85(1) K with the detector placed at a distance 42.00 mm from the crystal. A total of 3580 images were collected with an oscillation width of 1.0° in ω . The exposure time was 2 sec. for the low angle images, 6 sec. for high angle. The integration of the data yielded a total of 67413 reflections to a maximum 2θ value of 136.48° of which 5115 were independent and 5056 were greater than $2\sigma(I)$. The final cell constants were based on the xyz centroids of 49398 reflections above $10\sigma(I)$. Analysis of the data showed negligible decay during data collection; the data were processed with CrystalClear 2.0 and corrected for absorption. The structure was solved and refined with the Bruker SHELXTL (version 2008/4) software package, using the space group P2(1)/c with $Z = 4$ for the formula C₂₈H₂₂N₃Cl₄IPd. Full matrix least-squares refinement based on F^2 converged at $R1 = 0.0253$ and $wR2 = 0.0592$ [based on $I > 2\sigma(I)$], $R1 = 0.0257$ and $wR2 = 0.0603$ for all data. Additional details are presented below.

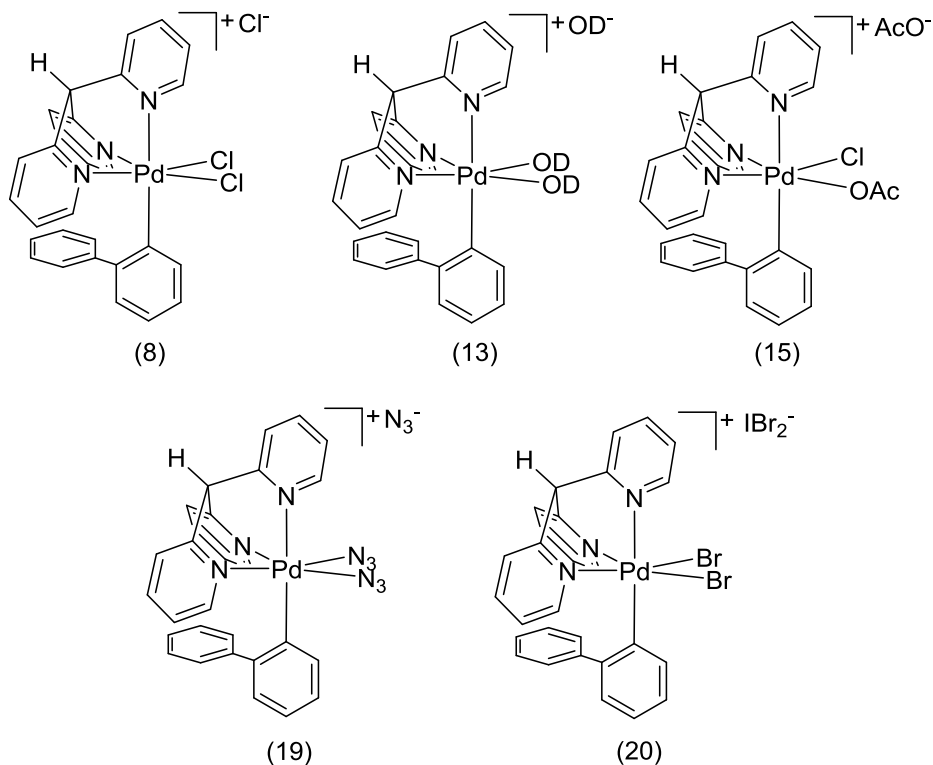
Crystal data and structure refinement for complex 7.

Identification code	am5380
Empirical formula	C ₂₈ H ₂₂ Cl ₄ I N ₃ Pd
Formula weight	775.59
Temperature	85(2) K
Wavelength	1.54178 Å
Crystal system, space group	Monoclinic, P 2(1)/c
Unit cell dimensions	a = 13.9340(3) Å alpha = 90 deg. b = 12.6639(2) Å beta = 92.745(7) deg. c = 15.8661(11) Å gamma = 90 deg.
Volume	2796.5(2) Å ³
Z, Calculated density	4,1842 Mg/m ³
Absorption coefficient	17.724 mm ⁻¹
F(000)	1512
Crystal size	0.08 x 0.06 x 0.06 mm
Theta range for data collection	3.18 to 68.24 deg.
Limiting indices	-16<=h<=16, -15<=k<=15, -19<=l<=19
Reflections collected / unique	67413 / 5115 [R(int) = 0.0543]
Completeness to theta = 68.24	99.9%
Absorption correction	Semi-empirical from equivalents
Max. and min. transmission	0.4161 and 0.3313
Refinement method	Full-matrix least-squares on F ²
Data / restraints / parameters	5115 / 0 / 334
Goodness-of-fit on F ²	1.105
Final R indices [I>2sigma(I)]	R1 = 0.0253, wR2 = 0.0592
R indices (all data)	R1 = 0.0257, wR2 = 0.0603
Largest diff. peak and hole	1.280 and -0.901 e.Å ⁻³

Atomic coordinates ($\times 10^4$) and equivalent isotropic displacement parameters ($\text{\AA}^2 \times 10^3$) for complex **7**. U(eq) is defined as one third of the trace of the orthogonalized Uij tensor.

	x	y	z	U(eq)
I(1)	5485(1)	6869(1)	1107(1)	18(1)
Pd(1)	1004(1)	5737(1)	3082(1)	9(1)
Cl(1)	9(1)	4361(1)	3391(1)	16(1)
Cl(2)	284(1)	6771(1)	4054(1)	19(1)
Cl(3)	5827(1)	6118(1)	2622(1)	20(1)
Cl(4)	5109(1)	7599(1)	-337(1)	26(1)
C(1)	1754(2)	4960(3)	4866(2)	18(1)
C(2)	2419(3)	4688(3)	5497(2)	21(1)
C(3)	3385(2)	4685(3)	5328(2)	21(1)
C(4)	3658(2)	4960(3)	4525(2)	18(1)
C(5)	2952(2)	5243(2)	3926(2)	12(1)
C(6)	3184(2)	5585(2)	3034(2)	12(1)
C(7)	2881(2)	6721(2)	2897(2)	12(1)
C(8)	3558(2)	7513(3)	2822(2)	16(1)
C(9)	3255(3)	8558(3)	2760(2)	22(1)
C(10)	2286(3)	8778(3)	2775(2)	22(1)
C(11)	1642(2)	7961(3)	2840(2)	17(1)
C(12)	1342(2)	4005(3)	1837(2)	15(1)
C(13)	1879(2)	3303(3)	1391(2)	16(1)
C(14)	2870(2)	3377(3)	1430(2)	18(1)
C(15)	3293(2)	4152(3)	1940(2)	17(1)
C(16)	2734(2)	4821(2)	2398(2)	12(1)
C(17)	26(2)	6239(2)	2128(2)	12(1)
C(18)	-915(2)	6326(3)	2384(2)	16(1)
C(19)	-1648(2)	6686(2)	1841(2)	16(1)
C(20)	-1450(2)	6954(2)	1021(2)	17(1)
C(21)	-517(2)	6848(2)	765(2)	17(1)
C(22)	247(2)	6493(2)	1298(2)	12(1)
C(23)	1190(2)	6437(2)	889(2)	14(1)
C(24)	1386(2)	5570(3)	379(2)	17(1)
C(25)	2235(3)	5521(3)	-49(2)	23(1)
C(26)	2883(2)	6352(3)	6(2)	20(1)
C(27)	2674(2)	7235(3)	476(2)	18(1)
C(28)	1834(2)	7283(3)	910(2)	16(1)
N(1)	2020(2)	5238(2)	4096(2)	13(1)
N(2)	1936(2)	6950(2)	2894(2)	12(1)
N(3)	1763(2)	4753(2)	2327(2)	11(1)

3.11.4 Complexes with [(Py₃CH)Pd^{IV}(biaryl)(Z)(Y)][X] General Structure (Z, Y = OD, OAc, Cl, Br, N₃)



Preparation of [(Py₃CH)Pd^{IV}([1,1'-biphenyl]-2-yl)(Cl)₂][Cl] (8). AgOOCFF₃ (265 mg; 1.2 mmol) was added to the solution of the corresponding Pd^{II} iodide complex **6** (645 mg; 1.0 mmol) in CH₂Cl₂ (25 mL). The resulting suspension was sonicated at 20 °C for 5 min and then it was filtered through a pad of diatomaceous earth. Iodobenzene dichloride (470 mg; 1.7 mmol) was then added and the solution was stirred at 20 °C for 5 min. The resulting bright orange solution was washed with water (3 × 40 mL) and then with brine (2 × 40 mL). The organic phase was dried over anhydrous Na₂SO₄ and evaporated under reduced pressure. Et₂O (80 mL) was added to the amorphous residue and the resulting suspension was sonicated for 15 minutes at 20 °C. The crystalline

product was filtered and washed with several portions of Et₂O (3 × 30 mL) and then with EtOAc (3 × 5 mL). After drying under vacuum 515 mg (83%) of **8** was obtained as an orange powder. ¹H NMR (CDCl₃): δ 9.07 (dd, *J* = 5.5 and 1.3 Hz, 1H), 8.99 (s, 1H), 8.88 (dd, *J* = 6.0 and 1.0 Hz, 2H), 8.83 (d, *J* = 7.6 Hz, 1H), 8.72 (d, *J* = 7.4 Hz, 2H), 8.55 (dd, *J* = 8.8 and 0.6 Hz, 1H), 8.03 (t, *J* = 6.9 Hz, 2H), 7.89 (td, *J* = 7.6 and 1.2 Hz, 1H), 7.49 (t, *J* = 6.5 Hz, 2H), 7.43 (t, *J* = 6.0 Hz, 1H), 7.30 (td, *J* = 7.0 and 2.0 Hz, 1H), 7.22 (td, *J* = 7.2 and 0.7 Hz, 1H), 6.81 (t, *J* = 7.6 Hz, 1H), 6.69 (dd, *J* = 7.2 and 2.2 Hz), 6.42 (t, *J* = 7.7 Hz, 2H), 5.74 (d, *J* = 7.1 Hz, 2H). ¹³C NMR (CDCl₃): δ 154.84, 153.36, 150.60, 150.27, 149.92, 143.21, 142.89, 141.72, 141.36, 140.69, 135.52, 129.58, 128.25, 127.77, 127.60, 127.56, 127.08, 126.33, 126.20, 125.29, 57.84. HRMS electrospray (*m/z*): [M – Cl]⁺ calcd for C₂₈H₂₂Cl₂N₃Pd, 576.0220; Found, 576.0211.

Preparation of [(Py₃CH)Pd^{IV}([1,1'-biphenyl]-2-yl)(OD)₂][OD] (13**).** The corresponding Pd^{IV} dichloride complex **8** (20.0 mg; 0.03 mmol) was dissolved in CDCl₃ (0.7 mL). NaOD (~8 mg; 0.2 mmol) in D₂O (1.0 mL) was added to the CDCl₃ solution and the resulting biphasic mixture was shaken intensively for two minutes. Then D₂O and CDCl₃ layers were separated and analyzed by NMR spectroscopy. ¹H NMR spectrum of the CDCl₃ layer did not contain any resonances of significant intensity. The ¹H NMR (of the D₂O layer): δ 8.71 (d, *J* = 5.3 Hz, 1H), 8.35 (d, *J* = 5.8 Hz, 2H), 8.06 (t, *J* = 7.5 Hz, 2H), 7.90 (t, *J* = 7.7 Hz, 1H), 7.81 (dd, *J* = 8.6 and 0.9 Hz, 1H), 7.75 (m, 3H), 7.52 (t, *J* = 6.4 Hz, 2H), 7.47 (td, *J* = 6.5 and 1.0 Hz, 1H), 7.38 (td, *J* = 8.4 and 1.2 Hz, 1H), 7.24 (td, *J* = 7.2 and 0.9 Hz, 1H), 6.68 (m, 2H), 6.35 (t, *J* = 7.4 Hz, 2H), 5.74 (d, *J* = 7.2 Hz, 2H). ¹³C NMR (D₂O): δ 153.12, 151.44, 149.91, 149.72, 148.32, 143.81, 143.52, 142.04,

140.43, 134.38, 133.38, 128.94, 127.73, 127.66, 127.65, 127.22, 127.02, 125.77, 125.75, 125.49, 60.72.

Preparation of [(Py₃CH)Pd^{IV}([1,1'-biphenyl]-2-yl)(Cl)(OAc)][OAc] (15). Bu₄NOAc (11.7 mg; 0.04 mmol) was added to a cooled (-30 °C) NMR tube containing a solution of complex **8** (10 mg; 0.013 mmol) in CD₂Cl₂ (0.5 mL). The NMR tube was inserted into the NMR spectrometer (precooled to -20 °C) and the progress of the reaction was monitored by ¹H NMR. With ~3 equivalents of Bu₄NOAc only ~50% conversion of **8** to **15** was observed. Upon the addition of ~3 more equivalents of Bu₄NOAc conversion reached 80%. Further addition of Bu₄NOAc resulted only in formation of complex mixture of products.

Preparation of [(Py₃CH)Pd^{IV}([1,1'-biphenyl]-2-yl)(N₃)₂][N₃] (19). The solution of Pd^{IV} dichloride complex **8** (115 mg; 0.15 mmol) in CH₂Cl₂ (15 mL) was washed with 4% aq NaN₃ (4×10 mL). The organic phase was dried over anhydrous Na₂SO₄ and the solvent was removed under reduced pressure. The amorphous residue was suspended in Et₂O (10 mL) and sonicated for 15 minutes at 20 °C. The Precipitate was collected by filtration, washed with EtOAc (2×3 mL) and dried under vacuum. 88 mg (94%) of **19** was obtained as a dark red powder. Complex **19** exist as a mixture of two equilibrating isomers **19a** and **19b**. The ratio between isomers **19a** and **19b** is ~70/30 in CD₂Cl₂ at 25°C. Because of the overlap between the peaks of the two isomers ¹H and ¹³C{¹H} NMR data for **19a/b** is not reported in detail. ¹H NMR of the isomer **19a** (CD₂Cl₂): δ 8.81 (d, *J* = 5.2 Hz, 1H), 8.59 (d, *J* = 5.7 Hz, 2H), 8.20 (t, *J* = 7.2 Hz, 2H), 8.14 (m, 3H), 8.06 (t, *J* = 7.5 Hz, 1H), 7.71 (d, *J* = 8.8 Hz, 1H), 7.65 (t, *J* = 6.5 Hz, 2H), 7.61 (m, 1H), 7.50 (m, 1H), 7.33 (t, *J* = 7.0 Hz, 1H), 6.92 (t, *J* = 7.5 Hz, 1H), 6.79 (d, *J* = 5.4 Hz, 1H), 6.62

(s, 1H), 6.51 (t, $J = 7.4$ Hz, 2H), 5.77 (d, $J = 7.2$ Hz, 2H). HRMS electrospray (m/z): $[M - N_3]^+$ calcd for $C_{28}H_{22}N_9Pd$, 590.1028; Found, 590.1032.

[(Py₃CH)Pd^{IV}([1,1'-biphenyl]-2-yl)(Br)₂][IBr₂] (20). The solution of Pd^{IV} dichloride complex **7** (100.0 mg; 0.13 mmol) in CH₂Cl₂ (25 mL) was washed with 10% aq KBr (6 × 30 mL). The organic phase was dried over anhydrous Na₂SO₄ and solvent was removed under reduced pressure. The amorphous residue was suspended in Et₂O (10 mL) and sonicated for 15 minutes at 20 °C. Precipitate was collected by filtration, washed with EtOAc (2 × 3 mL) and dried under vacuum. 89 mg (72%) of **20** was obtained as a dark red powder. X-ray quality crystals of **20** were grown by slow vapor diffusion of MTBE into CD₃NO₂ solution at 4 °C. ¹H NMR (CD₃NO₂): δ 9.37 (d, $J = 5.0$ Hz, 1H), 9.20 (d, $J = 5.3$ Hz, 2H), 8.95 (d, $J = 6.4$ Hz, 1H), 8.27 (t, $J = 7.4$ Hz, 2H), 8.06 (t, $J = 7.5$ Hz, 1H), 7.95 (m, 3H), 7.73 (t, $J = 6.4$ Hz, 2H), 7.57 (t, $J = 6.2$ Hz, 1H), 7.29 (t, $J = 7.1$ Hz, 1H), 7.23 (t, $J = 7.2$ Hz, 1H), 6.83 (t, $J = 7.4$ Hz, 1H), 6.76 (d, $J = 5.3$ Hz, 1H), 6.53 (t, $J = 7.0$ Hz, 2H), 6.41 (s, 1H), 5.91 (br, 2H). ¹³C NMR (CD₃NO₂): δ 155.56, 152.10, 151.14, 149.87, 148.98, 146.63, 144.53, 143.97, 141.88, 141.39, 135.91, 127.89, 127.68, 127.54, 127.41 (two overlapping resonances as determined by 2D ¹H/¹³C HSQC), 127.00, 125.85, 125.70, 125.44, 62.24. HRMS electrospray (m/z): $[M - IBr_2]^+$ calcd for $C_{28}H_{22}Br_2N_3Pd$, 663.9210; Found, 663.9194.

X-ray structure determination for [(Py₃CH)Pd^{IV}([1,1'-biphenyl]-2-yl)(Br)₂][IBr₂] (20). Orange plates of **am5390 (complex 20)** were grown from a methyl-t-butyl ether/nitromethane solution of the compound at 4 deg. C. A crystal of dimensions 0.13 x 0.10 x 0.06 mm was mounted on a Rigaku AFC10K Saturn 944+ CCD-based X-ray diffractometer equipped with a low temperature device and Micromax-007HF Cu-target micro-focus rotating anode ($\lambda = 1.54187$ Å) operated at 1.2 kW power (40 kV, 30 mA). The X-ray intensities were measured at 85(1) K with the detector placed at a distance 42.00 mm from the crystal. A total of 4081 images were collected with an oscillation width of 1.0° in ω . The exposure time was 1 sec. for the low angle images, 4 sec. for high angle. The integration of the data yielded a total of 80397 reflections to a maximum 2θ value of 136.44° of which 5317 were independent and 5271 were greater than $2\sigma(I)$. The final cell constants were based on the xyz centroids of 48097 reflections above $10\sigma(I)$. Analysis of the data showed negligible decay during data collection; the data were processed with CrystalClear 2.0 and corrected for absorption. The structure was solved and refined with the Bruker SHELXTL (version 2008/4) software package, using the space group P2(1)/c with Z = 4 for the formula C₂₈H₂₂N₃Br₃IPd. Full matrix least-squares refinement based on F² converged at R1 = 0.0251 and wR2 = 0.0588 [based on I > 2sigma(I)], R1 = 0.0253 and wR2 = 0.0589 for all data. Additional details are presented below.

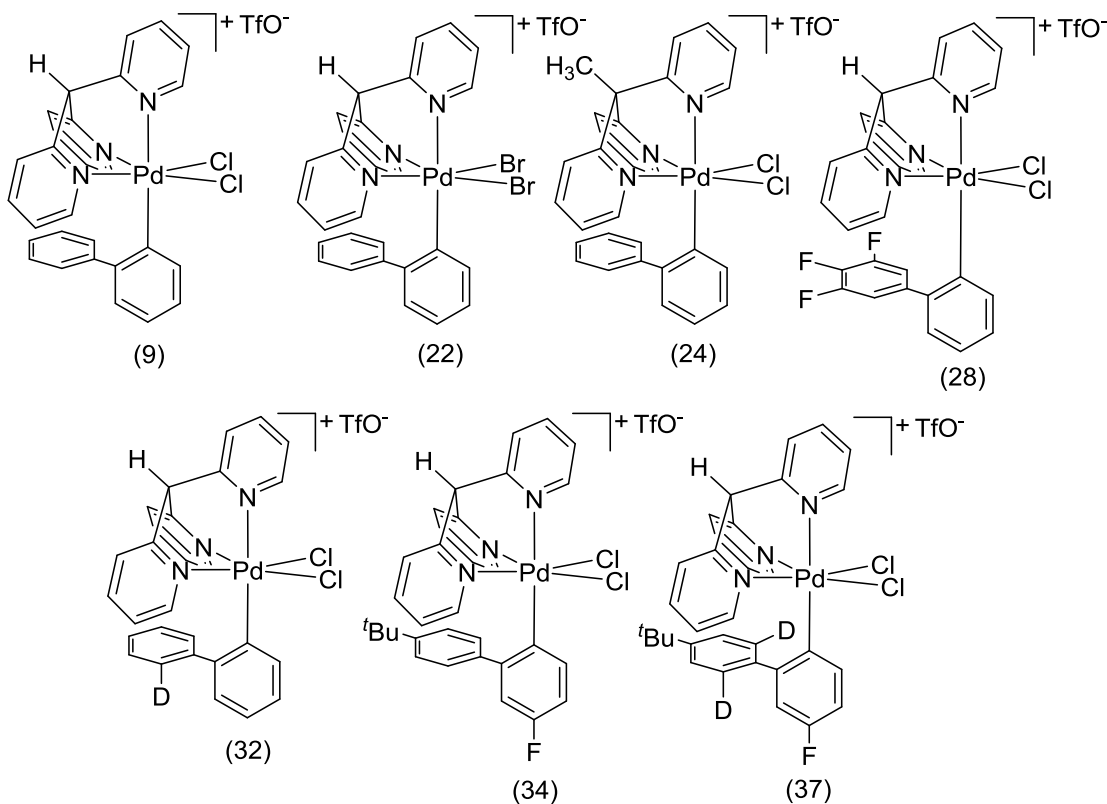
Crystal data and structure refinement for am5390 (**complex 20**).

Identification code	am5390
Empirical formula	C ₂₈ H ₂₂ Br ₄ I N ₃ Pd
Formula weight	953.43
Temperature	85(2) K
Wavelength	1.54178 Å
Crystal system, space group	Monoclinic, P2(1)/c
Unit cell dimensions	a = 13.5583(3) Å alpha = 90 deg. b = 12.5698(2) Å beta = 103.335(7) deg. c = 17.5426(12) Å gamma = 90 deg.
Volume	2909.1(2) Å ³
Z, Calculated density	4, 2.177 Mg/m ³
Absorption coefficient	20.096 mm ⁻¹
F(000)	1800
Crystal size	0.13 x 0.10 x 0.06 mm
Theta range for data collection	4.37 to 68.22 deg.
Limiting indices	-16<=h<=16, -15<=k<=15, -21<=l<=21
Reflections collected / unique	80357 / 5317 [R(int) = 0.0581]
Completeness to theta = 68.22	100.0%
Absorption correction	Semi-empirical from equivalents
Max. and min. transmission	0.545 and 0.287
Refinement method	Full-matrix least-squares on F ²
Data / restraints / parameters	5317 / 0 / 334
Goodness-of-fit on F ²	1.126
Final R indices [I>2sigma(I)]	R1 = 0.0251, wR2 = 0.0588
R indices (all data)	R1 = 0.0253, wR2 = 0.0589
Largest diff. peak and hole	0.708 and -0.777 e.Å ⁻³

Atomic coordinates ($\times 10^4$) and equivalent isotropic displacement parameters ($\text{Å}^2 \times 10^3$) for am5390 (**complex 20**). $U(\text{eq})$ is defined as one third of the trace of the orthogonalized U_{ij} tensor.

	x	y	z	$U(\text{eq})$
Pd(1)	3964(1)	1372(1)	8289(1)	8(1)
I(1)	8708(1)	2890(1)	2363(1)	12(1)
Br(1)	4910(1)	-248(1)	8713(1)	14(1)
Br(2)	5268(1)	1925(1)	7630(1)	16(1)
Br(3)	8444(1)	3029(1)	3824(1)	19(1)
Br(4)	9136(1)	2879(1)	916(1)	14(1)
N(1)	3163(2)	537(2)	7225(2)	12(1)
N(2)	2812(2)	815(2)	8778(2)	9(1)
N(3)	3108(2)	2670(2)	7802(2)	10(1)
C(1)	3624(3)	-73(3)	6785(2)	18(1)
C(2)	3098(3)	-540(3)	6104(3)	22(1)
C(3)	2061(3)	-385(3)	5870(2)	21(1)
C(4)	1583(3)	232(3)	6329(2)	17(1)
C(5)	2156(3)	683(3)	7007(2)	11(1)
C(6)	1693(2)	1389(3)	7535(2)	10(1)
C(7)	1859(3)	906(3)	8340(2)	11(1)
C(8)	1054(3)	490(3)	8616(2)	16(1)
C(9)	1241(3)	-46(3)	9321(3)	19(1)
C(10)	2230(3)	-146(3)	9748(2)	17(1)
C(11)	3003(3)	303(3)	9464(2)	14(1)
C(12)	2109(3)	2506(3)	7504(2)	9(1)
C(13)	1505(3)	3308(3)	7107(2)	12(1)
C(14)	1928(3)	4281(3)	6997(2)	15(1)
C(15)	2954(3)	4438(3)	7302(2)	15(1)
C(16)	3522(3)	3620(3)	7710(2)	12(1)
C(17)	4666(3)	2182(3)	9313(2)	11(1)
C(18)	5715(3)	2048(3)	9536(2)	14(1)
C(19)	6276(3)	2497(3)	10218(2)	15(1)
C(20)	5803(3)	3085(3)	10689(2)	20(1)
C(21)	4760(3)	3223(3)	10468(2)	18(1)
C(22)	4163(3)	2790(3)	9777(2)	13(1)
C(23)	3048(3)	3027(3)	9649(2)	14(1)
C(24)	2461(3)	2464(3)	10074(2)	17(1)
C(25)	1433(3)	2673(4)	9966(3)	24(1)
C(26)	978(3)	3473(4)	9459(3)	25(1)
C(27)	1568(3)	4087(4)	9077(3)	24(1)
C(28)	2601(3)	3870(3)	9185(2)	18(1)

3.11.5 Complexes with $[(\text{Py}_3\text{CH})\text{Pd}^{\text{IV}}(\text{biaryl})(\text{Y})_2][\text{OTf}]$ General Structure



General procedure 5: Preparation of Pd^{IV} complexes with $[(\text{Py}_3\text{CH})\text{Pd}^{\text{IV}}(\text{biphen-2-yl})(\text{Y})_2][\text{OTf}]$ general structure. AgOTf (82 mg; 0.32 mmol) was added to the solution of the corresponding Pd^{IV} complex (0.15 mmol) in CHCl₃ (15 mL). Resulting suspension was sonicated at 20 °C for 5 min and then it was filtered through a pad of diatomaceous earth. Volatiles were removed under reduced pressure and the residue was suspended in EtOAc (3 mL). EtOAc suspension was cooled to -25 °C for 30 min and then the product was collected by filtration, washed with EtOAc (2 mL) and finally with Et₂O (10 mL). The obtained orange powder was dried under high vacuum.

Preparation of [(Py₃CH)Pd^{IV}([1,1'-biphenyl]-2-yl)(Cl)₂][OTf] (9). **9** was obtained according to the general procedure **5** in 90% yield. ¹H NMR (CDCl₃): δ 9.09 (d, *J* = 5.2 Hz, 1H), 8.91 (d, *J* = 5.7 Hz, 2H), 8.53 (d, *J* = 8.8 Hz, 1H), 8.40 (d, *J* = 7.7 Hz, 2H), 8.31 (d, *J* = 7.7 Hz, 1H), 8.09 (t, *J* = 7.6 Hz, 2H), 7.92 (t, *J* = 7.6 Hz, 1H), 7.53 (t, *J* = 6.2 Hz, 2H), 7.46 (t, *J* = 6.4 Hz, 1H), 7.31 (m, 2H), 7.23 (t, *J* = 6.9 Hz, 1H), 6.84 (t, *J* = 7.5 Hz, 1H), 6.71 (dd, *J* = 7.0 and 2.1 Hz, 1H), 6.43 (t, *J* = 7.7 Hz, 2H), 5.73 (d, *J* = 7.2 Hz, 2H). ¹³C NMR (CDCl₃): δ 155.10, 153.58, 150.26, 149.97, 149.78, 143.35, 143.14, 141.69, 141.61, 140.60, 135.55, 129.08, 128.35, 127.89, 127.50, 127.14, 126.41, 126.26, 125.45, 120.87 (q, *J* = 319.8 Hz), 59.67. ¹⁹F NMR (CDCl₃): δ -78.20 (s). HRMS electrospray (*m/z*): [M – OTf]⁺ calcd for C₂₈H₂₂Cl₂N₃Pd, 576.0220; Found, 576.0217.

Preparation of [(Py₃CH)Pd^{IV}([1,1'-biphenyl]-2-yl)(Br)₂][OTf] (22). **22** was obtained according to the general procedure **5** in 73% yield. ¹H NMR (CDCl₃): δ 9.33 (d, *J* = 4.8 Hz, 1H), 9.09 (dd, *J* = 5.8 and 1.0 Hz, 2H), 8.94 (d, *J* = 8.8 Hz, 1H), 8.34 (d, *J* = 7.5 Hz, 2H), 8.28 (d, *J* = 7.7 Hz, 1H), 8.08 (t, *J* = 7.5 Hz, 2H), 7.90 (td, *J* = 7.8 and 1.7 Hz, 1H), 7.51 (t, *J* = 6.8 Hz, 2H), 7.39 (t, *J* = 7.2 Hz, 1H), 7.18 (m, 3H), 6.81 (t, *J* = 7.5 Hz, 1H), 6.69 (dd, *J* = 7.2 and 2.7 Hz, 1H), 6.41 (t, *J* = 7.8 Hz, 2H), 5.71 (d, *J* = 7.8 Hz, 2H). ¹³C NMR (CDCl₃): δ 154.88, 152.03, 150.53, 150.36, 150.18, 147.09, 144.16, 143.19, 141.55, 141.07, 135.88, 128.78, 127.76, 127.64, 127.51, 127.05, 126.82, 126.27, 126.06, 125.35, 120.88 (q, *J* = 320.2 Hz), 60.04. ¹⁹F NMR (CDCl₃): δ -78.14 (s). HRMS electrospray (*m/z*): [M – TfO]⁺ calcd for C₂₈H₂₂Br₂N₃Pd, 663.9215; Found, 663.9205.

Preparation of [(Py₃CCH₃)Pd^{IV}([1,1'-biphenyl]-2-yl)(Cl)₂][OTf] (24). **24** was obtained according to the general procedure **5** in 58% yield. ¹H NMR (CD₃NO₂): δ 9.29 (d, *J* = 4.9 Hz, 1H), 9.12 (d, *J* = 5.7 Hz, 2H), 8.57 (d, *J* = 8.6 Hz, 1H), 8.33 (t, *J* = 8.1 Hz,

2H), 8.10 (m, 3H), 8.01 (d, $J = 8.1$ Hz, 1H), 7.78 (t, $J = 6.6$ Hz, 2H), 7.67 (t, $J = 6.4$ Hz, 1H), 7.38 (td, $J = 7.1$ and 2.2 Hz, 1H), 7.33 (t, $J = 7.1$ Hz, 1H), 6.83 (t, $J = 7.6$ Hz, 1H), 6.78 (dd, $J = 6.9$ and 2.2 Hz, 1H), 6.53 (t, $J = 7.6$ Hz, 2H), 5.85 (d, $J = 7.3$ Hz, 2H), 2.75 (s, 3H). ^{13}C NMR (CD_3NO_2): δ 156.24, 154.93, 151.71, 151.20, 150.58, 144.02, 143.56, 141.76, 141.09, 140.96, 135.64, 127.79, 127.73 (two overlapping peaks as determined by 2D $^1\text{H}/^{13}\text{C}$ ASAPHMQC), 127.64, 127.10, 126.17, 125.65, 125.43, 123.22, 120.93 (q, $J = 320.4$ Hz), 57.88, 21.36. ^{19}F NMR (CD_3NO_2): δ -79.68 (s). HRMS electrospray (m/z): $[\text{M} - \text{TfO}]^+$ calcd for $\text{C}_{29}\text{H}_{24}\text{Cl}_2\text{N}_3\text{Pd}$, 592.0382; Found, 592.0376.

Preparation of $[(\text{Py}_3\text{CH})\text{Pd}^{\text{IV}}(\text{3',4',5'-trifluoro-[1,1'-biphenyl]-2-yl)(\text{Cl})_2][\text{OTf}]$ (28**).** **28** was obtained according to the general procedure **5** in 77% yield. The ratio between isomers **28a** and **28b** is approximately 50/50 in CDCl_3 at 25 °C. Because of the overlap between the peaks of the two isomers ^1H and $^{13}\text{C}\{^1\text{H}\}$ NMR data for **28a/b** is not reported in detail. ^{19}F NMR (CDCl_3 at 25°C): δ -78.28 (s, 6F), -133.05 (dd, $J = 19.9$ and 6.7 Hz, 2F), -137.94 (dd, $J = 19.9$ and 8.3 Hz, 2F), -159.42 (tt, $J = 19.9$ and 6.6 Hz, 1F), -163.01 (tt, $J = 21.6$ and 7.4 Hz, 1F). HRMS electrospray (m/z): $[\text{M} - \text{TfO}]^+$ calcd for $\text{C}_{28}\text{H}_{19}\text{Cl}_2\text{F}_3\text{N}_3\text{Pd}$, 629.9937; Found, 629.9939.

Preparation of $[(\text{Py}_3\text{CH})\text{Pd}^{\text{IV}}(\text{2'-deutero-[1,1'-biphenyl]-2-yl)(\text{Cl})_2][\text{OTf}]$ (32**).** **32** was obtained according to the general procedure **5** in 77% yield. ^1H NMR (CDCl_3): δ 9.12 (d, $J = 5.5$ Hz, 1H), 8.94 (d, $J = 6.0$ Hz, 2H), 8.55 (d, $J = 8.8$ Hz, 1H), 8.42 (d, $J = 7.4$ Hz, 2H), 8.33 (d, $J = 7.6$ Hz, 1H), 8.11 (t, $J = 7.4$ Hz, 2H), 7.94 (dt, $J = 7.7$ and 1.4 Hz, 1H), 7.56 (t, $J = 7.1$ Hz, 2H), 7.49 (t, $J = 6.5$ Hz, 1H), 7.34 (m, 2H), 7.25 (t, $J = 7.0$ Hz, 1H), 6.87 (t, $J = 7.6$ Hz, 1H), 6.73 (dd, $J = 7.1$ and 2.2 Hz, 1H), 6.46 (m, 2H), 5.75 (d, $J = 7.3$ Hz, 1H). ^{13}C NMR (CDCl_3): δ 155.14, 153.60, 150.27, 149.86, 149.74,

143.46, 143.12, 141.72, 141.56, 140.51, 135.56, 129.01, 128.32, 127.89, 127.54, 127.16, 127.03, 126.63, 126.54, 126.21, 125.49, 120.86 (q, $J = 320.2$ Hz), 59.80. ^{19}F NMR (CDCl_3 at 25°C): δ -78.20 (s). HRMS electrospray (m/z): $[\text{M} - \text{TfO}]^+$ calcd for $\text{C}_{28}\text{H}_{21}\text{DCl}_2\text{N}_3\text{Pd}$, 577.0283; Found, 577.0283.

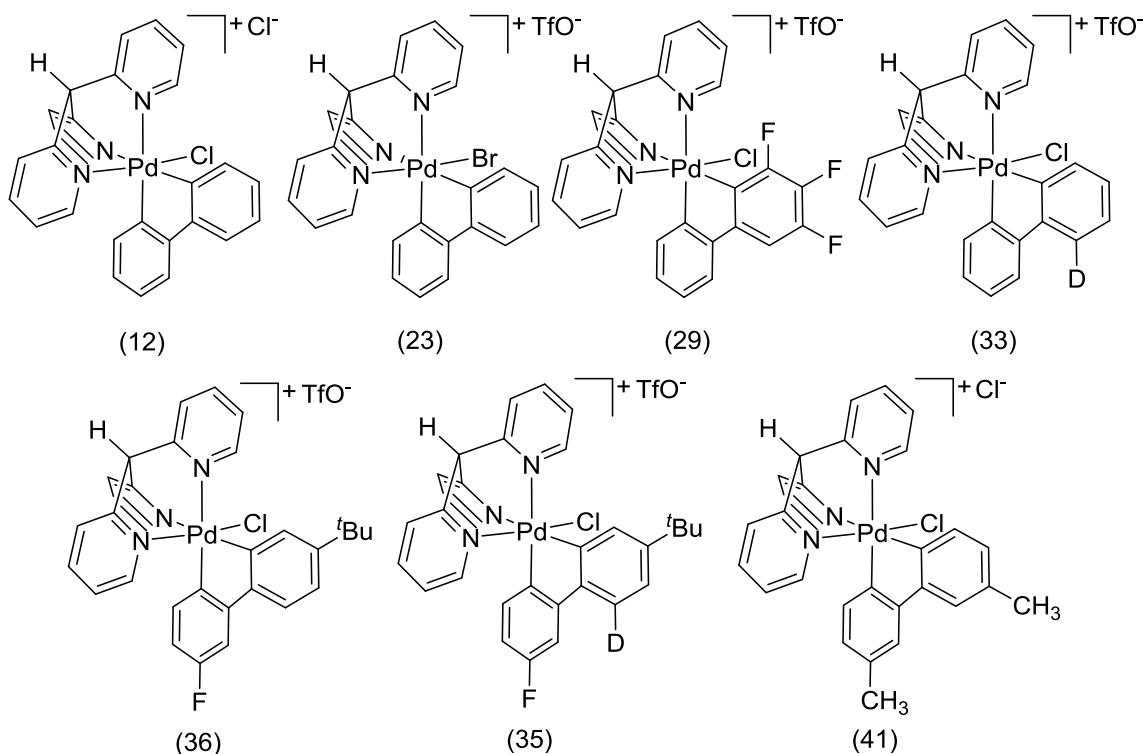
Preparatipon of $[(\text{Py}_3\text{CCH}_3)\text{Pd}^{\text{IV}}(\text{5-fluoro-4'-tert-butyl-[1,1'-biphenyl]-2-yl)(\text{Cl})_2][\text{OTf}]$ (34). **34** was obtained as an orange powder in 73% yield according to the general procedure **5** only using Et_2O for crystallization instead of EtOAc . ^1H NMR (CDCl_3): δ 9.09 (d, $J = 4.8$ Hz, 1H), 8.89 (d, $J = 5.9$ Hz, 1H), 8.54 (dd, $J = 9.5$ and 6.1 Hz, 1H), 8.44 (d, $J = 7.7$ Hz, 2H), 8.35 (d, $J = 7.7$ Hz, 1H), 8.11 (td, $J = 7.7$ and 1.1 Hz, 2H), 7.94 (td, $J = 7.7$ and 1.5 Hz, 1H), 7.57 (td, $J = 7.3$ and 1.5 Hz, 2H), 7.47 (t, $J = 7.0$ Hz, 1H), 7.39 (s, 1H), 7.09 (m, 1H), 6.53 (dd, $J = 9.2$ and 3.7 Hz, 1H), 6.43 (d, $J = 8.1$ Hz, 2H), 5.65 (d, $J = 8.4$ Hz, 2H), 1.17 (s, 9H). ^{13}C NMR (CDCl_3): δ 161.19 (d, $J = 249.9$ Hz), 153.48, 150.27, 149.93, 149.64, 149.44, 147.53, 144.72 (d, $J = 7.6$ Hz), 143.39, 142.57 (d, $J = 7.7$ Hz), 141.89, 136.84, 129.01, 127.09, 126.84, 126.54, 125.52, 124.12, 121.02 (d, $J = 21.9$ Hz), 120.83 (q, $J = 319.5$ Hz), 114.59 (d, $J = 20.1$ Hz), 59.52, 34.15, 30.88. ^{19}F NMR (CDCl_3): δ -78.13 (s, 3F), -115.97 (q, $J = 7.7$ Hz, 1F). HRMS electrospray (m/z): $[\text{M} - \text{TfO}]^+$ calcd for $\text{C}_{32}\text{H}_{29}\text{Cl}_2\text{FN}_3\text{Pd}$, 650.0752; Found, 650.0758.

Preparation of $[(\text{Py}_3\text{CH})\text{Pd}^{\text{IV}}(\text{4'-tert-butyl-2',6'-dideutero-5-fluoro-[1,1'-biphenyl]-2-yl)(\text{Cl})_2][\text{OTf}]$ (37). **37** was obtained as an orange powder in 91% yield according to the general procedure **5** only using Et_2O for crystallization instead of EtOAc . ^1H NMR (CDCl_3): δ 9.08 (dd, $J = 5.7$ and 1.2 Hz, 1H), 8.88 (dd, $J = 5.$ and 1.2 Hz, 1H), 8.53 (dd, $J = 9.7$ and 5.8 Hz, 1H), 8.44 (dd, $J = 7.7$ and 1.4 Hz, 2H), 8.35 (d, $J = 7.7$ Hz, 1H), 8.10 (td, $J = 7.7$ and 1.4 Hz, 2H), 7.92 (td, $J = 7.7$ and 1.3 Hz, 1H), 7.57 (m,

2H), 7.47 (m, 1H), 7.39 (s, 1H), 7.09 (m, 1H), 6.52 (dd, $J = 9.0$ and 3.4 Hz, 1H), 6.42 (s, 2H), 1.16 (s, 9H). ^{13}C NMR (CDCl_3): δ 161.19 (d, $J = 249.7$ Hz), 153.45, 150.26, 149.95, 149.65, 149.46, 147.55, 144.65 (d, $J = 7.2$ Hz), 143.37, 142.56 (d, $J = 7.5$ Hz), 141.87, 136.66, 129.01, 126.85, 126.76 (broad signal of low intensity overlapping with 126.85), 126.51, 125.51, 124.00, 121.01 (d, $J = 21.2$ Hz), 120.84 (q, $J = 320.2$ Hz), 114.57 (d, $J = 20.4$ Hz), 59.48, 34.14, 30.88. ^{19}F NMR (CDCl_3): δ -78.15 (s, 3F), -115.97 (q, $J = 7.9$ Hz, 1F). HRMS electrospray (m/z): $[\text{M} - \text{TfO}]^+$ calcd for $\text{C}_{32}\text{H}_{27}\text{D}_2\text{Cl}_2\text{FN}_3\text{Pd}$, 652.0877; Found, 652.0881.

3.11.6 Complexes with $[(\text{Py}_3\text{CH})\text{Pd}^{\text{IV}}([\text{1,1'-biphenyl-2,2'-diyl}(\text{X}))][\text{Y}]$ General

Structure



Preparation of [(Py₃CH)Pd^{IV}([1,1'-biphenyl]-2,2'-diyl)(Cl)][Cl] (12**).** Method A: with aq KOAc as the acetate source. Solution of Pd^{IV} dichloride **9** (200 mg; 0.33 mmol) in CH₂Cl₂ (10 mL) was washed with 5% aq KOAc (4×15 mL) then with water (2×15 mL) and finally with brine (2×15 mL). The organic phase was dried over anhydrous Na₂SO₄ and volatiles were evaporated under reduced pressure. The residue was suspended in Et₂O (20 mL) and sonicated for 5 minutes at 20 °C. The product was collected by filtration, washed with EtOAc (3×2 mL) and dried under vacuum. Yield: 73 mg (39%) of a pale yellow powder.

Method B: with AgOAc as the acetate source. AgOAc (167 mg; 1.0 mmol) was added to the solution of the Pd^{IV} dichloride **9** (200.0 mg; 0.33 mmol) in CHCl₃ (20 mL). The resulting suspension was sonicated for 5 min at 20 °C and then filtered through a pad of diatomaceous earth. The mother liquor was then washed with brine (4×10 mL). Organic layer was dried over anhydrous Na₂SO₄ and evaporated under reduced pressure. The residue was suspended in Et₂O (10 mL) and sonicated for 5 minutes at 20 °C. The fine powder was collected by filtration, washed with Et₂O (3×3 mL) then with EtOAc (3×3 mL) and dried under vacuum. Yield: 148 mg (78%) of a pale yellow powder. X-ray quality crystals of **12** were grown by slow vapor diffusion of MTBE into CD₃NO₂ solution of **12** at 4 °C. ¹H NMR (CDCl₃): δ 9.22 (d, *J* = 7.2 Hz, 1H), 9.11 (m, 3H), 8.96 (d, *J* = 7.6 Hz, 2H), 8.06 (t, *J* = 6.9 Hz, 2H), 7.95 (t, *J* = 7.4 Hz, 1H), 7.77 (d, *J* = 6.2 Hz, 2H), 7.61 (t, *J* = 6.2 Hz, 3H), 7.50 (d, *J* = 5.3 Hz, 1H), 7.31 (t, *J* = 7.1 Hz, 2H), 7.04 (t, *J* = 6.2 Hz, 1H), 6.96 (t, *J* = 7.0 Hz, 2H), 6.87 (d, *J* = 7.9 Hz, 2H). ¹³C NMR (CDCl₃): δ 161.47, 153.06, 152.89, 150.44, 150.04, 146.21, 142.19, 141.42, 130.47, 130.36, 128.87,

128.00, 127.67, 125.51, 125.48, 124.88, 57.23. HRMS electrospray (m/z): $[M - Cl]^+$ calcd for $C_{28}H_{21}ClN_3Pd$, 540.0453; Found, 540.0462.

General procedure 6: Preparation of Pd^{IV} complexes with [(Py₃CH)Pd^{IV}([1,1'-biphenyl]-2,2'-diyl)(X)][OTf] general structure. 4Å Molecular sieves were added to the solution of the corresponding [(Py₃CH)Pd^{IV}(aryl)(X)₂][OTf] complex (0.06 mmol) in CHCl₃ (7 mL). The solution was stirred 5 minutes at ambient temperature and then AgOAc (45 mg; 0.27 mmol) was added. The resulting suspension was stirred for 40 min at ambient temperature and then filtered through a pad of diatomaceous earth. The mother liquor was washed with water (2×5 mL), organic layer was dried over anhydrous Na₂SO₄ and evaporated under reduced pressure. The residue was suspended in Et₂O (5 mL) and sonicated for 5 minutes at 20°C. The product was collected by filtration, washed with EtOAc (3×2 mL) and dried under vacuum.

Preparation of [(Py₃CH)Pd^{IV}([1,1'-biphenyl]-2,2'-diyl)(Br)][OTf] (23). **23** was obtained according to the general procedure **6** in 53% yield as a pale yellow powder. ¹H NMR (CD₂Cl₂): δ 9.29 (d, *J* = 5.5 Hz, 2H), 8.60 (d, *J* = 8.9 Hz, 1H), 8.46 (d, *J* = 7.9 Hz, 2H), 8.15 (td, *J* = 7.9 and 1.7 Hz, 2H), 8.00 (td, *J* = 7.5 and 1.4 Hz, 1H), 7.80 (dd, *J* = 7.5 and 1.4 Hz, 2H), 7.67 (td, *J* = 6.7 and 1.4 Hz, 2H), 7.49 (d, *J* = 5.9 Hz, 1H), 7.33 (m, 3H), 7.10 (td, *J* = 7.5 and 1.4 Hz, 1H), 7.00 (td, *J* = 7.7 and 1.7 Hz, 2H), 6.91 (d, *J* = 8.2 Hz, 2H). ¹³C NMR (CD₂Cl₂): δ 157.35, 152.47, 151.77, 151.21, 150.07, 147.19, 142.45, 141.71, 130.96, 129.00, 128.90, 127.46, 127.04, 125.89, 125.64, 124.64, 121.04 (q, *J* = 320.8 Hz), 59.83. ¹⁹F NMR (CD₂Cl₂): δ -79.20 (s). HRMS electrospray (m/z): $[M - TfO]^+$ calcd for $C_{28}H_{21}BrN_3Pd$, 583.9954; Found, 583.9958.

Preparation of [(Py₃CH)Pd^{IV}(3,4,5-trifluoro-[1,1'-biphenyl]-2,2'-diyl)(Cl)][OTf] (28). **28** was obtained according to the general procedure **6** in 66% yield as a pale yellow powder. ¹H NMR (~1/2 mixture of CD₃NO₂ and CDCl₃): δ 9.16 (m, 2H), 8.38 (d, *J* = 7.8 Hz, 1H), 8.27 (m, 2H), 8.21 (m, 3H), 7.83 (ddd, *J* = 7.3, 5.7 and 2.0 Hz, 1H), 7.77 (dd, *J* = 7.7 and 1.7 Hz, 1H), 7.65 (m, 2H), 7.62 (m, 1H), 7.41 (t, *J* = 7.1 Hz, 1H), 7.33 (ddd, *J* = 7.5, 6.1 and 1.5 Hz, 1H), 7.07 (ddd, *J* = 7.7, 6.1 and 1.7 Hz, 1H), 6.91 (s, 1H), 6.86 (d, *J* = 8.2 Hz, 1H). ¹³C NMR (~1/2 mixture of CD₃NO₂ and CDCl₃): δ 161.92, 152.25, 152.21, 151.63, 151.26 (ddd, *J* = 250.0, 64.8 and 3.4 Hz), 151.22, 151.10, 150.88, 150.41, 146.47 (m), 143.58, 143.00 (m), 142.66, 142.02, 138.10 (ddd, *J* = 255.5, 19.8 and 15.8 Hz), 135.63 (dt, *J* = 23.8 and 3.0 Hz), 130.53, 130.04, 129.05, 128.10, 126.78, 126.59, 126.57, 126.37, 125.66, 124.54, 121.00 (q, *J* = 320.8 Hz), 107.66 (dd, *J* = 20.4 and 1.4 Hz), 61.22. ¹⁹F NMR (~1/2 mixture of CD₃NO₂ and CDCl₃): δ -79.03 (s, 3F), -123.44 (m, 1F), -137.92 (m, 1F), -158.36 (m, 1F). HRMS electrospray (m/z): [M – TfO]⁺ calcd for C₂₈H₁₈ClF₃N₃Pd, 594.0171; Found, 594.0183.

Preparation of [(Py₃CH)Pd^{IV}(6-deutero-[1,1'-biphenyl]-2,2'-diyl)(Cl)][OTf] (33). **33** was obtained according to the general procedure **6** in 84% yield as a pale yellow powder. ¹H NMR (CDCl₃): δ 9.14 (d, *J* = 5.1 Hz, 2H), 8.75 (d, *J* = 7.8 Hz, 1H), 8.57 (d, *J* = 7.8 Hz, 2H), 8.10 (td, *J* = 7.8 and 1.4 Hz, 2H), 7.99 (td, *J* = 7.8 and 1.3 Hz, 1H), 7.77 (dd, *J* = 7.5 and 1.2 Hz, 1H), 7.64 (t, *J* = 6.4 Hz, 1H), 7.53 (m, 2H), 7.32 (m, 2H), 7.08 (t, *J* = 6.0 Hz, 1H), 6.97 (t, *J* = 7.3 Hz, 2H), 6.86 (d, *J* = 8.2 Hz, 2H). ¹³C NMR (CDCl₃): δ 161.49, 161.43, 152.38, 152.06, 150.81, 150.34, 146.13, 146.09, 142.68, 141.84, 130.28, 129.75, 128.96, 127.78, 127.67, 127.30, 125.84, 125.76, 124.99, 120.91 (q, *J* = 320.2 Hz), 59.27. (Signal of the carbon attached to deuterium was not observed presumably

because it is a triplet of low intensity that overlaps with nearby more intense signals.) ^{19}F NMR (CDCl_3): δ -78.02. HRMS electrospray (m/z): $[\text{M} - \text{TfO}]^+$ calcd for $\text{C}_{28}\text{H}_{20}\text{DCIN}_3\text{Pd}$, 541.0516; Found, 541.0523.

Preparation of $[(\text{Py}_3\text{CH})\text{Pd}^{\text{IV}}(4'\text{-tert-butyl-5-fluoro-[1,1'\text{-biphenyl]-2,2'\text{-diyl}})(\text{Cl})][\text{OTf}]$ (36). **36** was obtained according to the general procedure **6** in 70% yield as a pale yellow powder. ^1H NMR (CDCl_3): δ 9.14 (d, $J = 5.6$ Hz, 1H), 9.10 (d, $J = 5.6$ Hz, 1H), 8.76 (d, $J = 7.8$ Hz, 1H), 8.61 (d, $J = 7.8$ Hz, 1H), 8.54 (d, $J = 8.0$ Hz, 1H), 8.14 (td, $J = 7.7$ and 1.5 Hz, 1H), 8.11 (td, $J = 7.8$ and 1.5 Hz, 1H), 8.03 (td, $J = 7.7$ and 1.4 Hz, 1H), 7.64 (m, 3H), 7.52 (m, 2H), 7.46 (dd, $J = 9.0$ and 2.9 Hz, 1H), 7.36 (dd, $J = 8.0$ and 1.4 Hz, 1H), 7.12 (td, $J = 6.8$ and 1.4 Hz, 1H), 6.83 (d, $J = 1.4$ Hz, 1H), 6.80 (dd, $J = 8.7$ and 4.8 Hz, 1H), 6.70 (td, $J = 7.8$ and 2.9 Hz, 1H), 1.17 (s, 9H). ^{13}C NMR (CDCl_3): δ 162.78 (d, $J = 245.9$ Hz), 161.53, 153.76, 153.50, 152.45, 152.43, 152.08, 150.73, 150.30, 150.18, 147.29 (d, $J = 6.8$ Hz), 142.78, 142.31 (d, $J = 2.7$ Hz), 142.09, 141.88, 130.79 (d, $J = 7.5$ Hz), 130.00, 127.63, 127.39, 126.81, 125.83, 125.81, 125.28, 125.08, 124.68, 120.91 (q, $J = 320.2$ Hz), 114.64 (d, $J = 22.5$ Hz), 111.51 (d, $J = 23.2$ Hz), 59.18, 35.84, 31.21. ^{19}F NMR (CDCl_3): δ -78.12 (s, 3F), -115.40 (m, 1F). HRMS electrospray (m/z): $[\text{M} - \text{TfO}]^+$ calcd for $\text{C}_{32}\text{H}_{28}\text{CFIN}_3\text{Pd}$, 614.0985; Found, 614.0995.

Preparation of $[(\text{Py}_3\text{CH})\text{Pd}^{\text{IV}}(4'\text{-t-Bu-2'\text{-deutero-5-fluoro-[1,1'\text{-biphenyl]-2,2'\text{-diyl}})(\text{Cl})][\text{OTf}]$ (35). **35** was obtained according to the general procedure **6** in 63% yield as a pale yellow powder. ^1H NMR (CDCl_3): δ 9.15 (d, $J = 4.9$ Hz, 1H), 9.11 (d, $J = 4.8$ Hz, 1H), 8.82 (d, $J = 7.8$ Hz, 1H), 8.65 (d, $J = 7.8$ Hz, 1H), 8.58 (d, $J = 7.8$ Hz, 1H), 8.14 (td, $J = 7.8$ and 1.1 Hz, 1H), 8.11 (td, $J = 7.8$ and 1.4 Hz, 1H), 8.02 (t, $J = 7.5$ Hz, 1H), 7.64 (m, 2H), 7.60 (s, 1H), 7.53 (d, $J = 5.3$ Hz, 1H), 7.47 (dd, $J = 9.0$ and 2.9 Hz, 1H),

7.37 (s, 1H), 7.12 (t, $J = 6.1$ Hz, 1H), 6.84 (d, $J = 1.0$ Hz, 1H), 6.80 (dd, $J = 8.7$ and 4.7 Hz, 1H), 6.71 (td, $J = 8.7$ and 2.9 Hz, 1H), 1.18 (s, 9H). ^{13}C NMR (CDCl_3): δ 162.79 (d, $J = 245.9$ Hz), 161.51, 153.75, 153.51 (d, $J = 1.5$ Hz), 152.45, 152.43, 152.08, 150.74, 150.31, 150.19, 147.27 (d, $J = 7.5$ Hz), 142.77, 142.25 (d, $J = 2.7$ Hz), 142.09, 141.89, 130.79 (d, $J = 7.5$ Hz), 130.01, 127.64, 127.40, 126.81, 125.83, 125.81, 125.28, 124.98, 124.39 (broad multiplet), 120.92 (q, $J = 320.2$ Hz), 114.64 (d, $J = 21.8$ Hz), 111.52 (d, $J = 23.2$ Hz), 59.16, 35.85, 31.21. ^{19}F NMR (CDCl_3): δ -78.12 (s, 3F), -115.35 (m, 1F). HRMS electrospray (m/z): $[\text{M} - \text{TfO}]^+$ calcd for $\text{C}_{32}\text{H}_{27}\text{DCFIn}_3\text{Pd}$, 615.1048; Found, 615.1064.

Preparation of $[(\text{Py}_3\text{CH})\text{Pd}^{\text{IV}}(5,5'\text{-dimethyl-[1,1'-biphenyl]-2,2'-diyl})(\text{Cl})](\text{Cl})$ (41**).** AgOAc (134 mg; 0.80 mmol) was added to the solution of the Pd^{IV} complex **40** (150 mg; 0.187 mmol) in CHCl_3 (20 mL). The resulting suspension was sonicated for 5 min at 20 °C and then filtered through a pad of diatomaceous earth. Mother liquor was washed with brine (4×10 mL). Organic layer was dried over anhydrous MgSO_4 and evaporated under reduced pressure. The residue was suspended in MTBE (10 mL) and sonicated for 5 minutes at 20 °C. The fine powder was collected by filtration, washed with MTBE (3×3 mL) and dried under vacuum. Yield: 78 mg (69%) of a pale yellow powder. Analytical sample was obtained by dissolving the crude product in minimal amount of CH_2Cl_2 and consecutive precipitation with ethanol. ^1H NMR (acetone- d_6 at 25 °C): δ 9.19 (dd, $J = 5.4$ and 1.0 Hz, 2H), 8.70 (d, $J = 7.5$ Hz, 1H), 8.58 (d, $J = 7.5$ Hz, 2H), 8.33 (t, $J = 7.5$ Hz, 2H), 8.24 (t, $J = 7.1$ Hz, 1H), 7.93 (bs, 1H), 7.89 (dd, $J = 5.8$ and 7.2 Hz, 2H), 7.75 (d, $J = 1.9$ Hz, 2H), 7.71 (dd, $J = 5.1$ and 1.0 Hz, 1H), 7.41 (t, $J = 6.6$ Hz, 1H), 6.91 (d, $J = 8.3$ Hz, 2H), 6.82 (dd, $J = 8.3$ and 1.5 Hz, 2H), 2.41 (s, 6H).

$^{13}\text{C}\{^1\text{H}\}$ NMR (acetone- d_6 at 25 °C): δ 158.61, 152.36, 151.93, 151.40, 150.84, 146.17, 142.96, 142.04, 136.98, 130.22, 129.13, 128.98, 126.55, 126.37, 126.19, 125.39, 59.90, 19.91. HRMS electrospray (m/z): $[\text{M} - \text{Cl}]^+$ calcd for $\text{C}_{30}\text{H}_{25}\text{ClN}_3\text{Pd}$, 568.0772; Found, 568.0763.

X-ray structure determination for $[(\text{Py}_3\text{CH})\text{Pd}^{\text{IV}}([\text{1,1}'\text{-biphenyl-2,2}'\text{-diyl})(\text{Cl})][\text{Cl}]$ (12**).** Orange needles of complex **12** were grown from a methyl-t-butyl ether /nitromethane solution of the compound at 4 deg. C. A crystal of dimensions 0.11 x 0.03 x 0.03 mm was mounted on a Rigaku AFC10K Saturn 944+ CCD-based X-ray diffractometer equipped with a low temperature device and Micromax-007HF Cu-target micro-focus rotating anode ($\lambda = 1.54187 \text{ \AA}$) operated at 1.2 kW power (40 kV, 30 mA). The X-ray intensities were measured at 85(1) K with the detector placed at a distance 42.00 mm from the crystal. A total of 3890 images were collected with an oscillation width of 1.0° in ω . The exposure time was 2 sec. for the low angle images, 8 sec. for high angle. The integration of the data yielded a total of 61924 reflections to a maximum 2θ value of 136.48° of which 2289 were independent and 270 were greater than $2\sigma(I)$. The final cell constants were based on the xyz centroids of 46351 reflections above $10\sigma(I)$. Analysis of the data showed negligible decay during data collection; the data were processed with CrystalClear 2.0 and corrected for absorption. The structure was solved and refined with the Bruker SHELXTL (version 2008/4) software package, using the space group Pnma with $Z = 4$ for the formula $\text{C}_{28}\text{H}_{21}\text{N}_3\text{Cl}_2\text{Pd}\cdot(\text{H}_2\text{O})_{0.5}$. Full matrix least-squares refinement based on F^2 converged at $R1 = 0.0219$ and $wR2 = 0.0548$ [based on $I > 2\sigma(I)$], $R1 = 0.0221$ and $wR2 = 0.0549$ for all data. The Pd-complex lies on a mirror plane in the crystal lattice. Additional details are presented in below.

Crystal data and structure refinement for complex **12**.

Identification code	am5405 (complex 12)
Empirical formula	C ₂₈ H ₂₂ Cl ₂ N ₃ O _{0.50} Pd
Formula weight	585.79
Temperature	85(2) K
Wavelength	1.54178 Å
Crystal system, space group	Orthorhombic, P n m a
Unit cell dimensions	a = 13.9621(10) Å alpha = 90 deg. b = 12.8717(2) Å beta = 90 deg. c = 13.3016(2) Å gamma = 90 deg.
Volume	2390.51(18) Å ³
Z, Calculated density	4, 1.628 Mg/m ³
Absorption coefficient	8.514 mm ⁻¹
F(000)	1180
Crystal size	0.11 x 0.03 x 0.03 mm
Theta range for data collection	4.59 to 68.24 deg.
Limiting indices	-16<=h<=16, -15<=k<=15, -16<=l<=16
Reflections collected / unique	61924 / 2289 [R(int) = 0.0440]
Completeness to theta = 68.24	100.0%
Absorption correction	Semi-empirical from equivalents
Max. and min. transmission	0.7843 and 0.4544
Refinement method	Full-matrix least-squares on F ²
Data / restraints / parameters	2289 / 3 / 182
Goodness-of-fit on F ²	1.051
Final R indices [I>2sigma(I)]	R1 = 0.0219, wR2 = 0.0548
R indices (all data)	R1 = 0.0221, wR2 = 0.0549
Largest diff. peak and hole	0.461 and -0.376 e.Å ⁻³

Atomic coordinates ($\times 10^4$) and equivalent isotropic displacement parameters ($\text{\AA}^2 \times 10^3$) for am5405 (**complex 12**). U(eq) is defined as one third of the trace of the orthogonalized Uij tensor.

	x	y	z	U(eq)
Pd(1)	3727(1)	2500	3816(1)	10(1)
Cl(1)	2373(1)	2500	2835(1)	16(1)
Cl(2)	3989(1)	2500	8797(1)	19(1)
N(1)	3107(1)	1381(1)	4856(1)	13(1)
N(2)	4952(1)	2500	4664(1)	12(1)
C(1)	2569(1)	572(1)	4570(1)	15(1)
C(2)	2238(1)	-160(1)	5252(1)	18(1)
C(3)	2465(1)	-35(1)	6262(1)	19(1)
C(4)	2988(1)	829(1)	6563(1)	17(1)
C(5)	3299(1)	1527(1)	5837(1)	14(1)
C(6)	3856(2)	2500	6119(2)	14(1)
C(7)	4854(2)	2500	5673(2)	14(1)
C(8)	5656(2)	2500	6284(2)	16(1)
C(9)	6564(2)	2500	5862(2)	19(1)
C(10)	6647(2)	2500	4825(2)	17(1)
C(11)	5830(2)	2500	4243(2)	15(1)
C(12)	4319(1)	1474(1)	2845(1)	13(1)
C(13)	4410(1)	419(1)	3028(1)	15(1)
C(15)	5120(1)	230(1)	1379(1)	17(1)
C(16)	5048(1)	1295(1)	1215(1)	17(1)
C(17)	4657(1)	1930(1)	1963(1)	14(1)
C(14)	4819(1)	-198(1)	2279(1)	17(1)
O(1)	6181(2)	2500	8864(3)	20(1)

Hydrogen bonds for am5405 (**complex 12**) [A and deg.].

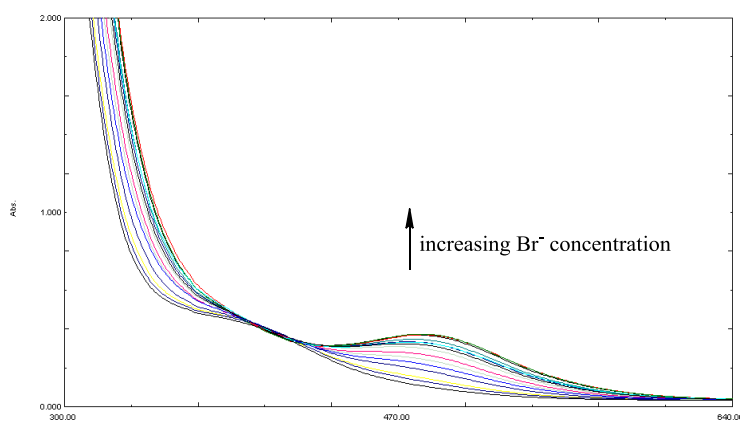
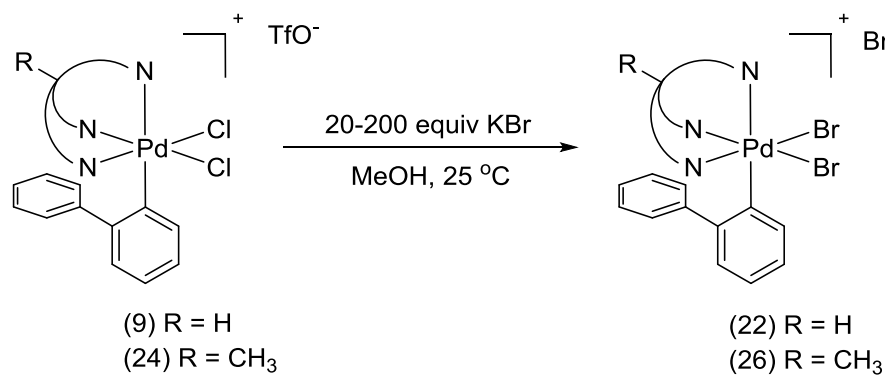
D-H...A	d(D-H)	d(H...A)	d(D...A)	<(DHA)
O(1)-H(1)...Cl(2)	0.824(17)	2.238(17)	3.061(4)	179(6)

Symmetry transformations used to generate equivalent atoms: #1 x,-y+1/2,z

3.11.7 Chloride-to-bromide ligand exchange rates for complexes **9** and **24**

Experimental procedures. First, **9** and **24** were titrated with potassium bromide (0-50 equivalents) and progress of the reaction was monitored with UV-VIS spectroscopy. Both reactions of **9** and **24** yielded very similar UV-VIS spectra and those of compound **24** are shown in Figure 3.8. Growing absorbance band centered at ~ 480 nm is likely due to a bromide-to-palladium charge transfer in the corresponding mono bromide intermediates and in final products **22** and **26**. From this absorbance band at 480 nm it was determined that for both complexes ~10 equivalents of bromide are necessary to drive the reaction to completion.

Figure 3.8 Absorbance of complex **24** as a function of added bromide (0 - 50 equiv)



Next, rate experiments were performed under pseudo first order conditions in bromide (10-200 equiv). Reactions were monitored at 480 nm and in all cases even and

reproducible reaction traces were obtained (Figure 3.9 and Figure 3.10). However, these reaction traces were not fitted to an exponential or two exponentials because the overall transformations shown in the scheme above are multi step processes that involve several ligand dissociation and association events and the relative rates of these elementary steps are unknown. Even though accurate rate constants were not extracted from the performed rate experiments, nevertheless, two important qualitative observations were made. First, it was determined that under identical conditions reaction of **9** with KBr reached completion in more than 10 times shorter time than the reaction of **24** with KBr. Second, for both complexes **10** and **24**, the reaction rate was dependent on the bromide concentration in a wide concentration range from 5-100 mM (10 to 200 equiv). These two observations support the hypothesis of reversible dissociation of one pyridine arm of the Py_3CH ligand and the proposed ligand exchange mechanism.

Figure 3.9 UV-Vis traces (480 nm) of reaction between complex **9** and bromide

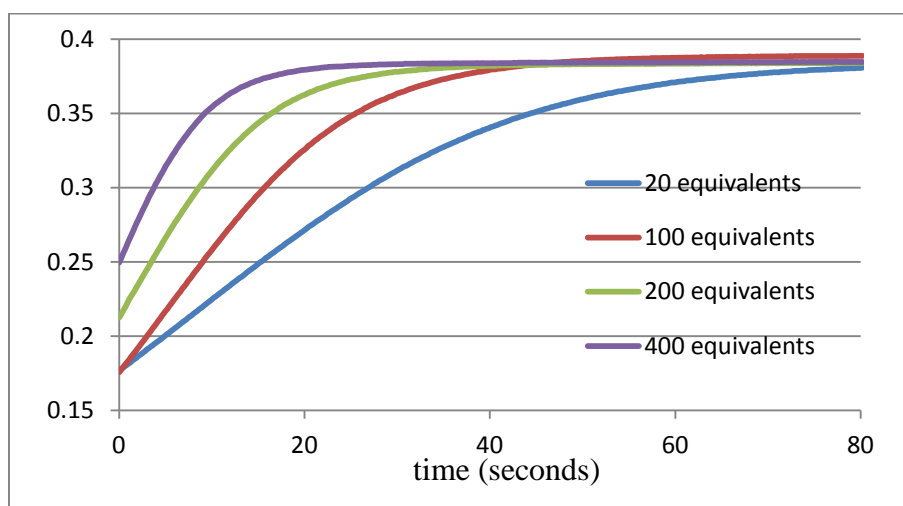
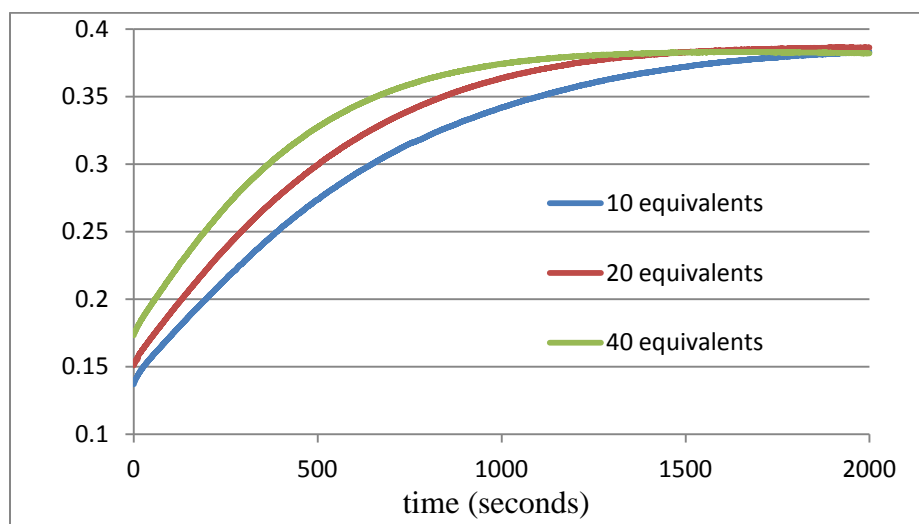


Figure 3.10 UV-Vis traces (480 nm) of reaction between complex **24** and bromide



3.11.8 Determination of Intramolecular Kinetic Isotope Effect

Experimental procedure for determination of intramolecular KIE: Complex **32** (9.8 mg; 0.015 mmol) was dissolved in CDCl_3 (0.5 mL) and 4Å molecular sieves were added to this solution. The solution was equilibrated to a set temperature and then the corresponding silver carboxylate (0.06 mmol) was added in one portion. The resulting suspension was stirred intensively for 20 minutes and then filtered through a plug of celite. The solution was first analyzed by ^1H NMR to ensure a complete consumption of the starting material and to verify that complex **33** is the main reaction product. CDCl_3 solution was then evaporated and the residue was analyzed by mass spectrometry in low resolution ESI+ mode. The MS data is provided in Table 3.3.

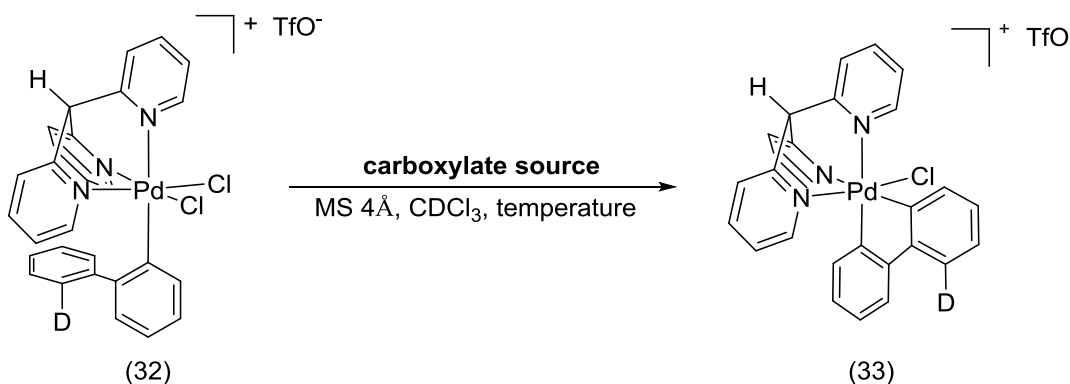
Calculation of KIE: KIEs were calculated from MS data (Table 3.3) according to the published method.²⁶ The MS data of **12** (showed in Table 3.2) was used as a standard from which extent of deuterium incorporation for compound **31** was calculated. The use

of theoretical isotope distribution pattern as standard yielded slightly different results, however, the discrepancies were negligible.

Table 3.2 MS data of $[(\text{Py}_3\text{CH})\text{Pd}^{\text{IV}}([\text{1,1'-biphenyl-2,2'-diyl})(\text{Cl})]^+$ (**12**)

m/z	538	539	540	541	542	543	544	545	546	547	548
	Relative intensity										
Complex 12	27.1	64.51	98.01	45.07	100	29.11	54.75	16.09	11.63	3.33	0

Table 3.3 MS data for intramolecular KIE determination



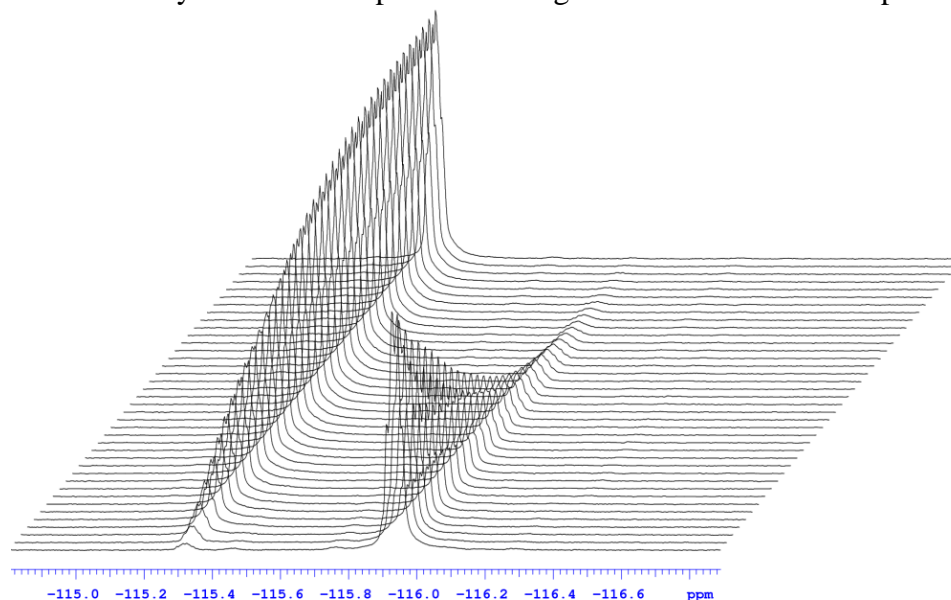
m/z	538	539	540	541	542	543	544	545	546	547	548	KIE
	Relative intensity											
AgOAc, 25 °C	3.86	34.38	73.82	99.24	55.04	100	34.33	54.69	17.11	11.47	2.99	9.4
AgOAc, 0 °C	3.47	32.99	72.96	97.61	53.39	100	32.91	54.53	16.68	11.28	3.23	10.34
AgOAc, 55 °C	4.83	36.42	75.53	100	58.74	98.53	35.64	55.83	16.8	11.24	3.16	6.93
AgOPiv, 25 °C	3.52	32.36	73.06	100	52.5	99.37	30.92	51.81	14.5	9.99	2.61	9.73
AgOOCFF ₃ , 25 °C	3.21	31.31	71.66	99.58	51.58	100.00	30.93	52.12	14.46	9.84	2.67	11.49
AgOOCCH ₃ , 25 °C	3.57	33.29	72.19	100.00	51.82	99.40	32.22	53.14	16.15	10.81	2.65	9.96
aq KOAc, 25 °C	3.40	32.43	71.90	100.00	51.16	99.41	30.48	51.46	14.67	10.02	2.73	10.89
AgOTf, 25 °C	11.66	49.67	95.74	100.00	78.06	95.29	43.14	49.61	16.11	9.59	2.41	1.97

3.11.9 Determination of Intermolecular Kinetic Isotope Effect

Experimental procedure: Complex **34** (12.3 mg; 0.015 mmol) was dissolved in dry CDCl_3 (0.6 mL) and the solution was cooled to $-30\text{ }^\circ\text{C}$. Silver pivalate (9.4 mg; 0.045) was then added and the resulting suspension was sonicated at $-30\text{ }^\circ\text{C}$ for 3 minutes. ^{19}F NMR and ^1H NMR analysis of this reaction mixture at $-30\text{ }^\circ\text{C}$ showed

almost complete conversion of **34** to the intermediate **35**. The kinetics of conversion of **35** into the final product **36** was monitored by ^{19}F NMR at 0 °C and spectra were recorded with 1 minute intervals (Figure 3.11 and Figure 3.12). Kinetics of conversion of the deuterated complex **37** into the final product **39** was monitored in the exactly same manner (Figure 3.13 and Figure 3.14). Complexes **36** and **39** were also synthesized on a preparative scale and fully characterized by NMR and MS (see above). The obtained reaction traces could not be fitted to a simple mathematical functions, however, it can be qualitatively estimated that **35** and **38** decays to the corresponding products **36** and **39** at approximately the same rate. The most likely explanation of why reaction traces could not be fitted to simple mathematical functions is that conversion of **35** to **36** (and **38** to **39**) is a multistep process.

Figure 3.11 Array of ^{19}F NMR spectra showing conversion of **34** to the product **35**



(intermediate **34** at approximately -116.0 ppm and product **35** ~ -115.3 ppm, spectra acquired at 500 MHz)

Figure 3.12 Plot of **35** formed and **34** consumed as a function of time

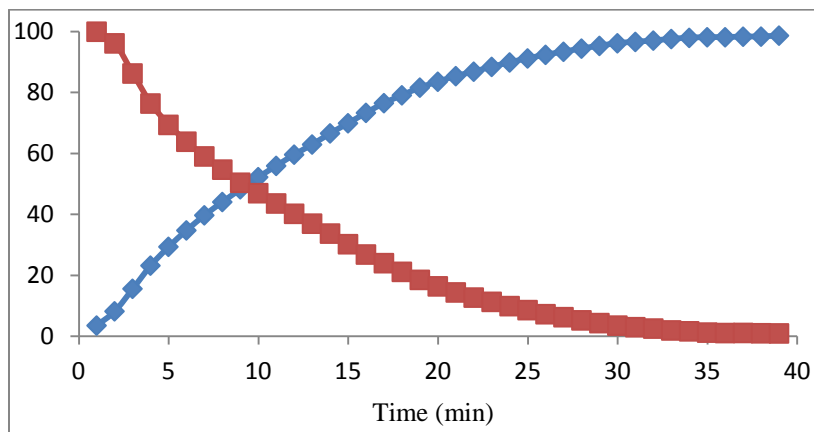
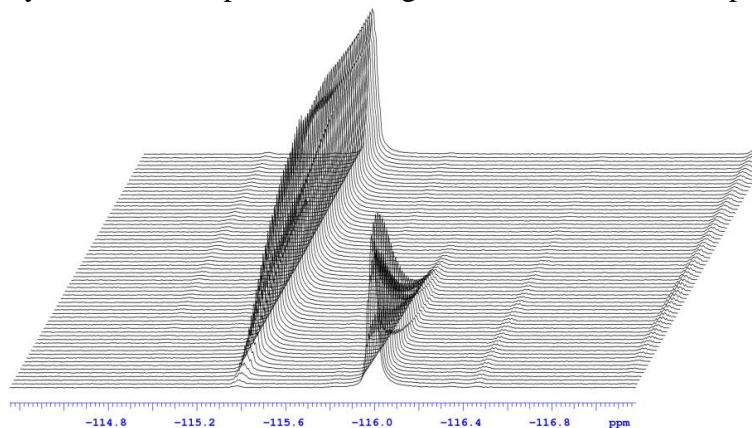
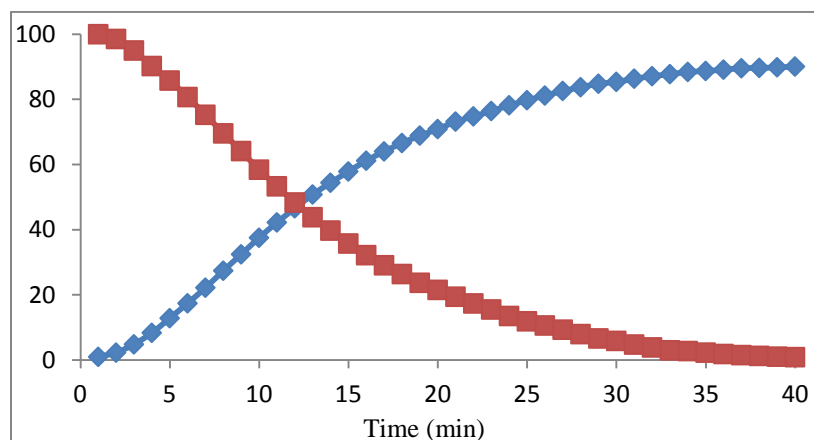


Figure 3.13 Array of ^{19}F NMR spectra showing conversion of **38** to the product **39**



(intermediate **38** at approximately -116.0 ppm and product **39** ~ -115.3 ppm, spectra acquired at 500 MHz)

Figure 3.14 Plot of **39** formed and **38** consumed as a function of time



3.12 References

-
- (1) Excerpts of Chapter 3 reprinted with permission from Maleckis, A.; Kampf, J. W.; Sanford, M. S. A Detailed Study of Acetate-Assisted C–H Activation at Palladium(IV) Centers. *J. Am. Chem. Soc.* **2013**, *135*, 6618-6625. Copyright 2013. American Chemical Society.
- (2) Wang, X.; Leow, D.; Yu, J.-Q. *J. Am. Chem. Soc.* **2011**, *133*, 13864-13867.
- (3) (a) Hickman, A. J.; Sanford, M. S. *ACS Catal.* **2011**, *1*, 170-174. (b) Pilarski, L. T.; Selander, N.; Bose, D.; Szabo, K. J. *Org. Lett.* **2009**, *11*, 5518-5521. (c) Kawai, H.; Kobayashi, Y.; Oi, S.; Inoue, Y. *Chem. Commun.* **2008**, 1464-1466.
- (4) Hull, K. L.; Lanni, E. L.; Sanford, M. S. *J. Am. Chem. Soc.* **2006**, *128*, 14047-14049.
- (5) (a) Sibbald, P. A.; Rosewall, C. F.; Swartz, R. D.; Michael, F. E. *J. Am. Chem. Soc.* **2009**, *131*, 15945-15951. (b) Rosewall, C. F.; Sibbald, P. A.; Liskin, D. V. Michael, F. E. *J. Am. Chem. Soc.* **2009**, *131*, 9488-9489.
- (6) (a) Canty, A. J.; van Koten, G. *Acc. Chem. Res.* **1995**, *28*, 406-413. (b) Powers, D. C.; Benitez, D.; Tkatchouk, E.; Goddard, W. A.; Ritter, T. *J. Am. Chem. Soc.* **2010**, *132*, 14092-14103. (c) Ye, Y.; Ball, N. D.; Sanford, M. S. *J. Am. Chem. Soc.* **2010**, *132*, 14682-14687. (d) Shabashov, D.; Daugulis, O. *J. Am. Chem. Soc.* **2010**, *132*, 3965-3972.
- (7) Racowski, J. M.; Ball, N. D.; Sanford, M. S. *J. Am. Chem. Soc.* **2011**, *133*, 18022-18025.
- (8) (a) Byers, P. K.; Canty, A. J.; Skelton, B. W.; White, A. H. *Organometallics* **1990**, *9*, 826-832. (b) Byers, P. K.; Canty, A. J.; Skelton, B. W.; White, A. H. *J. Chem. Soc. Chem. Commun.* **1987**, 1093-1095.
- (9) (a) McCall, A. S.; Wang, H.; Desper, J. M.; Kraft S. *J. Am. Chem. Soc.* **2011**, *133*, 1832-1848. (b) Brown, D. G.; Byers, P. K.; Canty A. J. *Organometallics*, **1990**, *9*, 1231-1235.
- (10) Ryabov, A. D.; Sakodinskaya, I. K.; Yatsimirsky, A. K. *J. Chem. Soc., Dalton Trans.* **1985**, 2629-2638.
- (11) Lafrance, M.; Gorelsky, S. I.; Fagnou, K. *J. Am. Chem. Soc.* **2007**, *129*, 14570-14571.
- (12) (a) Lapointe D.; Fagnou, K. *Chem. Lett.* **2010**, *39*, 1118-1126. (b) Gorelsky, S.; Lapointe, D.; Fagnou, K. *J. Org. Chem.* **2012**, *77*, 658-668. (c) Gorelsky, S. I.; Stuart, D. R.; Campeau, L.-C.; Fagnou, K. *J. Org. Chem.* **2010**, *75*, 8180-8189 (d) D. García-Cuadrado, D.; Braga, A. A. C.; Maseras, F.; Echavarren, A. M. *J. Am. Chem. Soc.* **2006**, *128*, 1066-1067.
- (13) For CMD at Rh(III) see Rhinehart, J. L.; Manbeck, K. A.; Buzak, S. K.; Lipka, G. M.; Brennessel, W. W.; Goldberg, K. I.; Jones, W. D. *Organometallics*, **2012**, *31*, 1943-1952.
- (14) For CMD at Ir(III) see (a) Davies, D. L.; Donald S. M. A.; Al-Duaij, O.; Macgregor S. A.; Pölleth M. *J. Am. Chem. Soc.* **2006**, *128*, 4210-4211. (b) Li, L.; Brennessel, W. W.; Jones, W. D. *Organometallics* **2009**, *28*, 3492-3500.
- (15) For CMD at Ru(II) see: Davies, D. L., Al-Duaij, O.; Fawcett, J.; Giardiello, M.; Hilton, S. T.; Russell, D. R. *Dalton Trans.* **2003**, 4132-4138.

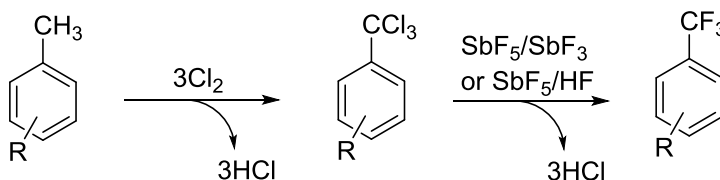
-
- (16) (a) Juwaini, N. A. B.; Ng, J. K. P.; Seayad, J. *ACS Catal.* **2012**, *2*, 1787-1791. (b) Wang, X.; Leow, D.; Yu, J.-Q. *J. Am. Chem. Soc.* **2011**, *133*, 13864–13867. (c) Hickman, A. J.; Sanford, M. S. *ACS Catal.* **2011**, *1*, 170-174. (d) Sibbald, P. A.; Rosewall, C. F.; Swartz, R. D.; Michael, F. E. *J. Am. Chem. Soc.* **2009**, *131*, 15945–15951. (e) Rosewall, C. F.; Sibbald, P. A.; Liskin, D. V.; Michael, F. E. *J. Am. Chem. Soc.* **2009**, *131*, 9488–9489. (f) Pilarski, L. T.; Selander, N.; Bose, D.; Szabo, K. J. *Org. Lett.* **2009**, *11*, 5518-5521 (g) Hull, K. L.; Lanni, E. L.; Sanford, M. S. *J. Am. Chem. Soc.* **2006**, *128*, 14047-14049.
- (17) For Pd^{II} κ^2 acetate complexes see: (a) Thirupathi, N.; Amoroso, D.; Bell, A.; Protasiewicz, J. D. *Organometallics* **2005**, *24*, 4099–4102. (b) Viciu, M. S.; Stevens, E. D.; Petersen, J. L.; Nolan, S. P. *Organometallics* **2004**, *23*, 3752–3755. (c) Lee, J.-C.; Wang, M.-G.; Hong, F.-E. *Eur. J. Inorg. Chem.* **2005**, 5011–5017.
- (18) Perrin, C. L.; Dwyer, T. J.; *Chem. Rev.* **1990**, *90*, 935-967.
- (19) (a) Heard, P. *J. Chem. Soc. Rev.* **2007**, *36*, 551-569. (b) Braunstein, P.; Naud, F. *Angew. Chem. Int. Ed.* **2001**, *40*, 680-699. (c) Álvarez, C. M.; Carrillo, R.; García-Rodríguez, R.; Miguel, D. *Chem. Commun.* **2011**, *47*, 12765-12767. (d) Abel, W. E.; Kite, K.; Perkins, P. S. *Polyhedron* **1987**, *6*, 549-562. (e) Yang, H.; Alvarez-Gressier, M.; Lugan, N.; Mathieu, R. *Organometallics* **1997**, *16*, 1401-1409.
- (20) (a) Berry, R. S. *J. Chem. Phys.* **1960**, *32*, 933–938. (b) Fortman, J. J. *Coord. Chem. Rev.* **1971**, *6*, 331-375.
- (21) Gómez-Gallego, M.; Sierra, M. A. *Chem. Rev.* **2011**, *111*, 4857–4963.
- (22) Analysis of **34** by ESI-MS showed that this complex is >99% mono-deuterated. For details of analysis, see: Gruber, C. C.; Oberdorfer, G.; Voss, C. V.; Kreamsner, J. M.; Kappe, C. O. Kroutil, W. *J. Org. Chem.* **2007**, *72*, 5778-5783.
- (23) (a) Sühnel, J. *J. Phys. Org. Chem.* **1990**, *3*, 62-68. (b) Bordwell, F. G.; Boyle, W. J. Jr. *J. Am. Chem. Soc.* **1975**, *97*, 3447-3452.
- (24) Kresge, A. J.; Brennan, J. F. *J. Org. Chem.* **1967**, *32*, 752–755.
- (25) Neugebauer, W.; Kos, A. J.; Schleyer, P. v. R. *J. Organomet. Chem.* **1982**, *228*, 107-118.
- (26) Gruber, C. C.; Oberdorfer, G.; Voss, C. V.; Kreamsner, J. M.; Kappe, C. O. Kroutil, W. *J. Org. Chem.* **2007**, *72*, 5778-5783.

Chapter 4: Synthesis of Trifluoromethyl Complexes Using TFAA as CF₃ Source

4.1 Introduction

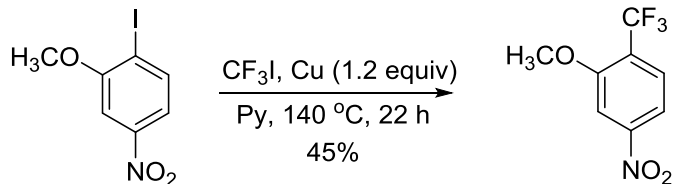
Swarts reaction is the oldest method for the preparation of trifluoromethylated arenes (Scheme 4.1).¹ Originally SbF₃ was used as a fluorinating reagent in the presence of a SbF₅ catalyst; however, a modern version of Swarts reaction involves use of HF in the presence of a Lewis acid catalyst to convert trichloromethylated starting material into the desired trifluoromethylated product. Even though the Swarts reaction requires highly corrosive reagents and generates three equivalents of HCl byproduct, it is still the only method for the synthesis of trifluoromethylated compounds that is used on industrial scale. It is even more surprising, considering that trichloromethylated starting material is usually synthesized via chlorination with Cl₂ thus generating three more equivalents of HCl. In addition, the Swarts reaction can be applied only to very simple building blocks since the harsh reaction conditions would degrade complex pharmaceutical and agrochemical intermediates containing acid or oxidant sensitive functional groups.

Scheme 4.1. Swarts reaction

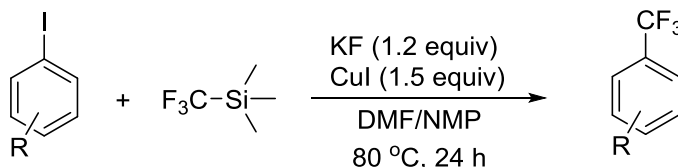


Transition metal catalyzed cross-couplings typically allow very efficient and completely regioselective formation of the C–C bond. Therefore, over the last several decades many attempts have been made to apply transition metal catalysis to the development of trifluoromethylation reactions.² Several practically useful trifluoromethylation methodologies have been discovered.^{2,3,4} For instance, treatment of aryl iodides with trifluoromethyl iodide (CF₃I) in the presence of superstoichiometric amounts of copper powder affords corresponding benzotrifluorides. Scheme 4.2 shows an example of such a reaction.⁵ Aryl iodides can be converted into benzotrifluorides also in copper(I) iodide mediated cross-coupling reactions with Ruppert's reagent (CF₃SiMe₃) (Scheme 4.3).^{2,6}

Scheme 4.2. McLoughlin-Thrower reaction



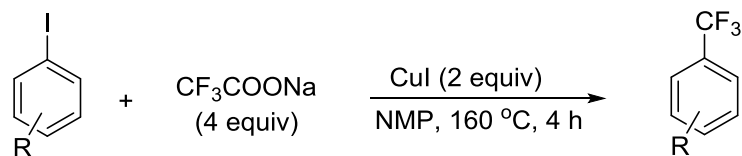
Scheme 4.3. Cross coupling of aryl iodides with Ruppert's reagent



R	<i>o</i> -CH ₃	<i>m</i> -CH ₃	<i>p</i> -CH ₃	<i>p</i> -CH ₃ O	<i>p</i> -Cl	<i>p</i> -CH ₃ CH ₂ O ₂ C	<i>p</i> -CH ₃ CO
Yield (%)	86	78	82	48	35	94	45

Most compounds that are used as a CF₃ source for transition metal catalyzed/mediated C–CF₃ bond formation (*e.g.*, CF₃I, CF₃-SiMe₃, CF₃-SiEt₃, Togni reagent) are expensive and/or toxic and volatile. Trifluoroacetate can be used as a cheap CF₃ source, however, super-stoichiometric amounts of transition metal catalyst and very harsh reaction conditions are typically required in decarboxylative trifluoromethylation reactions (Scheme 4.4).^{2,7,8} Therefore a mild and regioselective trifluoromethylation method that would employ cheap bulk chemicals such as trifluoroacetic anhydride (TFAA) or trifluoroacetic esters (TFA esters) as a CF₃ source is still highly desirable.

Scheme 4.4. Copper mediated decarboxylative trifluoromethylation

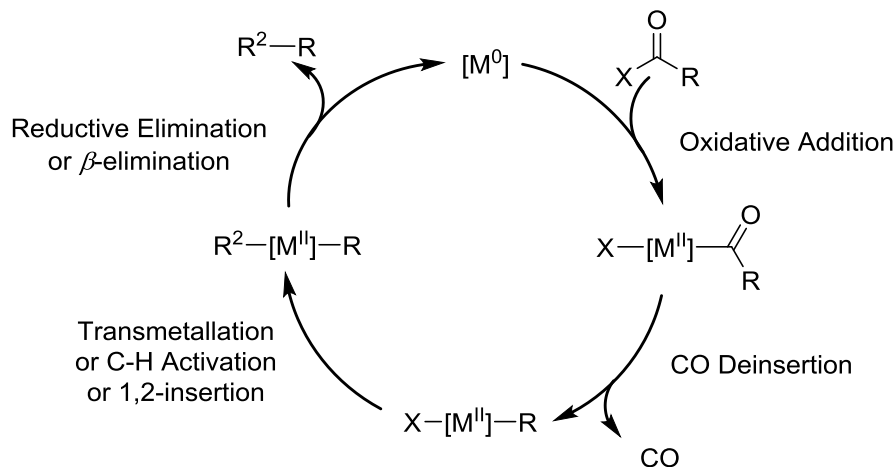


R	<i>m</i> -CH ₃	<i>p</i> -NO ₂	<i>p</i> -Cl	<i>p</i> -CH ₃ O
Yield (%)	88	47	68	59

Nickel and palladium are the most commonly used catalysts for traditional cross-coupling reactions. Ni and Pd are efficient catalysts also for decarbonylative coupling reactions.^{9,10,11,12} This prompted us to investigate nickel and palladium as catalysts for decarbonylative trifluoromethylation reactions with TFAA or TFA esters as cheap and available CF₃ donors. Scheme 4.5 shows the general mechanism for transition metal catalyzed decarbonylative C–C bond forming reactions. Oxidative addition of an ester to low valent transition metal species [M⁰] and consecutive CO deinsertion (decarbonylation) are the key steps in the catalytic turnover. After decarbonylation, a

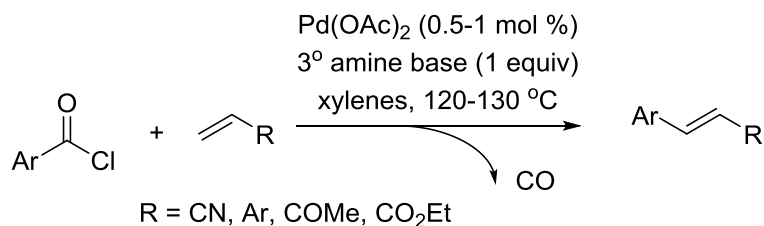
second coupling partner (R^2) is transferred to the Pd^{II} center via transmetalation, C–H activation, or 1,2-insertion. Finally, reductive elimination or β -elimination affords the product and returns $[M^0]$ species into the catalytic cycle.

Scheme 4.5 General mechanism of decarbonylative coupling reactions



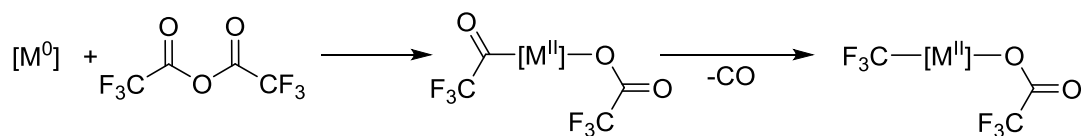
Scheme 4.6 shows an example of a palladium catalyzed decarbonylative coupling reaction. Only 0.5-1% of $Pd(OAc)_2$ is necessary for efficient decarbonylative coupling of acyl chlorides with activated alkenes.¹³

Scheme 4.6. Palladium catalyzed decarbonylative coupling



Our proposal that TFAA or TFA esters could also be used as reagents for decarbonylative trifluoromethylation reactions is supported by the fact that decarbonylation is a common method for the synthesis of transition metal CF₃ complexes (Scheme 4.7).^{14,15,16,17} It has been applied to first, second, and even third row metals such as iridium and platinum.

Scheme 4.7 Preparation of transition metal CF₃ complexes



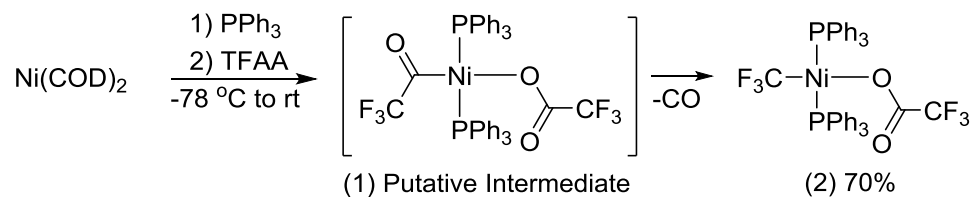
Surprisingly, TFAA and TFA esters have never been used for the synthesis of nickel and palladium trifluoromethyl complexes.^{18,19} In some cases CO deinsertion from M-COCF₃ complexes is a very difficult process, requiring heating to high temperatures. For example, transformation of CF₃COPt(Cl)(PPh₃)₂ to CF₃Pt(Cl)(PPh₃)₂ requires heating to 210 °C for 4 hours.²⁰ Therefore, at the outset of this project it was our concern that CO deinsertion could be a limiting process in the proposed nickel and palladium catalyzed decarbonylative trifluoromethylation reactions. Therefore, before attempting catalytic turnover, we decided to investigate TFAA and TFA esters as reagents for the decarbonylative synthesis of nickel and palladium trifluoromethyl complexes.

4.2 Decarbonylative Synthesis of Nickel Trifluoromethyl Complexes

Decarbonylation is generally a more facile process at first row metal centers; therefore, we decided to investigate decarbonylation at Ni first. For the investigation of

decarbonylation we chose Ni(COD)₂ as an available nickel(0) source and PPh₃ as a simple supporting ligand. Somewhat unexpectedly, treatment of Ni(COD)₂ with two equivalents of PPh₃ followed by the addition of a slight excess of TFAA afforded (PPh₃)₂Ni(CF₃)(OOCFF₃) (**2**) directly in 70% isolated yield (Scheme 4.8). The temperature of the reaction medium never exceeded 25 °C. Complex **2** was characterized by NMR and IR spectroscopies and composition of **2** was confirmed also by elemental analysis. ¹⁹F-NMR spectrum of **2** exhibits two resonances at -20 and 75 ppm in a 1:1 integral ratio and ³¹P{¹H}-NMR spectrum contains one resonance at 40 ppm. NMR signals of **2** are broad and ³J_{F-P} coupling is not resolved even at -50 °C which is likely a result of the highly fluxional nature of **2**.

Scheme 4.8 Preparation of (PPh₃)₂Ni(CF₃)(OOCFF₃)



Complex **2** undergoes facile ligand exchange with bidentate phosphine ligands. For example, treatment of **2** with slight excess of diphenylphosphinoethane (dppe) afforded **3** in 96% isolated yield (Scheme 4.9). Interestingly, treatment of Ni(COD)₂ with one equivalent of dppe, followed by TFAA did not afford **3**, but (dppe)Ni(OCOCF₃)₂ instead. Complex **3** was characterized by NMR, IR, and elemental analysis. ³J_{F-P} coupling observed in both ¹⁹F- and ³¹P-NMR spectra lend a strong support to the proposed structure (see Figure 4.1 and Figure 4.2 for spectra). Specifically, ³¹P-NMR

spectrum of **3** exhibits an apparent quintet at 45 ppm (${}^2J_{\text{P-P}} \approx {}^3J_{\text{P-F}} \approx 45$ Hz) and a doublet of quartets at 56 ppm (${}^2J_{\text{P-P}} = 46$ Hz and ${}^3J_{\text{P-F}} = 10$ Hz) in 1:1 integral ratio. In addition, ${}^{19}\text{F}$ -NMR spectrum of **3** exhibits two characteristic resonances in 1:1 integral ratio: doublet of doublets at -29 ppm (${}^3J_{(\text{F-P})} = 43.1$ Hz and 10.0 Hz) and a singlet at 75 ppm.

Scheme 4.9 Preparation of (dppe)Ni(CF₃)(OOC CF₃)

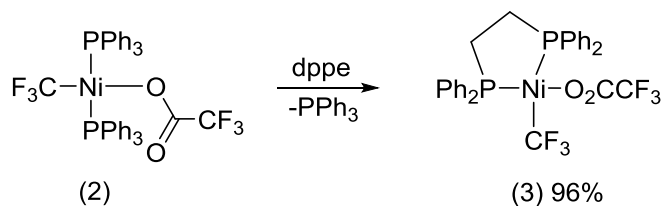
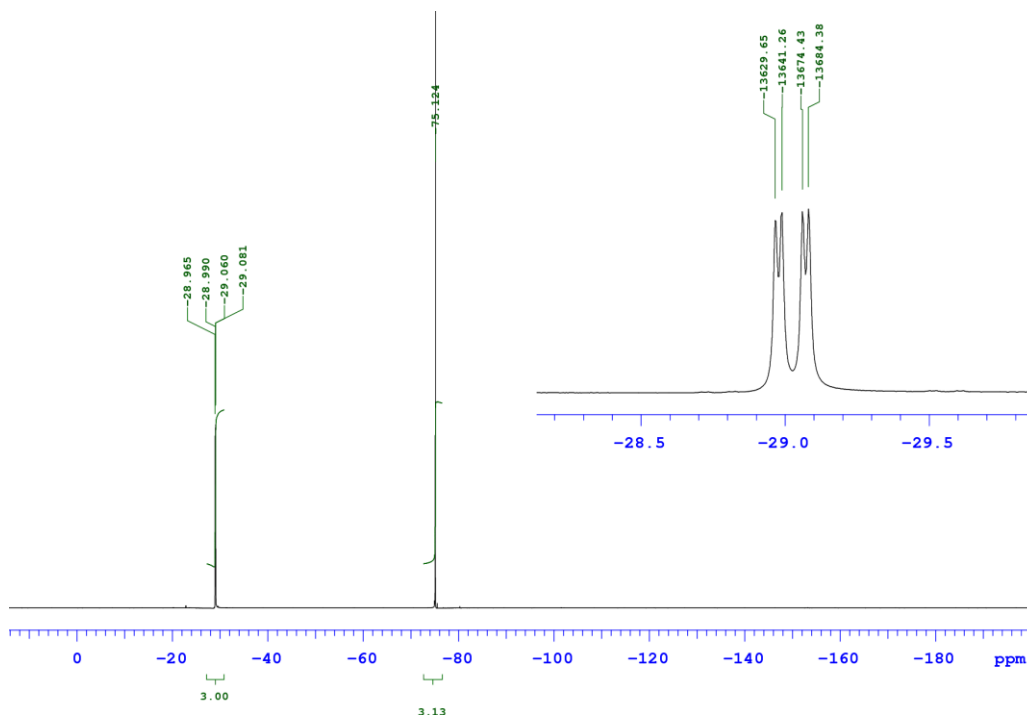
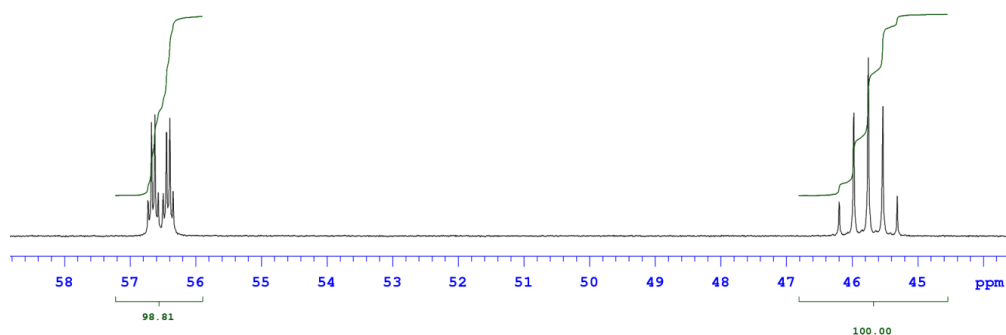


Figure 4.1 ${}^{19}\text{F}$ NMR spectrum of (dppe)Ni(CF₃)(OOC CF₃)



(spectrum acquired at 500 MHz)

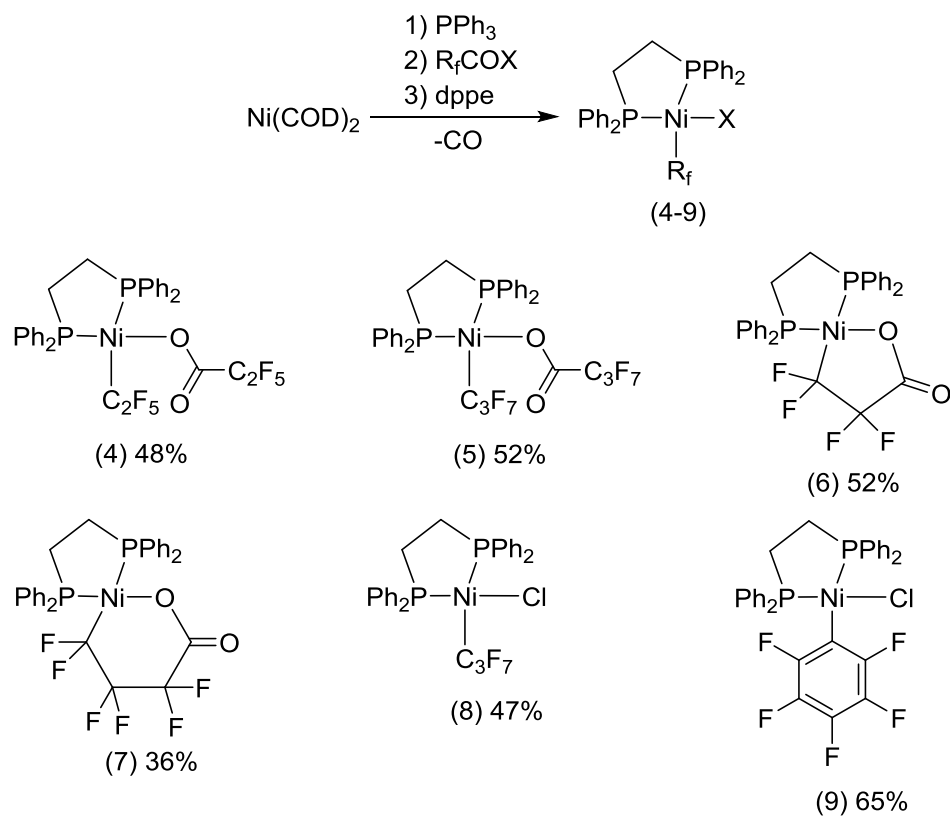
Figure 4.2 $^{31}\text{P}\{^1\text{H}\}$ NMR spectrum of $(\text{dppe})\text{Ni}(\text{CF}_3)(\text{OOC}\text{CF}_3)$



(spectrum acquired at 500 MHz)

Next, we investigated oxidative addition and decarbonylation of other carboxylic anhydrides and chloroanhydrides to Ni^0 . A convenient one pot procedure was developed (Scheme 4.10). First, $\text{Ni}(\text{COD})_2$ was treated with two equivalents of PPh_3 followed by slight excess of corresponding carboxylic anhydride or chloride. Next, to facilitate purification and characterization, *in situ* generated fluoroalkylnickel species were trapped with dppe. This approach proved successful for a number of complexes. For example, with simple higher analogues of TFAA, products **4** and **5** were isolated in 48% and 52% yields, respectively. Cyclic carboxylic anhydrides could also be used in this reaction. Thus, products **6** and **7** were isolated in 52% and 36% yield. Finally, with carboxylic chlorides, complexes **8** and **9** were obtained in 47% and 65% isolated yields. Moderate isolated yields of **4-9** are a result of losses during isolation and purification.

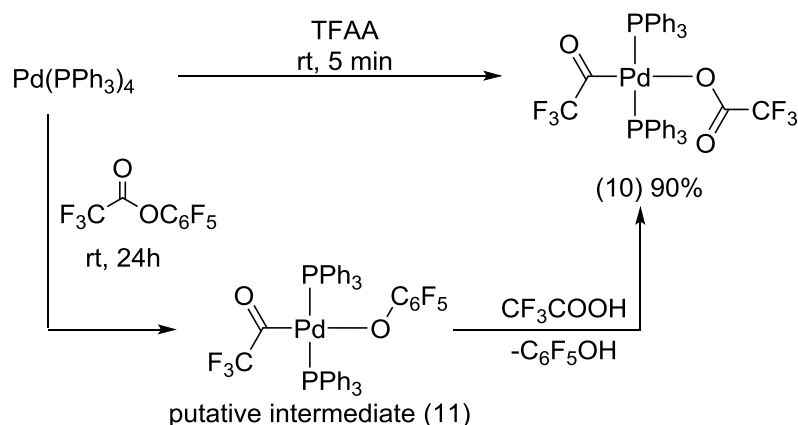
Scheme 4.10 Preparation of (dppe)Ni(R_f)(X) complexes



4.3 Decarbonylative Synthesis of Pd^{II} Trifluoromethyl Complexes

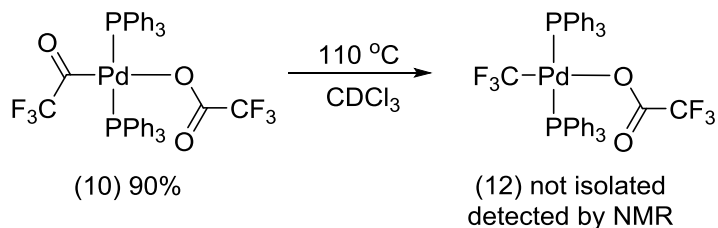
While decarbonylation at nickel is fast at or below room temperature, this is not the case for palladium. Treatment of Pd(PPh₃)₄ with TFAA resulted in formation of trifluoroacetyl complex **10** in 90% isolated yield (Scheme 4.11). Complex **10** is stable at room temperature in CDCl₃ solution and no decomposition was detected over the course of three days. Pentafluorophenyl trifluoroacetate also undergoes oxidative addition to Pd(PPh₃)₄. Unexpectedly, with C₆F₅OCOCF₃, the oxidative addition product was isolated as trifluoroacetate complex **10** and not as pentafluorophenoxide complex **11**. It is likely that initially formed **11** reacts with trifluoroacetic acid generated *in situ* during workup from excess C₆F₅OCOCF₃.

Scheme 4.11 Synthesis of $(PPh_3)_2Pd(COCF_3)(OCOCF_3)$



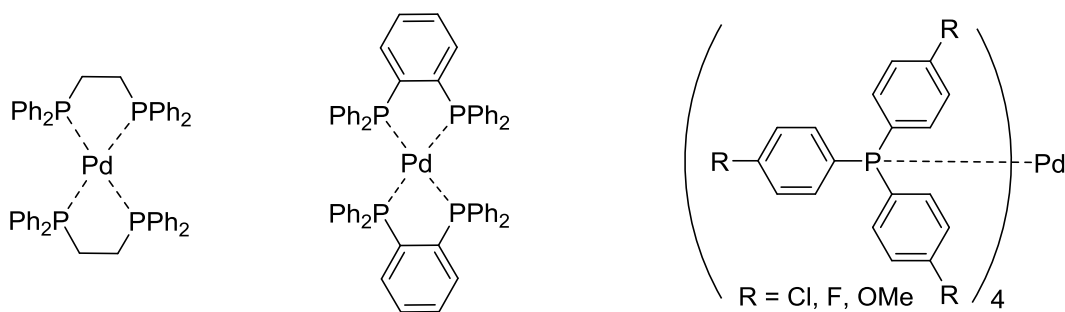
Decarbonylation at Pd^{II} was investigated next (Scheme 4.12). In order to promote CO deinsertion, **10** was heated in $CDCl_3$ solution to $110^\circ C$ and decarbonylation progress was monitored by ^{19}F - and ^{31}P -NMR spectroscopy. **10** underwent slow conversion to **12** as evidenced by the appearance of a triplet at -20 ppm in ^{19}F -NMR spectrum and a quartet at 40 ppm in ^{31}P -NMR spectrum ($^3J_{F-P} \approx 30$ Hz in both spectra). After 3 hours at $110^\circ C$ approximately 30% of **12** and 70% of **10** was detected in the reaction mixture. Unfortunately, **12** could not be isolated in pure form because after prolonged heating to $110^\circ C$ both starting material **10** and product **12** had decomposed to a complex mixture of unidentified side products.

Scheme 4.12 Reactivity of $(PPh_3)_2Pd(COCF_3)(OCOCF_3)$



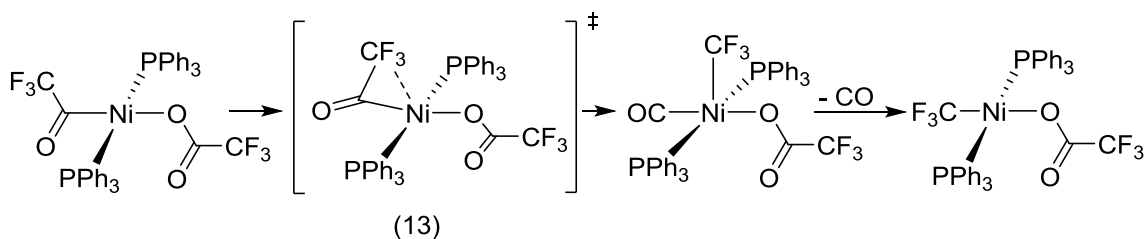
After unsuccessful but somewhat encouraging results with $\text{Pd}(\text{PPh}_3)_4$ as a Pd^0 source, a number of other palladium starting complexes were screened (Figure 4.3). Unfortunately, none of the complexes shown in Figure 4.3 gave significant improvement over $\text{Pd}(\text{PPh}_3)_4$.

Figure 4.3 Screened $\text{Pd}^0(\text{L})_n$ complexes

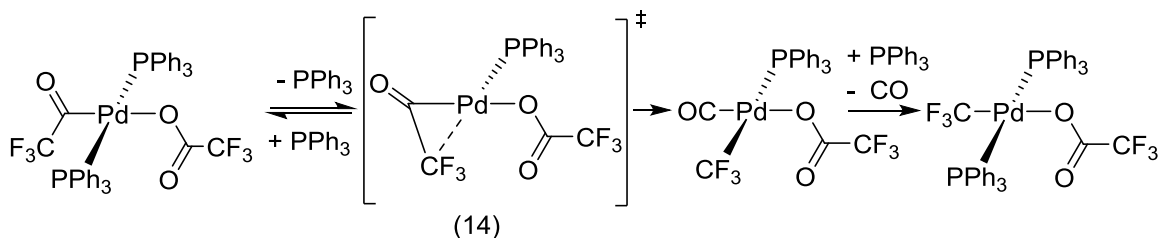


CO insertion/deinsertion is generally accepted to proceed via a three-center transition state (Scheme 4.13).^{19a,21} The very facile decarbonylation at nickel can be rationalized with the fact that square planar tetracoordinate Ni^{II} centers easily expand coordination number to five and thus the three-center transition state such as **13** is reached without prior dissociation of the spectator ligands (Scheme 4.13).^{19a,21} In contrast, CO insertion/deinsertion at square planar tetracoordinate Pd^{II} center via a pentacoordinate transition state analogous to **13** is feasible but it is a high energy pathway. For palladium, CO insertion/deinsertion via a tetracoordinate transition state such as **14** is, in general, a much more facile process (Scheme 4.14).²¹ We envisioned that substitution of PPh_3 supporting ligands with more labile analogues would accelerate the rate of decarbonylation at the Pd^{II} center via a transition state **14**.

Scheme 4.13 Viable mechanism for decarbonylation at Ni^{II}

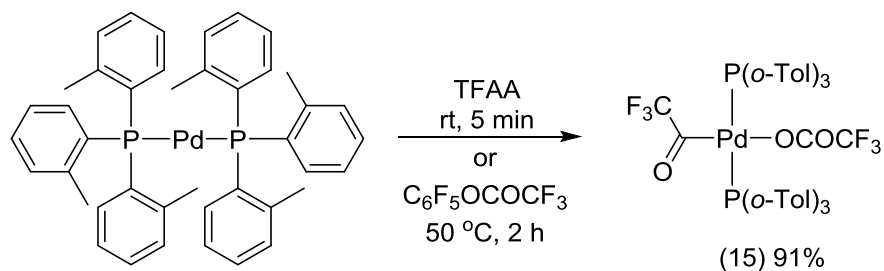


Scheme 4.14 Viable mechanism for decarbonylation at Pd^{II}



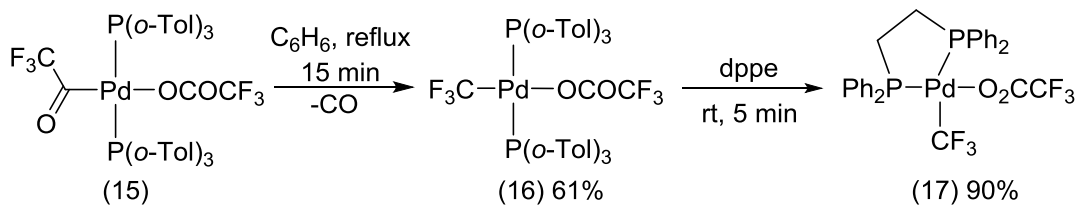
Based to the reasoning above, we chose to substitute PPh₃ with sterically more bulky and thus more labile P(*o*-Tol)₃ ligands. Treatment of Pd[P(*o*-Tol)₃]₂ with TFAA in THF at room temperature afforded complex **15** in 91% isolated yield (Scheme 4.15). Reaction of Pd[P(*o*-Tol)₃]₂ with C₆F₅OCOCF₃ also afforded **15**, only in this case 2 h at 50 °C was required for complete conversion. ¹⁹F- and ³¹P-NMR spectra of **15** are similar to those of **10**; however, peaks are much broader which is likely due to reversible dissociation of the phosphine ligand.

Scheme 4.15 Synthesis of (P(*o*-Tol)₃)₂Pd(COCF₃)(OCOCF₃)



Decarbonylation of the synthesized complex **15** was investigated next (Scheme 4.16). We found that simply refluxing **15** in benzene for 20 minutes leads to complete decarbonylation. Pure **16** was isolated as a crystalline solid in 61% yield. Although isolated **16** passed elemental analyses, NMR spectra of complex **16** are broad and show the presence of several species. We explain this with a reversible dissociation of the P(*o*-Tol)₃ ligand. In order to definitely confirm the structure of **16**, it was treated with dppe (Scheme 4.16). The resulting complex **17** was isolated in high purity. **17** passed elemental analyses and very distinctive ¹⁹F-, ³¹P- and ¹³C-NMR spectral data provides substantial evidence for the proposed structure.

Scheme 4.16 Decarbonylative decomposition of (P(*o*-Tol)₃)₂Pd(COCCF₃)(OCOCF₃)

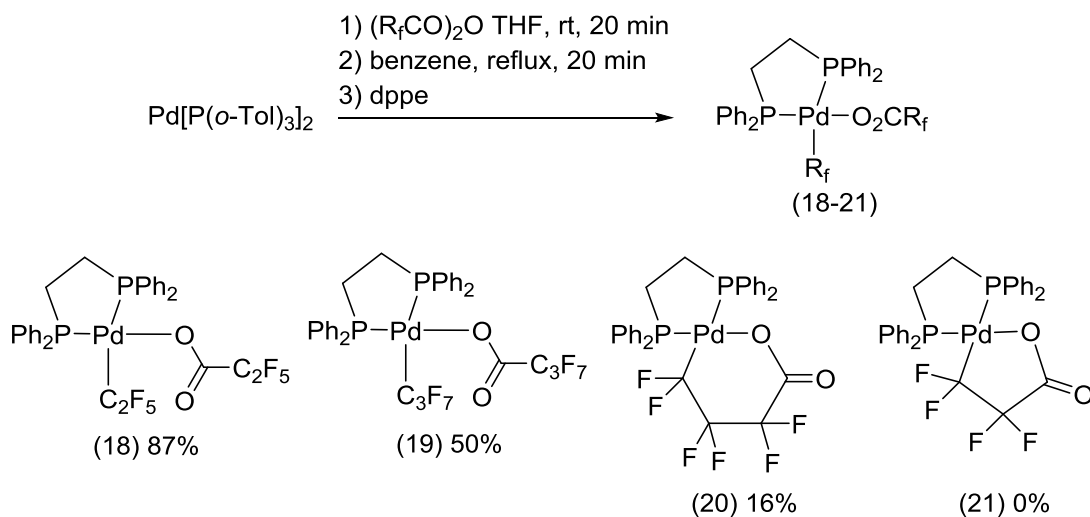


In order to test our theory that dissociation of the supporting ligand from Pd^{II} is necessary for facile decarbonylation, the reaction of **15** with excess ligand was carried out. 3 equivalents of P(*o*-Tol)₃ were added to the benzene solution of **15** and the resulting mixture was refluxed for 1 hour. P(*o*-Tol)₃ completely inhibited decarbonylation and pure **15** was recovered in 63% yield.

After we had determined appropriate spectator ligands for decarbonylation at Pd^{II}, preparation of palladium complexes with other fluoroalkyl groups was targeted next. A convenient one-pot procedure starting from Pd[P(*o*-Tol)₃]₂ was developed (Scheme 4.17).

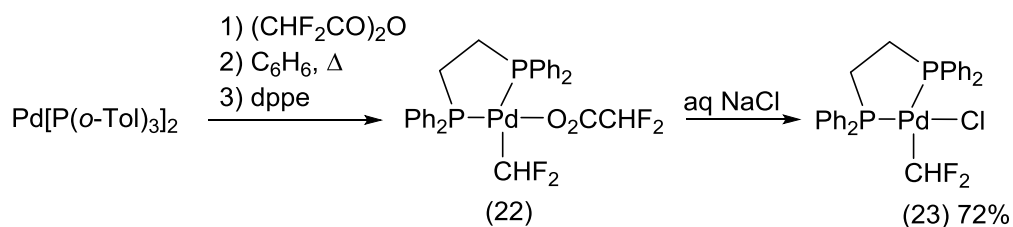
In order to facilitate purification and characterization, all products were isolated as dppe complexes. We found that higher analogues of TFAA are effective reagents in this reaction and thus complexes **18** and **19** were isolated in 87% and 50% yield, respectively. In contrast, use of cyclic anhydrides was not successful for the preparation of palladium complexes. **20** was obtained only in 16% isolated yield and attempted preparation of **21** resulted in the formation of an insoluble precipitate.

Scheme 4.17 Preparation of (dppe)Pd(R_f)(OCOR_f) complexes



We investigated the oxidative addition-decarbonylation sequence also with difluoroacetic anhydride (Scheme 4.18). We were unable to find appropriate solvent and conditions for the crystallization and purification of the initially targeted compound **22**. However, we found that treatment of the crude **22** with aqueous NaCl resulted in facile ligand exchange and chloride complex **23** was successfully isolated via crystallization in 72% yield starting from Pd[P(*o*-Tol)₃]₂.

Scheme 4.18 Preparation of (dppe)Pd(CHF₂)(Cl)

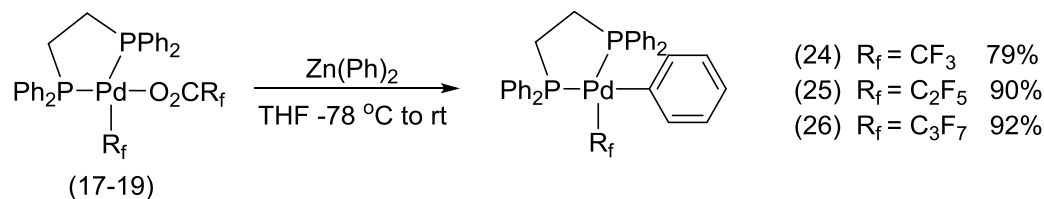


4.4 Reactivity of the Perfluoroalkyl Nickel and Palladium Complexes

We have shown that with selection of appropriate phosphine ligands decarbonylation of fluoroacyl ligands at Ni^{II} and Pd^{II} occurs under mild conditions. Next, we aimed to investigate the reactivity of the obtained Ni and Pd trifluoromethyl complexes towards transmetalation. Reaction of **2**, **3** and **12** with phenyllithium, phenylmagnesium bromide or diphenylzinc afforded inseparable mixture of products. Biphenyl was isolated as the organic product in all cases. It has been reported that complexes with (phosphine)Ni(CF₃)(aryl) and (phosphine)Pd(CF₃)(aryl) general structure decompose with concomitant formation of the corresponding biaryl.^{22,23} It is possible that arylnickel and arylpalladium species generated from **2**, **3** and **12** also undergo rapid decomposition in accordance with the literature precedents.

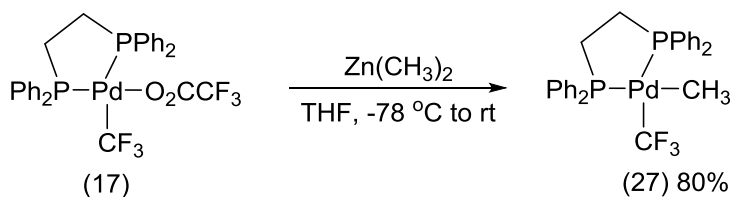
We also investigated transmetalation to perfluoroalkylpalladium complexes **17-19** anticipating that bidentate dppe ligand should stabilize the targeted arylpalladium species (Scheme 4.19). Gratifyingly, treatment of **17-19** with diphenylzinc afforded **24-26** in good isolated yields. Complexes **24-26** are stable under ambient conditions and their structures were confirmed unequivocally by NMR spectroscopy and elemental analyses.

Scheme 4.19 Preparation of (dppe)Pd(R_f)(C₆H₅) complexes



We found that dimethylzinc is also an appropriate transmetallating reagent. Treatment of complex **17** with Zn(CH₃)₂ in anhydrous THF resulted in formation of air stable complex **27** in 80% isolated yield (Scheme 4.20).

Scheme 4.20 Preparation of (dppe)Pd(CF₃)(CH₃)



4.5 Conclusions

This chapter describes the investigation of decarbonylation of –COR_f ligands at Ni^{II} and Pd^{II} centers. It was found that facile decarbonylation of (PPh₃)₂Ni(COCF₃)(CO₂CF₃) occurs at or below room temperature. In contrast, the analogous palladium complex (PPh₃)₂Pd(COCF₃)(CO₂CF₃) undergoes very slow decarbonylation when heated to 110 °C. However, acylpalladium complexes supported by sterically bulky and therefore more labile P(*o*-Tol)₃ ligands decarbonylate under milder reaction conditions. For example, complete decarbonylative decomposition of [P(*o*-Tol)₃]₂Pd(CF₃CO)(CO₂CF₃) in boiling benzene was achieved in only 20 minutes.

Performed experiments indicate that decarbonylation at nickel proceed without ligand dissociation via a pentacoordinate transition state. In contrast, decarbonylation at Pd^{II} most likely proceeds through a tetracoordinate transition state. This mechanism requires prior dissociation of the supporting phosphine ligand.

The results described in this chapter support the viability of decarbonylative trifluoromethylation methodology with TFAA or TFA esters as a CF₃ source. The fact that facile decarbonylation at Ni^{II} and Pd^{II} proceeds under mild conditions encouraged further investigation of processes relevant to the proposed trifluoromethylation reaction. The results of these investigations are described in the following chapter.

4.6 Experimental Section

General Procedures. All syntheses were conducted under nitrogen unless otherwise stated. All reagents were purchased from commercial sources and used as received. Pd[P(*o*-Tol)₃]₂ was obtained according to literature procedure.²⁴ Tetrahydrofuran, dichloromethane and diethyl ether were purified using an Innovative Technologies (IT) solvent purification system consisting of a copper catalyst, activated alumina, and molecular sieves. NMR spectra were acquired using 400, 500 and 700 MHz Varian spectrometers. All ¹H/¹H NOESY and ¹H/¹H ROESY correlation spectra were acquired on a 500 MHz instrument. ¹H, ¹⁹F and ¹³C chemical shifts are reported in parts per million (ppm) relative to TMS, with the residual solvent peak used as an internal reference. ¹H and ¹⁹F multiplicities are reported as follows: singlet (s), doublet (d), triplet (t), quartet (q), broad resonance (br) and multiplet (m). Overlapping signals in ¹H-NMR spectra were also reported as (m).

Preparation of $(\text{PPh}_3)_2\text{Ni}(\text{CF}_3)(\text{OOC}\text{CF}_3)$ (2). In a nitrogen filled glovebox a Schlenk flask was charged with a teflon coated stirbar, triphenylphosphine (4.20 g; 16 mmol) and $\text{Ni}(\text{cod})_2$ (2.00 g; 7.27 mmol). The flask was sealed with septum and then taken out of the glovebox. Dry THF (150 mL) was added via cannula and the resulting dark red mixture was stirred at r.t. for 15 minutes. The solution was then cooled to $-78\text{ }^\circ\text{C}$ and trifluoroacetic anhydride (TFAA) (1.70 ml; 12 mmol) was added dropwise. Solution was slowly warmed to rt and volatiles were then removed under reduced pressure via the sidearm of the reaction flask. Diethylether (200 ml) was added to the residue and product then precipitated in a form of yellow crystals. The product was collected by filtration and washed with several portions of diethyl ether. After drying in vacuum 4.04 g (70%) of yellow crystalline powder was obtained. ^1H NMR (CDCl_3 at $23\text{ }^\circ\text{C}$): δ 7.90-7.78 (m, 12H), 7.52-7.37 (m, 18H). $^{13}\text{C}\{\text{H}\}$ NMR (CDCl_3 at $23\text{ }^\circ\text{C}$): δ 160.11 (q, $^2J_{(\text{C-F})} = 37.5$ Hz), 134.39 (br), 130.49 (br), 130.07 (br), 128.40 (br), 123.28 (broad quartet, $^1J_{(\text{C-F})} = 361.7$ Hz), 113.88 (q, $^1J_{(\text{C-F})} = 290.9$ Hz). ^{19}F NMR (CDCl_3 at $23\text{ }^\circ\text{C}$): δ 75.54 (s, 3F), -8.83 (br, 3F). $^{31}\text{P}\{\text{H}\}$ NMR (CDCl_3 at $23\text{ }^\circ\text{C}$): δ 22.62 (br). $^{19}\text{F}/^{13}\text{C}$ HSQC NMR (CDCl_3 at $25\text{ }^\circ\text{C}$): $\delta_{\text{F}}/\delta_{\text{C}}$ -8.95/123.34, -75.67/114.03. IR (ATR): cm^{-1} 3058 (w), 1675 (s), 1482 (s), 1434 (s), 1415 (s), 1190 (s). Elemental analysis: Calculated for $\text{NiC}_39\text{H}_{30}\text{F}_6\text{O}_2\text{P}_2$ C = 61.21%, H = 3.95%, F = 14.90%; Found: C = 61.12%, H = 3.95%, F = 14.81%.

Preparation of $(\text{dppe})\text{Ni}(\text{CF}_3)(\text{OOC}\text{CF}_3)$ (3). A 20 mL vial was charged with $(\text{PPh}_3)_2\text{Ni}(\text{CF}_3)(\text{OOC}\text{CF}_3)$ (1) (153 mg; 0.20 mmol), 1,2-bis(diphenylphosphino)ethane (dppe) (105 mg; 0.26 mmol) and dry dichloromethane (10 ml). The resulting solution was stirred at rt for 5 minutes and then the reaction mixture was filtered through a pad of celite. Volatiles were removed under reduced pressure and residue was dissolved in

diisopropyl ether. Product slowly separated in a form of yellow crystals. The product was collected by filtration, washed with several portions of diisopropyl ether and dried under reduced pressure. The yield of the product was 123 mg (96%). Analytical sample was obtained after crystallization (3 times) from dichloromethane/diisopropyl ether. ^1H NMR (CD_2Cl_2 at 23 °C): δ 8.07-8.00 (m, 4H), 7.82-7.75 (m, 4H), 7.67-7.51 (m, 12H), 2.31-2.19 (m, 4H), 2.12-2.00 (m, 4H). $^{13}\text{C}\{^1\text{H}\}$ NMR (CD_2Cl_2 at 23 °C): δ 160.73 (d, $^2J_{\text{C-F}} = 36.1$ Hz), 133.48 (d, $^3J_{\text{C-P}} = 10.9$ Hz), 133.42 (qdd, $^1J_{\text{C-F}} = 234.3$ Hz, $^3J_{\text{C-P}} = 137.6$ Hz, $^3J_{\text{C-P}} = 39.5$ Hz), 133.07 (d, $^3J_{\text{C-P}} = 11.6$ Hz), 132.05 (d, $^4J_{\text{C-P}} = 2.7$ Hz), 131.82 (d, $^4J_{\text{C-P}} = 2.0$ Hz), 129.24 (d, $^2J_{\text{C-P}} = 10.2$ Hz), 129.14 (d, $^2J_{\text{C-P}} = 10.9$ Hz), 127.84 (d, $^1J_{\text{C-P}} = 50.4$ Hz), 127.00 (d, $^1J_{\text{C-P}} = 40.9$ Hz), 114.94 (q, $^1J_{\text{C-F}} = 290.2$ Hz), 29.40 (dd, $^1J_{\text{C-P}} = 33.4$ Hz, $^2J_{\text{C-P}} = 17.0$ Hz), 22.28 (dd, $^1J_{\text{C-P}} = 30.0$ Hz, $^2J_{\text{C-P}} = 7.9$ Hz). ^{19}F NMR (CD_2Cl_2 at 23 °C): δ -29.02 (dd, $^3J_{\text{F-P}} = 43.1$ Hz and 10.0 Hz, 3F), -75.12 (s, 3F). $^{31}\text{P}\{^1\text{H}\}$ NMR (CD_2Cl_2 at 23 °C): δ 56.54 (dq, $^2J_{\text{P-P}} = 45.8$ Hz, $^3J_{\text{P-F}} = 10.7$ Hz), 45.76 (apparent quintet, $^2J_{\text{P-P}} = ^3J_{\text{P-F}} = 44.7$ Hz). $^{19}\text{F}/^{13}\text{C}$ HSQC NMR (CD_2Cl_2 at 25 °C): $\delta_{\text{F}}/\delta_{\text{C}}$ - 29.16/133.48, -75.24/114.98. $^{19}\text{F}/^{13}\text{C}$ HMBC NMR (CD_2Cl_2 at 25 °C): $\delta_{\text{F}}/\delta_{\text{C}}$ - 75.14/160.71. IR (ATR): cm^{-1} 3054 (w), 1685 (s), 1573 (w), 1485 (m), 1436 (s), 1421 (s), 1313 (m), 1183 (s). Elemental analysis: Calculated for $\text{NiC}_{29}\text{H}_{24}\text{F}_6\text{O}_2\text{P}_2$ C = 54.50%, H = 3.78%, F = 17.84%; Found: C = 54.53%, H = 3.69%, F = 17.97%.

General procedure 1: Synthesis of dppe supported perfluoroalkynickel complexes 4-9. In a nitrogen filled glovebox a Schlenk flask was charged with triphenylphosphine (1.00 g; 3.81 mmol) and $\text{Ni}(\text{cod})_2$ (500 mg; 1.82 mmol). The flask was sealed with septum and then taken out of the glovebox. Dry THF (50 mL) was added via cannula and the resulting dark red mixture was stirred at r.t. for 15 minutes. The

solution was then cooled to -78 °C and corresponding carboxylic anhydride or carboxylic chloride (3 mmol) was added dropwise. Solution was slowly warmed to rt over the period of 1 hour and then dppe (876 mg; 2.20 mmol) was added. Resulting solution was stirred at rt for 5 minutes and then filtered through a pad of celite. Volatiles were removed under reduced pressure and the residue was suspended in diisopropyl ether (50 mL). Product separated in a form of yellow crystals. Product was collected by filtration, washed with several portions of diisopropyl ether and dried under reduced pressure. Analytical sample was obtained after crystallization (3 times) from DCM/diisopropyl ether.

Preparation of (dppe)Ni(C₂F₅)(OCC₂F₅) (4). **4** was obtained according to the general procedure **1** in 640 mg (48%) yield. ¹H NMR (CD₂Cl₂ at 23 °C): δ 8.06-8.00 (m, 4H), 7.82-7.76 (m, 4H), 7.66-7.59 (m, 4H), 7.59-7.50 (m, 8H), 2.21-2.12 (m, 4H), 2.10-2.00 (m, 4H). ¹³C{¹H} NMR (CD₂Cl₂ at 25 °C): δ 160.89 (t, ²J_(C-F) = 26.0 Hz), 133.60 (d, ³J_(C-P) = 10.2 Hz), 133.20 (d, ³J_(C-P) = 10.9 Hz), 131.97 (d, ⁴J_(C-P) = 2.7 Hz), 131.85 (d, ⁴J_(C-P) = 2.0 Hz), 129.19 (d, ²J_(C-P) = 10.2 Hz), 129.03 (d, ²J_(C-P) = 10.9 Hz), 128.47 (m, Ni-CF₂-CF₃ resonance not observed in ¹³C spectrum but shift extracted from ¹⁹F/¹³C HSQC and HMBC experiments), 127.62 (d, ¹J_(C-P) = 50.4 Hz), 126.67 (d, ¹J_(C-P) = 40.9 Hz), 120.63 (qtd, ¹J_(C-F) = 285.4 Hz, ²J_(C-F) = 32.0 Hz, ³J_(C-P) = 8.2 Hz, Ni-CF₂-CF₃), 118.26 (qt, ¹J_(C-F) = 286.1 Hz, ²J_(C-F) = 35.4 Hz, CO-CF₂-CF₃), 105.49 (tq, ¹J_(C-F) = 263.0 Hz, ²J_(C-F) = 38.1 Hz, CO-CF₂-CF₃), 28.98 (dd, ¹J_(C-P) = 35.4 Hz, ²J_(C-P) = 16.4 Hz), 22.30 (dd, ¹J_(C-P) = 30.0 Hz, ²J_(C-P) = 8.9 Hz). ¹⁹F NMR (CD₂Cl₂ at 23 °C): δ -80.31 (s, 3F, Ni-CF₂-CF₃), -83.56 (br, 3F, CO-CF₂-CF₃), -102.07 (broad triplet, ³J_(F-P) = 24.9 Hz, 2F, Ni-CF₂-CF₃), -119.83 (br, 2F, CO-CF₂-CF₃). ³¹P{¹H} NMR (CD₂Cl₂ at 23 °C): δ 54.91 (dt, ²J_(P-P) = 48.5 Hz, ³J_(P-F) = 25.9 Hz), 45.27 (dt, ²J_(P-P) = 48.5 Hz, ³J_(P-F) = 27.5 Hz). ¹⁹F/¹³C HSQC

NMR (CD₂Cl₂ at 25 °C): δ_F/ δ_C -80.43/120.72, -83.68/118.48, -102.19/128.47, -119.91/105.56. ¹⁹F/¹³C HMBC NMR (CD₂Cl₂ at 25 °C): δ_F/ δ_C -80.31/128.36, -80.31/120.82 (¹J correlation), -83.58/105.41, -83.58/118.32 (¹J correlation), -102.08/120.73, -119.78/105.41 (¹J correlation), -119.78/118.32, -119.78/161.00. IR (ATR): cm⁻¹ 1696 (s), 1485 (w), 1439 (s), 1393 (m), 1319 (s), 1296 (s), 1225 (m), 1154 (s). Elemental analysis: Calculated for NiC₃₁H₂₄F₁₀O₂P₂ C = 50.37%, H = 3.27%, F = 25.70%; Found: C = 50.23%, H = 3.32%, F = 25.76%.

Preparation of (dppe)Ni(C₃F₇)(OCC₃F₇) (5). **5** was obtained according to the general procedure **1** in 790 mg (52%) yield. ¹H NMR (CDCl₃ at 23 °C): δ 8.06-7.97 (m, 4H), 7.80-7.74 (m, 4H), 7.60-7.43 (m, 12H), 2.17-2.07 (m, 2H), 2.06-1.96 (m, 2H). ¹³C{¹H} NMR (CDCl₃ at 23 °C; resonances of fluoroalkyl groups are assigned from ¹⁹F/¹³C HSQC spectrum): δ 161.06 (br), 133.65 (d, ³J_(C-P) = 10.9 Hz), 133.18 (d, ³J_(C-P) = 10.9 Hz), 131.87, 131.83, 131.09 (m, Ni-CF₂-), 129.25 (d, ²J_(C-P) = 10.2 Hz), 129.05 (d, ²J_(C-P) = 10.9 Hz), 127.73 (d, ¹J_(C-P) = 50.4 Hz), 126.56 (d, ¹J_(C-P) = 40.2 Hz), 118.17 (m, -CF₃), 117.81 (m, -CF₃), 110.98 (m, -CF₂-), 108.21 (m, -CF₂-), 107.38 (m, -CF₂-), 28.95 (dd, ¹J_(C-P) = 34.1 Hz, ²J_(C-P) = 16.4 Hz), 22.32 (dd, ¹J_(C-P) = 29.3 Hz, ²J_(C-P) = 8.9 Hz). ¹⁹F NMR (CDCl₃ at 23 °C): δ -80.51 (s, 3F), -80.81 (s, 3F), -98.43 (br, 2F), -116.88 (br, 2F), -118.28 (s, 2F), -127.07 (s, 2F). ³¹P{¹H} NMR (CDCl₃ at 25 °C): δ 54.15 (dt, ²J_(P-P) = 43.5 Hz, ³J_(P-F) = 25.4 Hz, 1P), 44.33 (dt, ²J_(P-P) = 43.5 Hz, ³J_(P-F) = 28.6 Hz, 1P). ¹⁹F/¹³C HSQC NMR (CDCl₃ at 25 °C): δ_F/δ_C -80.63/118.17, -80.94/117.81, -98.54/131.09, -117.02/107.38, -118.40/110.98, -127.19/108.21. ¹⁹F/¹³C HMBC NMR (CDCl₃ at 25 °C): δ_F/δ_C -80.53/110.96, -80.83/108.17, -118.32/111.19 (¹J correlation), -118.32/118.14, -127.08/107.57, -127.08/117.96. IR (ATR): cm⁻¹ 1698 (s), 1486 (w), 1437 (m), 1385 (w),

1330 (s), 1210 (s), 1174 (s), 1119 (s), 1078 (s). Elemental analysis: Calculated for NiC₃₃H₂₄F₁₄O₂P₂ C = 47.23%, H = 2.88%, F = 31.70%; Found: C = 47.37%, H = 2.92%, F = 31.70%.

Preparation of (dppe)Ni(CF₂CF₂COO) (6). **6** was obtained according to the general procedure **1** in 572 mg (52%) yield. ¹H NMR (CD₂Cl₂ at 25 °C): δ 8.87-7.78 (m, 8), 7.63-7.48 (m, 12H), 2.44-2.34 (m, 2H), 2.21-2.10 (m, 2H). ¹³C{¹H} NMR (CD₂Cl₂ at 25 °C; resonances of fluoroalkyl group partially assigned from ¹⁹F/¹³C HSQC spectrum): δ 168.98 (t, ²J_(C-F) = 25.9 Hz), 133.24 (d, ³J_(C-P) = 10.9 Hz), 132.73 (d, ³J_(C-P) = 11.6 Hz), 132.03 (d, ⁴J_(C-P) = 2.7 Hz), 131.66 (d, ⁴J_(C-P) = 2.1 Hz), 129.59 (m, Ni-CF₂-), 129.41 (d, ²J_(C-P) = 10.2 Hz), 129.16 (d, ²J_(C-P) = 10.9 Hz), 128.46 (d, ¹J_(C-P) = 38.2 Hz), 126.97 (d, ¹J_(C-P) = 41.8 Hz), 110.83 (tt, ¹J_(C-F) = 267.0 Hz, ²J_(C-F) = 21.8 Hz), 29.91 (dd, ¹J_(C-P) = 34.8 Hz, ²J_(C-P) = 17.7 Hz), 21.93 (dd, ¹J_(C-P) = 30.7 Hz, ²J_(C-P) = 8.9 Hz). ¹⁹F NMR (CD₂Cl₂ at 25 °C): δ -110.31 (m, 2F), -120.00 (br, 2F). ³¹P{¹H} NMR (CD₂Cl₂ at 25 °C): δ 59.09 (dt, ²J_(P-P) = 28.6 Hz, ³J_(P-F) = 20.1 Hz, 1P), 38.46 (apparent quartet, ²J_(P-P) = ³J_(P-F) = 30.1 Hz, 1P). ¹⁹F/¹³C HSQC NMR (CD₂Cl₂ at 25 °C): δ_F/δ_C -110.31/129.59, -120.00/110.83. ¹⁹F/¹³C HMBC NMR (CD₂Cl₂ at 25 °C): δ_F/δ_C -110.31/110.83, -110.31/129.59 (¹J correlation), -110.31/168.98 -120.00/110.83 (¹J correlation), -120.00/129.59, -120.00/168.98. IR (ATR): cm⁻¹ 3054 (w), 2956 (w), 1698 (s), 1619 (w), 1587 (w), 1483 (m), 1436 (m), 1351 (m), 1245 (s), 1137 (m), 1098 (s), 1038 (s). Elemental analysis: Calculated for NiC₂₉H₂₄F₄O₂P₂ C = 57.94%, H = 4.02%, F = 12.64%; Found: C = 57.64%, H = 4.02%, F = 12.66%.

Preparation of (dppe)Ni(CF₂CF₂CF₂COO) (7). **7** was obtained according to the general procedure **1** in 422 mg (36%) yield. ¹H NMR (CD₂Cl₂ at 25 °C): δ 7.96-7.90 (m,

4H), 7.86-7.80 (m, 4H), 7.66-7.61 (m, 2H), 7.61-7.57 (m, 2H), 7.57-7.51 (m, 8H), 2.46-2.36 (m, 2H), 2.06-1.96 (m, 2H). $^{13}\text{C}\{\text{H}\}$ NMR (CD_2Cl_2 at 25 °C; resonances of fluoroalkyl partially assigned from $^{19}\text{F}/^{13}\text{C}$ HSQC spectrum): δ 163.72 (t, $^2J_{(\text{C-F})} = 22.5$ Hz), 133.47 (d, $^3J_{(\text{C-P})} = 10.9$ Hz), 132.88 (d, $^3J_{(\text{C-P})} = 10.2$ Hz), 132.21 (d, $^4J_{(\text{C-P})} = 2.0$ Hz), 131.75 (d, $^4J_{(\text{C-P})} = 2.7$ Hz), 129.35 (d, $^2J_{(\text{C-P})} = 10.2$ Hz), 129.17 (d, $^2J_{(\text{C-P})} = 10.9$ Hz), 127.97 (d, $^1J_{(\text{C-P})} = 38.8$ Hz), 126.87 (d, $^1J_{(\text{C-P})} = 51.1$ Hz), 126.75 (m, $-\text{CF}_2\text{-Ni}$), 111.65 (broad triplet, $^1J_{(\text{C-F})} = 261.6$ Hz), 107.79 (tt, $^1J_{(\text{C-F})} = 260.2$ Hz, $^2J_{(\text{C-F})} = 28.6$ Hz), 30.42 (dd, $^1J_{(\text{C-P})} = 36.1$ Hz, $^2J_{(\text{C-P})} = 17.7$ Hz), 21.23 (dd, $^1J_{(\text{C-P})} = 30.7$ Hz, $^2J_{(\text{C-P})} = 8.2$ Hz). ^{19}F NMR (CD_2Cl_2 at 25 °C): δ -100.75 (t, $^2J_{(\text{F-P})} = 31.5$ Hz, 2F), -120.35 (m, 2F), -130.03 (br, 2F). $^{31}\text{P}\{\text{H}\}$ NMR (CD_2Cl_2 at 25 °C): δ 58.29 (dt, $^2J_{(\text{P-P})} = 44.25$ Hz, $^3J_{(\text{P-F})} = 33.6$ Hz, 1P), 38.19 (m, 1P). $^{19}\text{F}/^{13}\text{C}$ HSQC NMR (CD_2Cl_2 at 25 °C): $\delta_{\text{F}}/\delta_{\text{C}}$ -100.75/126.75, -120.35/107.79, -130.03/111.65. $^{19}\text{F}/^{13}\text{C}$ HMBC NMR (CD_2Cl_2 at 25 °C): $\delta_{\text{F}}/\delta_{\text{C}}$ -100.75/111.65, -120.36/107.79 (1J correlation), -120.36/111.65, -120.36/163.79, -130.03/111.65 (1J correlation), -130.03/126.75. IR (ATR): cm^{-1} 3064 (w), 2956 (w), 2918 (w), 1687 (s), 1482 (m), 1434 (m), 1379 (m), 1288 (m), 1221 (m), 1164 (s), 1102 (s), 1052 (s). Elemental analysis: Calculated for $\text{NiC}_{30}\text{H}_{24}\text{F}_6\text{O}_2\text{P}_2$ C = 55.34%, H = 3.72%, F = 17.51%; Found: C = 55.19%, H = 3.70%, F = 17.25%.

Preparation of (dppe)Ni(C₃F₇)(Cl) (8). **8** was obtained according to the general procedure **1** in 570 mg (47%) yield. Compound slowly decomposes in solution. Analytical sample contains some unidentified decomposition product (~15% based on ^{31}P NMR) with (dppe)NiX₂ structure. All further attempts to purify the title complex resulted in extensive decomposition. ^1H NMR (CDCl_3 at 23 °C): δ 7.91-7.80 (m, 8H), 7.28-7.40 (m, 12H), 2.20-2.08 (m, 2H), 1.99-1.88 (m, 2H). $^{13}\text{C}\{\text{H}\}$ NMR (CDCl_3 at 23 °C): δ

133.72 (d, $^3J_{(C-P)} = 10.2$ Hz), 133.81 (Low intensity multiplet that overlaps with nearby peaks. Resonance observed in $^{19}\text{F}/^{13}\text{C}$ HSQC spectrum.), 133.51 (d, $^3J_{(C-P)} = 10.9$ Hz), 131.71, 131.29, 128.92-128.61 (four overlapping doublets.), 118.42 (qt, $^1J_{(C-F)} = 286.8$ Hz, $^2J_{(C-F)} = 40.87$ Hz), 111.62 (tq, $^1J_{(C-F)} = 256.8$ Hz, $^2J_{(C-F)} = 32.8$ Hz), 29.66 (dd, $^1J_{(C-P)} = 34.7$ Hz, $^2J_{(C-P)} = 18.4$ Hz), 24.63 (dd, $^1J_{(C-P)} = 27.2$ Hz, $^2J_{(C-P)} = 9.9$ Hz). ^{19}F NMR (CDCl_3 at 23 °C): δ -80.42 (t, $^3J_{(F-F)} = 9.6$ Hz, 3F), -89.88 (m, 2F), -115.33 (br, 2F). $^{31}\text{P}\{^1\text{H}\}$ NMR (CDCl_3 at 25 °C): δ 60.36 (dt, $^2J_{(P-P)} = 48.7$ Hz, $^3J_{(P-F)} = 35.0$ Hz, 1P), 44.39 (dt, $^2J_{(P-P)} = 48.8$ Hz, $^3J_{(P-F)} = 27.6$ Hz, 1P). $^{19}\text{F}/^{13}\text{C}$ HSQC NMR (CDCl_3 at 25 °C): $\delta_{\text{F}}/\delta_{\text{C}}$ -80.54/118.43, -89.99/133.81, -115.44/111.63. $^{19}\text{F}/^{13}\text{C}$ HMBC NMR (CDCl_3 at 25 °C): $\delta_{\text{F}}/\delta_{\text{C}}$ -80.42/111.72, -80.42/118.55 (1J correlation). IR (ATR): cm^{-1} 3055 (w), 1485 (m), 1438 (s), 1326 (s), 1211 (s), 1188 (s). Elemental analysis: Calculated for $\text{NiC}_{29}\text{H}_{24}\text{ClF}_7\text{P}_2$ C = 52.65%, H = 3.66%, Cl = 5.36% F = 20.10%; Found: C = 53.02%, H = 3.81%, Cl = 5.46, F = 18.16%.

Preparation of (dppe)Ni(C₆F₅)(Cl) (9). **9** was obtained according to the general procedure **1** in 775 mg (65%) yield. ^1H NMR (CD_2Cl_2 at 23 °C): δ 7.97 (m, 4H), 7.68 (m, 4H), 7.60 (m, 2H), 7.57-7.52 (m, 6H), 7.41 (m, 4H), 2.44-2.32 (m, 2H), 2.11-1.98 (m, 2H). $^{13}\text{C}\{^1\text{H}\}$ NMR (CD_2Cl_2 at 23 °C): δ 145.89 (dd, $^1J_{(C-F)} = 226.8$ Hz, $^3J_{(C-P)} = 27.3$ Hz), 138.19 (d, $^1J_{(C-F)} = 240$ Hz), 137.16 (d, $^1J_{(C-F)} = 252$ Hz), 133.62 (d, $^3J_{(C-P)} = 10.2$ Hz), 132.95 (d, $^3J_{(C-P)} = 10.2$ Hz), 131.81 (d, $^4J_{(C-P)} = 2.7$ Hz), 131.81 (d, $^4J_{(C-P)} = 2.0$ Hz), 129.15 (d, $^1J_{(C-P)} = 43.6$ Hz), 128.90 (d, $^2J_{(C-P)} = 10.2$ Hz) 128.67 (d, $^2J_{(C-P)} = 10.9$ Hz), 128.63 (d, $^1J_{(C-P)} = 41.8$ Hz), 123.37 (m), 27.80 (dd, $^1J_{(C-P)} = 31.3$ Hz, $^2J_{(C-P)} = 18.4$ Hz), 22.94 (dd, $^1J_{(C-P)} = 28.6$ Hz, $^2J_{(C-P)} = 12.3$ Hz). ^{19}F NMR (CD_2Cl_2 at 23 °C): δ -118.61 (m, 2F), -161.67 (apparent t, $^3J_{(F-F)} = 19.9$ Hz, 1F), -163.55 (m, 2F). $^{31}\text{P}\{^1\text{H}\}$ NMR (CD_2Cl_2 at

23 °C): δ 61.55 (d, $^2J_{(P-P)} = 51.9$ Hz), 48.03 (broad doublet, $^2J_{(P-P)} = 51.9$ Hz). $^{19}\text{F}/^{13}\text{C}$ HSQC NMR (CD_2Cl_2 at 25 °C): $\delta_{\text{F}}/\delta_{\text{C}}$ -118.63/145.87, -162.66/137.03, -164.41/135.79. $^{19}\text{F}/^{13}\text{C}$ HMBC NMR (CD_2Cl_2 at 25 °C): $\delta_{\text{F}}/\delta_{\text{C}}$ -118.55/123.44, -118.55/135.84, -118.55/137.01, -162.57/135.84, -162.57/137.01 (1J correlation), -162.57/145.86, -164.35/123.44, -164.35/135.84 (1J correlation), -164.35/137.01, -164.35/145.86. IR (ATR): cm^{-1} 3076 (w), 1495 (s), 1448 (s), 1435 (s), 1343 (m), 1102 (s).

Preparation of $(\text{PPh}_3)_2\text{Pd}(\text{COCF}_3)(\text{OCOCF}_3)$ (10). A Schlenk flask was charged with a stirbar and $(\text{PPh}_3)_4\text{Pd}$ (8.00 g; 6.92 mmol). The flask was sealed, evacuated under reduced pressure and then refilled with nitrogen four times. Dry THF (250 mL) was added via cannula. Trifluoroacetic anhydride (TFAA) (3.40 mL; 24.0 mmol) was then added dropwise over the period of 10 minutes. The resulting solution was stirred at rt for 20 minutes and then volatiles were removed under reduced pressure. The white crystalline residue was suspended in EtOAc (100 mL), filtered and washed with several portions of EtOAc. After drying in vacuum 5.23 g (90%) of a white solid was obtained. ^1H NMR (CDCl_3 at 25 °C): δ 7.64-7.58 (m, 12H), 7.49-7.44 (m, 6H), 7.44-7.38 (m, 12H). $^{13}\text{C}\{^1\text{H}\}$ NMR (CDCl_3 at 25 °C): δ 219.54 (q, $^2J_{(C-F)} = 38.2$ Hz), 159.69 (q, $^2J_{(C-F)} = 36.2$ Hz), 134.39 (t, $^2J_{(C-P)} = 6.9$ Hz), 131.0, two overlapping triplets 128.55 (t, $^3J_{(C-P)} = 4.9$ Hz) and 128.54 (t, $^1J_{(C-P)} = 23.5$ Hz), 115.51 (q, $^1J_{(C-F)} = 291.5$ Hz), 111.65 (qt, $^1J_{(C-F)} = 301.3$ Hz, $^3J_{(C-P)} = 16.6$ Hz). ^{19}F NMR (CDCl_3 at 25 °C): δ -75.01 (s, 3F), -75.46 (s, 3F). $^{31}\text{P}\{^1\text{H}\}$ NMR (CDCl_3 at 25 °C): δ 17.53 (s). $^{19}\text{F}/^{13}\text{C}$ HSQC NMR (CDCl_3 at 25 °C): $\delta_{\text{F}}/\delta_{\text{C}}$ -75.14/111.82, -75.59/115.66. $^{19}\text{F}/^{13}\text{C}$ HMBC NMR (CDCl_3 at 25 °C): $\delta_{\text{F}}/\delta_{\text{C}}$ -75.01/219.52, -75.60/111.82 (1J correlation), -75.46/159.66, -75.46/115.54 (1J correlation). IR (ATR): cm^{-1} 3059 (w), 1752 (w), 1684 (s), 1665 (s), 1481 (s), 1436 (s),

1422 (s), 1229 (s), 1177 (s), 1136 (s), 1095 (s). FAB MS (m/z): $[M - CF_3COO]^+$ calcd for $C_{38}H_{30}F_3OP_2Pd$, 727.1; Found, 727.5, $[(PPh_3)_2PdCF_3]^+$ calcd for $C_{37}H_{30}F_3P_2Pd$, 699.1; Found, 699.5 Elemental analysis: Calculated for $PdC_{40}H_{30}F_6O_3P_2$ C = 57.12%, H = 3.60%, F = 13.55%; Found: C = 57.09%, H = 3.70%, F = 13.66%.

Preparation of $(P(o-Tol)_3)_2Pd(COCF_3)(OCOCF_3)$ (15**).** A Schlenk flask was charged with a stirbar and $Pd[P(o-Tol)_3]_2$ (4.00 g; 6.92 mmol). The flask was sealed, evacuated under reduced pressure and then refilled with nitrogen. The flask was evacuated and refilled with nitrogen three more times. Dry THF (100 mL) was added via cannula. Trifluoroacetic anhydride (TFAA) (1.13 mL; 8 mmol) was then added dropwise over the period of 10 minutes. The resulting solution was stirred at rt for 20 minutes and then filtered through a pad of celite. Volatiles were removed under reduced pressure. The residue was suspended in diethyl ether (100 mL). Product slowly separated over the period of 4 hours in a form of yellowish crystals. Precipitate was filtered and washed with several portions of diethyl ether. After drying in vacuum 5.08 g (91%) of a white solid was obtained. 1H NMR and elemental analysis showed that crystallized compound contains exactly one equivalent of diethyl ether that could not be removed even after prolonged drying under vacuum. The cocrystallized ether was taken into account when the reaction yield was calculated. 1H -, ^{19}F - and ^{31}P -NMR spectra of **15** contain only very broad resonances. We explain this with reversible dissociation of the $P(o-Tol)_3$ ligand and dynamic equilibrium between several species in the solution. This is supported by the fact that ^{31}P -NMR spectrum of **15** contains a singlet at -29.6 ppm corresponding to a free $P(o-Tol)_3$ ligand. 1H NMR ($CDCl_3$ at 23 °C): δ 10.0-6.0 (br, 24H), 4.0-1.0 (br, 18 H), 3.48 (q, $J = 7.1$ Hz, 4H, diethyl ether), 1.21 (t, $J = 7.1$ Hz, 6H, diethyl ether). ^{19}F NMR ($CDCl_3$ at

23 °C): δ -73.2 (br, 3F), -74.8 (br, 3F). $^{31}\text{P}\{^1\text{H}\}$ NMR (CDCl_3 at 23 °C): δ 20.5-6.7 (br). IR (ATR): cm^{-1} 3058 (w), 2973 (m), 1700 (s), 1677 (s), 1590 (m), 1566 (m), 1444 (s), 1405 (s), 1381 (m), 1279 (m), 1231 (m), 1191 (s). Elemental analysis: Calculated for $\text{PdC}_{46}\text{H}_{42}\text{F}_6\text{O}_3\text{P}_2 \cdot \text{C}_2\text{H}_5\text{OC}_2\text{H}_5$ C = 60.10%, H = 5.24%, F = 11.41%; Found: C = 60.03%, H = 5.32%, F = 11.69%.

Preparation of $(\text{P}(o\text{-Tol})_3)_2\text{Pd}(\text{CF}_3)(\text{OCOCF}_3)$ (16**).** $(\text{P}(o\text{-Tol})_3)_2\text{Pd}(\text{COCF}_3)(\text{OCOCF}_3)$ (**15**) (2.50 g; 2.70 mmol) was refluxed in benzene (150 mL) for 1 hour. Reaction mixture was then filtered through a pad of celite and volatiles were removed under reduced pressure. The residue was dissolved in diisopropyl ether (150 mL) and product slowly separated in a form of yellowish crystals over the period of 4 hours. Product was collected by filtration and washed with several portions of diisopropylether. After drying under reduced pressure, 1.82g (67%) of a yellowish solid was obtained. ^1H NMR and elemental analysis showed that crystallized **16** contains exactly one equivalent of diisopropyl ether that could not be removed even after prolonged drying under vacuum. The cocrystallized diisopropyl ether was taken into account when the reaction yield was calculated. ^1H -, ^{19}F - and ^{31}P -NMR spectra of **16** contain broad resonances. We explain this with reversible dissociation of the $\text{P}(o\text{-Tol})_3$ ligand and dynamic equilibrium between several species in the solution. This is supported by the fact that ^{31}P -NMR spectrum of **16** contains a singlet at -29.6 ppm corresponding to a free $\text{P}(o\text{-Tol})_3$ ligand. NMR of **16** spectra are not reported here but they are provided in the SI. IR (ATR): cm^{-1} 3059 (w), 2968 (m), 2870 (w), 1698 (s), 1591 (m), 1566 (m), 1445 (s), 1405 (m), 1380 (m), 1281 (m), 1190 (s). FAB MS (m/z): $[\text{M} - \text{CF}_3\text{COO}]^+$ calcd for $\text{C}_{43}\text{H}_{42}\text{F}_3\text{P}_2\text{Pd}$, 783.2; Found, 783.5, Elemental analysis: Calculated for

PdC₄₅H₄₂F₆O₂P₂*C₃H₇OC₃H₇ C = 61.29%, H = 5.65%, F = 11.41%; Found: C = 60.04%, H = 5.34%, F = 11.50%.

Preparation of (dppe)Pd(CF₃)(OCOCF₃) (17). (P(*o*-Tol)₃)₂Pd(CF₃)(OCOCF₃)*C₃H₇OC₃H₇ (**16**) (250 mg; 0.25 mmol) and 1,2-bis(diphenylphosphino)ethane (dppe) (115 mg; 0.29 mmol) were dissolved in a small amount of DCM (~7 mL). Reaction mixture was stirred at rt for 5 minutes and then filtered through a pad of celite. Diisopropylether was slowly added to the solution until the product started to crystallize. Mixture was cooled to 5 °C for 4 hours and crystallized product was then collected by filtration. Product was washed with several portions of diisopropyl ether and dried under reduced pressure. Thus **17** was prepared in 154 mg (90%) yield. Analytical sample was obtained after crystallization (3 times) from DCM/diisopropyl ether. ¹H NMR (CD₂Cl₂ at 25 °C): δ 7.87-7.80 (m, 4H), 7.77-7.71 (m, 4H), 7.66-7.61 (m, 2H) 7.60-7.49 (m, 10H), 2.51-2.42 (m, 2H), 2.28-2.18 (m, 2H). ¹³C{¹H} NMR (CD₂Cl₂ at 25 °C): δ 160.73 (q, ³J_(C-F) = 36.1 Hz), 136.15 (qdd, ¹J_(C-F) = 381.47 Hz, ²J_(C-P) = 215.9 and 8.9 Hz), 133.50 (d, ³J_(C-P) = 11.6 Hz), 133.08 (d, ³J_(C-P) = 11.6 Hz), 132.39 (d, ⁴J_(C-P) = 2.7 Hz), 131.89 (d, ⁴J_(C-P) = 2.7 Hz), 129.36-129.16 (two overlapping doublets), 127.92 (d, ¹J_(C-P) = 40.9 Hz), 127.24 (d, ¹J_(C-P) = 55.2 Hz), 116.22 (qd, ¹J_(C-F) = 290.9 Hz, ⁴J_(C-P) = 7.5 Hz), 30.61 (dd, ¹J_(C-P) = 36.8 Hz, ²J_(C-P) = 18.4 Hz), 23.66 (dd, ¹J_(C-P) = 30.0 Hz, ²J_(C-P) = 8.2 Hz). ¹⁹F NMR (CD₂Cl₂ at 25 °C): δ -26.61 (dd, ³J_(F-P) = 66.3 and 26.5 Hz, 3F), -74.60 (s, 3F). ³¹P{¹H} NMR (CD₂Cl₂ at 25 °C): δ 56.55 (apparent quintet, ²J_(P-P) = ³J_(P-F) = 25.9 Hz, 1P), 44.04 (qd, ³J_(P-F) = 65.6 Hz, ²J_(P-P) = 27.5 Hz, 1P). ¹⁹F/¹³C HSQC NMR (CD₂Cl₂ at 25 °C): δ_F/δ_C -74.60/116.25 (Peak corresponding to the Pd-CF₃ group was not observed in ¹⁹F/¹³C HSQC. However Pd-CF₃

group was observed in $^{19}\text{F}/^{13}\text{C}$ HMBC as a 1J artifact. $^{19}\text{F}/^{13}\text{C}$ HMBC NMR (CD_2Cl_2 at 25 °C): $\delta_{\text{F}}/\delta_{\text{C}}$ -26.61/136.31 (1J correlation), -74.60/116.39 (1J correlation), -74.60/160.77. IR (ATR): cm^{-1} 3068 (w), 2976 (w), 1682 (s), 1486 (m), 1436 (s), 1418 (m), 1314 (m), 1182 (s), 1136 (s), 1082 (s). HRMS electrospray (m/z): $[\text{M} - \text{OCOCF}_3]^+$ calcd for $\text{C}_{27}\text{H}_{24}\text{F}_3\text{P}_2\text{Pd}$, 573.0335; Found, 573.0348, $[\text{M} - \text{CO}_2\text{CF}_3 + \text{CH}_3\text{CN}]^+$ calcd for $\text{C}_{29}\text{H}_{27}\text{F}_3\text{NP}_2\text{Pd}$, 614.0600; Found, 614.0610. Elemental analysis: Calculated for $\text{PdC}_{29}\text{H}_{24}\text{F}_6\text{O}_2\text{P}_2$ = 50.71%, H = 3.52%, F = 16.60%; Found: C = 50.46%, H = 3.59%, F = 16.37%.

General procedure 2: Preparation of dppe supported perfluoroalkylpalladium complexes 18-20. A Schlenk flask was charged with a stirbar and $\text{Pd}[\text{P}(o\text{-Tol})_3]_2$ (2.00g; 3.46 mmol). The flask was sealed, evacuated under reduced pressure and then refilled with nitrogen four times. Dry THF (100 mL) was added via cannula. Corresponding anhydride (5.0 mmol) was then added dropwise over the period of 5 minutes. The resulting solution was stirred at rt for 20 minutes, it was then filtered through a pad of celite and volatiles were removed under reduced pressure. Residue was refluxed in 150 mL of benzene for approximately 30 minutes, until the color of the solution changed from yellow to deep red and then back to yellow. Benzene solution was cooled to rt and dppe (1.35 g; 3.4 mmol) was added. Reaction mixture was filtered through a pad of celite and benzene was removed under reduced pressure. The residue was dissolved in diisopropyl ether (100 mL). Product slowly separated over the period of 4 hours in a form of yellowish crystals. Product was collected by filtration and washed with several portions of diisopropylether. Analytical sample was obtained after several crystallizations from DCM/isopropylether.

Preparation of (dppe)Pd(C₂F₅)(OCOC₂F₅) (18). **18** was obtained according to the general procedure **2** in 87% yield. ¹H NMR (CD₂Cl₂ at 25 °C): δ 7.85-7.79 (m, 4H), 7.74-7.69 (m, 4H), 7.66-7.61 (m, 2H), 7.60-7.50 (m, 10H), 2.43-2.34 (m, 2H), 2.24-2.14 (m, 2H). ¹³C{¹H} NMR (CD₂Cl₂ at 25 °C; resonances of fluoroalkyl groups are assigned from ¹⁹F/¹³C HSQC spectrum): δ 160.85 (t, ³J_(C-F) = 25.2 Hz), 133.62 (d, ³J_(C-P) = 11.6 Hz), 133.28 (d, ³J_(C-P) = 11.6 Hz), 132.31 (d, ⁴J_(C-P) = 2.7 Hz), 131.88 (d, ⁴J_(C-P) = 2.7 Hz), 129.68 (m, Pd-CF₂-), 129.24-129.07 (two overlapping doublets), 127.67 (d, ¹J_(C-P) = 42.2 Hz), 127.27 (d, ¹J_(C-P) = 54.5 Hz), 121.15 (m, CF₃), 118.50 (qt, ¹J_(C-F) = 286.1 Hz, ²J_(C-F) = 35.4 Hz, CF₃) 106.56 (m, CO-CF₂-), 30.48 (dd, ¹J_(C-P) = 36.1 Hz, ²J_(C-P) = 17.7 Hz), 24.28 (dd, ¹J_(C-P) = 29.3 Hz, ²J_(C-P) = 8.9 Hz). ¹⁹F NMR (CD₂Cl₂ at 25 °C): δ -81.49 (s, 3F), -83.51 (s, 3F), -96.55 (dd, ³J_(F-P) = 39.8 and 31.5 Hz, 2F), -119.55 (s, 2F). ³¹P{¹H} NMR (CD₂Cl₂ at 25 °C): δ 55.90 (td, ³J_(P-F) = 31.8 Hz, ²J_(P-P) = 26.5 Hz, 1P), 44.14 (tdq, ³J_(P-F) = 39.2 Hz, ²J_(P-P) = 26.5 Hz, ⁴J_(P-F) = 3.2 Hz, 1P). ¹⁹F/¹³C HSQC NMR (CD₂Cl₂ at 25 °C): δ_F/δ_C -81.60/121.15, -83.64/118.50, -96.67/129.68, -119.68/106.56. ¹⁹F/¹³C HMBC NMR (CD₂Cl₂ at 25 °C): δ_F/δ_C -81.60/121.15 (¹J correlation), -81.60/129.68, -83.64/106.56, -83.64/118.50 (¹J correlation), -96.67/121.15, -119.68/118.50, -119.68/160.91. IR (ATR): cm⁻¹ 3066 (w), 1693 (s), 1485 (w), 1437 (s), 1386 (m), 1319 (s), 1300 (s), 1226 (m), 1150 (s), 1104 (s). HRMS electrospray (m/z): [M - OCOC₂F₅]⁺ calcd for C₂₈H₂₄F₅P₂Pd, 623.0303; Found, 623.0312, [M - CO₂C₂F₅ + CH₃CN]⁺ calcd for C₃₀H₂₇F₅NP₂Pd, 664.0568; Found, 664.0575. Elemental analysis: Calculated for PdC₃₁H₂₄F₁₀O₂P₂ C = 47.32%, H = 3.07%, F = 24.14%; Found: C = 47.08%, H = 3.02%, F = 24.05%.

Preparation of (dppe)Pd(C₃F₇)(OCOC₃F₇) (19). **19** was obtained according to the general procedure **2** in 50% yield. ¹H NMR (CDCl₃ at 25 °C): δ 7.82-7.76 (m, 4H),

7.73-7.68 (m, 4H), 7.60-7.46 (m, 12H), 2.38-2.26 (m, 2H), 2.19-2.08 (m, 2H). $^{13}\text{C}\{^1\text{H}\}$ NMR (CDCl_3 at 25 °C; resonances of fluoroalkyl groups are assigned from $^{19}\text{F}/^{13}\text{C}$ HSQC spectrum): δ 161.15 (t, $^3J_{(\text{C-F})} = 25.9$ Hz), 133.66 (d, $^3J_{(\text{C-P})} = 12.3$ Hz), 132.59 (m, Pd-CF₂-), 133.27 (d, $^3J_{(\text{C-P})} = 11.6$ Hz), 132.25 (d, $^4J_{(\text{C-P})} = 2.7$ Hz), 131.88 (d, $^4J_{(\text{C-P})} = 2.7$ Hz), 129.26 (d, $^2J_{(\text{C-P})} = 10.2$ Hz), 129.14 (d, $^2J_{(\text{C-P})} = 11.6$ Hz), 127.70-127.27 (two overlapping doublets), 118.51 (m, -CF₃), 117.85 (m, -CF₃), 110.87 (m, -CF₂-), 108.47 (m, -CF₂-), 108.41 (m, -CF₂-), 30.20 (dd, $^1J_{(\text{C-P})} = 36.1$ Hz, $^2J_{(\text{C-P})} = 17.7$ Hz), 24.17 (dd, $^1J_{(\text{C-P})} = 29.3$ Hz, $^2J_{(\text{C-P})} = 8.9$ Hz). ^{19}F NMR (CDCl_3 at 25 °C): δ -80.31 (t, $^3J_{(\text{F-F})} = 8.3$ Hz, 3F), -80.78 (t, $^3J_{(\text{F-F})} = 8.3$ Hz, 3F), -93.34 (m, 2F), -116.49 (q, $^3J_{(\text{F-F})} = 10.0$ Hz, 2F), -120.43 (s, 2F), -126.96 (s, 2F). $^{31}\text{P}\{^1\text{H}\}$ NMR (CDCl_3 at 25 °C): δ 55.90 (apparent quartet, $^2J_{(\text{P-P})} = ^3J_{(\text{P-F})} = 27.5$ Hz, 1P), 44.14 (td, $^3J_{(\text{P-F})} = 39.7$ Hz, $^2J_{(\text{P-P})} = 27.5$ Hz, 1P). $^{19}\text{F}/^{13}\text{C}$ HSQC NMR (CDCl_3 at 25 °C): $\delta_{\text{F}}/\delta_{\text{C}}$ -80.43/118.51, -80.91/117.85, -93.43/132.59, -116.61/108.47, -120.54/110.87, -127.08/108.41. $^{19}\text{F}/^{13}\text{C}$ HMBC NMR (CDCl_3 at 25 °C): $\delta_{\text{F}}/\delta_{\text{C}}$ -80.43/110.87, -80.91/108.47, -116.61/108.47, -116.61/161.51, -120.54/110.87 (1J correlation), -120.54/118.51, -127.08/108.47, -127.08/117.85. IR (ATR): cm^{-1} 3065 (w), 1494 (s), 1486 (m), 1438 (s), 1384 (m), 1331 (s), 1210 (s), 1175 (s). HRMS electrospray (m/z): $[\text{M} - \text{OCOC}_3\text{F}_7]^+$ calcd for C₂₉H₂₄F₇P₂Pd, 673.0271; Found, 673.0278, $[\text{M} - \text{CO}_2\text{C}_3\text{F}_7 + \text{CH}_3\text{CN}]^+$ calcd for C₃₁H₂₇F₇NP₂Pd, 714.0536; Found, 714.0540. Elemental analysis: Calculated for PdC₃₃H₂₄F₁₄O₂P₂ = 44.69%, H = 2.73%, F = 29.99%; Found: C = 44.76%, H = 2.74%, F = 29.91%.

Preparation of (dppe)Pd(CF₂CF₂CF₂COO) (20). **20** was obtained according to the general procedure **2** in 16% yield. Methyl *tert*-butyl ether (MTBE) was used for crystallizations instead of diisopropyl ether. In order to remove cocrystallized solvent, the

analytical sample was dried under vacuum at at 90 °C for 8 hours. ^1H NMR (CD_2Cl_2 at 25 °C): δ 7.81-7.73 (m, 8H), 7.65-7.61 (m, 2H), 7.59-7.50 (m, 10H), 2.66-2.56 (m, 2H), 2.26-2.17 (m, 2H). $^{13}\text{C}\{^1\text{H}\}$ NMR (CD_2Cl_2 at 25 °C; resonances of fluoroalkyl partially assigned from $^{19}\text{F}/^{13}\text{C}$ HSQC spectrum): δ 164.01 (t, $^2J_{(\text{C-F})} = 25.2$ Hz), 133.60 (d, $^3J_{(\text{C-P})} = 11.6$ Hz), 132.76 (d, $^3J_{(\text{C-P})} = 11.6$ Hz), 132.56 (d, $^4J_{(\text{C-P})} = 2.7$ Hz), 131.92 (d, $^4J_{(\text{C-P})} = 2.1$ Hz), 129.48 (d, $^2J_{(\text{C-P})} = 10.2$ Hz), 129.25 (d, $^2J_{(\text{C-P})} = 11.6$ Hz), 128.30 (d, $^1J_{(\text{C-P})} = 39.5$ Hz), 128.15 (m, $-\text{CF}_2\text{-Pd}$), 126.39 (d, $^1J_{(\text{C-P})} = 55.9$ Hz), 113.08 (broad triplet, $^1J_{(\text{C-F})} = 265.7$ Hz), 108.81 (tt, $^1J_{(\text{C-F})} = 260.9$ Hz, $^2J_{(\text{C-F})} = 30.5$ Hz), 31.09 (dd, $^1J_{(\text{C-P})} = 36.8$ Hz, $^2J_{(\text{C-P})} = 18.4$ Hz), 21.83 (dd, $^1J_{(\text{C-P})} = 30.7$ Hz, $^2J_{(\text{C-P})} = 8.2$ Hz). ^{19}F NMR (CD_2Cl_2 at 25 °C): δ -96.04 (m, 2F), -118.93 (m, 2F), -128.66 (br, 2F). $^{31}\text{P}\{^1\text{H}\}$ NMR (CD_2Cl_2 at 25 °C): δ 57.49 (td, $^3J_{(\text{P-F})} = 41.3$ Hz, $^2J_{(\text{P-P})} = 32.84$ Hz, 1P), 37.30 (m, 1P). $^{19}\text{F}/^{13}\text{C}$ HSQC NMR (CD_2Cl_2 at 25 °C): $\delta_{\text{F}}/\delta_{\text{C}}$ -96.04/128.15, -118.93/108.81, -128.66/113.08. $^{19}\text{F}/^{13}\text{C}$ HMBC NMR (CD_2Cl_2 at 25 °C): $\delta_{\text{F}}/\delta_{\text{C}}$ -96.04/113.08, -96.04/128.15 (1J correlation), -118.93/108.81 (1J correlation), -118.93/113.08, -118.93/164.01, -128.66/108.81, -128.66/113.08 (1J correlation), -128.66/128.15. IR (ATR): cm^{-1} 3058 (w), 2919 (w), 1680 (s), 1483 (m), 1436 (s), 1374 (m), 1276 (m), 1222 (m), 1161 (s), 1104 (s), 1056 (s), 992 (s). HRMS electrospray (m/z): $[\text{M} + \text{H}]^+$ calcd for $\text{C}_{30}\text{H}_{25}\text{F}_6\text{O}_2\text{P}_2\text{Pd}$, 699.0263; Found, 699.0262.

Preparation of (dppe)Pd(CHF₂)(Cl) (23). A Schlenk flask was charged with a stirbar and Pd[P(*o*-Tol)₃]₂ (2.00g; 3.46 mmol). The flask was sealed, evacuated under reduced pressure and then refilled with nitrogen four times. Dry THF (100 mL) was added via cannula. Difluoroacetic anhydride (4.0 mmol; 0.89 mL) was then added dropwise over the period of 5 minutes. The resulting solution was stirred at rt for 20

minutes, and then filtered through a pad of celite and volatiles were removed under reduced pressure. Residue was refluxed in 150 mL of benzene for approximately 30 minutes, until the color of the solution changed from yellow to deep red and then back to yellow. Reaction mixture was cooled to rt and then dppe (1.35 g; 3.4 mmol) was added. Reaction mixture was filtered through a pad of celite and resulting benzene solution was stirred intensively with brine for 3 hours. Benzene layer was separated from the brine, dried over anhydrous Na₂SO₄ and evaporated under reduced pressure. The residue was dissolved in methyl *tert*-butyl ether (150 mL). Product slowly separated in a form of yellowish crystals. Product was collected by filtration and washed with several portions of MTBE. After drying in vacuum 1.19 g (72%) of product was obtained. Analytical sample was obtained after several crystallizations from DCM/MTBE. ¹H NMR (CDCl₃ at 25 °C): δ 7.90-7.79 (m, 4H), 7.75-7.65 (m, 4H), 7.55-7.35 (m, 12H), 6.85 (tdd, ²J_(H-F) = 49.3 Hz, ³J_(H-P) = 20.7 Hz and 2.9 Hz, 1H), 2.51-2.33 (m, 2H), 2.22-2.06 (m, 2H). ¹³C{¹H} NMR (CDCl₃ at 25 °C): δ 133.94 (tdd, ¹J_(C-F) = 304.5, ²J_(C-P) = 177.1 Hz and 19.1 Hz), 133.56 (d, ³J_(C-P) = 12.3 Hz), 133.26 (d, ³J_(C-P) = 11.6 Hz), 131.74 (d, ⁴J_(C-P) = 2.1 Hz), 131.06 (d, ⁴J_(C-P) = 2.1 Hz), 130.28 (d, ¹J_(C-P) = 34.1 Hz), 129.07 (d, ²J_(C-P) = 10.2 Hz), 128.98 (d, ²J_(C-P) = 10.9 Hz), 128.46 (d, ¹J_(C-P) = 50.4 Hz), 30.57 (dd, ¹J_(C-P) = 34.1 Hz, ²J_(C-P) = 20.4 Hz), 23.65 (dd, ¹J_(C-P) = 26.6 Hz, ²J_(C-P) = 10.2 Hz). ¹⁹F NMR (CDCl₃ at 23 °C): δ -89.00 (apparent quartet, ²J_(F-H) = ³J_(F-P) = 48.1 Hz). ³¹P{¹H} NMR (CDCl₃ at 25 °C): δ 53.71 (td, ³J_(P-F) = 48.8 Hz, ²J_(P-P) = 35.1 Hz), 31.66 (td, ³J_(P-F) = 53.4 Hz, ²J_(P-P) = 35.1 Hz). ¹⁹F/¹³C HSQC NMR (CDCl₃ at 25 °C): δ_F/δ_C -89.05/133.82. IR (ATR): cm⁻¹ 3053 (w), 2898 (w), 1572 (w), 1482 (m), 1434 (s), 1408 (s), 1310 (m), 1277(m), 1242 (m), 1186 (m), 1102 (s), 1010 (s), 996 (s). HRMS electrospray (m/z): [M – Cl]⁺ calcd for

C₂₇H₂₅F₂P₂Pd, 555.0429; Found, 555.0436, [M - Cl + CH₃CN]⁺ calcd for C₂₉H₂₈F₂NP₂Pd, 596.0694; Found, 596.0693, [M - CHF₂]⁺ calcd for C₂₆H₂₄ClP₂Pd, 539.0071; Found, 539.0074. Elemental analysis: Calculated for PdC₂₉H₂₆F₄O₂P₂ C = 54.84%, H = 4.26%, Cl = 6.00%, F = 6.43%; Found: C = 54.95%, H = 4.32%, Cl = 5.94%, F = 6.28%.

General procedure 3: Preparation of complexes 24-26 with (dppe)Pd(R_f)(Ph) general structure. In a glovebox, a Schlenk flask was charged with a stirbar, diphenylzinc (120 mg; 0.55 mmol) and corresponding (dppe)Pd(R_f)(OOCR_f) complex (0.36 mmol). The flask was sealed and removed from glovebox. Dry THF (20 mL) was added via cannula. The resulting solution was stirred at rt for 20 minutes, then water (0.2 mL) was introduced via septum. Reaction mixture was stirred at rt for additional 20 minutes until Zn(OH)₂ had completely precipitated. Then the THF solution was dried over anhydrous Na₂SO₄, filtered and volatiles were removed under reduced pressure. Residue was crystallized from diethylether. Product was collected by filtration, washed with several portions of ether and dried under vacuum. Analytical sample was obtained after several crystallizations from DCM/isopropylether.

Preparation of (dppe)Pd(CF₃)(Ph) (24). 24 was obtained according to the general procedure 3 in 79% yield. ¹H NMR (CDCl₃ at 25 °C): δ 7.80-7.74 (m, 4H), 7.52-7.44 (m, 6H), 7.43-7.38 (m, 2H), 7.33-7.26 (m, 10H), 7.20 (t, *J* = 6.9 Hz, 2H), 6.81 (apparent t, *J* = 6.9 Hz, 2H), 6.77 (t, *J* = 6.9 Hz, 1H), 2.34-2.16 (m, 4H). ¹³C{¹H} NMR (CDCl₃ at 25 °C): δ 158.85 (apparent doublet of quintets, ²*J*_(C-P) = 112.4 Hz, ³*J*_(C-F) = ²*J*_(C-P) = 8.9 Hz), 143.63 (qdd, ¹*J*_(C-F) = 373.3 Hz, ²*J*_(C-P) = 195.5 Hz and 13.6 Hz), 136.70, 133.35-133.19 (two overlapping doublets), 131.43 (d, ¹*J*_(C-P) = 34.1 Hz), 130.83 (d, ⁴*J*_(C-P) = 2.1 Hz),

130.76 (d, $^4J_{(C-P)} = 2.1$ Hz), 130.19 (d, $^1J_{(C-P)} = 41.5$ Hz), 128.95 (d, $^2J_{(C-P)} = 9.5$ Hz), 128.66 (d, $^2J_{(C-P)} = 10.2$ Hz), 126.64 (d, $^3J_{(C-P)} = 7.5$ Hz, Pd-C-CH), 122.34, 27.48 (dd, $^1J_{(C-P)} = 25.9$ Hz, $^2J_{(C-P)} = 18.4$ Hz), 26.40 (dd, $^1J_{(C-P)} = 25.2$ Hz, $^2J_{(C-P)} = 15.0$ Hz). ^{19}F NMR (CDCl_3 at 25 °C): δ -17.48 (dd, $^3J_{(F-P)} = 51.4$ Hz and 11.8 Hz, 3F). $^{31}\text{P}\{^1\text{H}\}$ NMR (CDCl_3 at 25 °C): δ 40.11 (qd, $^3J_{(P-F)} = 50.4$ Hz, $^2J_{(P-P)} = 16.8$ Hz), 38.26 (apparent quintet, $^3J_{(P-F)} = ^2J_{(P-P)} = 18.3$ Hz). $^{19}\text{F}/^{13}\text{C}$ HSQC NMR (CDCl_3 at 25 °C): $\delta_{\text{F}}/\delta_{\text{C}}$ -17.62/143.74. $^{19}\text{F}/^{13}\text{C}$ HMBC NMR (CDCl_3 at 25 °C): $\delta_{\text{F}}/\delta_{\text{C}}$ -17.48/143.74 (1J correlation), -17.48/158.84. IR (ATR): cm^{-1} 3052 (w), 1565 (m), 1470 (m), 1434 (s), 1308 (w), 1239 (m), 1103 (m), 1080 (s), 950 (s). HRMS electrospray (m/z): $[\text{M} - \text{Ph}]^+$ calcd for $\text{C}_{27}\text{H}_{24}\text{F}_3\text{P}_2\text{Pd}$, 573.0335; Found, 573.0343, $[\text{M} - \text{F}]^+$ calcd for $\text{C}_{33}\text{H}_{29}\text{F}_2\text{P}_2\text{Pd}$, 631.0742; Found, 631.0747.

Preparation of (dppe)Pd(C₂F₅)(Ph) (25). **25** was obtained according to the general procedure **3** in 90% yield. ^1H NMR (CDCl_3 at 25 °C): δ 7.77-7.72 (m, 4H), 7.52-7.45 (m, 4H), 7.41 (t, $J = 7.2$ Hz, 2H), 7.33-7.29 (m, 4H), 7.29-7.24 (m, 4H), 7.15 (t, $J = 7.0$ Hz, 2H), 6.75 (apparent t, $J = 7.3$ Hz, 2H), 6.72 (t, $J = 6.8$ Hz, 1H), 2.24-2.14 (m, 4H). $^{13}\text{C}\{^1\text{H}\}$ NMR (CDCl_3 at 25 °C): δ 158.22 (apparent doublet, $^2J_{(C-P)} = 107.7$ Hz), 136.93, 136.11 (m, Pd-CF₂-), 133.35 (d, $^3J_{(C-P)} = 12.3$ Hz), 133.21 (d, $^3J_{(C-P)} = 11.6$ Hz), 131.55 (d, $^1J_{(C-P)} = 33.4$ Hz), 130.77 (d, $^4J_{(C-P)} = 2.0$ Hz), 130.73 (d, $^4J_{(C-P)} = 2.1$ Hz), 130.24 (d, $^1J_{(C-P)} = 42.2$ Hz), 128.85 (d, $^2J_{(C-P)} = 10.2$ Hz), 128.66 (d, $^2J_{(C-P)} = 10.2$ Hz), 126.50 (d, $^3J_{(C-P)} = 7.5$ Hz, Pd-C-CH), 122.72 (qtd, $^1J_{(C-F)} = 284.8$ Hz, $^2J_{(C-F)} = 30.0$ Hz, $^3J_{(C-P)} = 9.5$ Hz, -CF₃), 122.02, 27.01 (dd, $^1J_{(C-P)} = 25.9$ Hz, $^2J_{(C-P)} = 18.4$ Hz), 26.60 (dd, $^1J_{(C-P)} = 25.9$ Hz, $^2J_{(C-P)} = 15.0$ Hz). ^{19}F NMR (CDCl_3 at 25 °C): δ -80.11 (s, 3F), -89.55 (dd, $^3J_{(F-P)} = 41.5$ Hz and 31.5 Hz, 2F). $^{31}\text{P}\{^1\text{H}\}$ NMR (CDCl_3 at 25 °C): δ 39.60 (tdq,

$^3J_{(P-F)} = 31.8$ Hz, $^2J_{(P-P)} = 17.0$ Hz, $^4J_{(P-F)} = 3.2$ Hz, 1P), 38.90 (td, $^3J_{(P-F)} = 41.3$ Hz, $^2J_{(P-P)} = 17.0$ Hz, 1P). $^{19}\text{F}/^{13}\text{C}$ HSQC NMR (CDCl_3 at 25 °C): $\delta_{\text{F}}/\delta_{\text{C}}$ -80.11/122.72, -89.55/136.11. $^{19}\text{F}/^{13}\text{C}$ HMBC NMR (CDCl_3 at 25 °C): $\delta_{\text{F}}/\delta_{\text{C}}$ -80.11/122.72 (1J correlation), -80.11/136.11, -89.55/122.72. IR (ATR): cm^{-1} 3055 (w), 1564 (m), 1472 (m), 1434 (s), 1292 (s), 1191 (s), 1145 (s), 1099 (m). HRMS electrospray (m/z): $[\text{M} - \text{Ph}]^+$ calcd for $\text{C}_{28}\text{H}_{24}\text{F}_5\text{P}_2\text{Pd}$, 623.0303; Found, 623.0314, $[\text{M} - \text{Ph} + \text{CH}_3\text{CN}]^+$ calcd for $\text{C}_{30}\text{H}_{27}\text{F}_5\text{NP}_2\text{Pd}$, 664.0568; Found, 664.0577. Elemental analysis: Calculated for $\text{PdC}_{34}\text{H}_{29}\text{F}_5\text{P}_2$ C = 58.26%, H = 4.17%, F = 13.55%; Found: C = 58.22%, H = 4.15%, F = 13.46%.

Preparation of (dppe)Pd(C₃F₇)(Ph) (26). **26** was obtained according to the general procedure **3** in 92% yield. ^1H NMR (CDCl_3 at 25 °C): δ 7.77-7.72 (m, 4H), 7.52-7.45 (m, 4H), 7.42 (t, $J = 7.5$ Hz, 2H), 7.33-7.29 (m, 4H), 7.29-7.25 (m, 4H), 7.17 (t, $J = 7.0$ Hz, 2H), 6.75 (apparent t, $J = 7.3$ Hz, 2H), 6.72 (t, $J = 6.9$ Hz, 1H), 2.24-2.14 (m, 4H). $^{13}\text{C}\{^1\text{H}\}$ NMR (CDCl_3 at 25 °C): δ 157.87 (apparent dd, $^2J_{(C-P)} = 117.1$ and 12.3 Hz), 139.31 (m, Pd- $\underline{\text{C}}\text{F}_2^-$), 136.98, 133.38 (d, $^3J_{(C-P)} = 12.3$ Hz), 133.17 (d, $^3J_{(C-P)} = 10.9$ Hz), 131.57 (d, $^1J_{(C-P)} = 32.7$ Hz), 130.74 (two overlapping signals), 130.3 (d, $^1J_{(C-P)} = 42.9$ Hz), 128.81 (d, $^2J_{(C-P)} = 9.5$ Hz), 128.67 (d, $^2J_{(C-P)} = 7.5$ Hz), 126.50 (d, $^3J_{(C-P)} = 7.5$ Hz, Pd-C- $\underline{\text{C}}\text{H}$), 121.99, 119.21 (qt, $^1J_{(C-F)} = 289.5$ Hz, $^2J_{(C-F)} = 34.7$ Hz, $-\underline{\text{C}}\text{F}_3$), 112.04 (tq, $^1J_{(C-F)} = 252.0$ Hz, $^2J_{(C-F)} = 30.7$ Hz, $-\underline{\text{C}}\text{F}_2\text{CF}_3$), 26.97 (dd, $^1J_{(C-P)} = 24.5$ Hz, $^2J_{(C-P)} = 18.4$ Hz), 26.42 (dd, $^1J_{(C-P)} = 25.2$ Hz, $^2J_{(C-P)} = 15.7$ Hz). ^{19}F NMR (CDCl_3 at 23 °C): δ -79.66 (t, $^3J_{(F-F)} = 13.0$ Hz, 3F), -87.62 (m, 2F), -118.33 (s, 2F). $^{31}\text{P}\{^1\text{H}\}$ NMR (CDCl_3 at 25 °C): δ 39.47-38.92 (two overlapping multiplets). $^{19}\text{F}/^{13}\text{C}$ HSQC NMR (CDCl_3 at 25 °C): $\delta_{\text{F}}/\delta_{\text{C}}$ -79.66/119.21, -87.62/139.31, -118.33/112.04. $^{19}\text{F}/^{13}\text{C}$ HMBC NMR (CDCl_3 at 25

$^{\circ}\text{C}$): $\delta_{\text{F}}/\delta_{\text{C}}$ -79.66/112.04, -79.66/119.21 (1J correlation), -87.62/112.04, -118.33/112.04 (1J correlation), -118.33/119.21. IR (ATR): cm^{-1} 3061 (w), 1566 (m), 1473 (m), 1436 (s), 1325 (s), 1213 (s), 1180 (s), 1142 (s), 1099 (m). HRMS electrospray (m/z): $[\text{M} - \text{Ph}]^+$ calcd for $\text{C}_{29}\text{H}_{24}\text{F}_7\text{P}_2\text{Pd}$, 673.0271; Found, 673.0283, $[\text{M} - \text{Ph} + \text{CH}_3\text{CN}]^+$ calcd for $\text{C}_{31}\text{H}_{27}\text{F}_7\text{NP}_2\text{Pd}$, 714.0536; Found, 714.0542. Elemental analysis: Calculated for $\text{PdC}_{35}\text{H}_{29}\text{F}_7\text{P}_2$ C = 55.98%, H = 3.89%, F = 17.71%; Found: C = 55.86%, H = 3.89%, F = 17.90%.

Preparation of (dppe)Pd(CF₃)(CH₃) (27). A Schlenk flask was charged with a stirbar and (dppe)Pd(CF₃)(OOCFCF₃) (300 mg; 0.44 mmol). The flask was sealed, evacuated under reduced pressure and then refilled with nitrogen four times. Dry THF (15 mL) was added via cannula followed by dimethylzinc (1 mL of 1.2 M solution in THF). The resulting solution was stirred at rt for 20 minutes, then water (0.2 mL) was introduced via septum. Reaction mixture was stirred at rt for additional 20 minutes until Zn(OH)₂ had completely precipitated. Then THF solution was dried over anhydrous Na₂SO₄, filtered and volatiles were removed under reduced pressure. Residue was crystallized from diethylether. Product was collected by filtration, washed with several portions of ether and dried under vacuum affording **27** as a white crystalline solid (207 mg, 80%). Analytical sample was obtained after crystallization from DCM/isopropylether. ^1H NMR (CDCl_3 at 25 $^{\circ}\text{C}$): δ 7.71-7.65 (m, 4H), 7.62-7.57 (m, 4H), 7.49-7.38 (m, 12H), 2.34-2.24 (m, 2H), 2.21-2.12 (m, 2H), 0.59 (apparent triplet, $^3J_{(\text{H-P})} = 6.6$ Hz, 3H). $^{13}\text{C}\{^1\text{H}\}$ NMR (CDCl_3 at 25 $^{\circ}\text{C}$): δ 146.60 (qdd, $^1J_{(\text{C-F})} = 374.7$ Hz, $^2J_{(\text{C-P})} = 201.0$ Hz and 15.6 Hz), 133.35 (d, $^3J_{(\text{C-P})} = 11.6$ Hz), 133.18 (d, $^3J_{(\text{C-P})} = 12.9$ Hz), 132.03 (d, $^1J_{(\text{C-P})} = 31.3$ Hz), 130.95 (d, $^4J_{(\text{C-P})} = 2.1$ Hz), 130.56 (d, $^4J_{(\text{C-P})} = 1.4$ Hz), 130.29 (d,

$^1J_{(C-P)} = 40.2$ Hz), 128.95 (d, $^2J_{(C-P)} = 9.5$ Hz), 128.79 (d, $^2J_{(C-P)} = 9.5$ Hz), 28.44 (dd, $^1J_{(C-P)} = 27.2$ Hz, $^2J_{(C-P)} = 19.8$ Hz), 27.38 (dd, $^1J_{(C-P)} = 25.2$ Hz, $^2J_{(C-P)} = 15.7$ Hz), 0.25 (ddq, $^2J_{(C-P)} = 89.2$ Hz and 8.9 Hz, $^3J_{(C-F)} = 6.8$ Hz). ^{19}F NMR (CDCl_3 at 25 °C): δ -19.27 (dd, $^3J_{(F-P)} = 53.1$ Hz and 18.2 Hz, 3F). $^{31}\text{P}\{^1\text{H}\}$ NMR (CDCl_3 at 25 °C): δ 47.42 (qd, $^3J_{(P-F)} = 51.9$ Hz, $^2J_{(P-P)} = 15.9$ Hz), 47.42 (apparent quintet, $^3J_{(P-F)} = ^2J_{(P-P)} = 16.9$ Hz). $^{19}\text{F}/^{13}\text{C}$ HSQC NMR (CDCl_3 at 25 °C): $\delta_{\text{F}}/\delta_{\text{C}}$ -19.41/146.78. $^{19}\text{F}/^{13}\text{C}$ HMBC NMR (CDCl_3 at 25 °C): $\delta_{\text{F}}/\delta_{\text{C}}$ -19.27/0.25, -19.27/146.60 (1J correlation). IR (ATR): cm^{-1} 3053 (w), 2955 (w), 2888(w), 1587 (w), 1573 (w), 1483 (m), 1435 (s), 1411 (m), 1309 (m), 1186 (m), 1158 (m), 1102 (m), 1074 (s). HRMS electrospray (m/z): $[\text{M} - \text{CH}_3]^+$ calcd for $\text{C}_{27}\text{H}_{24}\text{F}_3\text{P}_2\text{Pd}$, 573.0335; Found, 573.0342, $[\text{M} - \text{CH}_3 + \text{CH}_3\text{CN}]^+$ calcd for $\text{C}_{29}\text{H}_{27}\text{F}_3\text{NP}_2\text{Pd}$, 614.0600; Found, 614.0603. Elemental analysis: Calculated for $\text{PdC}_{28}\text{H}_{27}\text{F}_3\text{P}_2$ C = 57.11%, H = 4.62%, F = 9.68%; Found: C = 56.04%, H = 4.57%, F = 9.81%.

4.7 References

- (1) Swarts, F. *Bull. Akad. R. Belg.* **1898**, 35, 375-420.
- (2) Reviews: (a) Tomashenko, O. A.; Grushin, V. V. *Chem. Rev.* **2011**, 111, 4475-4521. (b) Furuya, T.; Kamlet, A. S.; Ritter, T. *Nature* **2011**, 473, 470-477. (c) Besset, T.; Schneider, C.; Cahard, D. *Angew. Chem. Int. Ed.* **2012**, 51, 5048-5050.
- (3) Copper mediated reactions: (a) Ye, Y. Sanford, M. S. *J. Am. Chem. Soc.* **2012**, 134, 9034-9037. (b) Novák, P.; Lishchynskiy, A.; Grushin, V. V. *Angew. Chem. Int. Ed.* **2012**, 51, 7767-7770. (c) Morimoto, H.; Tsubogo, T.; Litvinas, N. D.; Hartwig, J. F. *Angew. Chem.* **2011**, 123, 3877-3882. (d) Oishi, M.; Kondo, H.; Amii, H. *Chem. Commun.* **2009**, 1909-1911. (e) Knauber, T.; Arikan, F.; Rösenthaller, G.-V.; Gooßen, L. *J. Chem. Eur. J.* **2011**, 17, 2689-2697.
- (4) Palladium catalyzed reactions (a) Cho, E. J.; Senecal, T. D.; Kinzel, T.; Zhang, Y.; Watson, D. A.; Buchwald, S. L. *Science*, **2010**, 328, 1679-1681. (b) Kitazume, T.; Ishikawa, N. *Chem. Lett.* **1982**, 137-140.
- (5) Potashman, M. H.; Bready, J.; Coxon, A.; DeMelfi, T. M.; DiPietro, L.; Doerr, N.; Elbaum, D.; Estrada, J.; Gallant, P.; Germain, J.; Gu, Y.; Harmange, J.-C.; Kaufman, S.

-
- A.; Kendall, R.; Kim, J. L.; Kumar, G. N.; Long, A. M.; Neervannan, S.; Patel, V. F.; Polverino, A.; Rose, P.; van der Plas, S.; Whittington, D.; Zanon, R.; Zhao, J. *J. Med. Chem.* **2007**, *50*, 4351-4373.
- (6) Urata, H.; Fuchikami, T. *Tetrahedron Lett.* **1991**, *32*, 91-94.
- (7) Matsui, K.; Tobita, E.; Ando, M.; Kondo, K. *Chem. Lett.* **1981**, 1719-1720.
- (8) McReynolds, K. A.; Lewis, R. S.; Ackerman, L. K. G.; Dubinina, G. G.; Brennessel, W. W.; Vivic, D. A. *J. Fluorine Chem.* **2010**, *131*, 1108-1112 and references therein.
- (9) For a review on decarbonylative couplings, see Alpay, D.; GuangBin, D. *Sci. China. Chem.* **2013**, *56*, 685-701.
- (10) For an example of Pd-catalyzed decarbonylative coupling of acid chlorides with disilanes and 1,3-dienes, see Obora Y.; Tsuji, Y.; Kawamura, T. *J. Am. Chem. Soc.* **1993**, *115*, 10414-10415.
- (11) For examples of Ni-catalyzed decarbonylative couplings of azoles with aryl esters, see (a) Amaike, K.; Muto, K.; Yamaguchi, J.; Itami, K. *J. Am. Chem. Soc.* **2012**, *134*, 13573-13576. (b) Correa, A.; Cornella, J.; Martin, R. *Angew. Chem. Int. Ed.* **2013**, *52*, 1878-1880.
- (12) For examples of Ni-catalyzed decarbonylative coupling of anhydrides with alkynes, see Kajita, Y.; Kurahashi, T.; Matsubara, S. *J. Am. Chem. Soc.* **2008**, *130*, 17226-17227. (b) Havlik, S. E.; Simmons, M. J.; Winton, J. V.; Johnson, J. B. *J. Org. Chem.* **2011**, *76*, 3588-3593.
- (13) Blaser, H. U.; Spencer, A. *J. Organomet. Chem.* **1982**, *233*, 267-274.
- (14) For reviews, see: (a) Brothers, P. J.; Roper, W. R. *Chem. Rev.* **1988**, *88*, 1293-1326. (b) Morrison, J. A. *Adv. Inorg. Chem. Radiochem.* **1983**, *27*, 293-316.
- (15) Synthesis of first row metal trifluoromethyl complexes via decarbonylation: (a) King, R. B. *Acc. Chem. Res.* **1970**, *3*, 417-427. (b) McClellan, W. R. *J. Am. Chem. Soc.* **1961**, *83*, 1598-1600.
- (16) Synthesis of second row metal trifluoromethyl complexes via decarbonylation: Panthi, B. D.; Gipson, S. L.; Franken, A. *Organometallics*, **2010**, *29*, 5890-5896.
- (17) For examples of the synthesis of Iridium trifluoromethyl complexes via decarbonylation, see: (a) Brothers, P. J.; Burrell, A. K.; Clark, G. R. Rickard, C. E. F.; Roper, W. R. *J. Organomet. Chem.* **1990**, *394*, 615-642. (b) Blake, D. M.; Shields, S.; Wyman, L. *Inorg. Chem.* **1974**, *13*, 1595-1600.
- (18) Nickel and Palladium metallatoms have been shown to react with perfluoroacyl chlorides in the gas phase. For reactions of metallatoms with perfluoroacyl chlorides, see Klabunde, K. G. *Angew. Chem.* **1975**, *87*, 309-314.
- (19) For examples of decarbonylation of non-fluorinated acyl ligands at Pd^{II} and Ni^{II}, see: (a) Otsuka, S.; Nakamura, A.; Yoshida, T.; Naruto, M.; Ataka, K. *J. Am. Chem. Soc.* **1973**, *93*, 3180-3188. (b) Yamamoto, T.; Ishizu, J.; Kohara, T.; Komiya, S.; Yamamoto, A. *J. Am. Chem. Soc.* **1980**, *102*, 3758-3764.
- (20) Bennett, M. A.; Chee, H.-K.; Robertson, G. B. *Inorg. Chem.* **1979**, *18*, 1061-1070.
- (21) Cavell, K. J. *Coord. Chem. Rev.* **1996**, *155*, 209-243.
- (22) Grushin, V. V.; Marshall, W. J. *J. Am. Chem. Soc.* **2006**, *128*, 4632-4641.
- (23) Dubinina, G. G.; Brennessel, W. W.; Miller, J. L.; Vivic, D. A. *Organometallics* **2008**, *27*, 3933-3938.
- (24) Beller, M.; Riermeier, T. H. *Eur. J. Inorg. Chem.* **1998**, *1*, 29-35.

Chapter 5: Catalytic Cycle of Trifluoromethylation with TFAA as a CF₃ Source¹

5.1 Introduction

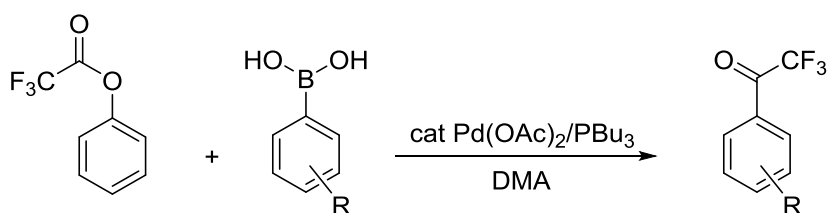
In the previous chapter we introduced the concept of decarbonylative trifluoromethylation (Scheme 4.5 and Scheme 4.7). We also demonstrated that with appropriately selected supporting ligands the two key steps of decarbonylative trifluoromethylation catalytic cycle are facile at nickel and palladium. Specifically, TFAA and pentafluorophenyl trifluoroacetate undergo clean oxidative addition to Ni(COD)₂/PPh₃ and Pd[P(*o*-Tol)₃]₂ and the resulting (PR₃)₂M(COCF₃)(O₂CCF₃) (M = Ni and Pd) intermediates decompose to (PR₃)₂M(CF₃)(O₂CCF₃) with elimination of carbon monoxide. Even though these initial results are very encouraging, there are several major complications that have to be solved before catalytic turnover is attempted. These issues will be addressed in this chapter.

First, highly electrophilic TFAA and to a lesser degree TFA esters are incompatible with organolithium, organomagnesium and other reactive transmetallating agents. Additionally, TFAA is likely incompatible also with electron-rich phosphine ligands. Therefore, milder alternatives to TFAA and less reactive transmetallating reagents have to be found for decarbonylative trifluoromethylation.

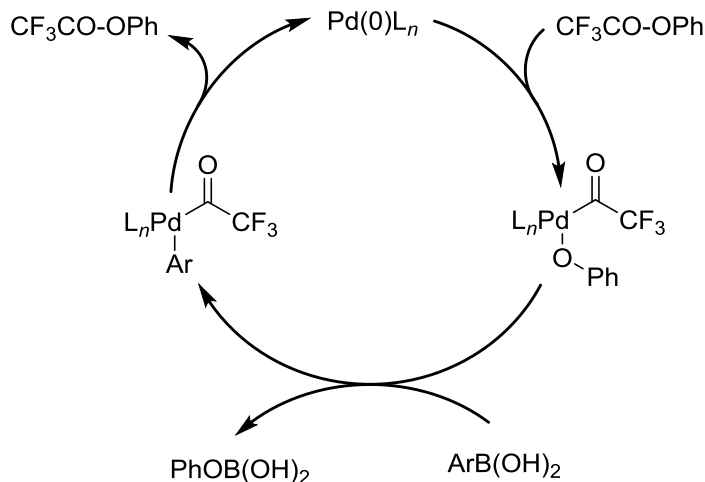
Second, the relative rates of all elementary steps in the catalytic cycle have to be considered. To obtain the desired trifluoromethylated product it is essential that CO

deinsertion is faster than transmetalation. There is an example in the literature of palladium catalyzed trifluoroacetylation of boronic acids (Scheme 5.1).² A viable catalytic cycle was proposed for this reaction (Scheme 5.2). This catalytic cycle differs from the one of decarbonylative trifluoromethylation only by fast transmetalation relative to decarbonylation.

Scheme 5.1 Palladium catalyzed trifluoroacetylation



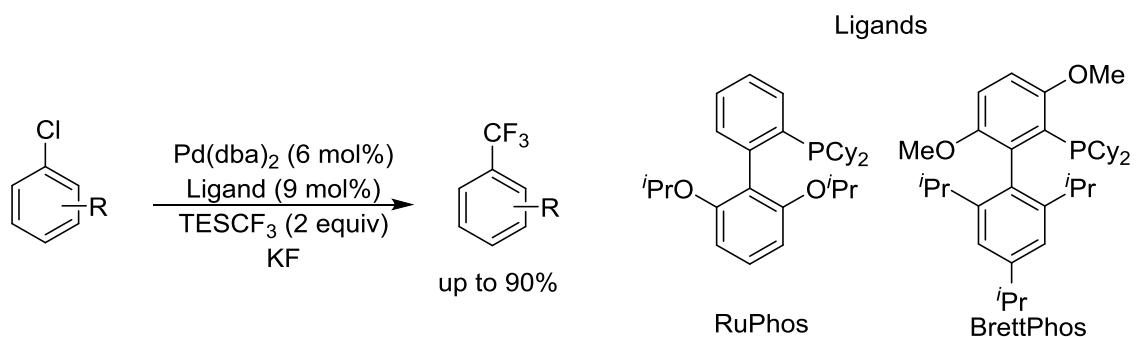
Scheme 5.2 Mechanism of palladium catalyzed trifluoroacetylation



Thirdly, C–CF₃ bond forming reductive elimination from palladium and nickel has extremely high activation barrier.³ While PPh₃ and P(*o*-Tol)₃ are suitable ligands for oxidative addition and decarbonylation, these ligands will likely inhibit reductive

elimination.³ Therefore, for the development of decarbonylative trifluoromethylation methodology, single supporting ligand has to be selected enabling all elementary steps of the catalytic turnover. Several ligands have been reported in the literature to promote C–CF₃ bond forming reductive elimination. For example, heating of [XantphosPd(CF₃)(C₆H₅)] to 80 °C affords trifluorotoluene in essentially quantitative yield.⁴ Furthermore, in 2010, the palladium-catalyzed synthesis of trifluoromethylated compounds via a classical cross-coupling catalytic manifold was reported by Buchwald and coworkers (Scheme 5.3).⁵ The biarylmonophosphines BrettPhos and RuPhos were shown to be the most effective ligands for this methodology. BrettPhos was also demonstrated to promote C–CF₃ bond forming reductive elimination from well defined Pd^{II} model complexes.

Scheme 5.3 Trifluoromethylation developed by Buchwald and coworkers



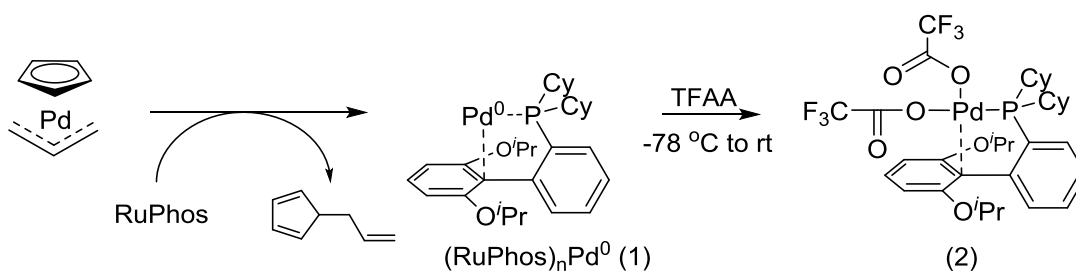
In order to address these issues and select appropriate reagents and reaction conditions for the proposed trifluoromethylation sequence, we sought to assess the feasibility of each elementary step in the proposed catalytic cycle with RuPhos supporting ligand. Based on results presented in the previous chapter we envisaged that biarylmonophosphine ligand such as RuPhos is also likely to promote not only reductive

elimination but also CO deinsertion at Pd^{II} under reasonable reaction conditions. Specifically, sterically bulky biarylmonophosphines (*e.g.*, RuPhos or XPhos) often act as bidentate ligands with the aromatic ring of the biaryl functionality serving as the second binding site.⁶ Such binding of Pd^{II} to the aromatic ring is weak and thus coordinatively unsaturated tricoordinate Pd^{II} species are readily accessible. We hypothesized that bulky biarylmonophosphines such as RuPhos would enable CO deinsertion at Pd^{II} via tetracoordinate transition state according to the mechanism depicted in Scheme 4.14.^{7,8}

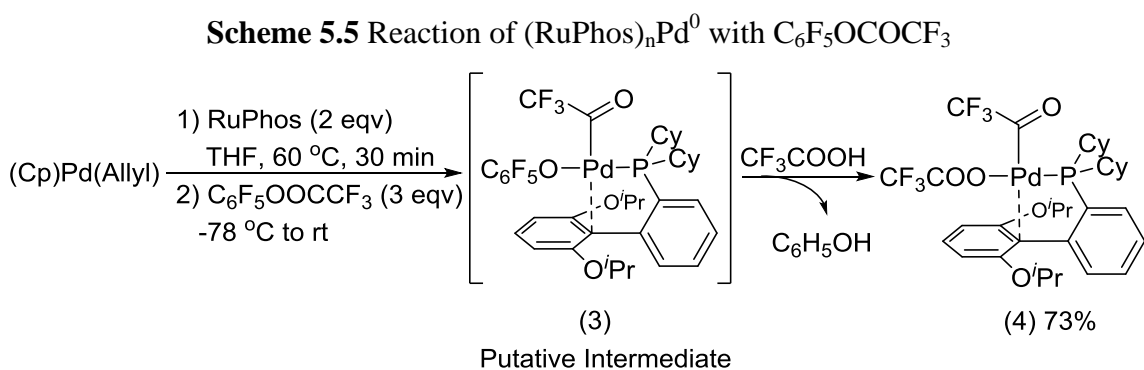
5.2 Oxidative Addition of TFA Esters to (RuPhos)_nPd⁰

A RuPhos-ligated Pd⁰ species was generated by treatment of (Cp)Pd(allyl) with 2 equiv of RuPhos at 60 °C for 30 min (Scheme 5.4).⁹ Then, the *in situ* formed (RuPhos)_nPd⁰ (**1**) was reacted with slight excess of TFAA and TFA esters.¹⁰ Reaction progress was monitored by ¹⁹F-NMR and ¹⁹F/¹³C HMBC NMR spectroscopy. Use of TFAA resulted in the formation of trifluoroacetate complex **2** (Scheme 5.4). *tert*-Butyl- and phenyl- trifluoroacetate showed no reactivity with (RuPhos)Pd⁰ at rt or 60 °C. Use of methyl- and ethyl- trifluoroacetate resulted in the formation of mixture of products. Such an outcome can be rationalized with β-hydride elimination from the alkoxide.

Scheme 5.4 Reaction of (RuPhos)_nPd⁰ with TFAA



Fortunately, when pentafluorophenyl trifluoroacetate was used, NMR showed formation of the oxidative addition product **3** within 30 min at rt (Scheme 5.5). Upon workup, **3** undergoes ligand exchange with trifluoroacetate (presumably generated by hydrolysis of the excess ester) to yield **4** as the product in 73% isolated yield. Such an outcome was not unexpected since Pd(PPh₃)₄ and Pd[P(*o*-Tol)]₃₂ exhibited similar reactivity with C₆F₅OCOCF₃ (Scheme 4.11 and Scheme 4.15).

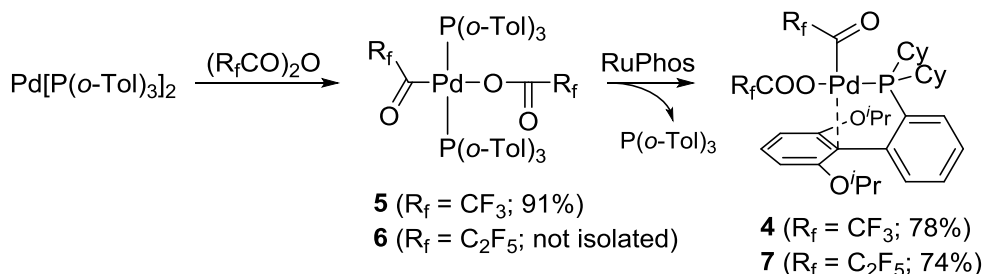


The structure of **4** was determined by 1D ¹³C-, ³¹P- and ¹⁹F-NMR as well as 2D heteronuclear correlation NMR experiments and HRMS. In particular, C–F and C–P couplings observed in the ¹³C-NMR spectrum of **4** provide strong evidence in support of the assigned structure. For example, signals of the trifluoroacetyl ligand are observed as quartet of doublets at 207.5 ppm (²J_(C-F) = 38.2 Hz and ³J_(C-P) = 7.5 Hz) and quartet of doublets at 110.0 ppm (¹J_(C-F) = 300.4 Hz and ³J_(C-P) = 17.0 Hz). In contrast, signals of the trifluoroacetate ligand are observed as quartet at 160.7 ppm (²J_(C-F) = 34.7 Hz) and quartet of doublets at 117.4 ppm (¹J_(C-F) = 292.2 Hz, ⁴J_(C-P) = 7.5 Hz). This assignment is confirmed by 2D ¹⁹F/¹³C HSQC and HMBC NMR experiments.

In addition, the ^{13}C NMR spectrum of **4** shows a doublet at 106 ppm ($J_{\text{C-P}} = 4.1$ Hz) corresponding to a carbon atom bound to Pd as shown in in Scheme 5.5. Such chemical shift and splitting is consistent with coordination of RuPhos through both phosphorous and the carbon atoms. Similar bidentate binding of biarylmonophosphines has been reported previously.¹¹

The structure of **4** was confirmed also by independent synthesis through an alternative route (Scheme 5.6). Previously synthesized **5** (Scheme 4.15) underwent fast ligand exchange with 1.1 equiv of RuPhos to afford **4** in 78% isolated yield. The approach shown in Scheme 5.6 could also be used to prepare the perfluoroethyl complex **7** starting from $\text{Pd}[\text{P}(o\text{-Tol})_3]_2$ and pentafluoropropionic anhydride.

Scheme 5.6 Synthesis of $(\text{RuPhos})\text{Pd}(\text{COR}_f)(\text{OCOR}_f)$ via ligand exchange



5.3 Decarbonylative Decomposition of $(\text{RuPhos})\text{Pd}(\text{COR}_f)(\text{OCOR}_f)$

We next investigated CO deinsertion reactions of the perfluoroacyl complexes **4** and **7** (Scheme 5.7). We were pleased to find that heating benzene solutions of **4** and **7** to reflux for 1.5 h resulted in clean conversion to the corresponding perfluoroalkyl complexes **8** and **9**. The reactions were quantitative by ^{19}F and ^{31}P NMR spectroscopy,

and pure products could be isolated via crystallization in 78% and 62% yield, respectively.

Scheme 5.7 Preparation of (RuPhos)Pd(R_f)(OCOR_f) complexes

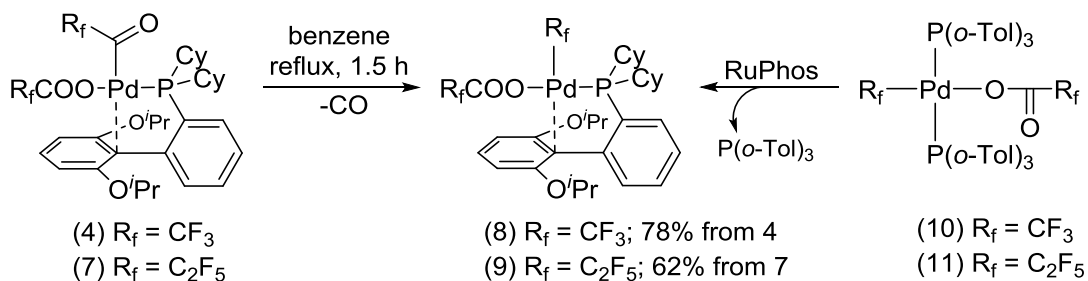
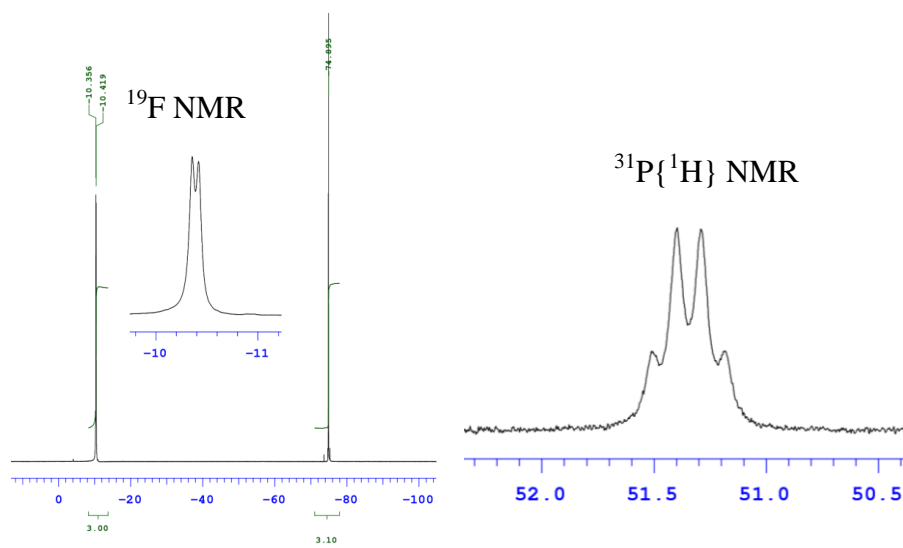


Figure 5.1 ¹⁹F- and ³¹P{¹H}-NMR spectra of RuPhosPd(CF₃)(OCOCF₃)



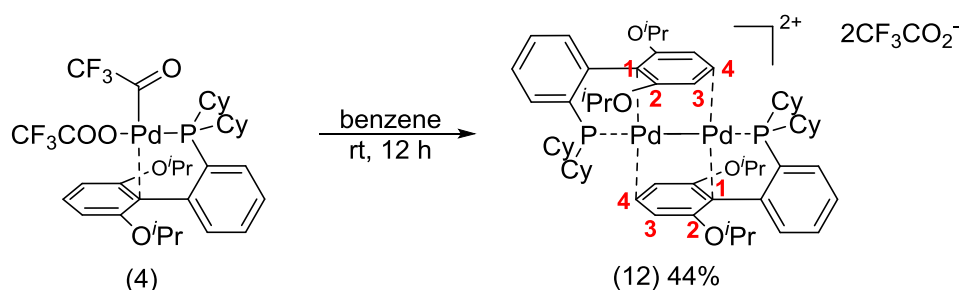
(spectra acquired at 500 MHz)

The identity of **8** and **9** was confirmed through independent synthesis. Treatment of previously synthesized complexes **10** and **11** with slight excess of RuPhos for 5 min at rt resulted in quantitative formation of **8** and **9**, correspondingly (Scheme 5.7). **8** and **9** were characterized by NMR, IR and HRMS. ³J_{P-F} coupling (~30 Hz) observed both in

^{19}F - and $^{31}\text{P}\{^1\text{H}\}$ -NMR spectra corroborates the assigned structures of **8** and **9** (Figure 5.1).

Interestingly, when benzene solutions of **4** are allowed to stand at room temperature completely different reactivity is observed (Scheme 5.8). Under these conditions, **4** slowly decomposes to form the dicationic dipalladium(I) complex **12**, which was isolated in 44% yield after 12 h at room temperature.

Scheme 5.8 Formation of $[(\text{RuPhos})_2\text{Pd}_2](\text{CF}_3\text{COO})_2$

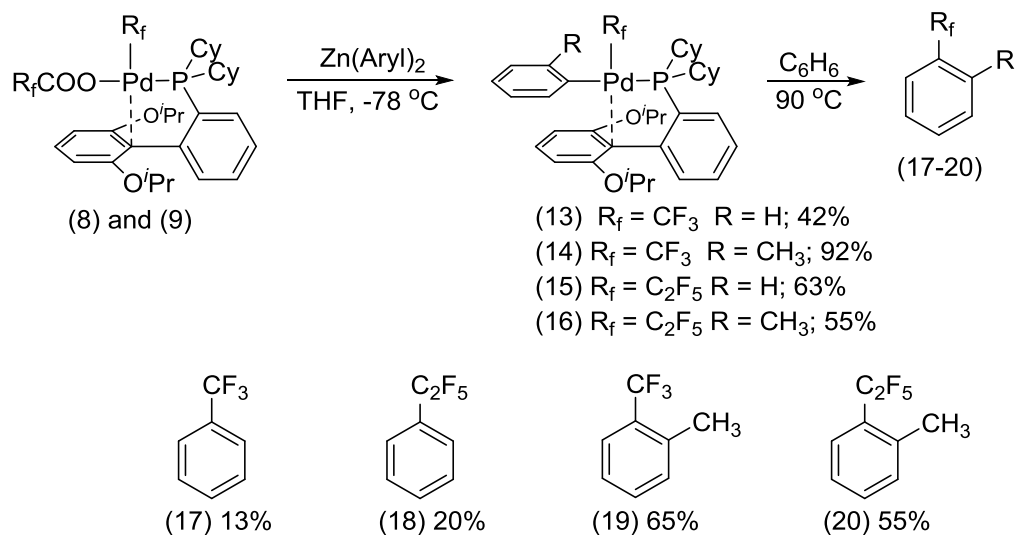


The structure of **12** was determined based on NMR and HRMS analysis. Specifically, **8** is C_{2h} symmetric; therefore, both phosphine ligands are chemically equivalent and only one set of signals is observed in ^{13}C - and ^1H -NMR spectra. However, virtual coupling is detected in the ^{13}C NMR spectrum, which is a very characteristic feature of symmetric trans-diphosphine complexes.¹² In addition, in the ^{13}C NMR spectrum signals of the carbon atoms C1-C4 are shifted to 94.1, 151.4, 86.7 and 80.5 ppm, correspondingly (see Scheme 5.8 for labeling). Such chemical shifts present strong evidence that aromaticity in the benzene rings is partially lost due to π -coordination to the dicationic Pd-Pd unit. Moreover, a molecular ion isotope pattern between 571-575 Da with 0.5 Da spacing in the HRMS of **12** is indicative of a species with molecular formula

$[(\text{RuPhos})_2\text{Pd}_2]^{2+}$.¹³ A preliminary X-ray diffraction analysis further confirmed the connectivity of **12**; however, the low quality of crystals precluded obtaining a high resolution structure. While the exact mechanism for the formation of **12** is unclear, it likely involves comproportionation between $(\text{RuPhos})\text{Pd}^0$ and a $(\text{RuPhos})\text{Pd}^{2+}$ species.¹⁴ A number of related dinuclear $\text{Pd}^{\text{I}}\text{-Pd}^{\text{I}}$ complexes stabilized by π -coordination to arenes have been reported in the literature.¹⁵

5.4 Transmetalation and Reductive Elimination

Scheme 5.9 Transmetalation and reductive elimination reactions



We next investigated transmetalation reactions of the $(\text{RuPhos})\text{Pd}(\text{R}_f)(\text{OCOR}_f)$ complexes **8** and **9** (Scheme 5.9). We found that diarylzincs are particularly effective transmetalating reagents for this system. Specifically, the reaction of **8** and **9** with diphenylzinc and diorthotolylzinc afforded complexes **13-16** in 42-92% isolated yields. It is essential to use salt-free zinc reagents in this reaction. Use of diarylzincs containing

LiCl led to a formation of complex mixture of products. ^{19}F and ^{31}P NMR analysis of the crude reaction mixtures of **13-16** showed no side products; thus the variation in isolated yield simply reflects loss of product during the isolation process. The structures of **13-16** were determined using 1D ^1H -, ^{13}C -, ^{31}P - and ^{19}F -NMR as well as by 2D $^{19}\text{F}/^{13}\text{C}$ and $^1\text{H}/^{13}\text{C}$ NMR correlation experiments. The stereochemistry of **13-16** was assigned based on $^1\text{H}/^1\text{H}$ ROESY NMR spectra.

With **13-16** in hand we next set to investigate aryl- CF_3 bond-forming reductive elimination (Scheme 5.9). We found that complexes **13-16** are stable in both CDCl_3 and benzene solution at room temperature for at least 10 h. However, heating benzene solutions of **13-16** at $90\text{ }^\circ\text{C}$ for 12 h resulted in reductive elimination to yield **17-20**. The yields of **17-20** were determined using ^{19}F -NMR spectroscopy with 1,4-di(trifluoromethyl)benzene as an internal standard. In all cases, complete conversion of the starting complexes **13-16** was observed. Compounds **17** and **18** were obtained in only 13% and 20% NMR yields respectively. However, the 2-tolylpalladium complexes **15** and **16** afforded reductive elimination products **19** and **20** in more respectable 65% and 55% yields. These results are consistent with Buchwald's prior report of the trifluoromethylation of aryl chlorides with TESCF_3 .⁴ In this system, RuPhos provided modest yields with simple aryl chlorides; however, a dramatic enhancement in yield was observed with sterically hindered aryl chlorides. Interestingly, in our system the conversion rate for for all of the complexes **13-16** is approximately the same. This suggests that additional steric bulk on the aryl ligand does not significantly increase the rate of reductive elimination but more likely prevents unproductive decomposition pathways.

5.5 Conclusions

Each step of the proposed catalytic cycle has been interrogated using RuPhos as supporting ligand. It was found that pentafluorophenyltrifluoroacetate undergoes oxidative addition to $(\text{RuPhos})_n\text{Pd}^0$ under mild conditions. The resulting product $(\text{RuPhos})\text{Pd}(\text{COCF}_3)(\text{CO}_2\text{CF}_3)$ eliminates CO in refluxing benzene 80 °C to afford $(\text{RuPhos})\text{Pd}(\text{CF}_3)(\text{CO}_2\text{CF}_3)$. Next, transmetalation with diarylzinc reagents yields $(\text{RuPhos})\text{Pd}(\text{CF}_3)(\text{Aryl})$. Finally, heating of $(\text{RuPhos})\text{Pd}(\text{CF}_3)(\text{Aryl})$ complexes to 90 °C for 12 h affords Aryl- CF_3 reductive elimination products. These results demonstrate the potential feasibility of using perfluoroalkyl esters as CF_3 sources in cross-coupling reactions. The current challenge is to integrate these elementary steps into a complete catalytic cycle for arene fluoroalkylation. Key to this enterprise is identifying perfluoroalkyl ester and transmetalating reagents that are compatible with one another. In addition, the relative rates of CO deinsertion, transmetalation, and reductive elimination must be controlled such that the desired aryl- R_F bond-formation outcompetes undesired aryl- COR_F coupling.

5.6 Experimental Section

General Procedures. All syntheses were conducted under nitrogen unless otherwise stated. All reagents were purchased from commercial sources and used as received. $\text{Pd}[\text{P}(o\text{-Tol})_3]_2$ was obtained according to literature procedure.¹⁶ Tetrahydrofuran, dichloromethane and diethyl ether were purified using an Innovative Technologies (IT) solvent purification system consisting of a copper catalyst, activated

alumina, and molecular sieves. NMR spectra were acquired using 400, 500 and 700 MHz Varian spectrometers. All $^1\text{H}/^1\text{H}$ NOESY and $^1\text{H}/^1\text{H}$ ROESY correlation spectra were acquired on a 500 MHz instrument. ^1H , ^{19}F and ^{13}C chemical shifts are reported in parts per million (ppm) relative to TMS, with the residual solvent peak used as an internal reference. ^1H and ^{19}F multiplicities are reported as follows: singlet (s), doublet (d), triplet (t), quartet (q), broad resonance (br) and multiplet (m). Overlapping signals in ^1H -NMR spectra were also reported as (m).

Preparation of (RuPhos)Pd(COCF₃)(OCOCF₃) (4). Method 1: oxidative addition of $\text{CF}_3\text{COOC}_6\text{F}_5$ to *in situ* generated $(\text{RuPhos})_n\text{Pd}^0$. $\text{CpPd}(\text{allyl})$ (200 mg; 0.94 mmol) and RuPhos (933 mg; 2.00 mmol) were sealed in a Schlenk flask. The Schlenk flask was flushed with nitrogen for 15 minutes and then degassed THF (20 mL) was added via cannula. Resulting red solution was heated to 60 °C for 30 minutes. Solution was cooled to -78 °C and $\text{CF}_3\text{COOC}_6\text{F}_5$ (840 mg; 3.00 mmol) was added dropwise over the period of 5 minutes. Reaction mixture was slowly warmed to rt. After being stirred at rt for 1h, reaction mixture was concentrated under reduced pressure at rt. Residue was dissolved in 100 mL of isopropylether and the solution was filtered through celite. 60 mL of hexanes were added to the isopropylether solution and the resulting mixture was left at -20 °C for 8 hours. During this period product separated in a form of yellowish crystals. Product was collected by filtration and it was washed with two 5 mL portions of cold isopropylether. After drying in vacuum 541 mg (73%) of yellowish crystalline solid was obtained. **Method 2:** ligand exchange reaction of $\text{P}(o\text{-Tol})_3)_2\text{Pd}(\text{COCF}_3)(\text{OCOCF}_3)$ with RuPhos. Under nitrogen atmosphere solution of $\text{P}(o\text{-Tol})_3)_2\text{Pd}(\text{COCF}_3)(\text{OCOCF}_3)\cdot\text{Et}_2\text{O}$ (1.00 g, 1.00 mmol) and RuPhos (513 mg; 1.1 mmol) in THF (20 mL) were stirred at 0

$^{\circ}\text{C}$ for 10 minutes. The solution was then concentrated under reduced pressure at 0°C . Diethylether (10 mL) was added to the residue and resulting suspension was stirred at 0°C for 15 minutes. Product was separated by filtration and then washed with two 5 mL portions of cold ether. After drying in vacuum 615 mg (78%) of yellowish crystalline solid was obtained. ^1H NMR (acetone- d_6 at 25°C): δ 7.87 (apparent triplet, $J = 7.7$ Hz, 1H), 7.56 (t, $J = 7.5$ Hz, 1H), 7.53-7.48 (m, 2H), 6.85 (dd, $J = 7.9$ and 3.2 Hz, 1H), 6.59 (d, $J = 8.6$ Hz, 2H), 4.64 (septet, $J = 6.1$ Hz, 2H), 2.40 (m, 2H), 2.24 (m, 2H), 1.90 (m, 2H), 1.83 (m, 4H), 1.73 (m, 2H), 1.57 (m, 2H), 1.44 (m, 2H), 1.40 (d, $J = 6.1$ Hz, 6H), 1.36 (m, 2H), 1.16 (m, 2H), 1.04 (m, 2H), 1.02 (d, $J = 6.1$ Hz, 6H). $^{13}\text{C}\{^1\text{H}\}$ NMR (acetone- d_6 at 25°C): δ 207.53 (qd, $^2J_{(\text{C-F})} = 38.2$ Hz, $^3J_{(\text{C-P})} = 7.5$ Hz), 161.99, 160.65 (q, $^2J_{(\text{C-F})} = 34.7$ Hz), 145.61 (d, $J = 17.7$ Hz), 138.25, 133.92 (d, $J = 45.0$ Hz), 132.76-132.40 (three overlapping signals as revealed by $^1\text{H}/^{13}\text{C}$ HMBC), 127.82 (d, $J = 6.1$ Hz), 117.37 (qd, $^1J_{(\text{C-F})} = 292.2$ Hz, $^4J_{(\text{C-P})} = 7.5$ Hz), 109.99 (qd, $^1J_{(\text{C-F})} = 300.4$ Hz, $^3J_{(\text{C-P})} = 17.0$ Hz), 106.12 (d, $^2J_{(\text{C-P})} = 4.1$ Hz), 106.05, 71.83, 33.31 (d, $J = 29.3$ Hz), 29.56 (d, $J = 2.1$ Hz), 29.05 (d, $J = 1.3$ Hz), 27.27 (d, $J = 14.3$ Hz), 27.09 (d, $J = 11.6$ Hz), 26.76, 22.08, 21.92. ^{19}F NMR (acetone- d_6 at 25°C): δ -74.32 (s, 3F), -75.03 (s, 3F). $^{31}\text{P}\{^1\text{H}\}$ NMR (acetone- d_6 at 25°C): δ 45.45 (s). $^{19}\text{F}/^{13}\text{C}$ HSQC NMR (acetone- d_6 at 25°C): $\delta_{\text{F}}/\delta_{\text{C}}$ -74.32/109.99, -75.03/117.37. $^{19}\text{F}/^{13}\text{C}$ HMBC NMR (acetone- d_6 at 25°C): $\delta_{\text{F}}/\delta_{\text{C}}$ -74.32/207.53, -75.03/117.37 (1J correlation), -75.03/160.65. IR (ATR): cm^{-1} 2978 (w), 2937 (m), 2853 (m), 1747 (m), 1702 (s), 1686 (s), 1588 (m), 1450 (m), 1410 (m), 1377 (w), 1256 (s), 1224 (s), 1190 (s), 1178 (s), 1128 (s), 1108 (s). HRMS electrospray (m/z): $[\text{M} - \text{OOCFF}_3]^+$ calcd for $\text{C}_{32}\text{H}_{43}\text{F}_3\text{O}_3\text{PPd}$, 669.1931 Found, 669.1947, $[\text{M} - \text{OOCFF}_3 - \text{CO}]^+$ calcd for $\text{C}_{31}\text{H}_{43}\text{F}_3\text{O}_2\text{PPd}$, 641.1982; Found, 641.2001.

Preparation of (RuPhos)Pd(COC₂F₅)(OOC₂CF₅) (7). A Schlenk flask was charged with a stirbar and Pd[P(*o*-Tol)₃]₂ (1.90 g; 2.66 mmol). The flask was sealed, evacuated under reduced pressure and then refilled with nitrogen. The flask was evacuated and refilled with nitrogen three more times. Dry THF (100 mL) was added via cannula. Perfluoropropionic anhydride (0.66 mL, 3.0 mmol) was then added dropwise over the period of 5 minutes. The resulting solution was stirred at rt for 20 minutes at r.t., then it was filtered through a pad of celite and volatiles were removed under reduced pressure. The residue was redissolved in benzene (35 mL) and RuPhos (700 mg; 1.5 mmol) was added in one portion. The homogenous solution was stirred at rt for 20 minutes and then volatiles were removed under reduced pressure. The residue was dissolved in butylether (30 mL). Product then slowly separated in the form of yellowish crystals. Product was collected by filtration and washed with several portions of butylether and then with hexanes. After drying in vacuum 989 mg (74% based on RuPhos) of product was obtained. NMR (CDCl₃ at 25 °C): δ 7.59 (apparent triplet, *J* = 7.5 Hz, 1H), 7.49 (t, *J* = 8.4 Hz, 1H), 7.43 (t, *J* = 7.5 Hz, 1H), 7.39 (t, *J* = 7.3 Hz, 1H), 6.76 (dd, *J* = 7.5 and 2.2 Hz, 1H), 6.48 (d, *J* = 8.5 Hz, 2H), 4.54 (septet, *J* = 6.0 Hz, 2H), 2.22-2.15 (m, 4H), 1.85-1.76 (m, 6H), 1.72-1.66 (m, 2H), 1.62-1.53 (m, 2H), 1.40-1.31 (m, 2H), 1.36 (d, *J* = 6.0 Hz, 6H), 1.29-1.22 (m, 2H), 1.22-1.12 (m, 4H), 1.00 (d, *J* = 6.0 Hz, 6H). ¹³C{¹H} NMR (CDCl₃ at 25 °C): δ 207.98 (td, ²*J*_(C-F) = 40.2 Hz, ³*J*_(C-P) = 7.0 Hz), 161.37 (t, ²*J*_(C-F) = 25.9 Hz), 161.04, 144.68 (d, *J* = 17.0 Hz), 137.38, 133.07 (d, *J* = 43.6 Hz), 131.78 (d, *J* = 11.6 Hz), 131.47 (d, *J* = 1.7 Hz), 130.94, 126.71 (d, *J* = 6.1 Hz), 121.44-114.17 (two overlapping multiplets, 2 x CF₂), 106.64 (m, CF₃), 105.98, 105.29, 101.53 (tqd, ¹*J*_(C-F) = 269.8 Hz, ²*J*_(C-F) = 36.1 Hz, ³*J*_(C-P) = 14.3 Hz), 71.19, 34.28 (d, *J* =

29.3 Hz), 28.26 (two overlapping signals), 26.75 (two overlapping doublets), 25.85, 21.74, 21.67. ^{19}F NMR (CDCl_3 at 25 °C): δ -80.18 (s, 3F), -82.40 (s, 3F), -112.23 (s, 2F), -118.44 (broad s, 2F). $^{31}\text{P}\{^1\text{H}\}$ NMR (CDCl_3 at 25 °C): δ 42.25 (s). $^{19}\text{F}/^{13}\text{C}$ HSQC NMR (CDCl_3 at 25 °C): $\delta_{\text{F}}/\delta_{\text{C}}$ -80.18/117.33, -82.40/118.70, -112.23/101.53, -118.44/106.64. $^{19}\text{F}/^{13}\text{C}$ HMBC NMR (CDCl_3 at 25 °C): $\delta_{\text{F}}/\delta_{\text{C}}$ -80.18/101.53, -80.18/117.33 (1J correlation), -112.23/101.53 (1J correlation), -112.23/117.33, 112.23/207.98. IR (ATR): cm^{-1} 2978 (w), 2987 (w), 2937 (m), 2855 (w), 1716 (s), 1684 (s), 1588 (m), 1569 (m), 1451 (s), 1384 (m), 1327 (s), 1256 (s), 1202 (s), 1162 (s), 1110 (s), 1069 (s). HRMS electrospray (m/z): $[\text{M} - \text{OOC}_2\text{F}_5]^+$ calcd for $\text{C}_{33}\text{H}_{43}\text{F}_5\text{O}_3\text{PPd}$, 719.1899 Found, 719.1916, $[\text{M} - \text{OOCF}_3 - \text{CO}]^+$ calcd for $\text{C}_{32}\text{H}_{43}\text{F}_5\text{O}_2\text{PPd}$, 691.1950; Found, 691.1969.

Preparation of (RuPhos)Pd(CF₃)(OOCF₃) (8). (RuPhos)Pd(COCF₃)(OCOCF₃) (4) (300 mg; 0.38 mmol) was refluxed in benzene (25 mL) for 1.5 hours. ^{19}F - and ^{31}P -NMR analysis of the crude reaction mixture showed complete conversion to product **8**. The benzene solution was filtered through a pad of celite and volatiles were removed under reduced pressure. The residue was dissolved in diisopropylether (5 mL). The product slowly crystallized over the period of 12 hours. Yellowish crystals were collected by filtration, washed with small amount of diisopropylether and dried under vacuum. 227 mg (78%) of product was obtained. ^1H NMR (CDCl_3 at 25 °C): δ 7.63 (apparent triplet, $J = 7.3$ Hz, 1H), 7.54 (t, $J = 8.5$ Hz), 7.43 (t, $J = 7.3$ Hz), 7.38 (t, $J = 7.3$ Hz), 6.68 (broad doublet, $J = 6.2$ Hz), 6.50 (d, $J = 8.5$ Hz), 4.60 (septet, $J = 6.2$ Hz), 2.26 (m, 2H), 2.16 (m, 2H), 1.90 (m, 2H), 1.80 (m, 4H), 1.68 (m, 2H), 1.58 (m, 2H), 1.41-1.11 (m, 8H), 1.30 (d, $J = 5.8$ Hz, 6H), 0.99 (d, $J = 6.2$ Hz, 6H). $^{13}\text{C}\{^1\text{H}\}$ NMR (CDCl_3 at 25 °C): δ 163.49,

161.25 (q, $J = 34.1$ Hz), 144.85 (d, $J = 16.3$ Hz), 138.82, 134.17 (d, $J = 44.3$ Hz), 131.75 (d, $J = 12.3$ Hz), 131.54 (d, $J = 1.5$ Hz), 131.40, 126.58 (d, $J = 6.1$ Hz), 118.59 (qd, $^1J_{(C-F)} = 379.4$ Hz, $^3J_{(C-P)} = 15.0$ Hz), 116.39 (q, $^1J_{(C-F)} = 290.9$ Hz), 105.73, 102.92, 71.60, 35.93 (d, $J = 27.9$ Hz), 29.28, 29.01, 27.00 (two overlapping doublets), 25.93, 21.96, 21.30. ^{19}F NMR (CDCl_3 at 25°C): δ -10.38 (d, $J = 29.8$ Hz, 3F), -74.90 (s, 3F). $^{31}\text{P}\{^1\text{H}\}$ NMR (CDCl_3 at 25°C): δ 51.35 (q, $J = 29.7$ Hz). $^{19}\text{F}/^{13}\text{C}$ HSQC NMR (CDCl_3 at 25°C): $\delta_{\text{F}}/\delta_{\text{C}}$ - 10.38/118.59, -74.90/116.39. $^{19}\text{F}/^{13}\text{C}$ HMBC NMR (CDCl_3 at 25°C): $\delta_{\text{F}}/\delta_{\text{C}}$ - 74.90/161.33. IR (ATR): cm^{-1} 2978 (w), 2931 (m), 2856 (m), 1698 (s), 1589 (m), 1445 (s), 1405 (m), 1378 (m), 1258 (s), 1193 (s), 1173 (s), 1130 (s), 1108 (s), 1068 (s). HRMS electrospray (m/z): $[\text{M} - \text{OOCF}_3]^+$ calcd for $\text{C}_3\text{H}_4\text{F}_3\text{O}_2\text{PPd}$, 641.1982; Found, 641.1994.

Preparation of (RuPhos)Pd(C₂F₅)(OOC C₂F₅) (9).

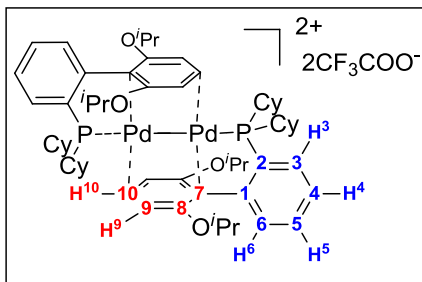
(RuPhos)Pd(COC₂F₅)(OCOC₂F₅) (7) (220 mg; 0.25 mmol) was refluxed in benzene (50 mL) for 1.5 hours. ^{19}F - and ^{31}P -NMR analysis of the crude reaction mixture showed complete conversion to product **9**. The benzene solution was filtered through a pad of celite and volatiles were removed under reduced pressure. The residue was dissolved in diethylether (5 mL). The product slowly crystallized over the period of several hours. Yellowish crystals were collected by filtration, washed with small amounts of ether and dried under vacuum. 133 mg (62%) of **9** was obtained. ^1H NMR (CDCl_3 at 25°C): δ 7.63 (apparent triplet, $J = 7.3$ Hz, 1H), 7.54 (t, $J = 7.5$ Hz), 7.42 (t, $J = 7.7$ Hz), 7.37 (t, $J = 7.7$ Hz), 6.69 (broad doublet, $J = 7.3$ Hz), 6.46 (d, $J = 8.5$ Hz), 4.55 (septet, $J = 6.2$ Hz), 2.29 (m, 2H), 2.22 (m, 2H), 1.91 (m, 2H), 1.81 (m, 4H), 1.69 (m, 2H), 1.61 (m, 2H), 1.38-1.22 (m, 6H), 1.34 (d, $J = 5.8$ Hz, 6H), 1.18 (m, 2H), 1.00 (d, $J = 6.2$ Hz, 6H). $^{13}\text{C}\{^1\text{H}\}$ NMR

(CDCl₃ at 25 °C): δ 163.45, 161.63 (t, $J = 22.5$ Hz), 144.78 (d, $J = 16.4$ Hz), 139.14, 133.86 (d, $J = 44.3$ Hz), 131.90 (d, $J = 11.6$ Hz), 131.41 (d, $J = 1.4$ Hz), 131.30, 126.54 (d, $J = 6.1$ Hz), 121.53-115.68 (three overlapping multiplets CF₂, CF₃ and CF₃), 106.69 (tqd, $^1J_{(C-F)} = 263.0$ Hz, $^2J_{(C-F)} = 37.5$ Hz, $^3J_{(C-P)} = 6.8$ Hz), 105.61, 103.01, 71.60, 36.14 (d, $J = 26.6$ Hz), 29.32, 28.92 (d, $J = 3.4$ Hz), 27.22-26.96 (two overlapping doublets), 25.96, 21.73, 21.48. ¹⁹F NMR (CDCl₃ at 25 °C): δ -76.10 (d, $J = 34.8$ Hz, 2F), -78.98 (s, 3F), -82.58 (s, 3F), -119.10 (s, 3F). ³¹P{¹H} NMR (CDCl₃ at 25 °C): δ 49.11 (t, $J = 33.9$ Hz). ¹⁹F/¹³C HSQC NMR (CDCl₃ at 25 °C): δ_F/δ_C -76.10/118.35, -78.98/118.46, -82.58/118.75, -119.10/106.64. ¹⁹F/¹³C HMBC NMR (CDCl₃ at 25 °C): δ_F/δ_C -76.10/118.35 (1J correlation), -76.10/118.46, -78.98/118.35, -78.98/118.46 (1J correlation), -82.58/106.64, -82.58/118.75 (1J correlation), -119.10/106.64 (1J correlation), 119.10/118.75, 119.10/161.61. IR (ATR): cm⁻¹ 2987 (w), 2938 (m), 2922 (m), 2859 (m), 1692 (s), 1588 (s), 1570 (m), 1447 (s), 1386 (s), 1333 (s), 1287 (m), 1255 (s), 1206 (s), 1161 (s), 1108 (s), 1061 (s), 1026 (s). HRMS electrospray (m/z): [M – OOCF₃]⁺ calcd for C₃₂H₄₃F₅O₂PPd, 691.1950; Found, 691.1962.

Preparation of [(RuPhos)₂Pd₂](CF₃COO)₂ (12). A solution of (RuPhos)Pd(COCF₃)(OCOCF₃) (7) (200 mg; 0.26 mmol) in benzene (7 mL) was left unperturbed for 24 hours. During this time the color of the solution changed from yellow to deep red and bright red crystals slowly separated from the solution. The benzene supernatant was decanted and two 2 mL portions of benzene were used to wash the crystals. After drying under vacuum 78 mg (44%) of bright orange powder was obtained. ¹H NMR (acetone-d₆ at 25 °C): δ 8.61 (m, 1H), 8.12 (m, 1H), 7.80 (t, $J = 7.3$ Hz, 1H), 7.75 (t, $J = 7.7$ Hz, 1H), 7.41 (d, $J = 7.7$ Hz, 1H), 5.60 (d, $J = 7.0$ Hz, 2H), 4.39 (septet, J

= 6.1 Hz), 3.26 (m, 2H), 2.19-2.09 (m, 4H), 1.83 (m, 4H), 1.74 (m, 2H), 1.59 (m, 2H), 1.51 (m, 2H), 1.46-1.35 (m, 4H), 1.23 (m, 2H), 0.95 (d, $J = 6.1$ Hz, 6H), 0.81 (d, $J = 6.0$ Hz, 6H). $^{13}\text{C}\{^1\text{H}\}$ NMR (acetone- d_6 at 25 °C): δ 159.03 (q, $J = 36.7$ Hz), 151.39, 144.54 (virtual triplet, $J = 27.2$ Hz), 138.27 (virtual triplet, $J = 42.2$ Hz), 133.31, 132.90, 131.41 (virtual triplet, $J_{\text{C-P}} = 16.4$ Hz), 129.37 (virtual triplet, $J_{\text{C-P}} = 6.2$ Hz), 116.42 (q, $J = 290.9$ Hz), 94.08, 86.69, 80.45, 73.30, 36.18 (virtual triplet, $J = 20.6$ Hz), 29.83, 29.32, 26.17-26.00 (two overlapping triplets), 25.74, 20.58, 19.95. ^{19}F NMR (acetone- d_6 at 25 °C): δ -76.38 (s). $^{31}\text{P}\{^1\text{H}\}$ NMR (acetone- d_6 at 25 °C): δ 61.46 (s). $^{19}\text{F}/^{13}\text{C}$ HSQC NMR (acetone- d_6 at 25 °C): $\delta_{\text{F}}/\delta_{\text{C}}$ -76.38/116.45. $^{19}\text{F}/^{13}\text{C}$ HMBC NMR (acetone- d_6 at 25 °C): $\delta_{\text{F}}/\delta_{\text{C}}$ -76.38/116.45 (1J correlation), -76.38/159.03. HRMS electrospray (m/z): $[\text{M} - \text{OCOCF}_3]^+$ calcd for $\text{C}_{62}\text{H}_{86}\text{F}_3\text{O}_6\text{P}_2\text{Pd}$, 1257.3905; Found, 1257.3921, $[\text{M} - 2\text{OCOCF}_3]^{2+}$ calcd for $[\text{C}_{30}\text{H}_{43}\text{O}_2\text{PPd}]^{2+}$, 572.2030; Found, 572.2049.

NMR Assignment for 12 (based on $^1\text{H}/^1\text{H}$ COSY and $^1\text{H}/^{13}\text{C}$ HSQC and HMBC)



carbon	δ (ppm)	proton	δ (ppm)
C^1	144.54 (virtual triplet, $J_{\text{C-P}} = 27.2$ Hz)		
C^2	138.27 (virtual triplet, $J_{\text{C-P}} = 42.2$ Hz)		
C^3	131.41 (virtual triplet, $J_{\text{C-P}} = 16.4$ Hz)	H^3	8.12 (multiplet)
C^4	129.37 (virtual triplet, $J_{\text{C-P}} = 6.2$ Hz)	H^4	7.75 (t, $J = 7.7$ Hz)
C^5	133.31	H^5	7.80 (t, $J = 7.3$ Hz)
C^6	132.90	H^6	7.41 (d, $J = 7.7$ Hz)
C^7	94.08		
C^8	151.39		
C^9	86.69	H^9	5.60 (d, $J = 7.0$ Hz)
C^{10}	80.45	H^{10}	8.61 (multiplet)

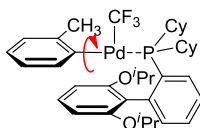
Preparation of (RuPhos)Pd(CF₃)(Ph) (13). A Schlenk flask was charged with a stirbar, diphenylzinc (200 mg; 0.91 mmol) and (RuPhos)Pd(CF₃)(OOCF₃) (**8**) (450 mg; 0.60 mmol). The flask was sealed, evacuated under reduced pressure and then refilled with nitrogen. The flask was evacuated and refilled with nitrogen three more times. Dry THF (20 mL) was added via cannula. The resulting solution was stirred at rt for 20 minutes, then water (0.2 mL) was introduced via septum. Reaction mixture was stirred at rt for additional 20 minutes. Then, the THF solution was dried over anhydrous Na₂SO₄ and filtered. Volatiles were removed under reduced pressure. The residue was dissolved in diisopropyl ether and product slowly crystallized over the period of several hours. Colorless crystals were collected by filtration, washed with small amount of diisopropylether and dried under vacuum. 180 mg (42%) of **13** was obtained. ¹H NMR (CDCl₃ at 25 °C): δ 7.53 (apparent triplet, *J* = 6.9 Hz, 1H), 7.42-7.32 (m, 3H), 7.23 (d, *J* = 7.4 Hz, 2H), 7.18 (broad d, *J* = 4.7 Hz, 1H), 7.02 (d, *J* = 8.3 Hz, 1H), 6.88 (t, *J* = 7.4 Hz, 2H), 6.82 (t, *J* = 7.1 Hz, 1H), 4.52 (septet, *J* = 6.0 Hz, 2H), 1.88-1.78 (m, 2H), 1.76-1.44 (multiple peaks, 12H, Cy protons), 1.32-1.02 (m, 8H, Cy protons), 1.28 (d, *J* = 6.0 Hz, 6H), 0.99 (d, *J* = 6.0 Hz, 6H). ¹³C{¹H} NMR (CDCl₃ at 25 °C): δ 154.11, 145.09 (broad), 141.31 (d, *J* = 13.6 Hz), 140.84 (m, CF₃), 136.54 (d, *J* = 2.0 Hz), 134.73 (d, *J* = 6.8 Hz), 130.73, 129.81, 128.60, 127.20 (d, *J* = 21.8 Hz), 126.56 (d, *J* = 4.1 Hz), 126.09, 123.34, 122.57, 110.93, 74.09, 31.82 (d, *J* = 19.8 Hz), 28.20, 27.28 (d, *J* = 13.0 Hz), 26.87 (d, *J* = 9.5 Hz), 26.67, 25.99, 22.30, 21.18. ¹⁹F NMR (CDCl₃ at 25 °C): δ -27.80 (d, *J* = 44.8 Hz). ³¹P{¹H} NMR (CDCl₃ at 25 °C): δ 14.77 (q, *J* = 45.8 Hz). ¹⁹F/¹³C HSQC NMR (CDCl₃ at 25 °C): δ_F/δ_C -27.80/140.84. ¹⁹F/¹³C HMBC NMR (CDCl₃ at 25 °C):

δ_F/δ_C -27.80/140.84 (1J correlation), -27.80/145.09. IR (ATR): cm^{-1} 3051 (w), 2968 (w), 2928 (s), 2850 (m), 1598 (m), 1579 (w), 1566 (m), 1450 (s), 1374 (m), 1331 (w), 1270 (s), 1224 (m), 1088 (s), 1046 (s). HRMS electrospray (m/z): $[\text{M} - \text{F}]^+$ calcd for $\text{C}_{37}\text{H}_{48}\text{F}_2\text{O}_2\text{PPd}$, 699.2389; Found, 699.2383.

Preparation of (RuPhos)Pd(CF₃)(*o*-C₆H₄CH₃) (14). 2-Iodotoluene (6.00 g; 27.5 mmol) and dry diethyl ether (120 mL) were introduced into a flame-dried 250 mL Schlenk flask. The ether solution was cooled to -78 °C and 2.5 M solution of *n*BuLi in hexanes (11.5 mL; 28 mmol) was added dropwise. The resulting suspension was stirred at -78 °C for 30 minutes. Then 1.9 M ZnCl₂ solution in 2-methyltetrahydrofuran (7.2 mL; 13.7 mmol) was added slowly over the period of 10 minutes (at -78 °C). Reaction mixture was warmed to rt and stirred at rt for 30 minutes. Volatiles were removed via the sidearm of the Schlenk flask and the residue was washed with several portions of dry pentane. Dry toluene (25 mL) was added to the residue and resulting suspension was cannula-transferred to a septum-sealed centrifuge tube. LiCl precipitate was separated by centrifugation and remaining clear toluene solution of Zn(*o*-C₆H₄CH₃)₂ reagent was used directly in the step below. It was assumed that the concentration of the Zn(*o*-C₆H₄CH₃)₂ reagent in toluene is 0.5 M.

A Schlenk flask was charged with a stirbar and (RuPhos)Pd(CF₃)(OOCCF₃) (**9**) (400 mg; 0.50 mmol). The flask was sealed, evacuated under reduced pressure and then refilled with nitrogen. The flask was evacuated and refilled with nitrogen three more times. Dry THF (20 mL) was added via cannula. The resulting solution was cooled to -78 °C and then Zn(*o*-C₆H₄CH₃)₂ solution in toluene (1.2 mL; approximately 0.6 mmol) was added dropwise. Reaction mixture was stirred at rt for 20 minutes, then water (0.2 mL)

was introduced via septum. Reaction was stirred at rt for additional 20 minutes. Then the THF solution was dried over anhydrous Na_2SO_4 and filtered. Volatiles were removed under reduced pressure. Residue was dissolved in acetone (1.5 mL) and product slowly crystallized over the period of several hours. Crystals were collected by filtration, washed with a small amount of acetone and dried under vacuum. 230 mg (63%) of colorless crystals was obtained.



Analytical data for 14. Rotation about Pd-(*o*-Tol) bond is hindered on the NMR timescale at 25 °C. Therefore several signals in ^1H - and ^{13}C -NMR spectra are broadened at 25 °C. VT ^1H -NMR experiments revealed that at -40 °C rotation about Pd-(*o*-Tol) is slow on the ^1H -NMR timescale (RuPhos fragment loses the plane of symmetry in the ^1H -NMR spectrum). ^1H NMR (CDCl_3 at 25 °C): δ 7.50 (apparent triplet, $J = 6.6$ Hz, 1H), 7.39-7.33 (m, 3H), 7.17 (d, $J = 7.5$ Hz, 1H), 7.14 (br, 1H), 7.00 (br, 2H), 6.81 (dd, $J = 8.3, 1.0$ Hz, 1H), 6.77 (t, $J = 7.0$ Hz, 1H), 6.71 (t, $J = 7.7$ Hz, 1H), 4.59-4.50 (two overlapping septets, 2H), 2.47 (s, 3H), 1.99-0.63 (overlapping broad resonances, 22H, Cy protons), 1.31 (d, $J = 6.0$ Hz, 3H), 1.27 (broad d, $J = 5.5$ Hz, 3H), 1.01 (broad d, $J = 4.6$ Hz, 3H), 0.97 (d, $J = 6.1$ Hz, 3H). $^{13}\text{C}\{^1\text{H}\}$ NMR (CDCl_3 at 25 °C): δ 154.40, 154.33, 146.47 (broad), 141.65 (d, $J = 12.9$ Hz), 141.35, 140.35 (m, CF_3), 135.84, 134.58 (broad), 130.91 (broad), 129.93 (broad), 128.61 (broad), 127.88 (broad d, $J = 19.1$ Hz), 127.42, 126.48 (d, $J = 4.1$ Hz), 123.14 (broad), 122.92 (broad), 122.58, 110.83, 110.72, 73.98 (broad), 73.74 (broad), 32.55 (two overlapping broad resonances, Cy signals), 28.61-25.59 (overlapping broad resonances, Cy signals), 27.47, 27.40, 26.19, 22.34, 22.27, 21.24 (two overlapping broad resonances). ^{19}F NMR (CDCl_3 at 25 °C): δ -27.74 (d, $J = 53.6$ Hz). $^{31}\text{P}\{^1\text{H}\}$ NMR (CDCl_3 at 25 °C): δ 13.79 (q,

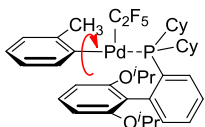
$J = 45.8$ Hz). $^{19}\text{F}/^{13}\text{C}$ HSQC NMR (CDCl_3 at 25°C): $\delta_{\text{F}}/\delta_{\text{C}}$ -27.74/140.19. $^{19}\text{F}/^{13}\text{C}$ HMBC NMR (CDCl_3 at 25°C): $\delta_{\text{F}}/\delta_{\text{C}}$ -27.74/140.19 (1J correlation), -27.74/146.47. IR (ATR): cm^{-1} 3064 (w), 2918 (s), 2850 (m), 2361 (w), 2338 (w), 2162 (w), 1599 (m), 1578 (m), 1453 (s), 1384 (m), 1373 (m), 1269 (m), 1225 (m), 1105 (m), 1084 (s), 1040 (s), 978 (s). HRMS electrospray (m/z): $[\text{M} - \text{F}]^+$ calcd for $\text{C}_{39}\text{H}_{50}\text{F}_4\text{O}_2\text{PPd}$, 763.2519; Found, 763.2514, $[\text{M} - o\text{-C}_6\text{H}_4\text{CH}_3]^+$ calcd for $\text{C}_{32}\text{H}_{43}\text{F}_5\text{O}_2\text{PPd}$, 691.1956; Found, 691.1929.

Preparation of (RuPhos)Pd(C₂F₅)(Ph) (15). A Schlenk flask was charged with a stirbar, diphenylzinc (180 mg; 0.82 mmol) and (RuPhos)Pd(C₂F₅)(OCCF₃) (7) (500 mg; 0.58 mmol). The flask was sealed, evacuated under reduced pressure and then refilled with nitrogen. The flask was evacuated and refilled with nitrogen three more times. Dry THF (20 mL) was added via cannula. The resulting solution was stirred at rt for 20 minutes, then water (0.2 mL) was introduced via septum. Reaction mixture was stirred at rt for additional 20 minutes. Then, the THF solution was dried over anhydrous Na_2SO_4 and filtered. Volatiles were removed under reduced pressure. Residue was dissolved in diethyl ether and product slowly crystallized over the period of several hours. Colorless crystals were collected by filtration, washed with a small amount of diethyl ether and dried under vacuum. 413 mg (92%) of **15** was obtained. ^1H NMR (CDCl_3 at 25°C): δ 7.52 (apparent triplet, $J = 6.7$ Hz, 1H), 7.41-7.36 (m, 2H), 7.34 (t, $J = 7.1$ Hz, 1H), 7.18 (ddd, $J = 7.5, 3.2, 1.2$ Hz, 2H), 7.11 (d, $J = 7.5$ Hz, 1H), 7.02 (d, $J = 8.3$ Hz, 1H), 6.81 (t, $J = 6.7$ Hz, 2H), 6.78 (t, $J = 7.2$ Hz, 1H), 4.50 (septet, $J = 6.1$ Hz, 2H), 1.81-1.73 (m, 2H), 1.73-1.67 (m, 2H), 1.63-1.56 (m, 6H, Cy protons), 1.50-1.40 (m, 2H), 1.34-1.27 (m, 2H), 1.25 (d, $J = 6.1$ Hz, 6H), 1.18-1.09 (m, 4H), 1.08-1.00 (m, 2H), 0.98 (d, $J = 6.0$ Hz, 6H). $^{13}\text{C}\{^1\text{H}\}$ NMR (CDCl_3 at 25°C): δ 153.98, 143.41 (broad), 141.34

(d, $J = 14.3$ Hz), 136.63 (d, $J = 2.7$ Hz), 134.69 (d, $J = 7.5$ Hz), 133.08 (m, CF₂), 130.80, 129.40, 128.55, 127.37 (d, $J = 21.8$ Hz), 126.49 (d, $J = 4.8$ Hz), 125.94, 123.69, 122.40, 122.26 (qtd, $^1J_{(C-F)} = 286.1$ Hz, $^2J_{(C-F)} = 31.3$ Hz, $^3J_{(C-P)} = 8.2$ Hz), 111.10, 74.05, 32.02 (d, $J = 19.1$ Hz), 28.15, 27.30 (d, $J = 12.3$ Hz), 27.10 (d, $J = 4.1$ Hz), 26.92 (d, $J = 9.5$ Hz), 26.01, 22.28, 21.19. ¹⁹F NMR (CDCl₃ at 25 °C): δ -79.83 (s, 3F), -102.50 (d, $J = 23.2$ Hz, 2F). ³¹P{¹H} NMR (CDCl₃ at 25 °C): δ 13.57 (t, $J = 28.6$ Hz). ¹⁹F/¹³C HSQC NMR (CDCl₃ at 25 °C): δ_F/δ_C -79.83/122.26, -102.50/133.08. ¹⁹F/¹³C HMBC NMR (CDCl₃ at 25 °C): δ_F/δ_C -79.83/122.26 (1J correlation), -79.83/133.08. IR (ATR): cm⁻¹ 3057 (w), 2974 (w), 2929 (m), 2848 (w), 1596 (m), 1564 (m), 1452 (s), 1384 (m), 1292 (m), 1267 (m), 1231 (w), 1187 (m), 1138 (m), 1101 (m), 1039 (s). HRMS electrospray (m/z): [M – F]⁺ calcd for C₃₈H₄₈F₄O₂PPd, 749.2363; Found, 749.2345, [M – Ph]⁺ calcd for C₃₂H₄₃F₅O₂PPd, 691.1956; Found, 691.1938.

Preparation of (RuPhos)Pd(C₂F₅)(*o*-C₆H₄CH₃) (16). A Schlenk flask was charged with a stirbar and (RuPhos)Pd(C₂F₅)(OOCC₂F₅) (**9**) (400 mg; 0.50 mmol). The flask was sealed, evacuated under reduced pressure and then refilled with nitrogen. The flask was evacuated and refilled with nitrogen three more times. Dry THF (20 mL) was added via cannula. The resulting solution was cooled to -78 °C and then Zn(*o*-C₆H₄CH₃)₂ solution in toluene (1.2 mL; approximately 0.6 mmol) was added dropwise. Reaction mixture was stirred at rt for 20 minutes, then water (0.2 mL) was introduced via septum. Reaction was stirred at rt for additional 20 minutes. Then, the THF solution was dried over anhydrous Na₂SO₄ and filtered. Volatiles were removed under reduced pressure. The residue was dissolved in methanol (1.5 mL) and product slowly crystallized over the

period of several hours. Crystals were collected by filtration, washed with small amount of methanol and dried under vacuum. 214 mg (55%) of **16** was obtained.



Analytical data for 16. ^1H -, ^{19}F - and ^{13}C -NMR spectra showed that rotation about Pd-(*o*-Tol) bond is slow on the NMR timescale at 25 °C.

According to ^1H - and ^{13}C -NMR spectra RuPhos fragment does not pose the plane of symmetry. Moreover, according to ^{19}F -NMR spectrum fluorine atoms of the CF_2 group are diastereotopic. ^1H NMR (CDCl_3 at 25 °C): δ 7.52 (apparent triplet, $J = 6.5$ Hz, 1H), 7.40-7.34 (m, 2H), 7.32 (t, $J = 7.3$ Hz, 1H), 7.19 (m, 2H), 7.12 (m, 1H), 6.85 (d, $J = 8.3$ Hz, 1H), 6.70 (m, 2H), 6.65 (m, 1H), 4.56-4.48 (two overlapping septets, 2H), 2.23 (m, 1H, Cy proton), 2.12 (s, 3H), 1.93-0.83 (many overlapping multiplets, 19H, Cy protons), 1.21 (two overlapping doublets, 6H), 1.12 (d, $J = 6.0$ Hz, 3H), 0.78 (d, $J = 6.0$ Hz, 3H), 0.63 (m, 1H, Cy proton), 0.46 (m, 1H, Cy proton). $^{13}\text{C}\{^1\text{H}\}$ NMR (CDCl_3 at 25 °C): δ 155.45, 153.24, 144.63 (broad), 141.31 (d, $J = 15.0$ Hz), 140.98, 136.94, 134.73 (d, $J = 8.2$ Hz), 133.23 (m, CF_2), 131.06, 129.63, 128.58 (d, $J = 2.0$ Hz), 127.76 (broad d, $J = 22.9$ Hz), 127.54, 126.38 (d, $J = 4.1$ Hz), 123.56 (broad multiplet), 122.74, 122.50, 122.45 (m, CF_3), 112.35, 109.54, 76.73, 71.03, 34.32 (d, $J = 19.1$ Hz), 32.07 (d, $J = 18.4$ Hz), 29.83, 29.80, 27.62 (d, $J = 12.3$ Hz), 27.13 (d, $J = 10.3$ Hz), 26.97 (d, $J = 2.3$ Hz), 26.92 (d, $J = 8.8$ Hz), 26.71 (d, $J = 12.9$ Hz), 26.41, 26.35 (d, $J = 3.4$ Hz), 25.98, 25.87, 22.45, 21.95, 21.64, 20.91. ^{19}F NMR (CD_2Cl_2 at 25 °C): δ -79.87 (s, 3F), -101.19 (dd, $^2J_{(\text{F-F})} = 31.5$ Hz, $^3J_{(\text{F-P})} = 275.3$ Hz, 1F), -102.44 (dd, $^2J_{(\text{F-F})} = 275.3$ Hz, $^3J_{(\text{F-P})} = 23.2$ Hz, 1F). $^{31}\text{P}\{^1\text{H}\}$ NMR (CD_2Cl_2 at 25 °C): δ 11.31 (broad multiplet). $^{19}\text{F}/^{13}\text{C}$ HSQC NMR (CDCl_3 at 25 °C): $\delta_{\text{F}}/\delta_{\text{C}}$ -79.87/122.45. $^{19}\text{F}/^{13}\text{C}$ HMBC NMR (CDCl_3 at 25 °C): $\delta_{\text{F}}/\delta_{\text{C}}$ -79.87/122.45 (1J correlation), -79.83/133.23. IR (ATR): cm^{-1} 3048 (w), 2976 (w),

2927 (m), 2850 (m), 1596 (m), 1577 (m), 1449 (s), 1384 (m), 1373 (m), 1292 (m), 1266 (m), 1228 (m), 1185 (s), 1148 (s), 1101 (s), 1037 (s). HRMS electrospray (m/z): [M – F]⁺ calcd for C₃₈H₅₀F₂O₂PPd, 713.2551; Found, 713.2546.

5.7 References

- (1) Excerpts of Chapter 5 reprinted with permission from Maleckis, A.; Sanford, M. S. A Catalytic Cycle for Palladium-Catalyzed Decarbonylative Trifluoromethylation using Trifluoroacetic Esters as the CF₃ Source. *Organometallics* **2014**, Article ASAP. Copyright 2014. American Chemical Society.
- (2) Kakino, R.; Shimizu, I.; Yamamoto, A. *Bull. Chem. Soc. Jpn.* **2001**, *74*, 371-376.
- (3) (a) Culkin, D. A.; Hartwig, J. F. *Organometallics* **2004**, *23*, 3398-3416. (b) Grushin, V. V.; Marshall, W. J. *J. Am. Chem. Soc.* **2006**, *128*, 4632-4641. (c) Grushin, V. V. *Acc. Chem. Res.* **2010**, *43*, 160-171. (d) Ball, N. D.; Kampf, J. W.; Sanford, M. S. *J. Am. Chem. Soc.* **2010**, *132*, 2878-2879.
- (4) Grushin, V. V.; Marshall, W. J. *J. Am. Chem. Soc.* **2006**, *128*, 12644-12645.
- (5) Cho, E. J.; Senecal, T. D.; Kinzel, T.; Zhang, Y.; Watson, D. A.; Buchwald, S. L. *Science*, **2010**, *328*, 1679-1681.
- (6) Milner, P. J.; Maimone, T. J.; Su, M.; Chem, J. Müller, P.; Buchwald, S. L. *J. Am. Chem. Soc.* **2012**, *134*, 19922-19934 and references therein.
- (7) Cavell, K. J. *Coord. Chem. Rev.* **1996**, *155*, 209-243.
- (8) Otsuka, S.; Nakamura, A.; Yoshida, T.; Naruto, M.; Ataka, K. *J. Am. Chem. Soc.* **1973**, *95*, 3180-3188.
- (9) (a) Norton, D. M.; Mitchell, E. A.; Botros, N. R.; Jessop, P. G.; Baird, M. C. *J. Org. Chem.* **2009**, *74*, 6674-6680. (b) Hayashi, Y.; Wada, S.; Yamashita, M.; Nozaki, K. *Organometallics* **2012**, *31*, 1073-1081. (c) Novak, B. M.; Wallow, T. I.; Goodson, F. E. *Organometallics* **1996**, *15*, 3708-3716.
- (10) While phenyl trifluoroacetate is known to undergo oxidative addition to transition metals, there are no reports in the literature of oxidative addition of pentafluorophenyl trifluoroacetate to Pd(0) or Ni(0). For oxidative addition of phenyl trifluoroacetate to Rh(I), see Zhu, Y.; Smith, D. A.; Herbert, D. E.; Gatard, S.; Ozerov, O. V. *Chem. Commun.* **2012**, *48*, 218-220.
- (11) (a) Walker, S. D.; Barder, T. E.; Martinelli, J. R.; Buchwald, S. L. *Angew. Chem. Int. Ed.* **2004**, *43*, 1871-1876 (b) O'Connor, A. R.; Kaminsky, W.; Heinekey, D. M.; Goldberg, K. I. *Organometallics* **2011**, *30*, 2105-2116. (c) Hubig, S. M.; Lindeman, S. V.; Kochi, J. K. *Coord. Chem. Rev.* **2000**, *200*, 831-873.
- (12) Jenkins, J. M.; Shaw, B. L. *J. Chem. Soc. A* **1966**, 770-775.
- (13) The observed HRMS pattern coincides with theoretically calculated isotopic distribution.

-
- (14) (a) Murahashi, T.; Nagai, T.; Okuno, T.; Matsutani, T.; Kurosawa, H. *Chem. Commun.* **2000**, 1689-1690. (b) Benner L. S., Balch, A. L. *J. Am. Chem. Soc.* **1978**, *100*, 6099-6106.
- (15) (a) Murahashi, T.; Kimura, S.; Takase, K.; Ogoshi, S.; Yamamoto, K. *Chem. Commun.* **2013**, *49*, 4310-4312. (b) Murahashi, T.; Takase, K.; Oka, M.; Ogoshi, S. *J. Am. Chem. Soc.* **2011**, *133*, 14908-14911. (c) Allegra, G.; Immirzi, A.; Porri, L. *J. Am. Chem. Soc.* **1965**, *87*, 1394-1395.
- (16) Beller, M.; Riermeier, T. H. *Eur. J. Inorg. Chem.* **1998**, *1*, 29-35.